



II. Second Investigation

1. Purpose

The purpose of this report is to provide results of additional investigation of I type mockups and boat samples collected from the U3B and U3A RSGs.

2. Background

Cracks were discovered on the divider plate-to-channel head weld, during the inspections of tube-to-tube sheet welds in secondary side hydrostatic test of Unit 3B RSG. The cracks were caused by the separation of the divider plate and channel head. The same separation was also confirmed in Unit 3A RSG. The I type mockups were made for a part of root cause analysis.

3. Investigation Methodology

2 boat samples were additionally collected from Unit 3A RSG at the location as shown in Figure A.44. The detail of the each sample was shown in Table A.5.

I type mockups and boat samples already taken were also used for additional investigation.

Table A.5 Locations and purpose of boat samples

Sample No.	Location	Purpose
Sample F	LAS under 152 buttering (sample E)	To investigate the situation of the separation between 152 buttering and LAS in U3A.
Sample G	Area of typical 152 buttering without separation in UT	To investigate the situation of the HAZ (heat affected zone) of LAS and fusion boundary between 152 buttering and LAS in U3A.

As for the boat samples already taken (sample A, B and C), grain size measurement was performed.

The investigation methodology matrix of sample F and G was summarized in Table A.6

As for the I type mockups, grain size measurement and hardness test was also performed.

Grain size in heat affected zone (HAZ) of low alloy steel (LAS) was measured with comparison method: some photographs of micro structure of the cross section were compared to figures of JIS G0551:2005 standard grain size number.

Grain size number G is described by equation 1 using m: number of grains per 1mm² in cross section. The grain size D is obtained by equation 2.

$$m = 8 \times 2^G \quad (\text{eq. 1})$$

$$D = 1/\sqrt{m} = 1/\sqrt{8 \times 2^G} \quad (\text{eq. 2})$$



Table A.6 Investigation Methodology of sample F and G

Item	Method	Purpose
Sample appearance	Visual examination	Confirm that the sample conditions (contains expected materials)
Separation surface	Visual examination at low magnification	Evaluate the macro-structure of the separation surface
Macro-structure	Visual examination of the cross-section at low magnification after etching	Evaluate the macro-structure of the materials constituting the sample
Micro-structure	Visual examination of the cross-section at high magnification after etching	Evaluate the micro-structure of near the fusion boundary Examine the existence of micro-cracking in LAS Measure the grain size of HAZ
Hardness	Measure Vickers hardness	Evaluate the hardness distribution near the fusion boundary and HAZ

4. Results of investigation

4.1 Boat samples A, B and C

Table A.7 shows the result of the grain size measurement in HAZ. The photographs used for grain size measurement were shown in Figures A.45.

The HAZ of 152 buttering tends to reveal larger grains (mean grain size was about 0.1mm) compared with HAZ of stainless steel clad (mean grain size was 0.02mm to 0.01mm). It was considered that the HAZ of stainless steel clad was refined by heat input of 2nd layer welding.

4.2 Sample F

Figure A.46 shows appearance of boat sample F collected from U3A. The sample contains low alloy steel part after sampling of 152 buttering part (sample E).

Figure A.47 shows appearance of fracture surface of the sample. A rough surface was observed on the fracture surface as observed in sample F. It is supposed that the rough surface corresponds to welding bead shape of 152 buttering.

Figures A.48 show macro-structures and micro-structures of cross section of sample F. The separation occurs along the fusion boundary between 152 weld metal and LAS base metal. In higher magnification pictures, the crack paths seem to be similar to the boat samples collected from U3B; crack path in LAS or crack path in the weld metal locate adjacent to the fusion boundary. Any micro-cracking in HAZ was not observed in the cross section.



Table A.8-1 shows the results of grain size measurement of HAZ of 152 buttering in sample F. The grain size distribution of HAZ of 152 buttering was almost similar to that of boat samples collected from U3B. There were both coarse grained region and small grained region in HAZ of 152 buttering.

Figure A.49 shows result of Vickers hardness measurement of cross section of sample F. There is no abnormality in hardness of LAS base metal and heat affected zone of LAS.

4.3 Sample G

Figure A.50 shows appearance of boat sample G collected from 152 buttering area without separation in U3A. The sample contains low alloy steel and 152 buttering. Any surface cracks were not observed.

Figures A.51 show macro-structures and micro-structures of cross section of sample G. Any separations were not observed. The micro structure of sample G was similar to that of sample F and those of boat samples collected from U3B. Any micro-cracking or defect were not observed in HAZ.

Table A.9-1 shows the results of grain size measurement of HAZ of 152 buttering in sample G. The grain size distribution of HAZ of 152 buttering was almost similar to those of other boat samples. There were both coarse grained region and small grained region in HAZ of 152 buttering. Mean grain size of the HAZ of 152 buttering was approximately 0.1mm.

Figure A.52 shows result of Vickers hardness measurement of cross section of sample G. The 152 buttering revealed high hardness (HV440 to 480) in colored zone adjacent to the fusion boundary as observed in boat samples collected from U3B.

4.4 I type mockups

Table A.10-1 shows the result of the grain size measurement in HAZ of I type mockups. The photographs used for grain size measurement were shown in Figures A.53.

Any difference in grain size was not observed between machining and grinding after 152 buttering in I type mockups as shown in Figure A. 53(1). The effect of gouging on grain size was observed before 152 buttering as shown in Figure A. 53(2).

The grain size of HAZ of 152 buttering in I type mockups tend to be smaller than that of boat samples. It was considered that the grain refining with heat input of 2nd layer of 152 buttering occurred in I type mockups compared to boat samples, since the distance between fusion line and 2nd layer of 152 buttering of I type mockups was smaller than that of boat samples.



Figures A.54 show result of additional Vickers hardness measurement of cross section of I type mockups. Any significant differences were not confirmed in Vickers hardness distribution and width of HAZ of 152 buttering between machining and grinding after 152 buttering. The widths of HAZ of ESW were varied by hardness measurement location.

5. Summaries of the investigation

The summaries of the investigation were as follows

5.1 Boat samples already taken

- 1) The HAZ of 152 buttering tends to reveal larger grains (mean grain size was approximately 0.1mm) compared with HAZ of stainless steel clad (mean grain size was 0.02mm to 0.01mm).

5.2 Sample F

- 1) Sample F revealed similar rough fracture surface as observed in U3B.
- 2) The separation occurs in LAS or in weld metal adjacent to fusion boundary.
- 3) Micro-cracking in HAZ was not observed in the cross section.
- 4) The grain size distribution of HAZ of 152 buttering was almost similar to those of boat samples collected from U3B. There were both coarse grained region and small grained region in HAZ of 152 buttering.

5.3 Sample G

- 1) Any surface cracks were not observed.
- 2) Any micro-cracking or defect were not observed in HAZ in cross section.
- 3) There were both coarse grained region and small grained region in HAZ of 152 buttering. Mean grain size of the HAZ of 152 buttering was approximately 0.1mm.
- 4) The 152 buttering revealed high hardness (HV440 to 480) in colored zone adjacent to the fusion boundary as observed in boat samples collected from U3B.

5.4 I type mockups

- 1) Any difference in grain size was not observed between machining and grinding after 152 buttering in I type mockups
- 2) The grain size of HAZ of 152 buttering in I type mockups tend to be smaller than those of boat samples. It was considered that the difference of distance between fusion line and 2nd layer of 152 buttering affected to grain size distribution of HAZ.
- 3) Any significant differences were not observed in Vickers hardness distribution and width of HAZ of 152 buttering between machining and grinding after 152 buttering. The widths of HAZ of ESW were varied by hardness measurement location.

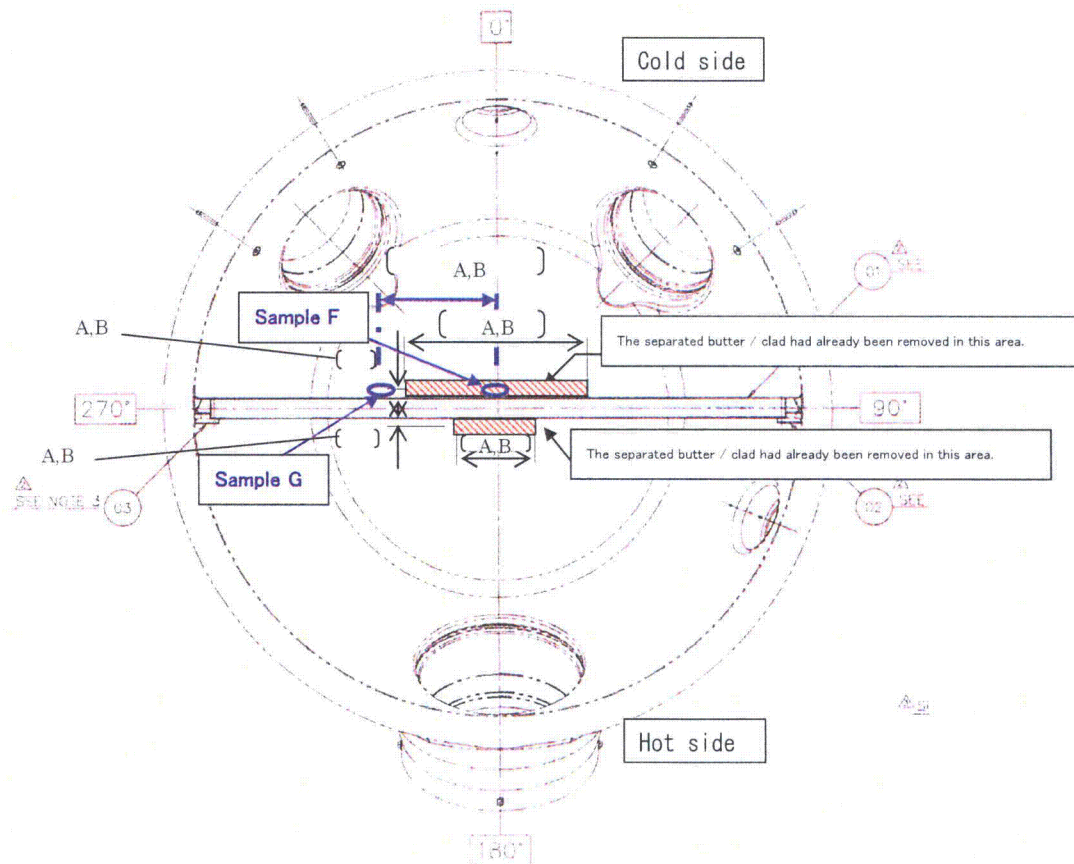


Figure A.44(1) The collecting location and schematic illustration of boat samples.
(collecting location of boat samples)

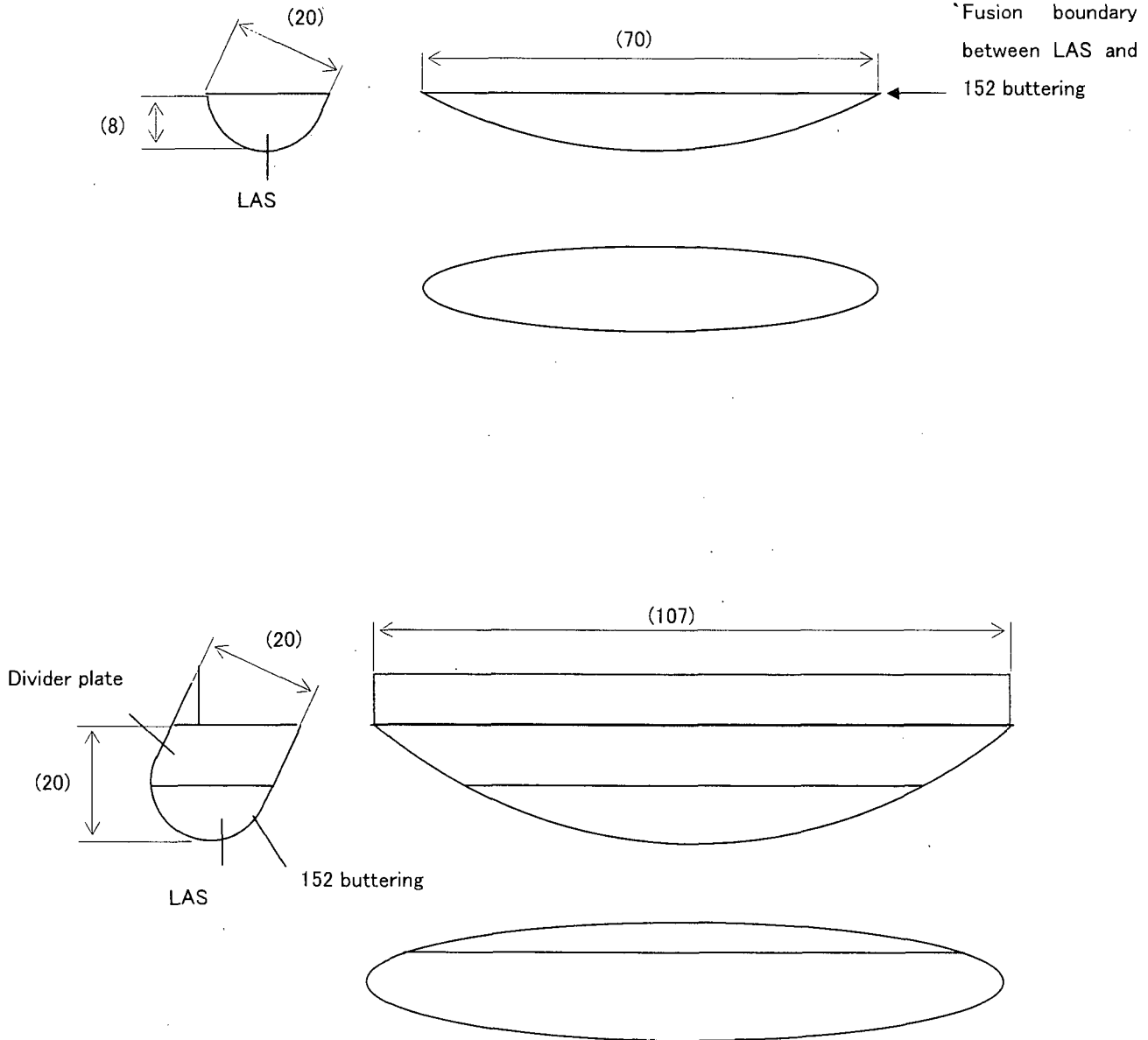


Figure A.44(2) The collecting location and schematic illustration of boat samples.
(schematic illustration of boat samples)

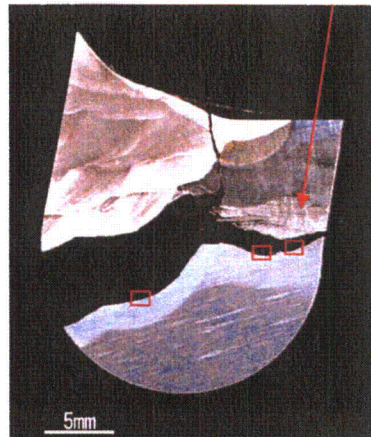


Table A.7 The results of grain size measurement in HAZ of boat samples A, B and C

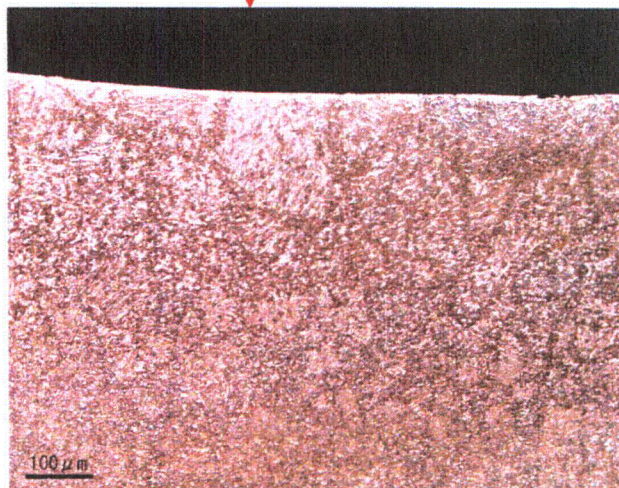
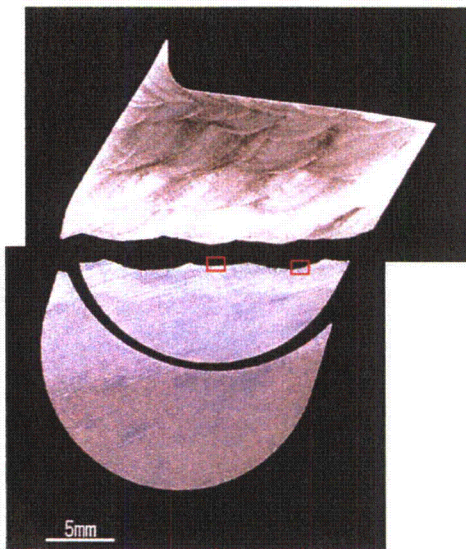
Weld metal	Welding process	Grain size number/ Grain size measured			Mean grain size
		4/ 0.088mm	3/ 0.125mm	5/ 0.063mm	
152	SMAW				0.09mm
	ESW	6/ 0.044mm	9.5/ 0.013mm	9/ 0.016mm	0.024mm
Stainless steel	SMAW	10.5/ 0.009mm	12/ 0.006mm		0.008mm



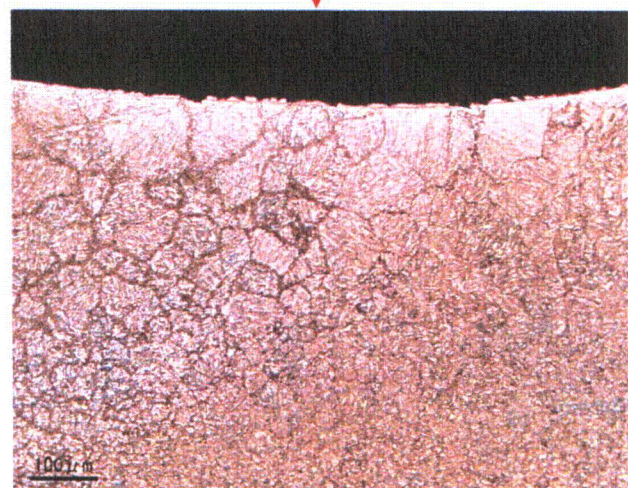
Details are shown in next page



Sample A, HAZ by 152 buttering (SMAW)
Grain size number: 4, Grain size: 0.088mm

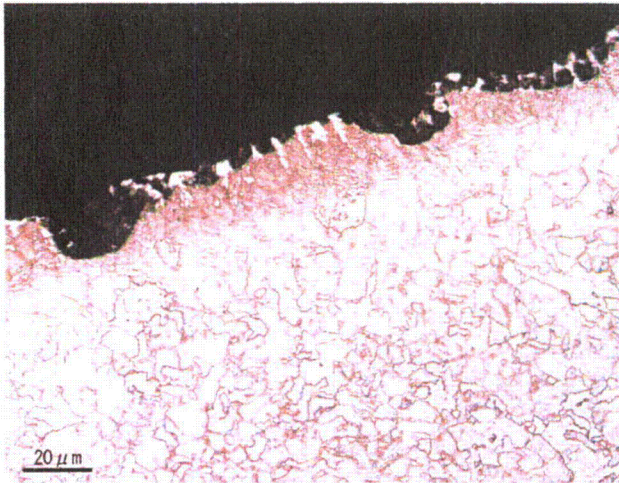


Sample B, HAZ by 152 buttering (SMAW)
Grain size number: 3, Grain size: 0.125mm

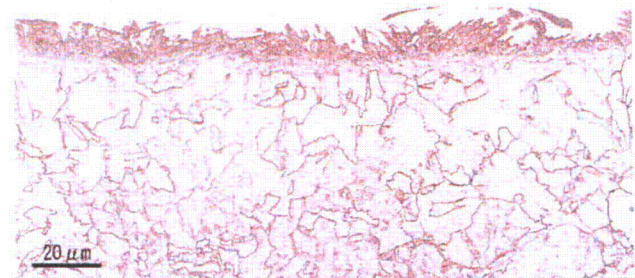
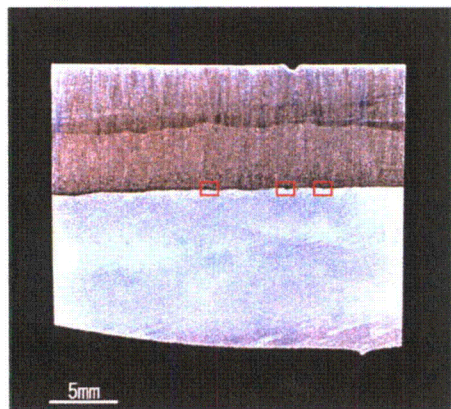
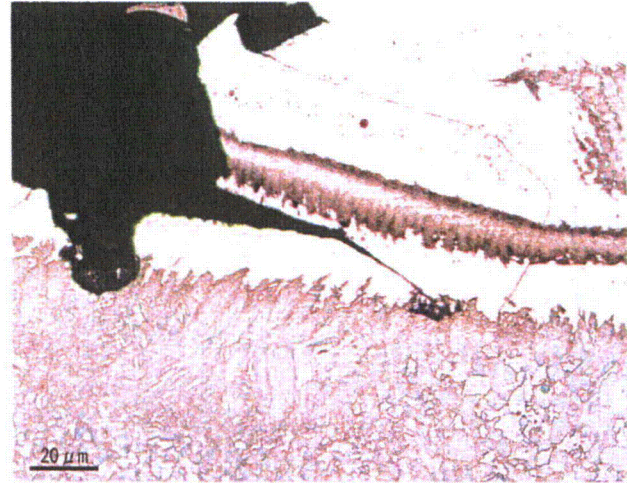


Sample B, HAZ by 152 buttering (SMAW)
Grain size number: 5, Grain size: 0.063mm

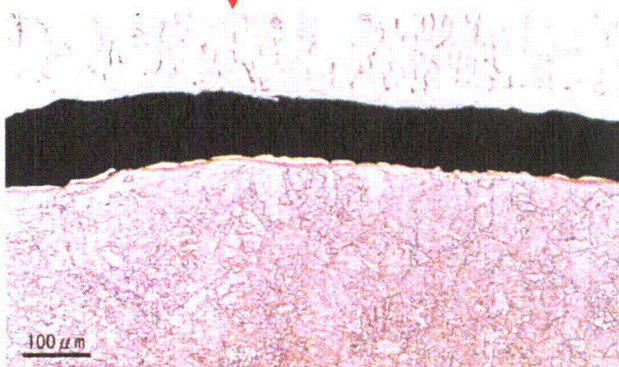
Figure A.45(1) Microstructure of the cross section of LAS channel head in boat samples A and B(152 buttering)



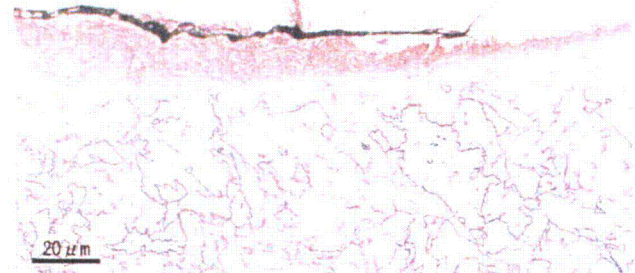
Sample A, HAZ by Stainless steel (SMAW)
Grain size number: 10.5, Grain size: 0.009mm



Sample C, HAZ by Stainless steel (ESW)
Grain size number: 9.5, Grain size: 0.013mm



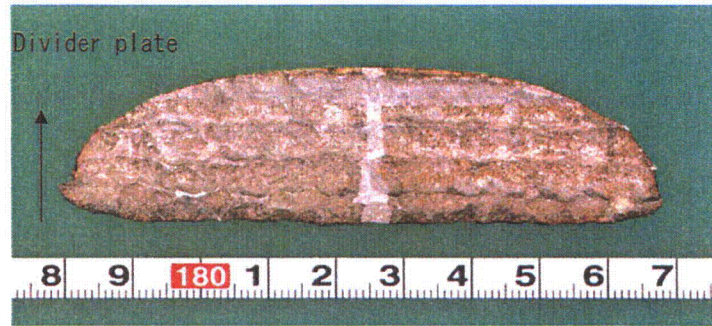
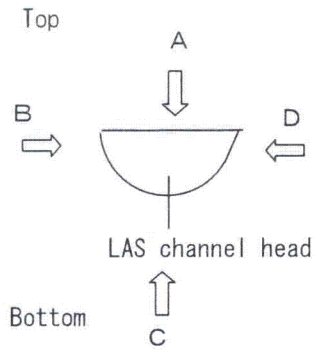
Sample C, HAZ by Stainless steel (ESW)
Grain size number: 6, Grain size: 0.044mm



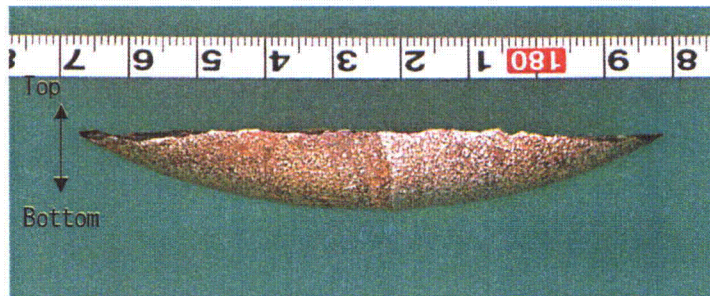
Sample C, HAZ by Stainless steel (ESW)
Grain size number: 9, Grain size: 0.0193mm

Figure A.45(2) Microstructure of the cross section of LAS channel head in boat samples A and C

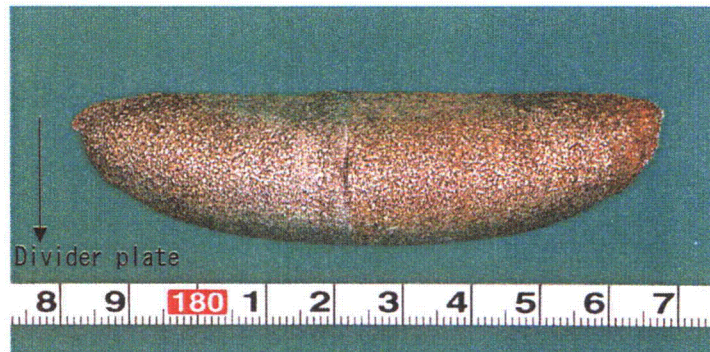
Divider plate ←



Fracture surface (direction A)



Electron discharge machined surface (direction B)

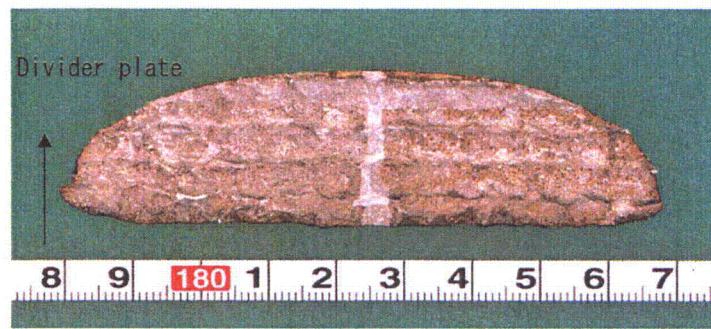


Electron discharge machined surface (direction C)

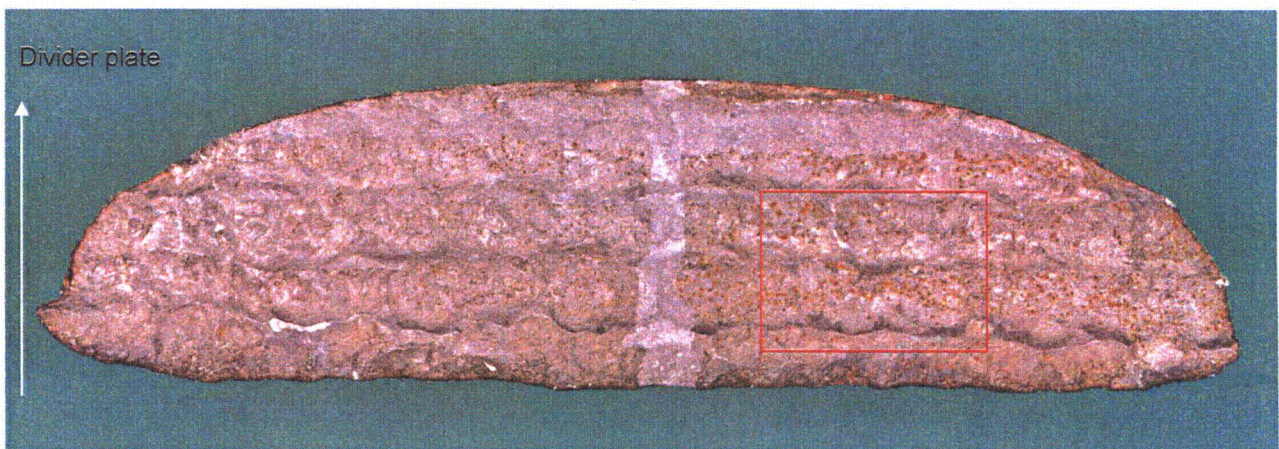


Electron discharge machined surface (direction D)

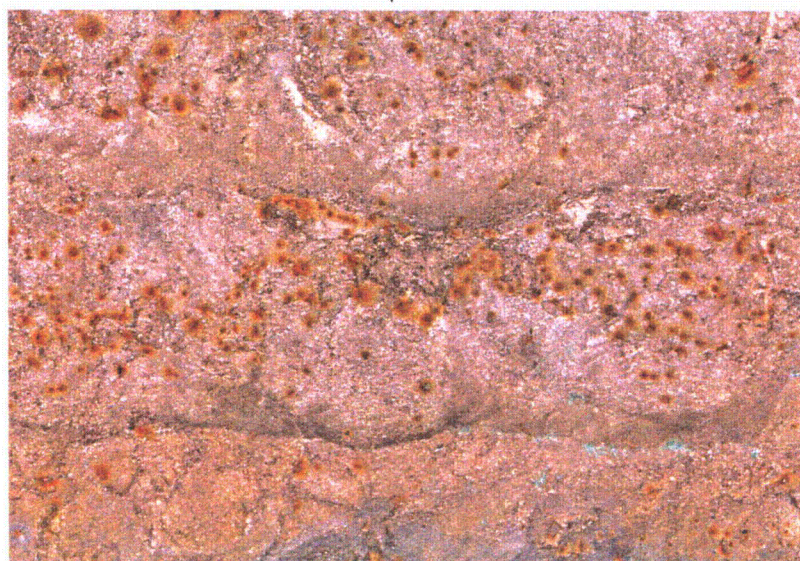
Figure A.46 Appearance of sample F collected from U3A



Fracture surface of sample F

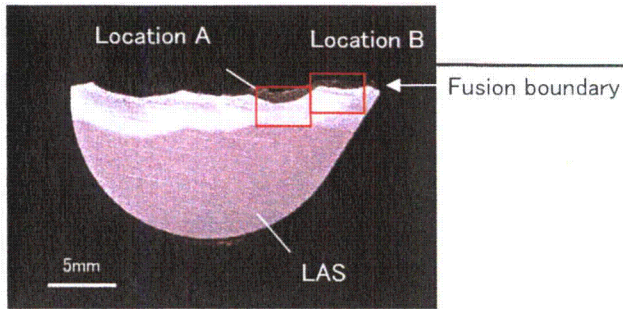


3mm



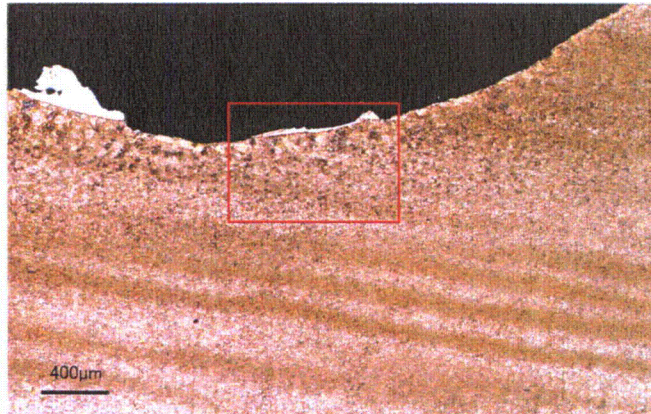
1mm

Figure A.47 Appearance of fracture surface of sample F

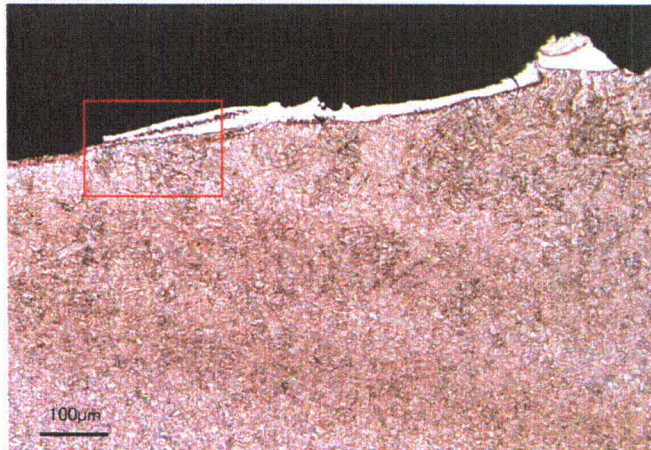


The location for detail observation

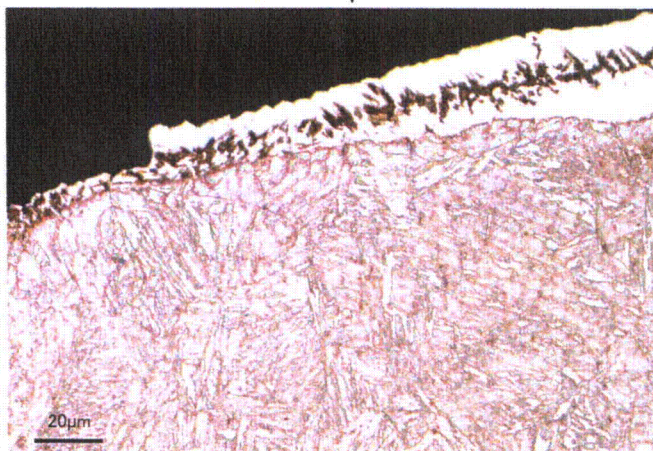
Detail observation of location A



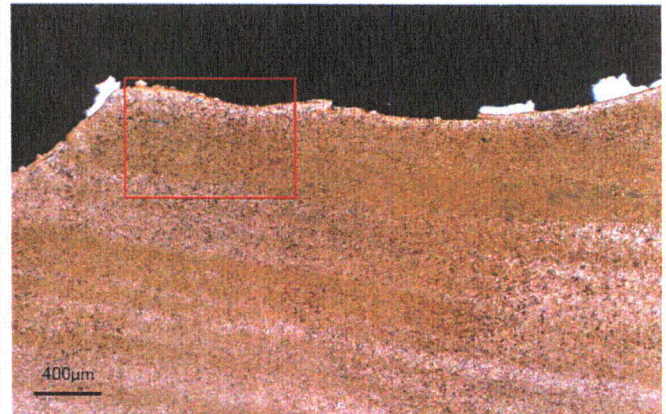
↓ Enlarged



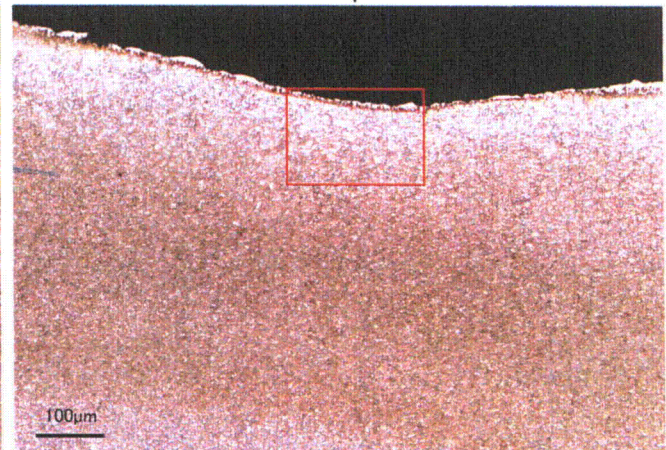
↓ Enlarged



Detail observation of location B



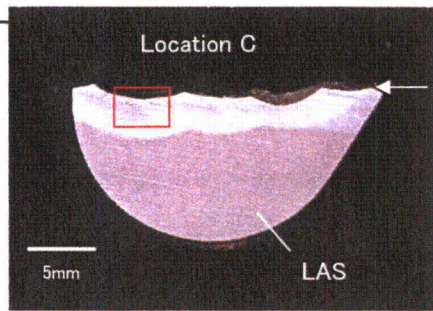
↓ Enlarged



↓ Enlarged



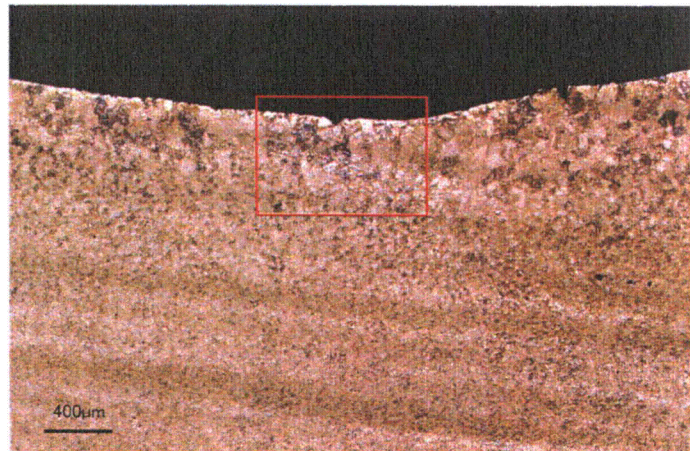
Figure A.48(1) Macro structure and micro structure of cross section of sample F



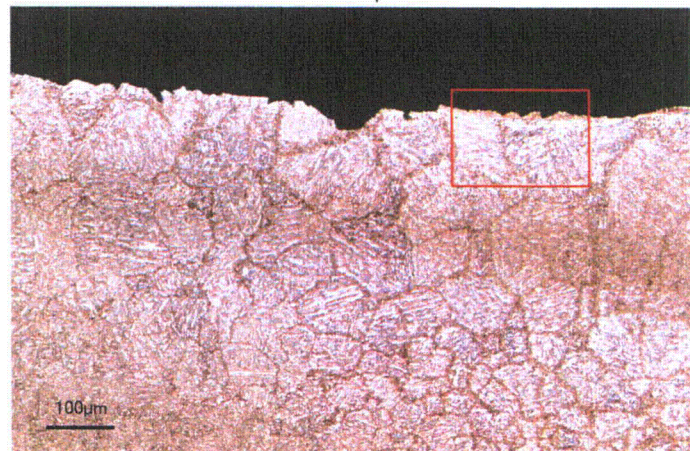
The location for detail observation

Fusion boundary

Detail observation of location C



Enlarged



Enlarged

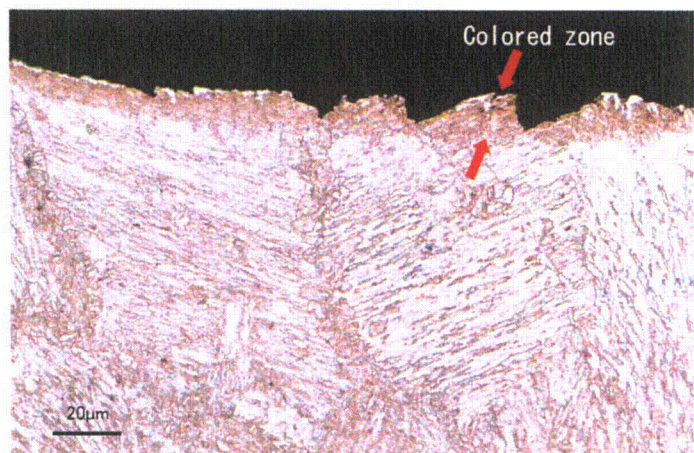
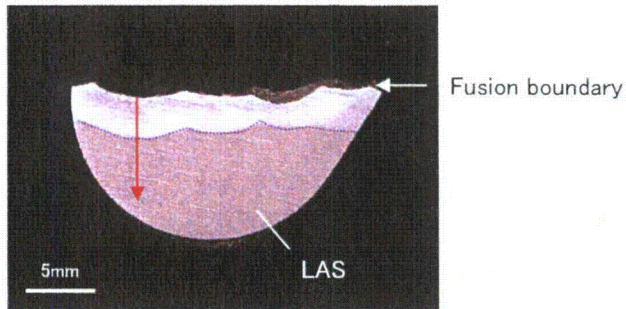


Figure A.48(2) Macro structure and micro structure of cross section of sample F



Table A.8-1 The results of grain size measurement in HAZ of sample F

Weld metal	Welding process	Grain size number/ Grain size measured			Mean grain size
		10.5/ 0.009mm (Location A)	5/ 0.063mm (Location B)	3.5/ 0.105mm (Location C)	
152	SMAW				0.059mm



Hardness measurement location

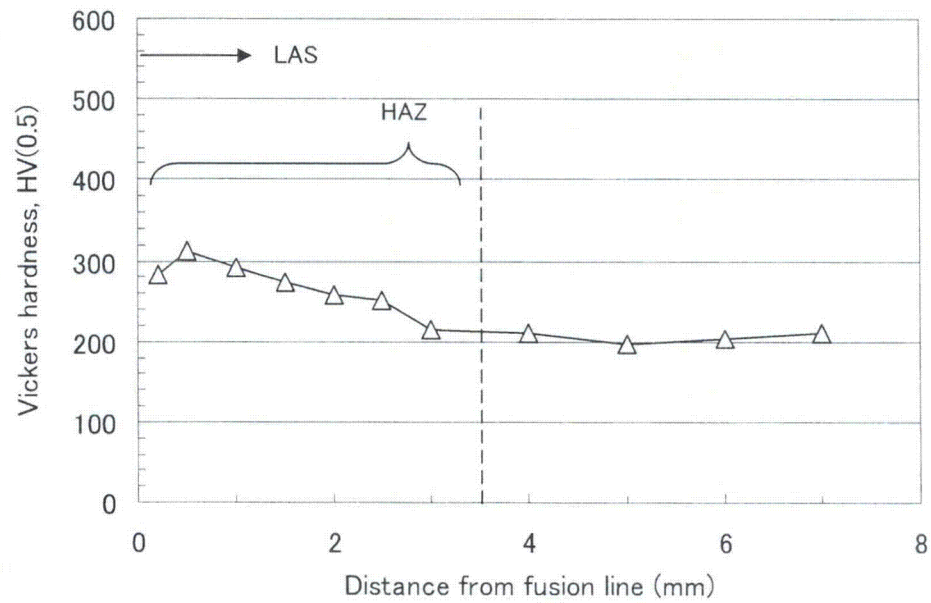
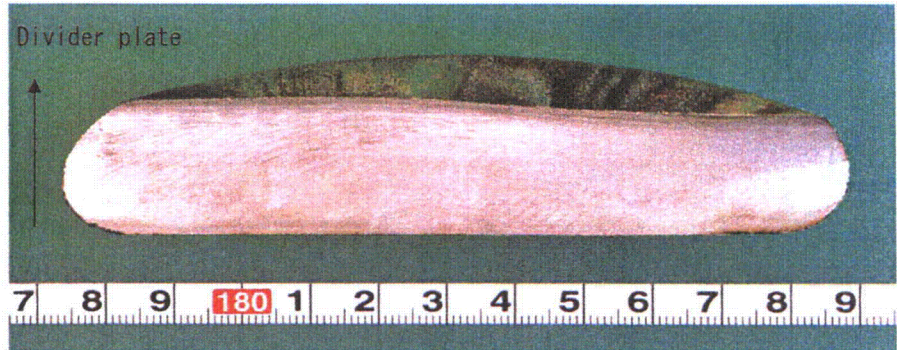
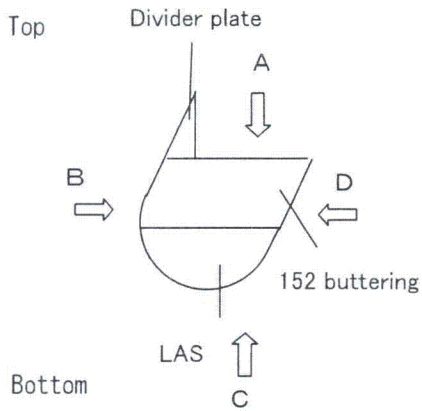
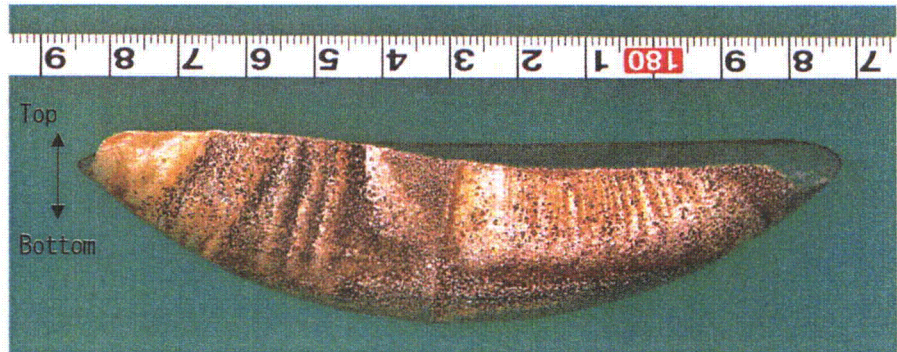


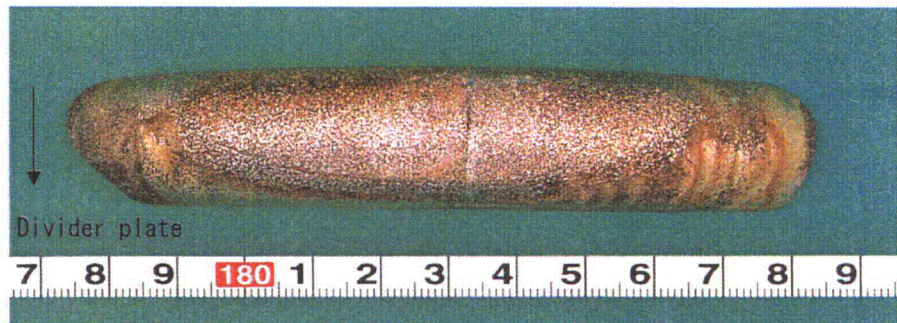
Figure A.49 Vickers hardness of cross section of sample F



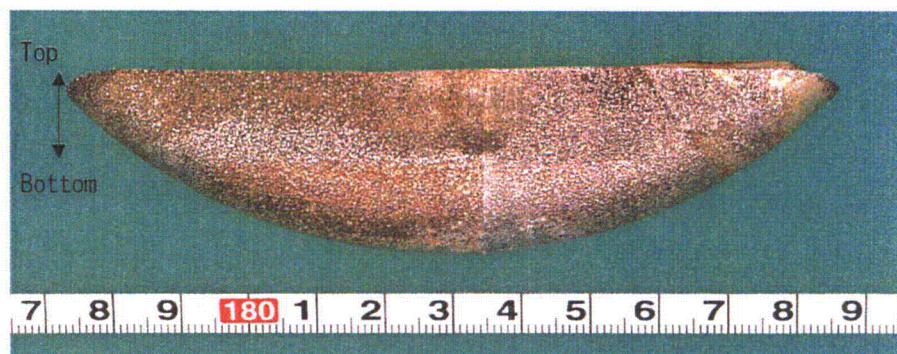
Surface of 152 buttering (direction A)



Electron discharge machined surface (direction B)

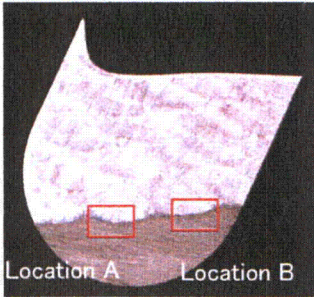
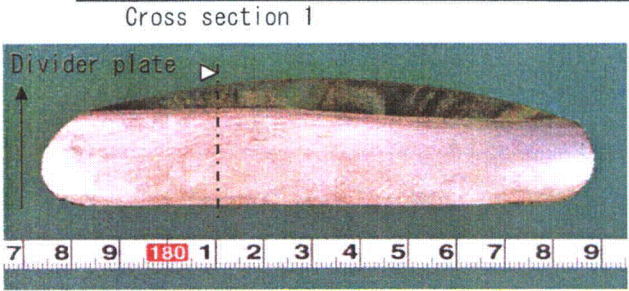


Electron discharge machined surface (direction C)



Electron Discharge Machined Surface (Direction D)

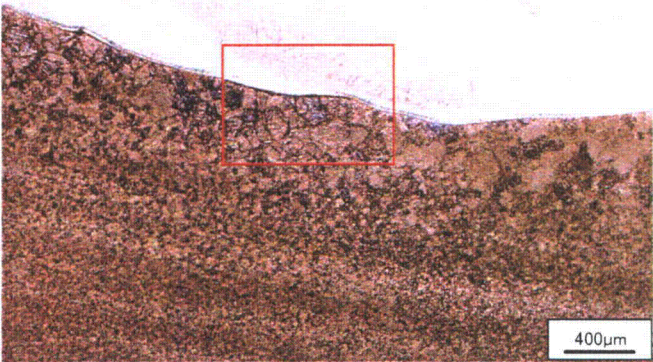
Figure A.50 Appearance of boat sample G



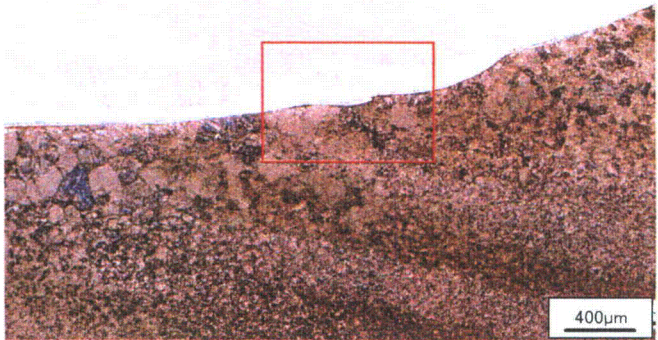
The location for
detail observation

Detail observation of location A

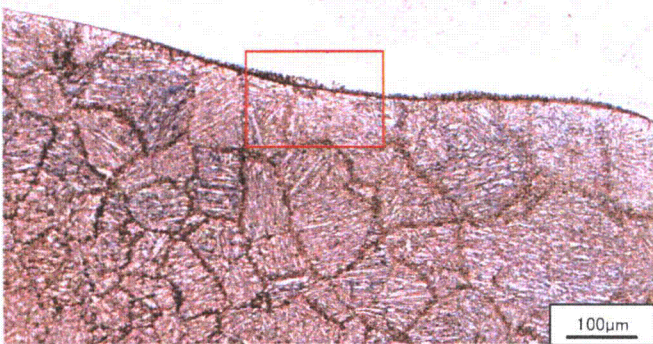
Detail observation of location B



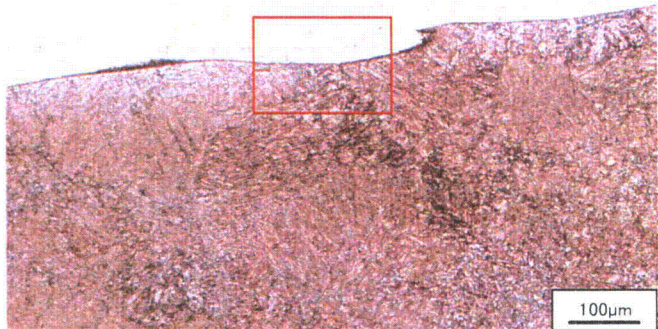
Enlarged



Enlarged



Enlarged



Enlarged

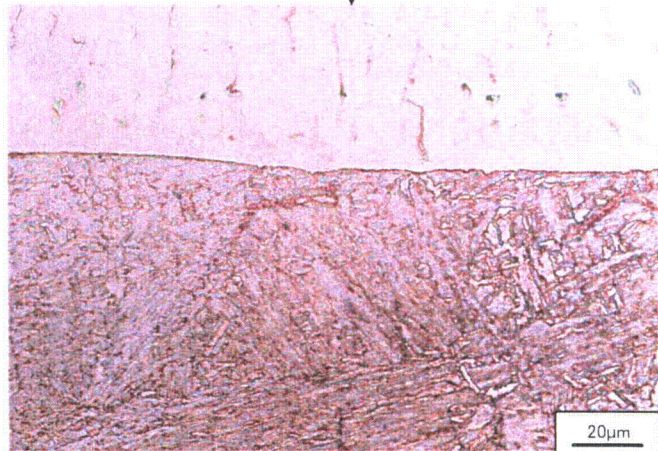
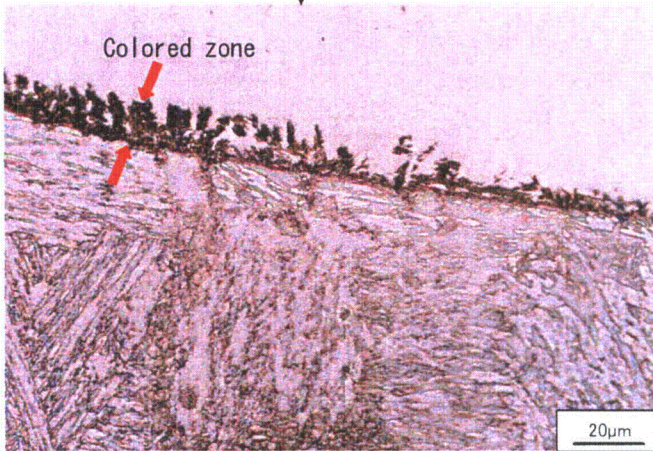
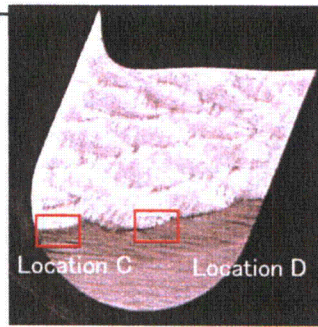
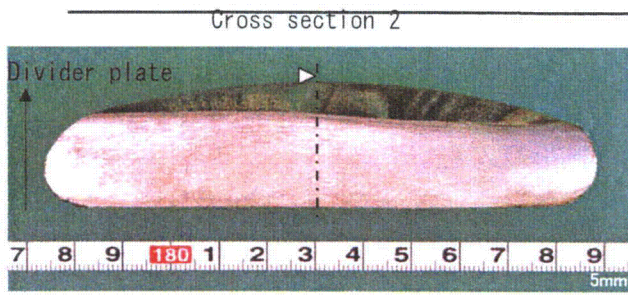


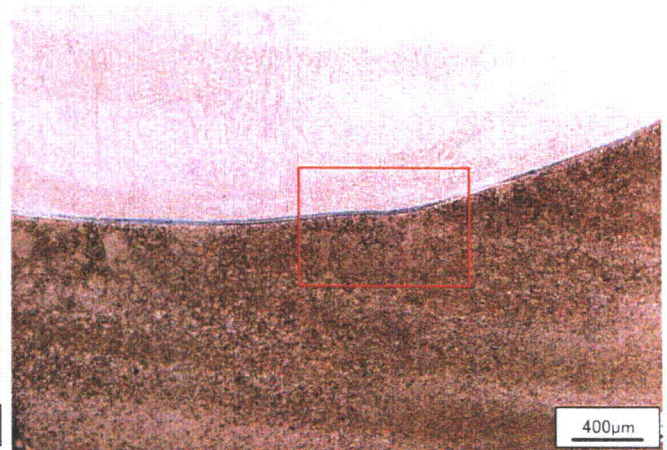
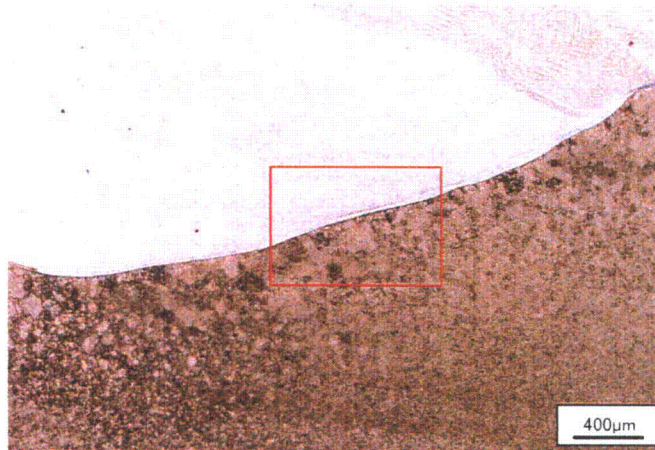
Figure A. 51(1) Macro structure and micro structure of cross section 1 of sample G



The location for
detail observation

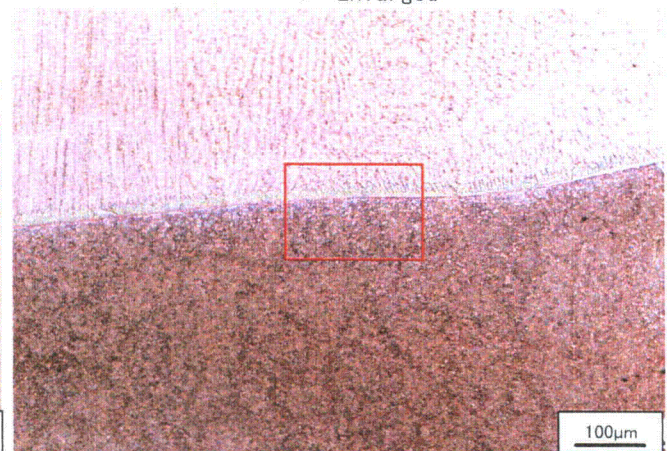
Detail observation of location C

Detail observation of location D



↓ Enlarged

↓ Enlarged



↓ Enlarged

↓ Enlarged

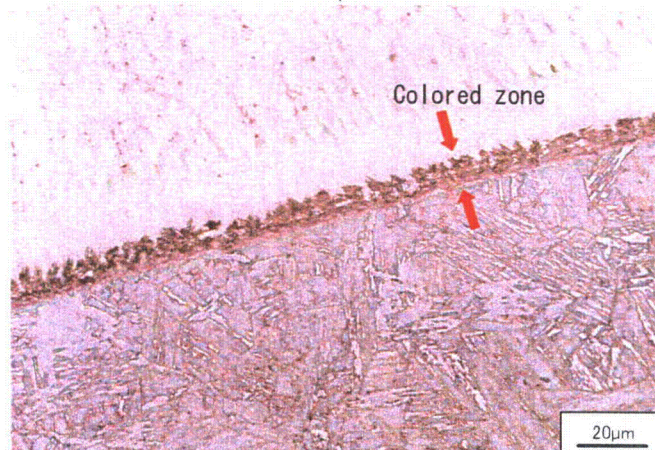
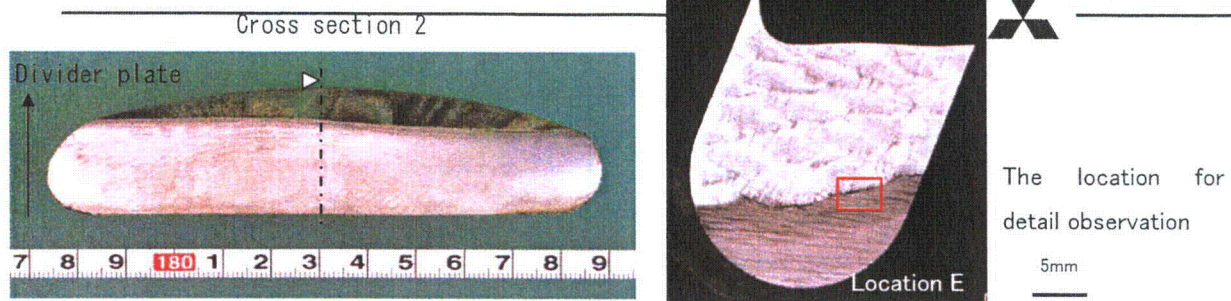
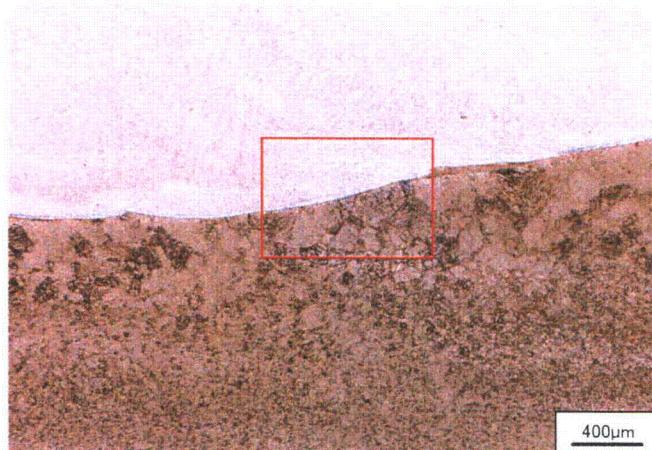


Figure A. 51(2) Macro structure and micro structure of cross section 2 of sample G



Detail observation of location E



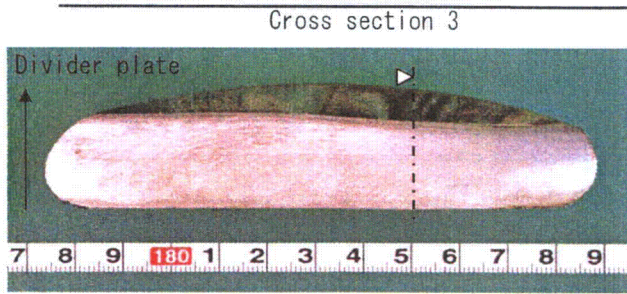
↓ Enlarged



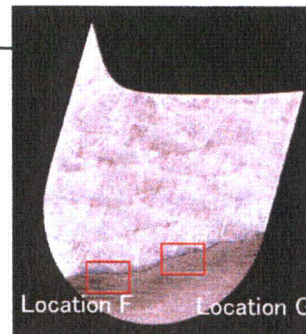
↓ Enlarged



Figure A. 51(3) Macro structure and micro structure of cross section 2 of sample G

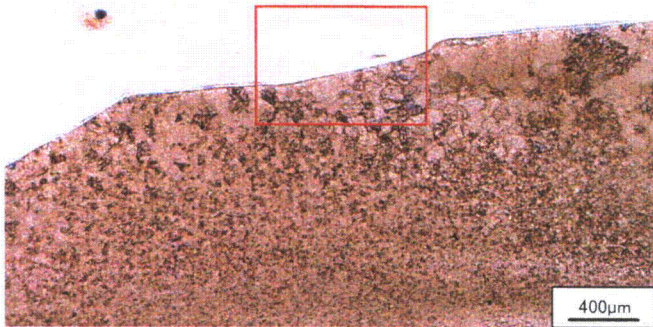


Detail observation of location F

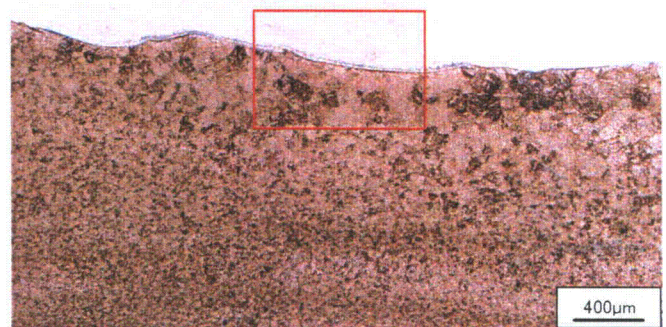


Detail observation of location G

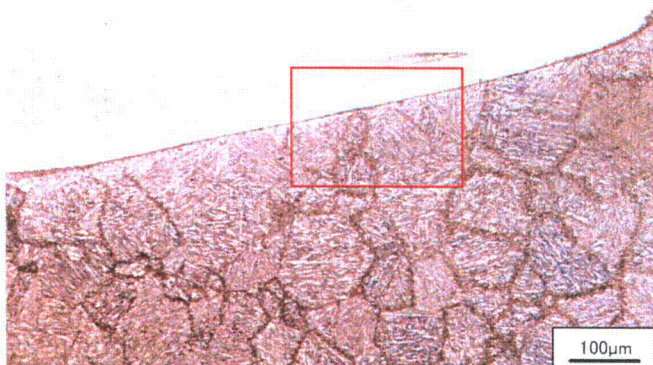
The location for
detail observation



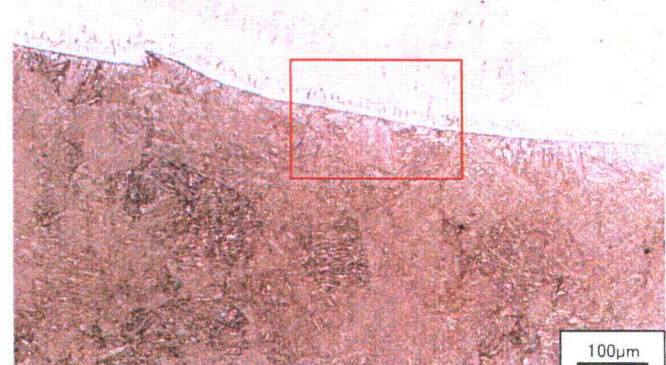
↓ Enlarged



↓ Enlarged



↓ Enlarged



↓ Enlarged

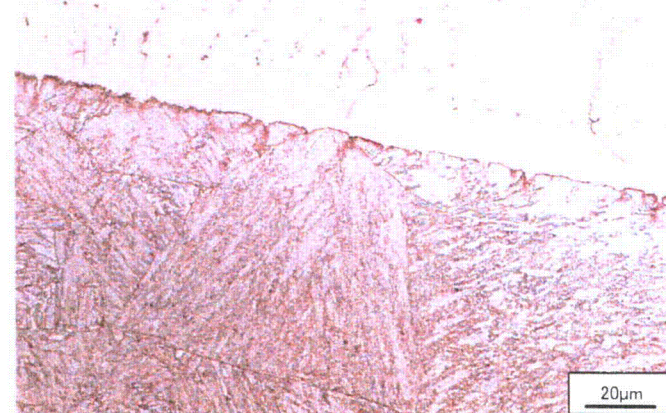
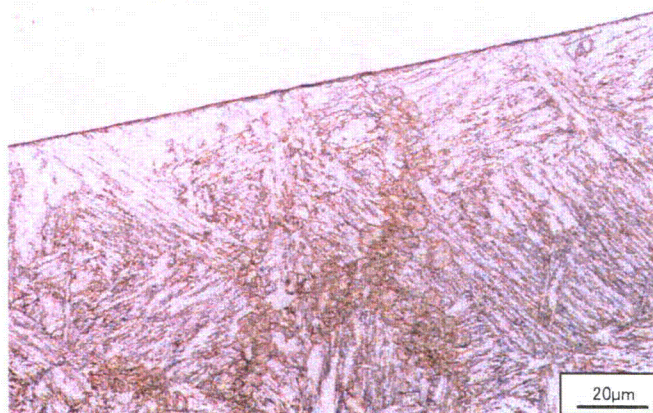
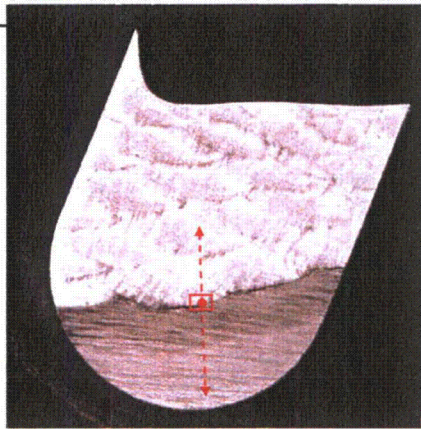


Figure A. 51(4) Macro structure and micro structure of cross section 3 of sample G

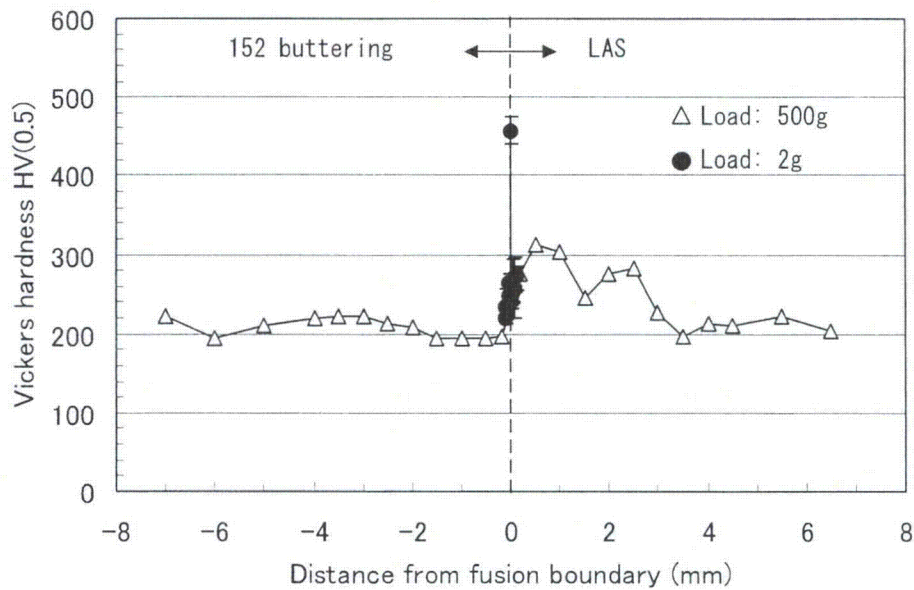


Table A.9-1 The results of grain size measurement in HAZ of sample G

Weld metal	Welding process	Grain size number/ Grain size measured			Mean grain size
		3.5/ 0.105mm (Location A)	3/ 0.125mm (Location B)	—	
152	SMAW	10.5/ 0.009mm (Location C)	4.5/ 0.074mm (Location D)	2.5/ 0.148mm (Location E)	0.096mm
		2.5/ 0.148mm (Location F)	5/ 0.063mm (Location G)	—	



The location for hardness
test (cross section 2)



Enlarged

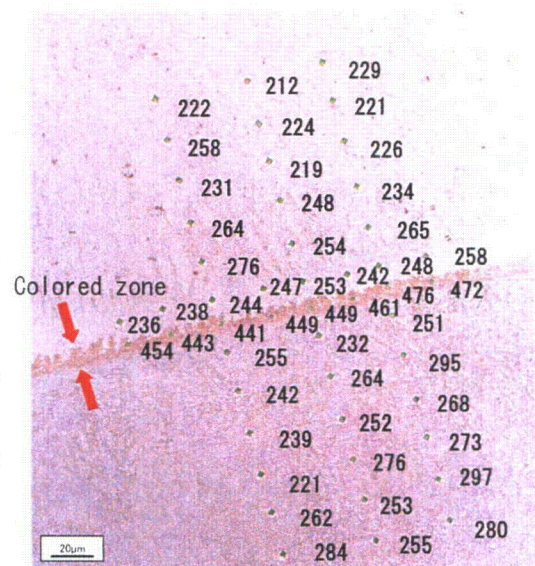
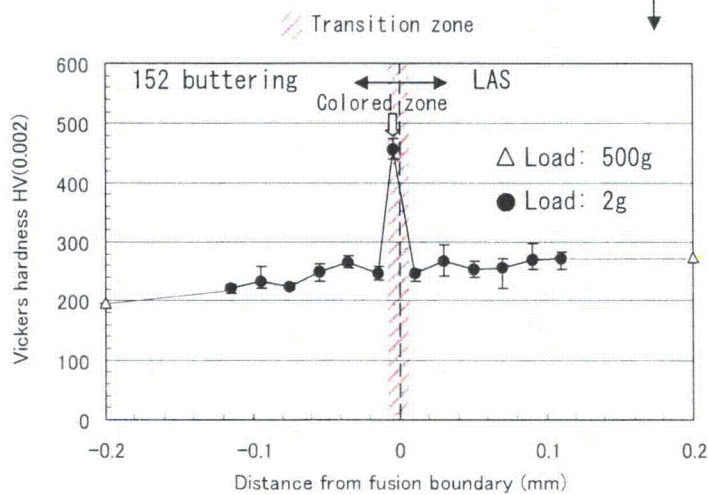


Figure A.52 Vickers hardness of cross section of sample G

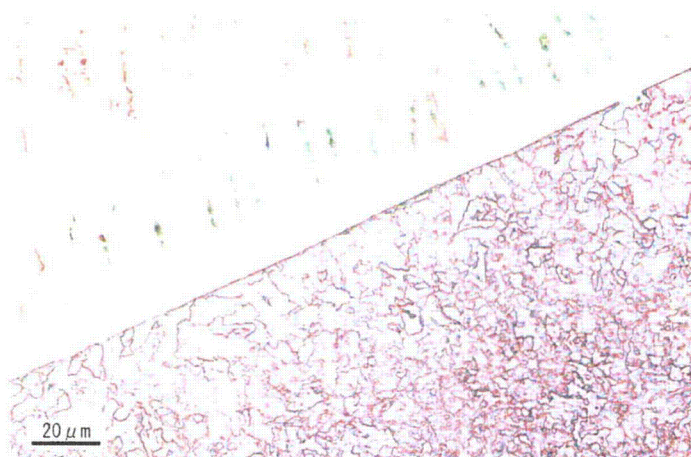
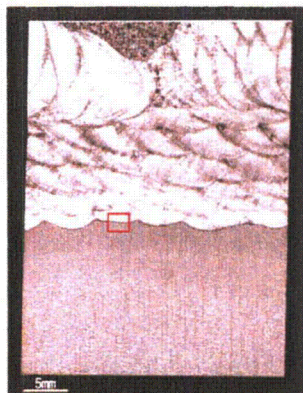


Table A.10-1 The results of grain size measurement in HAZ of I type mockups

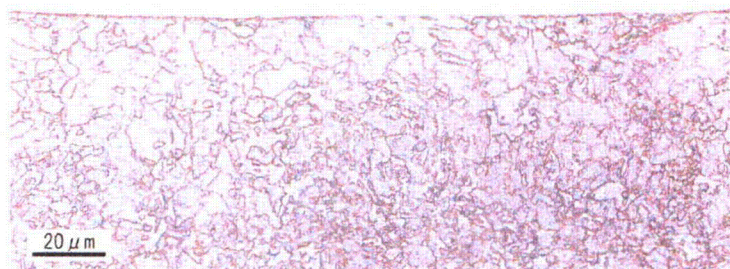
Process of clad removing	Welding process	Grain size number/ Grain size measured		Mean grain size
Gouging and grinding	SMAW (152 buttering)	10.5/ 0.009mm	10.5/ 0.009mm	0.009mm
Machining	SMAW (152 buttering)	10.5/ 0.009mm	—	0.009mm
Gouging (without ESW clad)	—	14/ 0.003mm	—	0.003mm
Gouging and grinding	—	13/ 0.004mm *1	—	0.004mm
Machining	—	10/ 0.011mm *2	—	0.011mm

*1 Grain size of HAZ of gouging

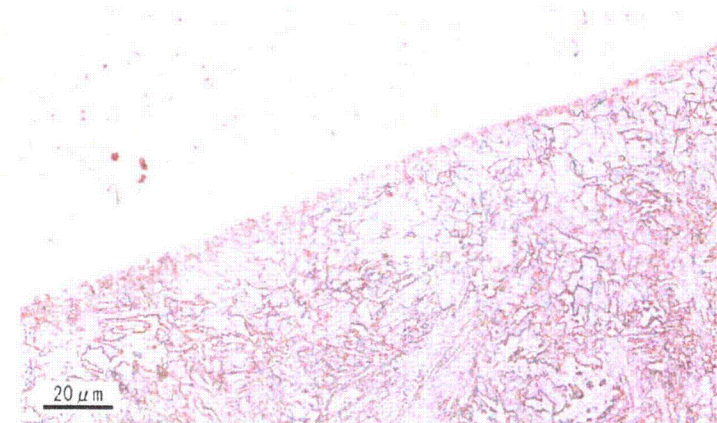
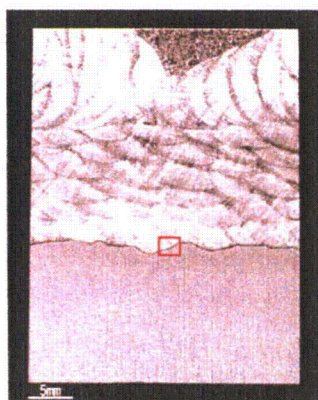
*2 Grain size of LAS base metal machined



TP.2-2, ESW + Gouging + grinding + 152 buttering (SMAW)
Grain size number: 10.5, Grain size: 0.009mm

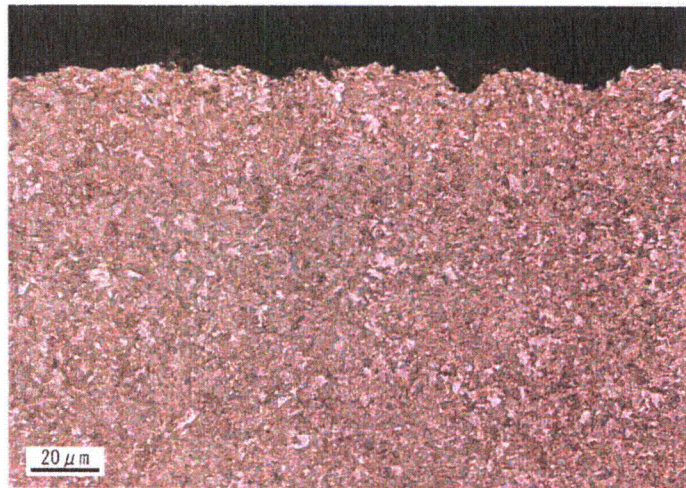
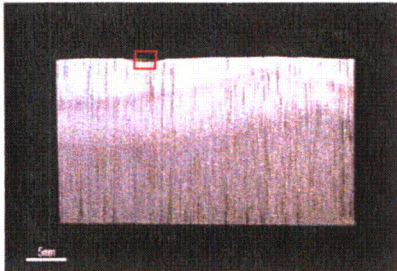


TP.2-2, ESW + Gouging + grinding + 152 buttering (SMAW)
Grain size number: 10.5, Grain size: 0.009mm

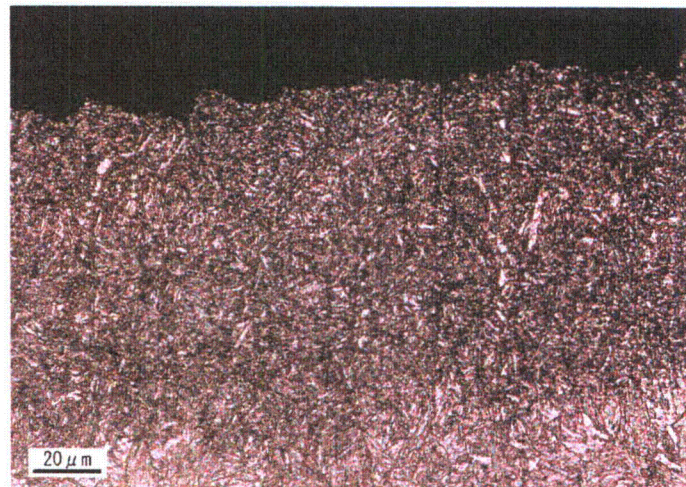
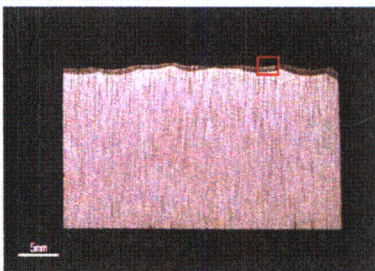


TP.3-1, ESW + Machining + 152 buttering (SMAW)
Grain size number: 10.5, Grain size: 0.009mm

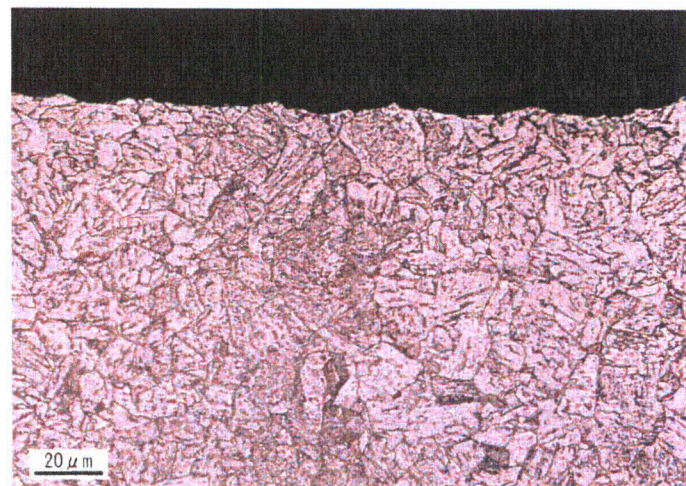
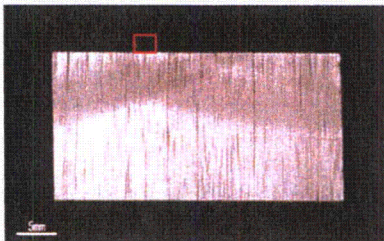
Figure A. 53(1) Microstructure of the cross section of LAS in I type model (after 152 buttering)



TP.2-1, ESW + Gouging + grinding
Grain size number: 13, Grain size: 0.004mm

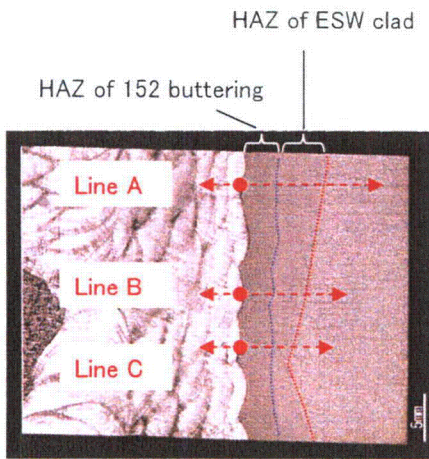


TP.4-2, As gouging
Grain size number: 14, Grain size: 0.003mm



TP.3-1, As machining
Grain size number: 10, Grain size: 0.011mm

Figure A. 53(2) Microstructure of the cross section of LAS in I type model (before 152 buttering)



Hardness measurement location

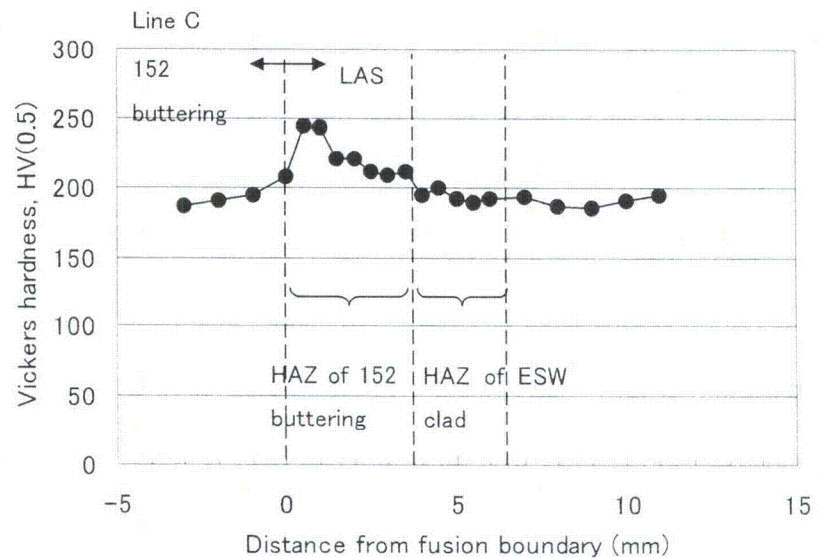
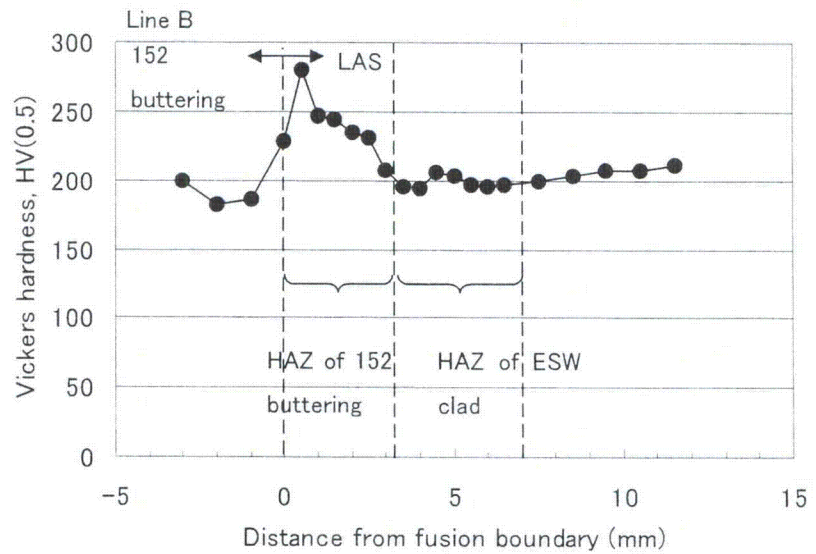
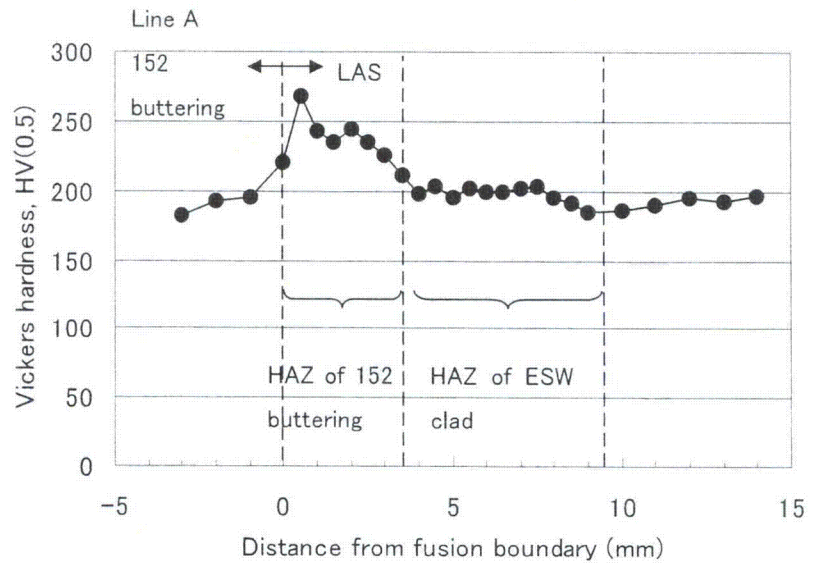
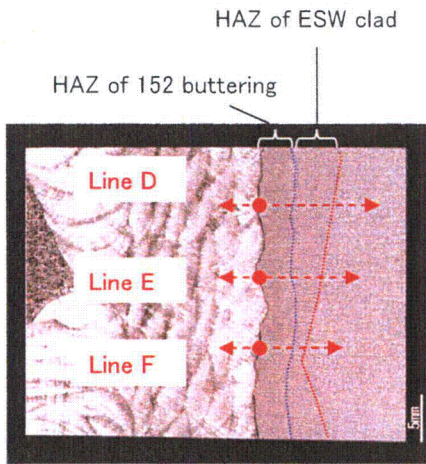


Figure A. 54(1) Vickers hardness of cross section of I type mockup 2-2



Hardness measurement location

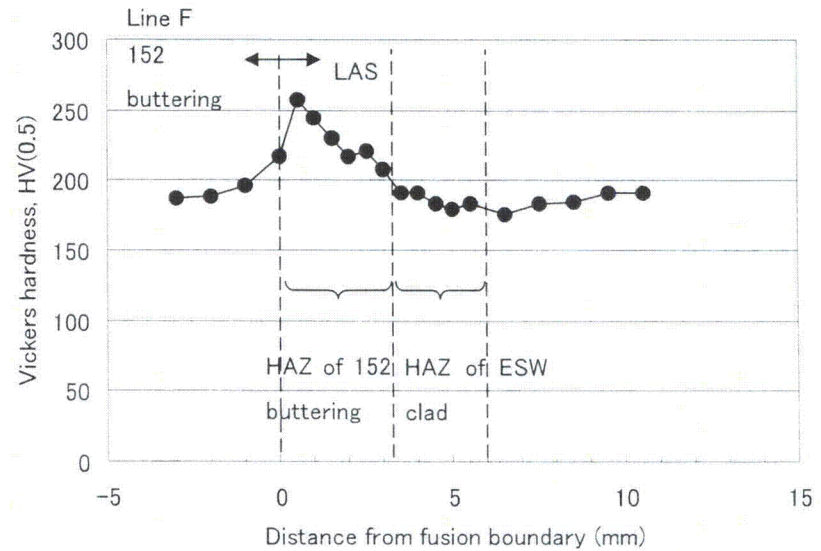
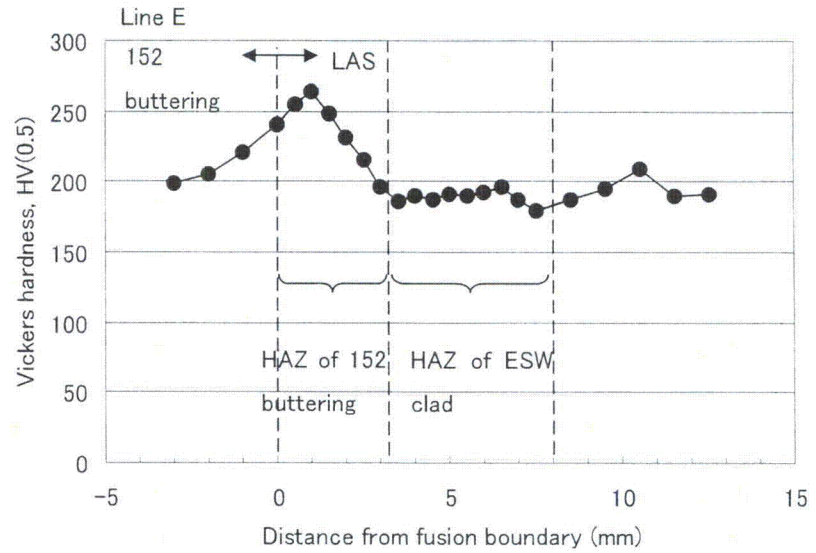
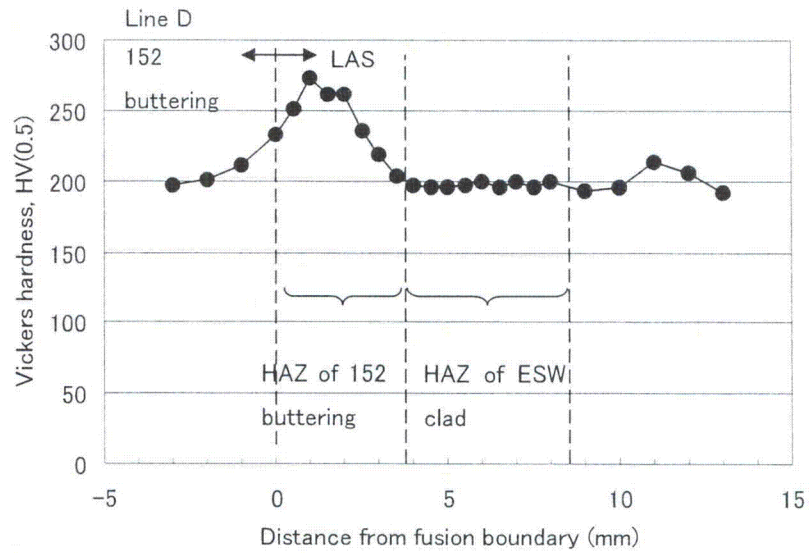


Figure A. 54(2) Vickers hardness of cross section of I type mockup 3-2



Attachment-B

I-Type Tensile Test



1. Purpose

The main purpose of this test is to confirm whether the small mockup tensile test (I type model) can reproduce the fracture at fusion boundary of weld which occurred in Unit 3. The secondary purpose is to examine the difference between gouging and machining on the fracture at fusion boundary.

2. Outline of test

The mockups (I type model) were fabricated, simulating the fractured weld between LAS and alloy 152. Two types of methods to remove stainless steel cladding were employed. One was gouging which was applied for Unit 3 and the other was machining which was applied for Unit 2.

Smooth and notched tensile specimens were machined from these mockups and tensile tests at room temperature in air and fracture surface observations were conducted.

3. Test method

3.1 Mockup (I type model)

The fabrication flow chart of mockup (I type model) is shown in Fig. B.1. The manufacturing procedure for the actual SG was reproduced including heat treatment and inspection. To examine metallurgical feature of mockup at intermediate stage of fabrication, test sample was machined from the mockup and metallurgical examination was conducted. To confirm the gouging effect, gouging was applied to the surface of mockup without stainless steel cladding and metallurgical examination of it was conducted.

The configuration of mockups is shown in Fig. B.2.

3.2 Tensile specimen

Three types of tensile specimens were tested. One was typical smooth specimen and the other two were notched specimens which radius of notch root was 2mm and 4mm (See Fig. B.3). The notched specimens were applied to examine the effects of constraint on fracture mode because there is three-dimensional constraint around fracture location in the actual SG.

The specimens were machined from mockups to make the longitudinal direction of specimens same as the height direction of mockups. The fusion boundary of weld was set at the center of smooth specimen or the root of notched specimen.



3.3 Tensile test

Tensile tests were conducted in room temperature air with 10tonf(98kN) universal test machine. The test procedure was according to JIS Z 2241(98).

4. Test results

4.1 Tensile test

The results of all tensile tests are shown in Table B.1 and Photographs of specimen and fracture surface were shown in Fig. B.4 and B.5.

As shown in Fig.B.4, all smooth specimens were broken at 152 buttering or welding portions and did not fracture at the boundary between LAS and 152 buttering. As shown in Fig.B.5, all notched specimens were broken at the notch but all fractured surfaces shows ductile feature and brittle fracture surface which was observed in the actual SG was not reproduced.

No difference between gouging and machining on the tensile strength was observed.

4.2 Metallurgical examination

The results of metallurgical examination (macro structure, micro structure, hardness measurement and surface etching) on mockups are summarized in Attachment C.

The following results were obtained.

- (1) Metallurgical structure observed near the fusion boundary of the mockup to which gouging was applied was similar to that observed near the fusion boundary of Unit 3, but were found to have a smaller grain size than the as-built (boat/strip) samples. It is considered that this was because grain refining occurred in the I-Type samples under the heat input during application of the second layer of the butter, because the distance between the butter/base metal fusion boundary and the second layer of the butter was smaller on the I-Type samples than on the actual RSGs.
- (2) Hardness near the fusion boundary of the mockup to which gouging was applied was lower than that measured in Unit 3, but it is estimated that this difference can be due to scattering.
- (3) It is estimated that there is no difference of metallurgical structure and hardness near the fusion boundary between the mockup gouged and the one machined.



5. Summary

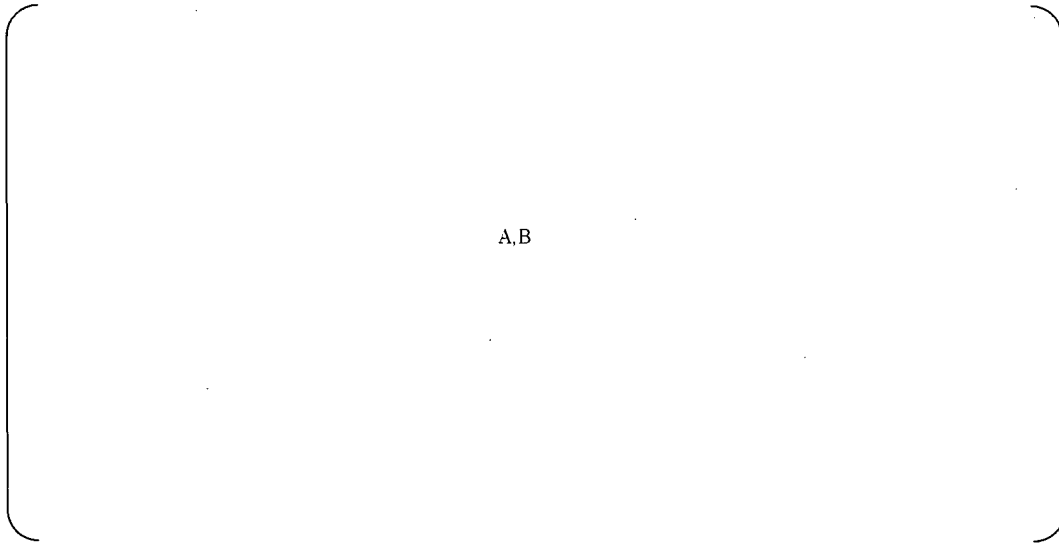
The small mockup tensile test (I type model) did not reproduce the fracture at fusion boundary of weld which occurred in Unit 3.

Metallurgical feature near the fusion boundary of the fabricated mockup was similar to that observed near the fusion boundary of Unit 3.



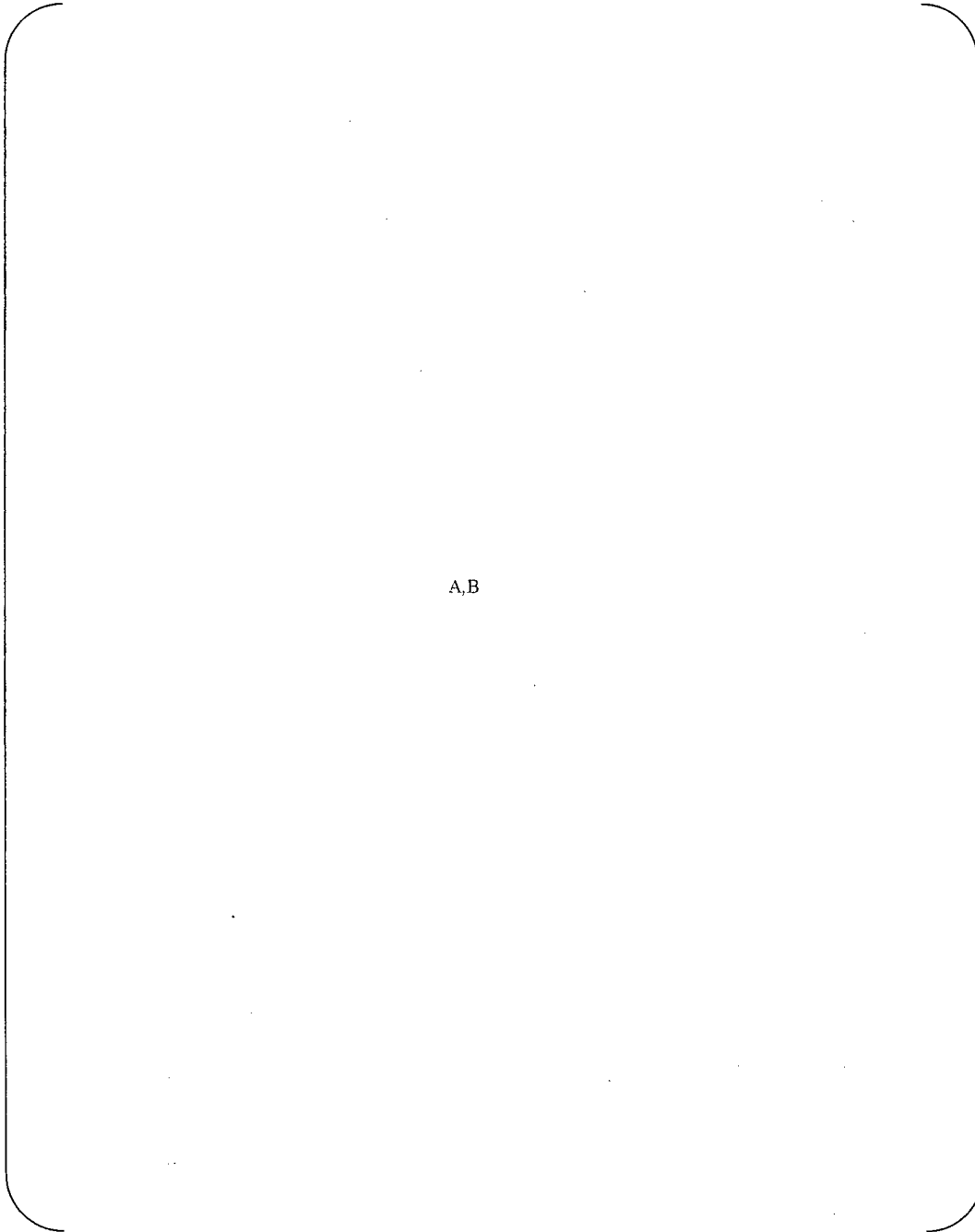
A,B

Fig. B.1 Flow chart of manufacturing I type mockup



A,B

Fig. B.2 Appearance of I type mockup



A,B

Fig.B.3 Tensile test specimen



Table B.1 Result of Tension Test

A,B

Spec	Test.No	Specimen Type					
Effect of gouging (Simulating U3)	②-2-1	R2 notched					
	②-2-2						
	②-2-3						
	②-2-4	R4 notched					
	②-2-5						
	②-2-6						
	②-2-11	Smooth					
	②-2-12						
Effect of machining (Simulating U2)	③-2-1	R2 notched					
	③-2-2						
	③-2-3						
	③-2-4	R4 notched					
	③-2-5						
	③-2-6						
	③-2-11	Smooth					

A,B



Spec	Test.No	Specimen Type	Appearance
Effect of gouging	②-2-11	JIS 4	
	②-2-12		
Effect of machining	③-2-11	JIS 4	
	③-2-12		

Fig.B.4 Photograph of smooth specimen after test (Sample ③-2)



A,B

Fig.B.5-1 Photograph of fracture surface (Sample ②-2)



A,B

Fig.B.5-2 Photograph of fracture surface (Sample ②-2)



A,B

Fig.B.5-3 Photograph of fracture surface (Sample ③-2)



A,B

Fig.B.5-4 Photograph of fracture surface (Sample ③-2)



Attachment-C

I-Type Metallurgical Examination



1. Sample ①-1

(1) Purpose

To examine the metallurgical structure and hardness in heat affected zone of low alloy steel after electrosag welding.

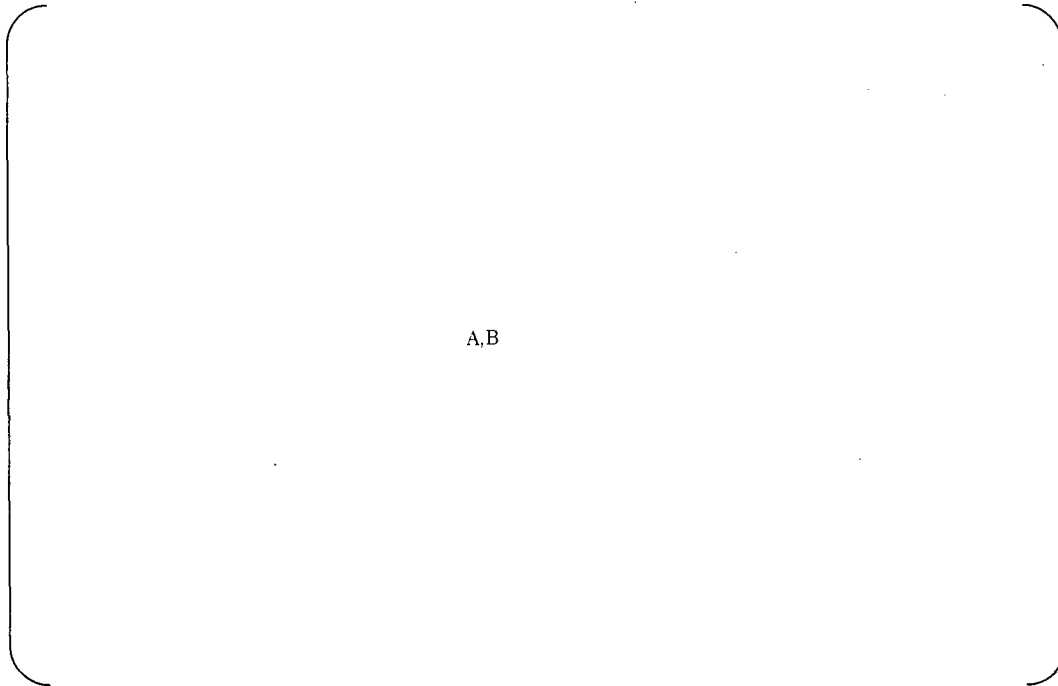
	Fabrication process			Tensile test
	electrosag welding	Gouging + grinding	Machining	
Effect of gouging (Simulating U3)	①-1 Macro-structure Micro-structure Hardness	②-1 Macro-structure Micro-structure Hardness Surface etching	-	②-2 Macro-structure Micro-structure Hardness Tensile test
Effect of removal of HAZ by gouging		④-1、④-2 Macro-structure Micro-structure Hardness	-	-
Effect of machining (Simulating U2)		-	③-1 Macro-structure Micro-structure Hardness Surface etching	③-2 Macro-structure Micro-structure Hardness Tensile test

(2)Results

Macro-structure observation: The maximum depth of heat affected zone by electrosag welding is{ A,B } as shown in Fig.C.1.

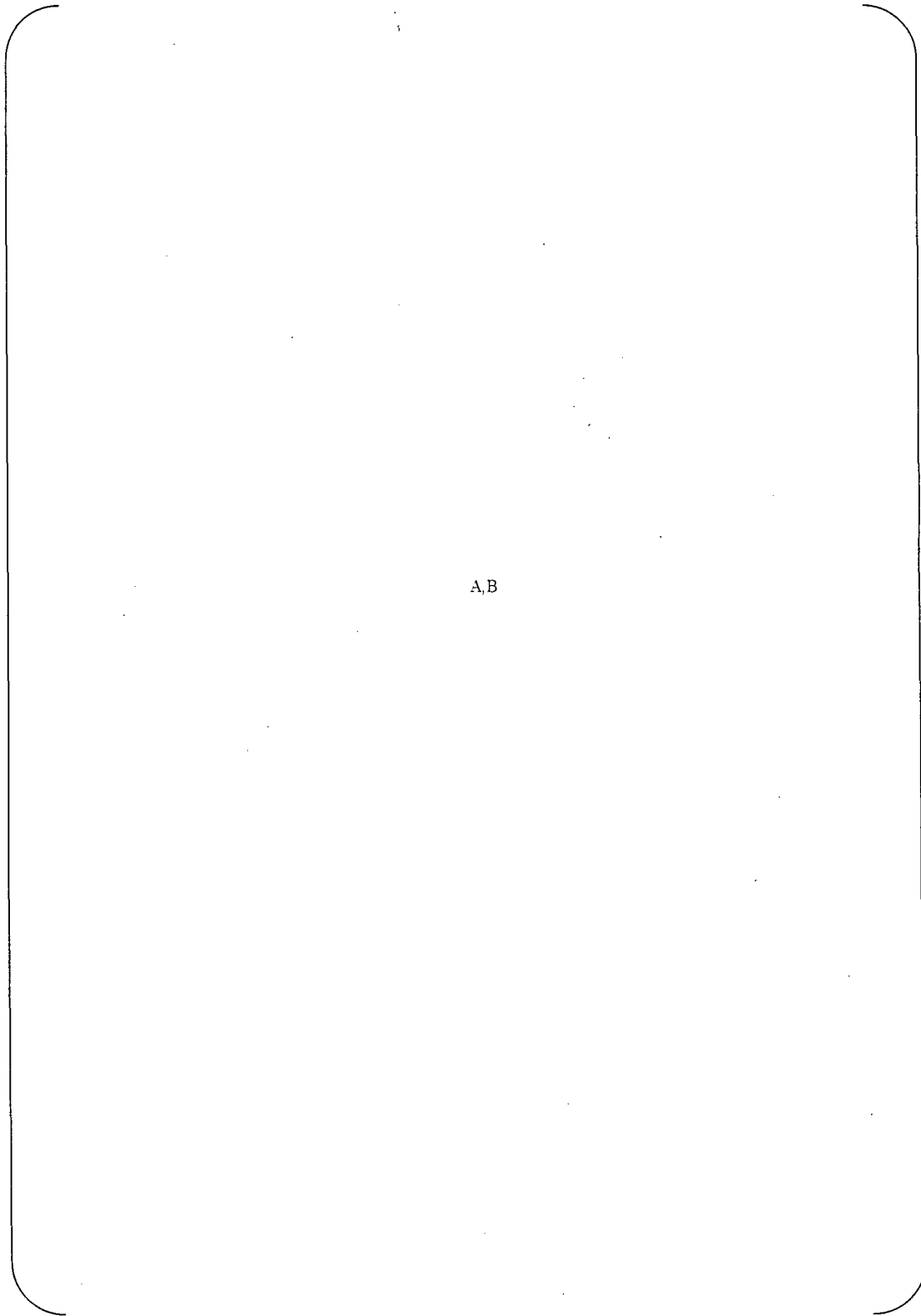
Micro-structure observation: The colored zone with width of { A,B } is observed in fusion boundary between stainless steel clad and LAS as shown in Fig.C.2.

Hardness measurement: The hardness of stainless steel clad is about HV(0.5){A,B}as shown in Fig.C.3. The hardness of heat affected LAS is HV(0.5){ A,B }and hardness of colored zone along fusion line is high and HV(0.002){ A,B }.



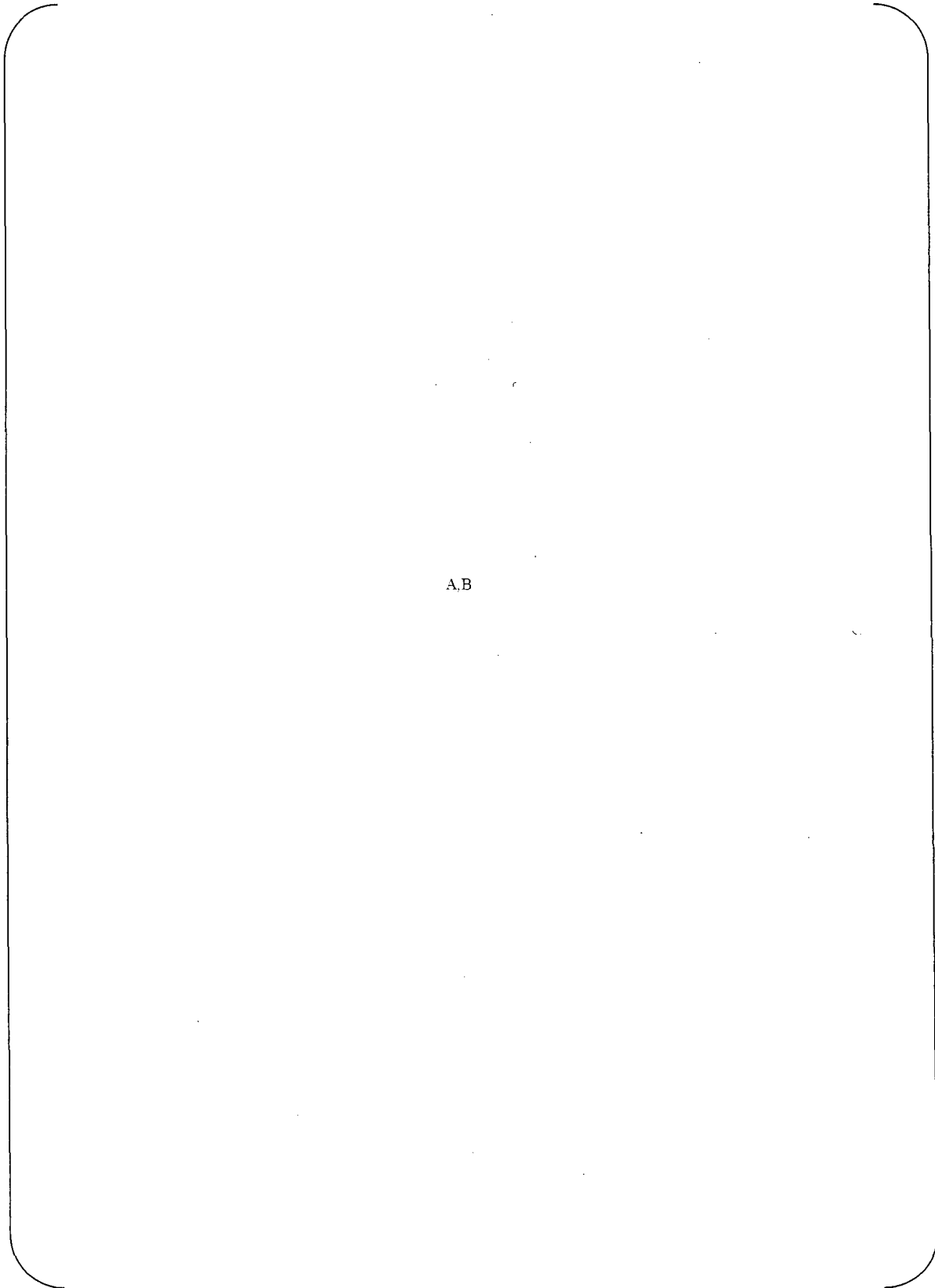
A,B

Fig.C.1 Macro-structure observation



A,B

Fig.C.2 Micro-structure observation



A,B

Fig. C.3 Result of Vickers hardness measurement



2. Sample ②-1

(1) Purpose

To examine the metallurgical structure and hardness of low alloy steel after removing electrosag welding by gouging and grinding the surface

	Fabrication process			Tensile test
	electrosag welding	Gouging + grinding	Machining	
Effect of gouging (Simulating U3)	①-1 Macro-structure Micro-structure Hardness	②-1 Macro-structure Micro-structure Hardness Surface etching	-	②-2 Macro-structure Micro-structure Hardness Tensile test
Effect of removal of HAZ by gouging		④-1、④-2 Macro-structure Micro-structure Hardness	-	-
Effect of machining (Simulating U2)		-	③-1 Macro-structure Micro-structure Hardness Surface etching	③-2 Macro-structure Micro-structure Hardness Tensile test

(2) Results

Macro-structure observation: The partial heat affected zones by gouging are observed as shown in Fig.C.4.

Surface etching: Some circular heat affected zones by gouging are observed as shown in Fig.C.5.

Micro-structure observation: The partial heat affected zones by gouging are observed as shown in Fig.C.6. The size of one is { A,B } of width, { A,B } of depth and that of the other is { A,B } of width, { A,B } of depth.

Hardness measurement: The hardness of heat affected zones by gouging is about HV(0.5){A,B} as shown in Fig.C.7. The hardness of LAS at the location 4mm from heat affected zone by gouging is HV(0.5){A,B}. The cause of hardening in heat affected zones by gouging is estimated by the effect of gouging and the effect of cold working by grinding. (Detail estimations are described later in sec. of ④-1.)

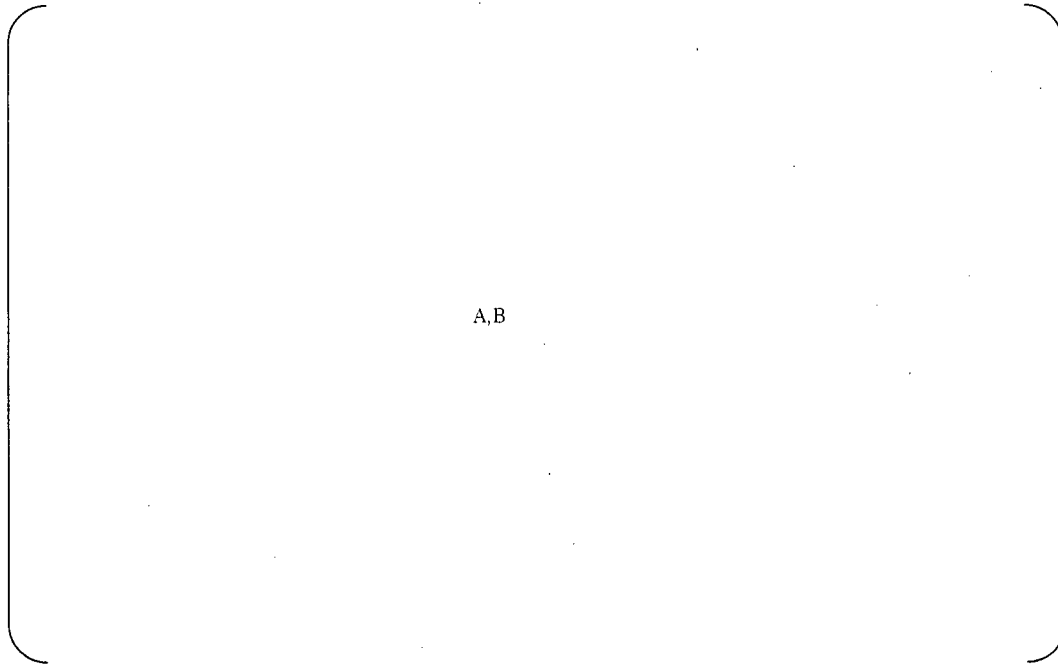


Fig.C.4 Macro-structure observation

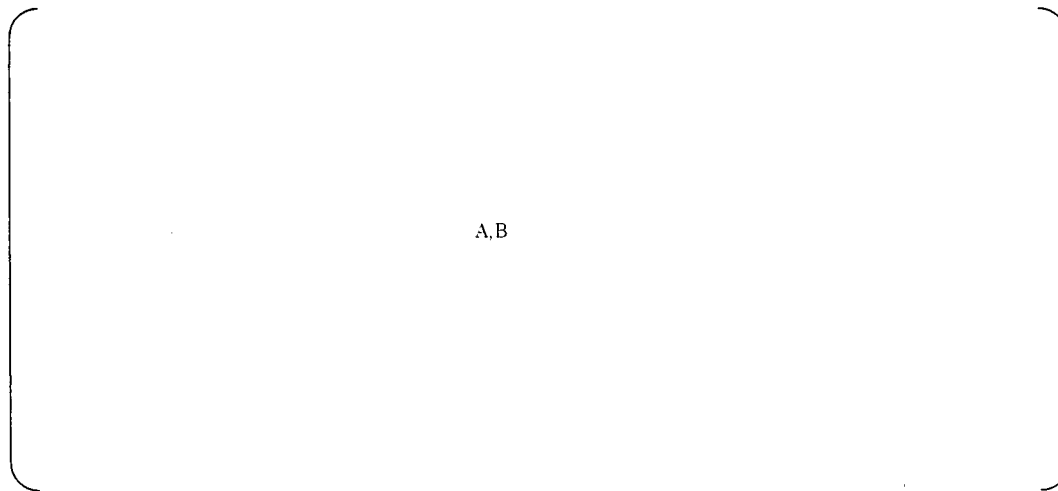
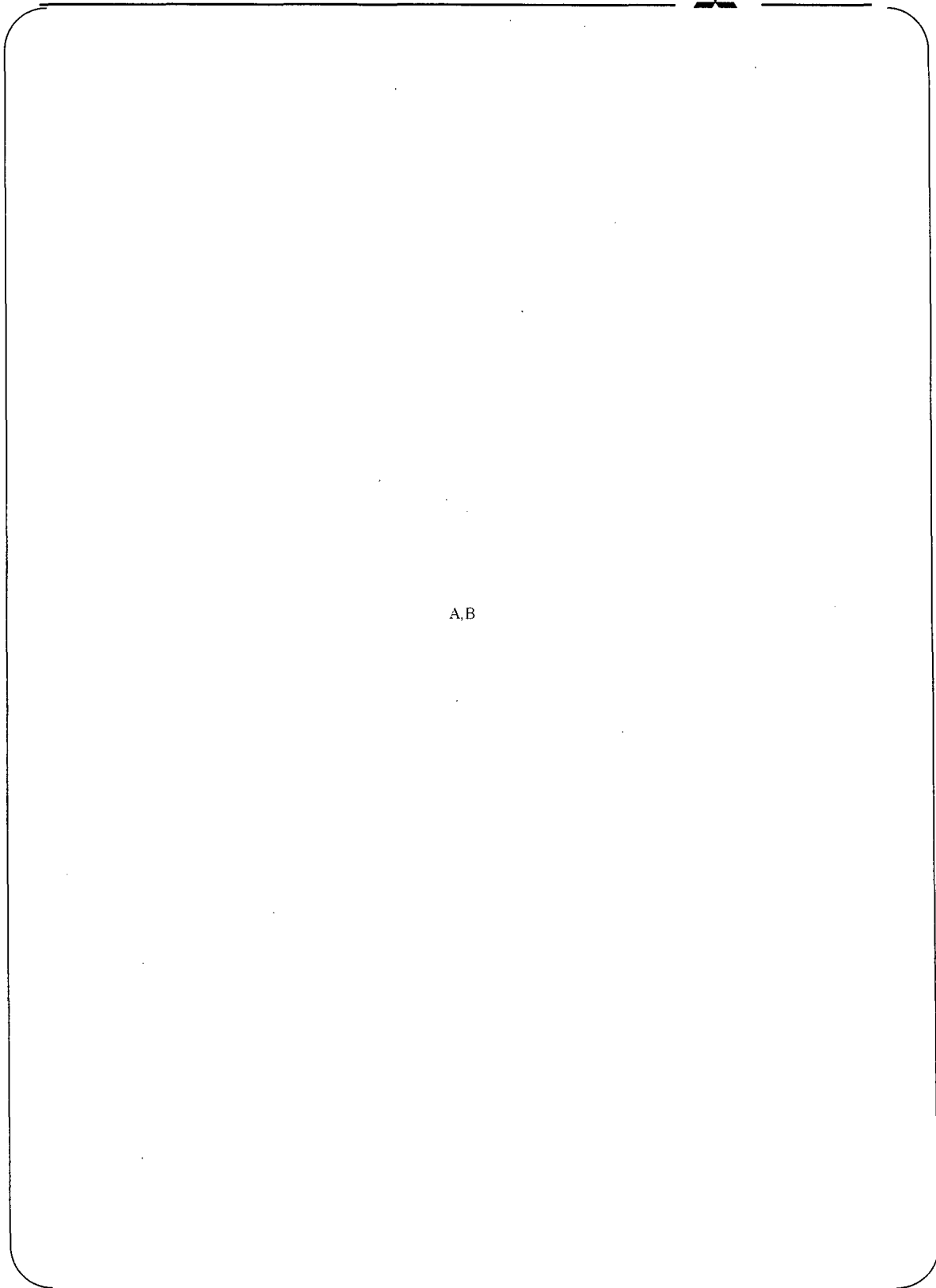


Fig.C.5 Surface observation after etching



A,B

Fig.C.6(1) Micro-structure observation



A,B

Fig.C.6(2) Micro-structure observation



A,B

Fig. C.7 Result of Vickers hardness measurement



3. Sample ③-1

(1) Purpose

To examine the metallurgical structure and hardness of low alloy steel after removing electroslag welding by machining

	Fabrication process			Tensile test
	electroslag welding	Gouging + grinding	Machining	
Effect of gouging (Simulating U3)	①-1 Macro-structure Micro-structure Hardness	②-1 Macro-structure Micro-structure Hardness Surface etching	-	②-2 Macro-structure Micro-structure Hardness Tensile test
Effect of removal of HAZ by gouging		④-1、④-2 Macro-structure Micro-structure Hardness	-	-
Effect of machining (Simulating U2)		-	③-1 Macro-structure Micro-structure Hardness Surface etching	③-2 Macro-structure Micro-structure Hardness Tensile test

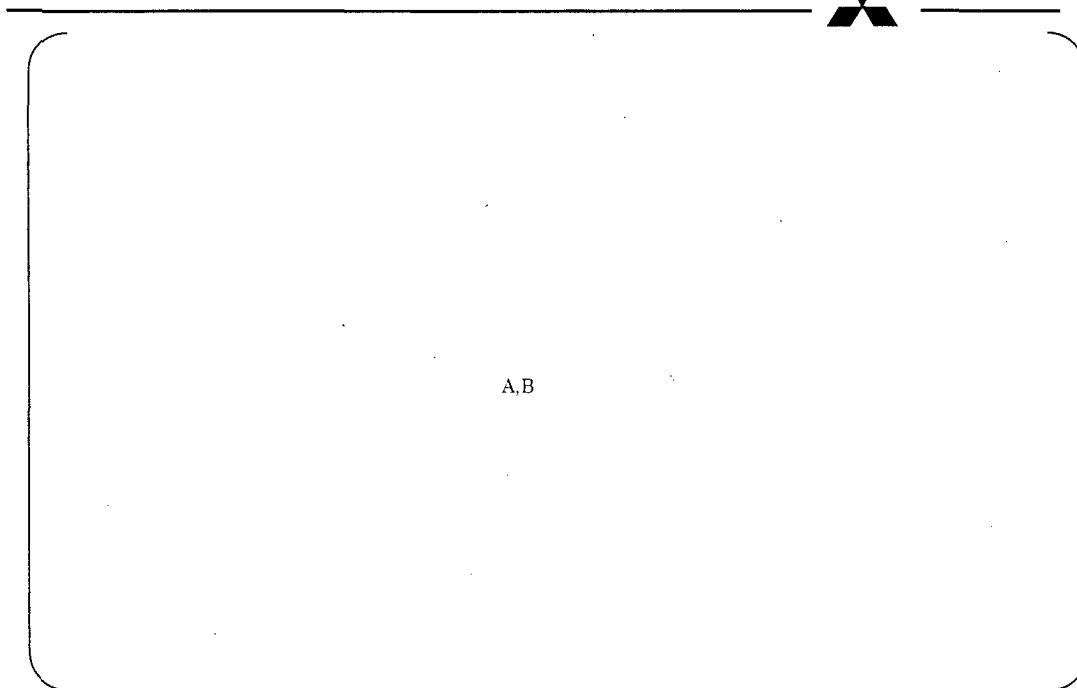
(2)Results

Macro-structure observation: Heat affected zone by machining or stainless clad is not observed as shown in Fig.C.8.

Surface etching: Heat affected zone by machining or stainless clad is not observed as shown in Fig.C.9.

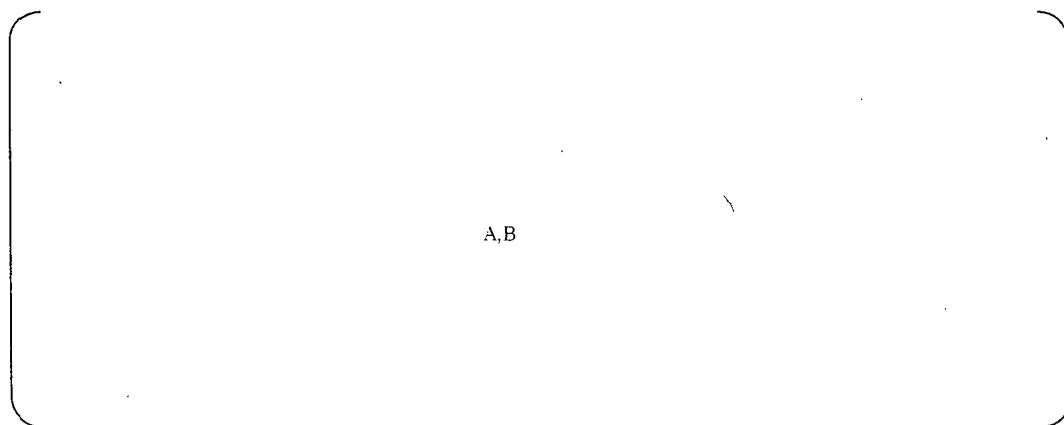
Micro-structure observation: Heat affected zone by machining or stainless clad is not observed as shown in Fig.C.10.

Hardness measurement: The hardness of LAS near the machined surface is about HV(0.5)[A,B] while at the location 2mm from the surface is HV(0.5)[A,B] as shown in Fig.C.11. The hardening near the machined surface is assumed to be produced by electroslag welding. The hardened zone of about HV(0.002)[A,B] is observed very near the machined surface and this hardening is assumed to be produced by electroslag welding and machining.



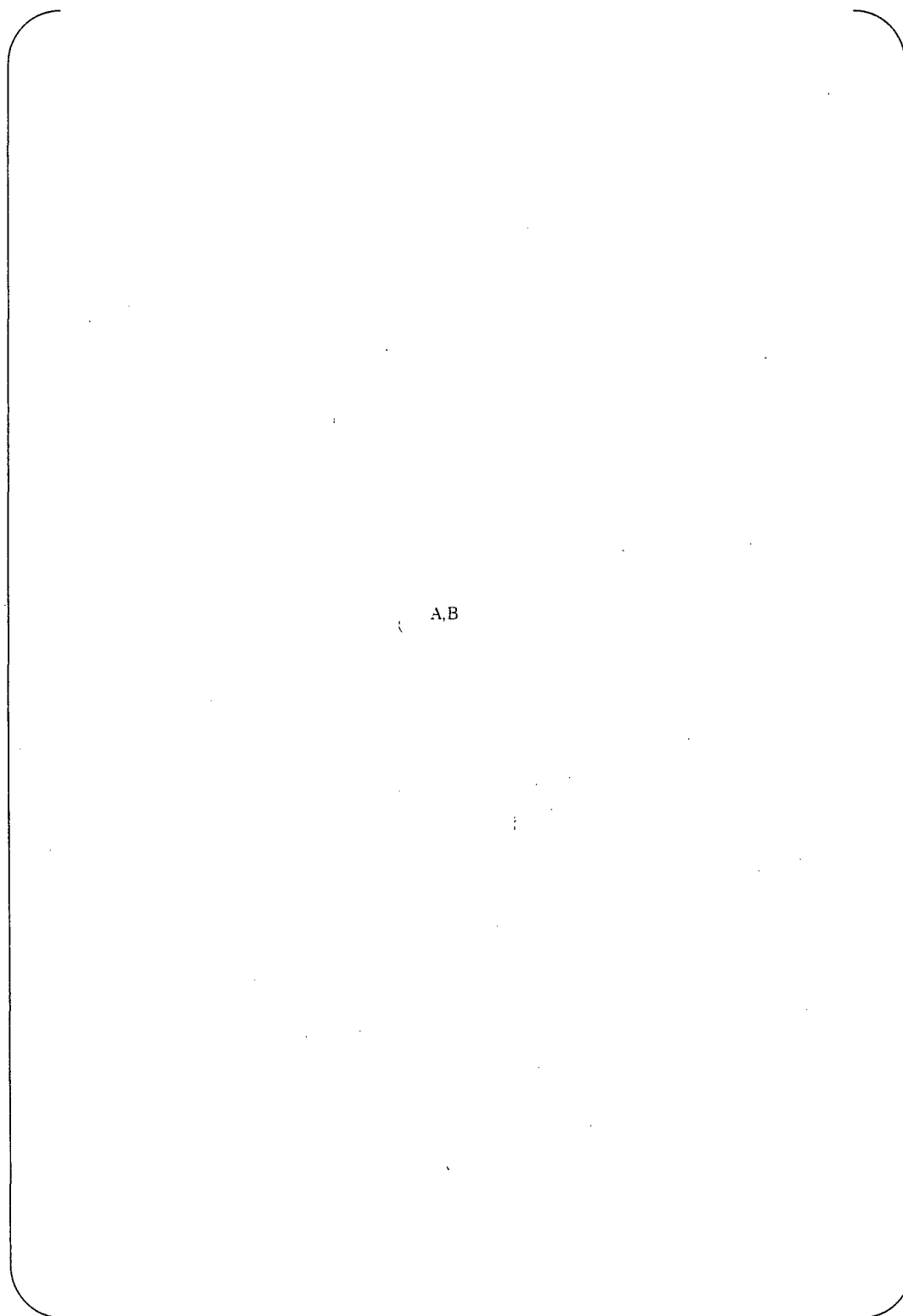
A,B

Fig.C.8 Macro-structure observation



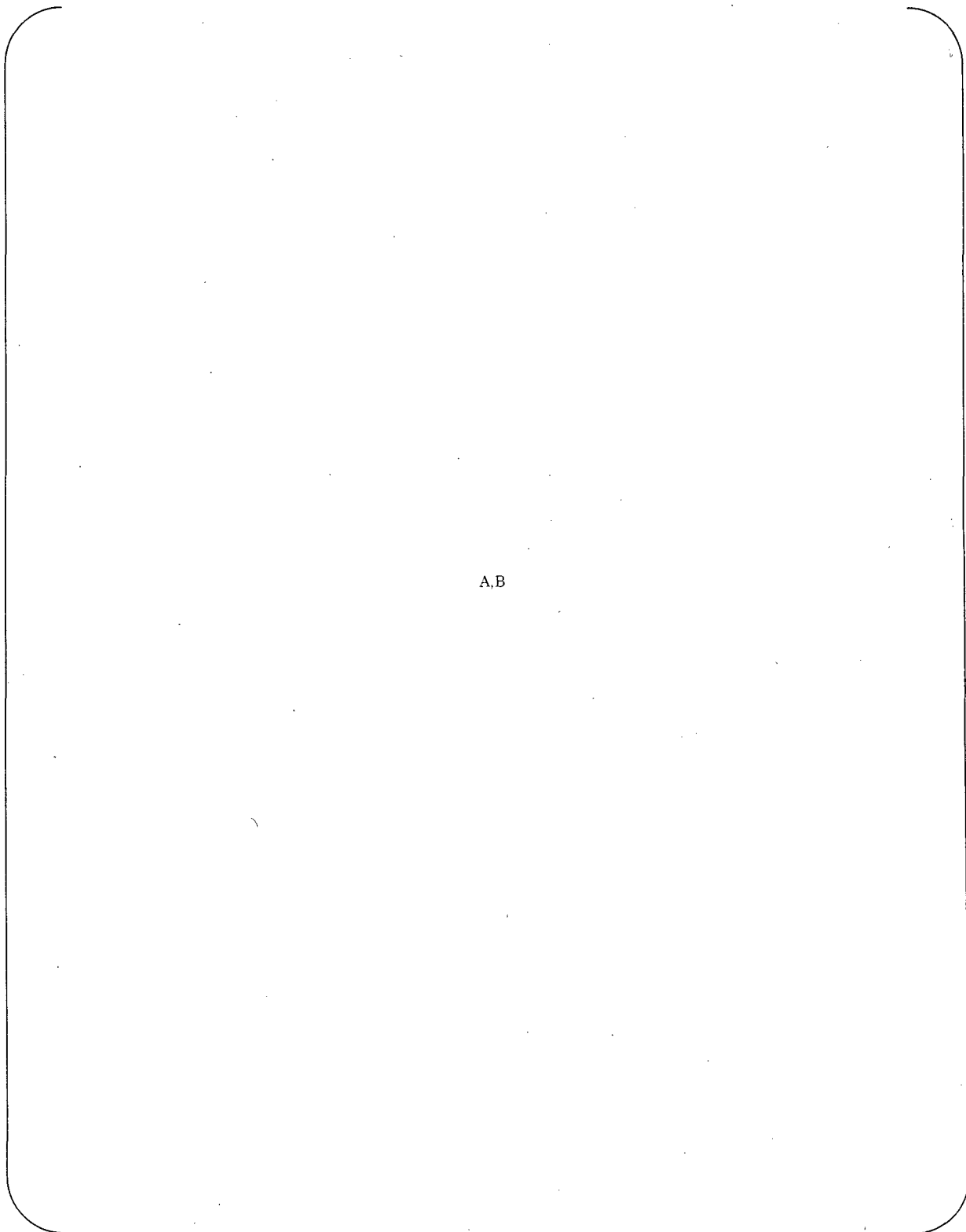
A,B

Fig.C.9 Surface observation after etching



A,B

Fig.C.10 Micro-structure observation



A,B

Fig. C.11 Result of Vickers hardness measurement



4. Sample ④-1

(1) Purpose

To examine the metallurgical structure and hardness of low alloy steel just after gouging

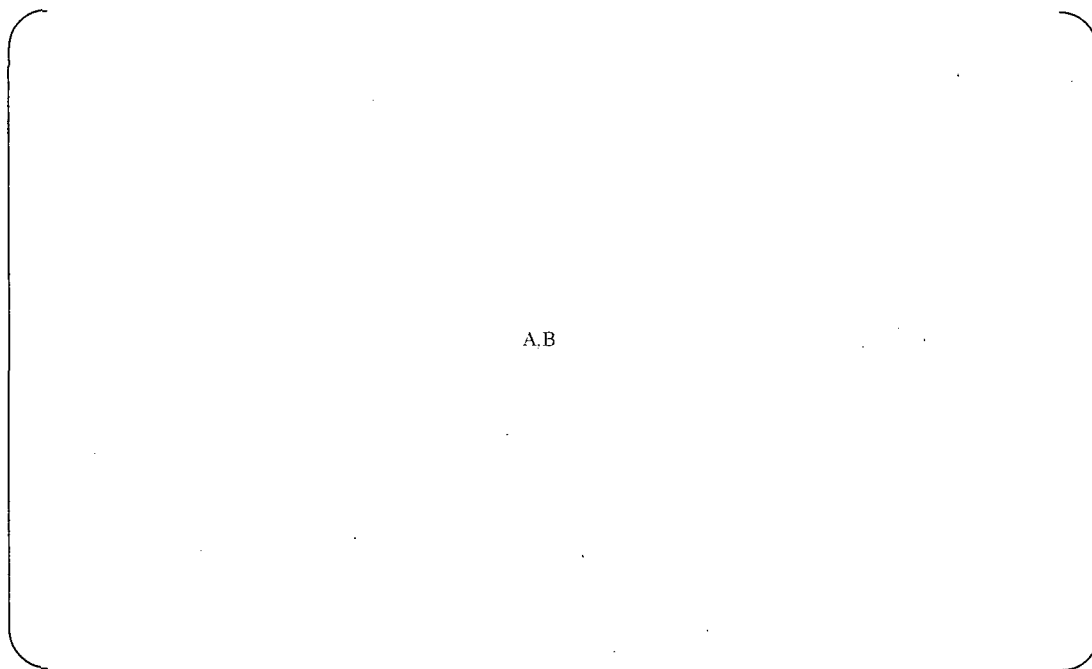
	Fabrication process			Tensile test
	electroslag welding	Gouging + grinding	Machining	
Effect of gouging (Simulating U3)	①-1 Macro-structure Micro-structure Hardness	②-1 Macro-structure Micro-structure Hardness Surface etching	-	②-2 Macro-structure Micro-structure Hardness Tensile test
Effect of removal of HAZ by gouging		④-1、④-2 Macro-structure Micro-structure Hardness	-	-
Effect of machining (Simulating U2)		-	③-1 Macro-structure Micro-structure Hardness Surface etching	③-2 Macro-structure Micro-structure Hardness Tensile test

(2) Results

Macro-structure observation: The maximum [A,B]thick heat affected zones by gouging are observed as shown in Fig.C.12.

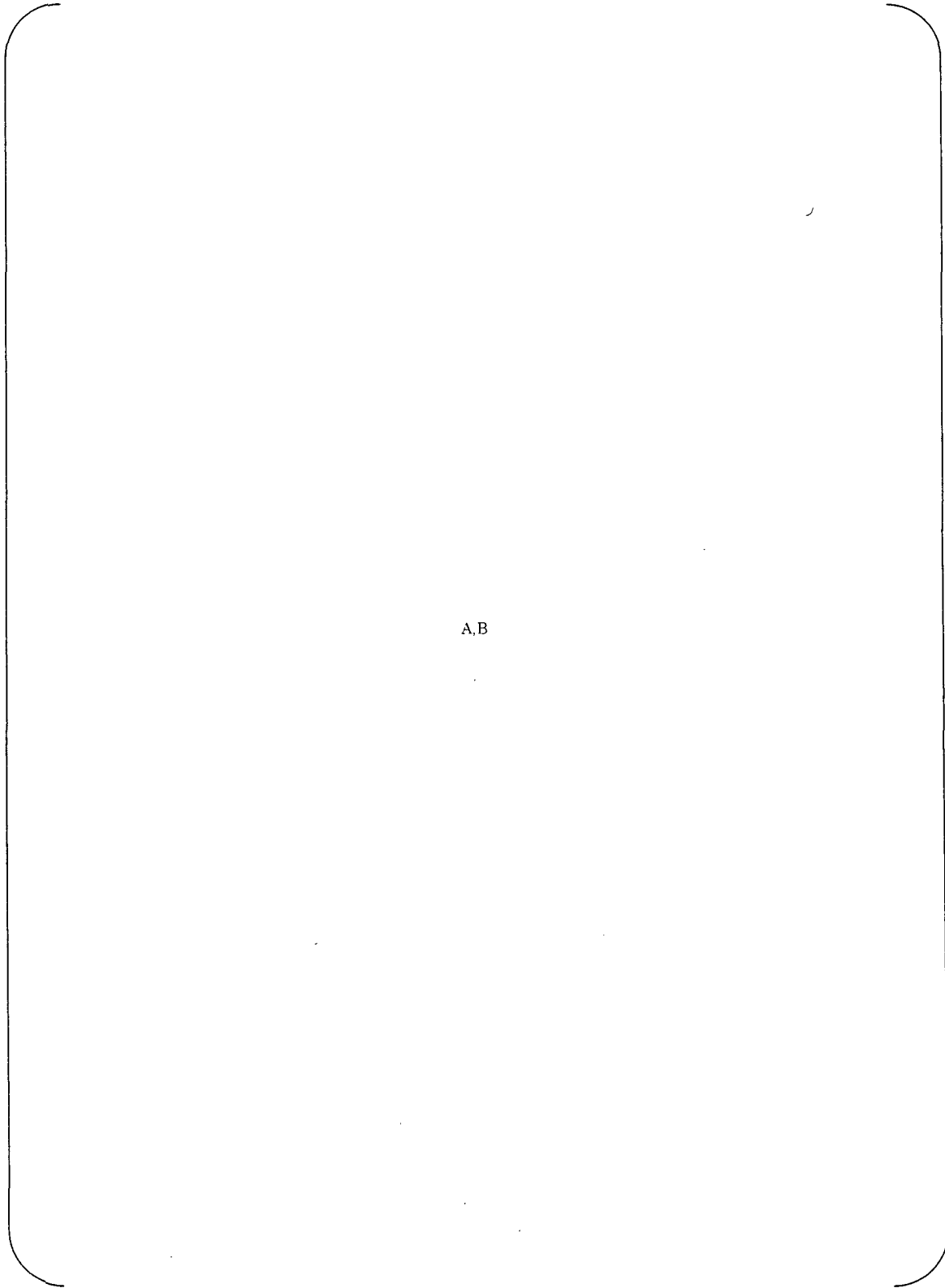
Micro-structure observation: The heat affected zones by gouging and black deposit near surface are observed as shown in Fig.C.13. The deposit is estimated to be a layer of carbon which is main composition of arc welding electrode.

Hardness measurement: The hardness of heat affected zones by gouging is about HV(0.5)[A,B] as shown in Fig.C.14. The hardness with light load of 0.002g is also same value. This hardness of LAS is lower than HV(0.5)[A,B] in heat affected zone in Fig.C.7. The cause of hardening in heat affected zones by gouging in Fig.C.7 is estimated by the effect of gouging and the effect of cold working by grinding.



A.B

Fig.C.12 Macro-structure observation



A,B

Fig.C.13 Micro-structure observation



A,B

Fig. C.14 Result of Vickers hardness measurement



5. Sample ④-2

(1) Purpose

To examine the metallurgical structure and hardness of low alloy steel after gouging and final stress relief heat treatment (595±30°C 5 hours)

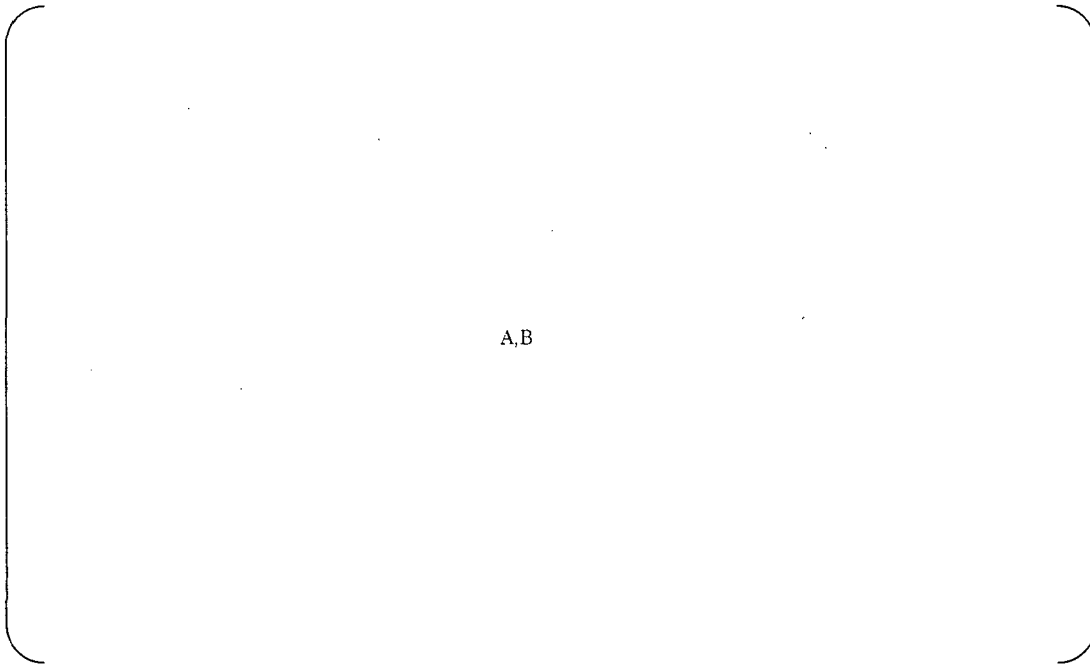
	Fabrication process			Tensile test
	electroslag welding	Gouging + grinding	Machining	
Effect of gouging (Simulating U3)	①-1 Macro-structure Micro-structure Hardness	②-1 Macro-structure Micro-structure Hardness Surface etching	-	②-2 Macro-structure Micro-structure Hardness Tensile test
Effect of removal of HAZ by gouging		④-1、④-2 Macro-structure Micro-structure Hardness	-	-
Effect of machining (Simulating U2)		-	③-1 Macro-structure Micro-structure Hardness Surface etching	③-2 Macro-structure Micro-structure Hardness Tensile test

(2) Results

Macro-structure observation: The maximum [A,B] thick heat affected zones by gouging are observed as shown in Fig.C.15.

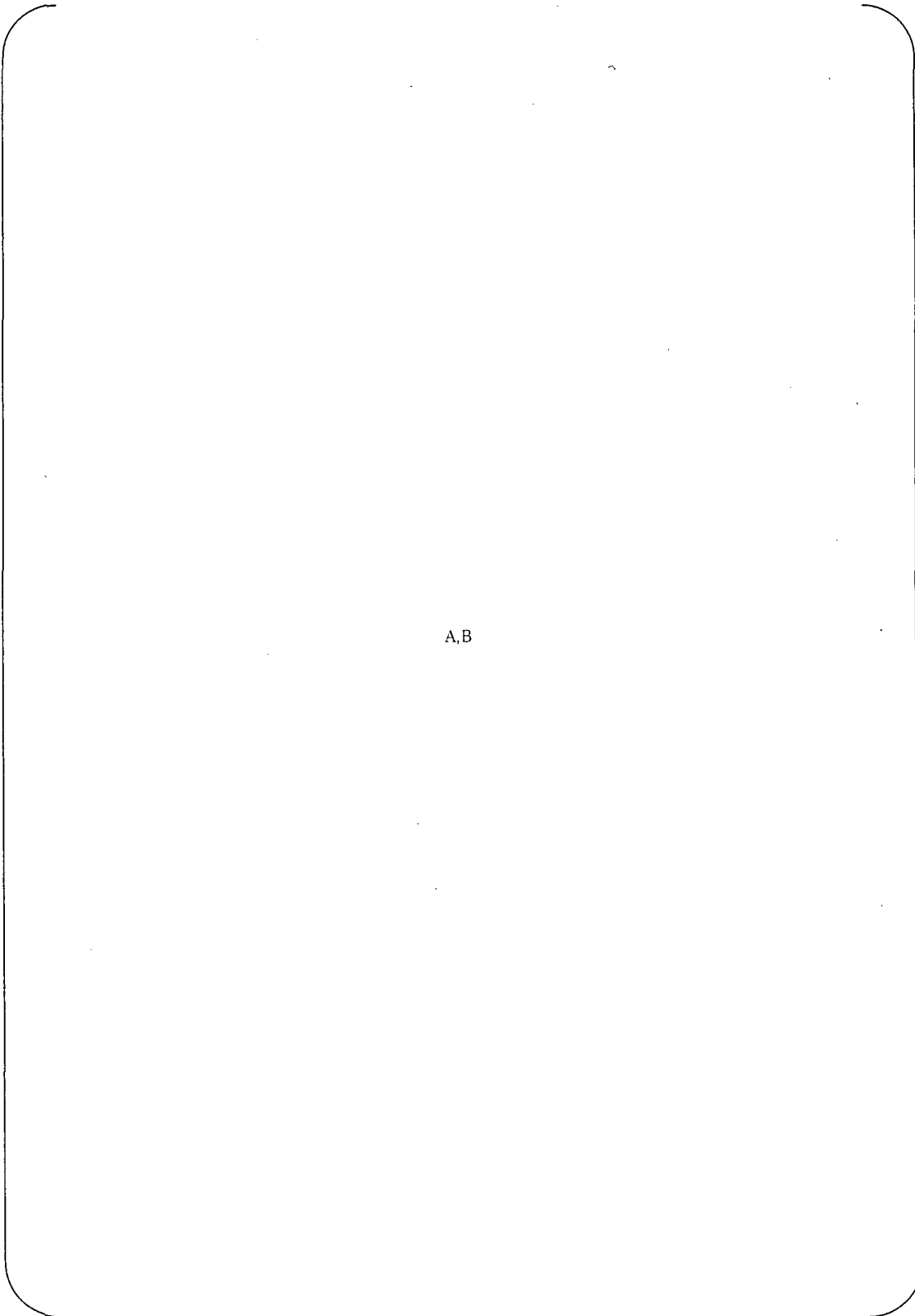
Micro-structure observation: The heat affected zones by gouging and black deposit near surface are observed as shown in Fig.C.16.

Hardness measurement: The hardness of heat affected zones by gouging is about HV(0.5)(A,B) as shown in Fig.C.17. The hardness with light load of 0.002g is also same value. Compared with Fig.C.14 and Fig.C.17, the hardness in heat affected zones by gouging is decreased about 50 by final stress relief heat treatment.



A,B

Fig.C.15 Macro-structure observation



A,B

Fig.C.16 Micro-structure observation



A.B

Fig. C.17 Result of Vickers hardness measurement



6. Sample ②-2

(1) Purpose

To examine the metallurgical structure and hardness near fusion boundary between 152 buttering and LAS of mockup test specimen

	Fabrication process			Tensile test
	electroslag welding	Gouging + grinding	Machining	
Effect of gouging (Simulating U3)	①-1 Macro-structure Micro-structure Hardness	②-1 Macro-structure Micro-structure Hardness Surface etching	-	②-2 Macro-structure Micro-structure Hardness (Tensile test)
Effect of removal of HAZ by gouging		④-1、④-2 Macro-structure Micro-structure Hardness	-	-
Effect of machining (Simulating U2)		-	③-1 Macro-structure Micro-structure Hardness Surface etching	③-2 Macro-structure Micro-structure Hardness (Tensile test)

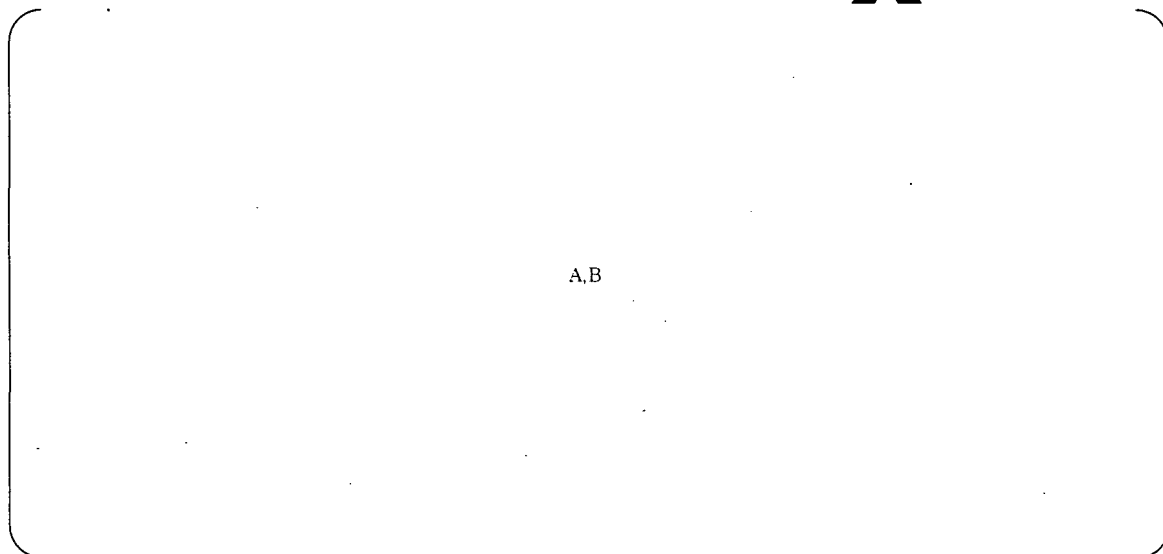
(2) Results

Macro-structure observation: The [A,B] depth heat affected zones by 152 buttering in LAS is observed as shown in Fig.C.18. The clear trace of heat affected zone by gouging can not be confirmed.

Micro-structure observation: The white zone is observed near fusion boundary as shown in Fig.C.19.

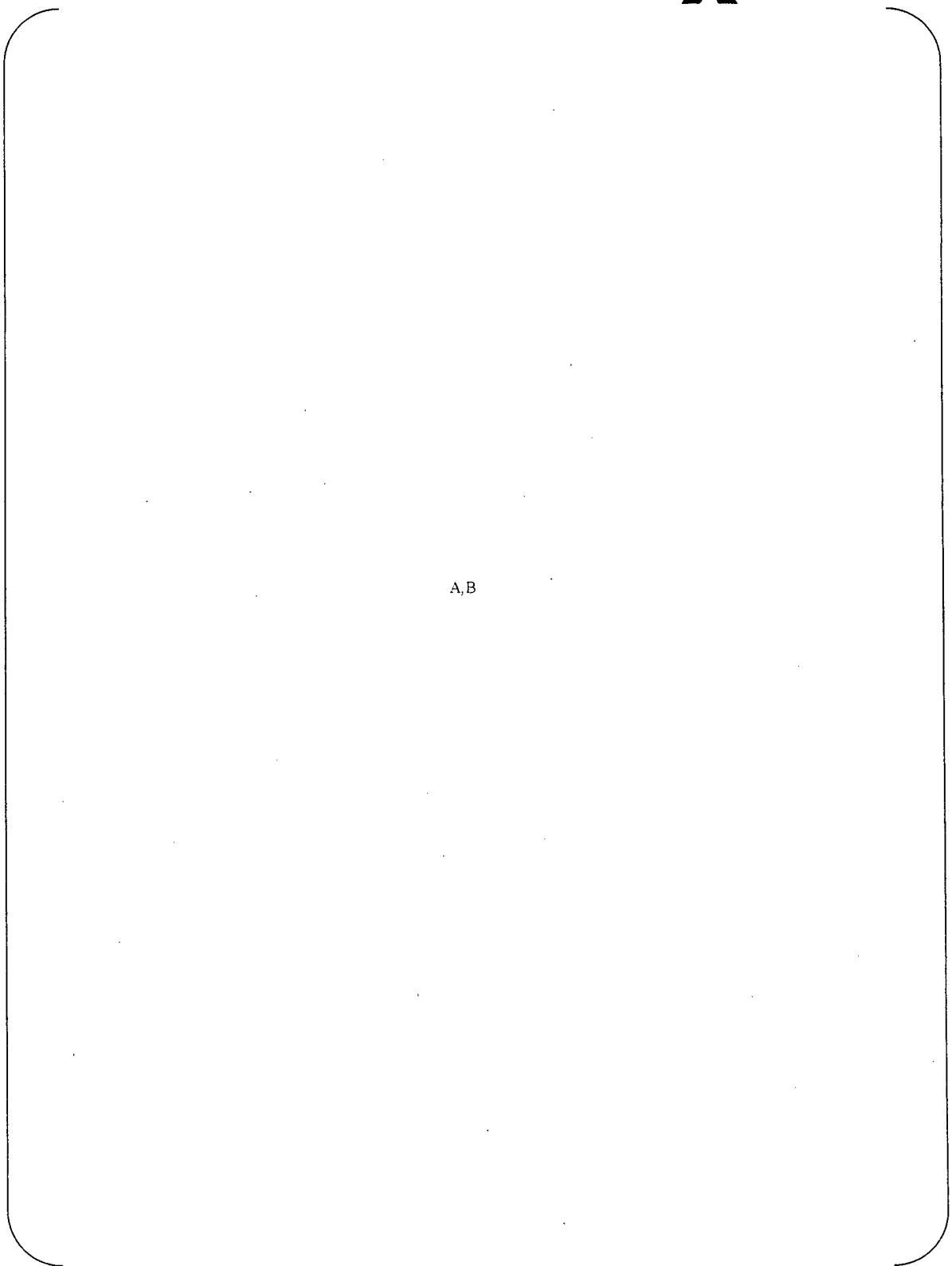
Hardness measurement: The hardness of 152 buttering is about HV(0.5)[A,B] as shown in Fig.C.20(1). The hardness of LAS near fusion boundary is about HV (0.5) [A,B] and that at the location 2mm from the fusion boundary is HV(0.5)[A,B].

The hardness of 152 buttering very near fusion boundary is from HV(0.002){ A,B }
The hardness of LAS very near fusion boundary is from HV(0.002){ A,B }, but the hardness of colored zone very near fusion boundary is from HV(0.002){ A,B } in Fig.C.20 (2). There is large scattering of hardness very near fusion boundary.



A,B

Fig.C.18 Macro-structure observation



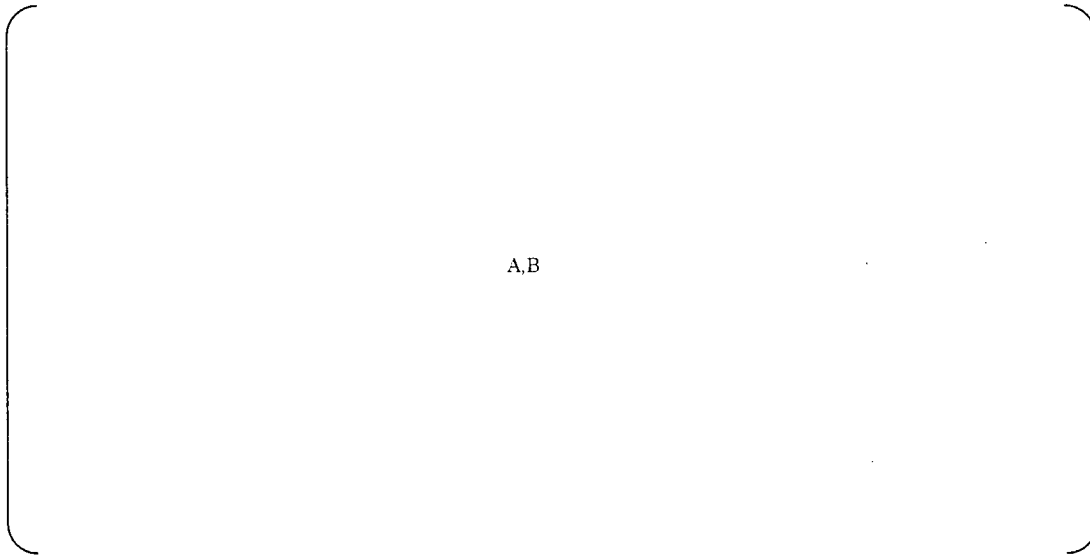
A,B

Fig.C.19 Micro-structure observation



A,B

Fig. C.20(1) Result of Vickers hardness measurement



A,B

Fig. C.20(2) Result of Vickers hardness measurement



7. Sample ③-2

(1) Purpose

To examine the metallurgical structure and hardness near fusion boundary between 152 buttering and LAS of mockup test specimen

	Fabrication process			Tensile test
	electroslag welding	Gouging + grinding	Machining	
Effect of gouging (Simulating U3)	①-1 Macro-structure Micro-structure Hardness	②-1 Macro-structure Micro-structure Hardness Surface etching	-	②-2 Macro-structure Micro-structure Hardness (Tensile test)
Effect of removal of HAZ by gouging		④-1、④-2 Macro-structure Micro-structure Hardness	-	-
Effect of machining (Simulating U2)		-	③-1 Macro-structure Micro-structure Hardness Surface etching	③-2 Macro-structure Micro-structure Hardness (Tensile test)

(2) Results

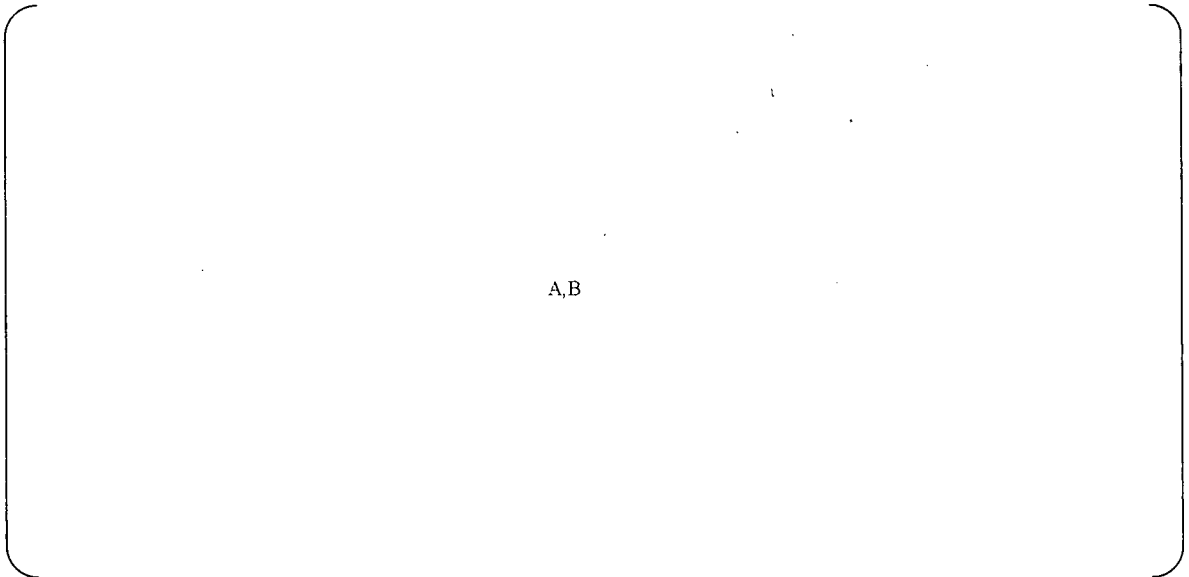
Macro-structure observation: The heat affected zones by 152 buttering in LAS is observed as shown in Fig.C.21.

Micro-structure observation: The white zone is observed near fusion boundary as shown in Fig.C.22.

Hardness measurement: The hardness of 152 buttering is about HV(0.5){A,B} as shown in Fig.C.23. The hardness of LAS near fusion boundary is about HV (0.5) {A,B} and that at the location 3mm from the fusion boundary is HV(0.5){A,B}.

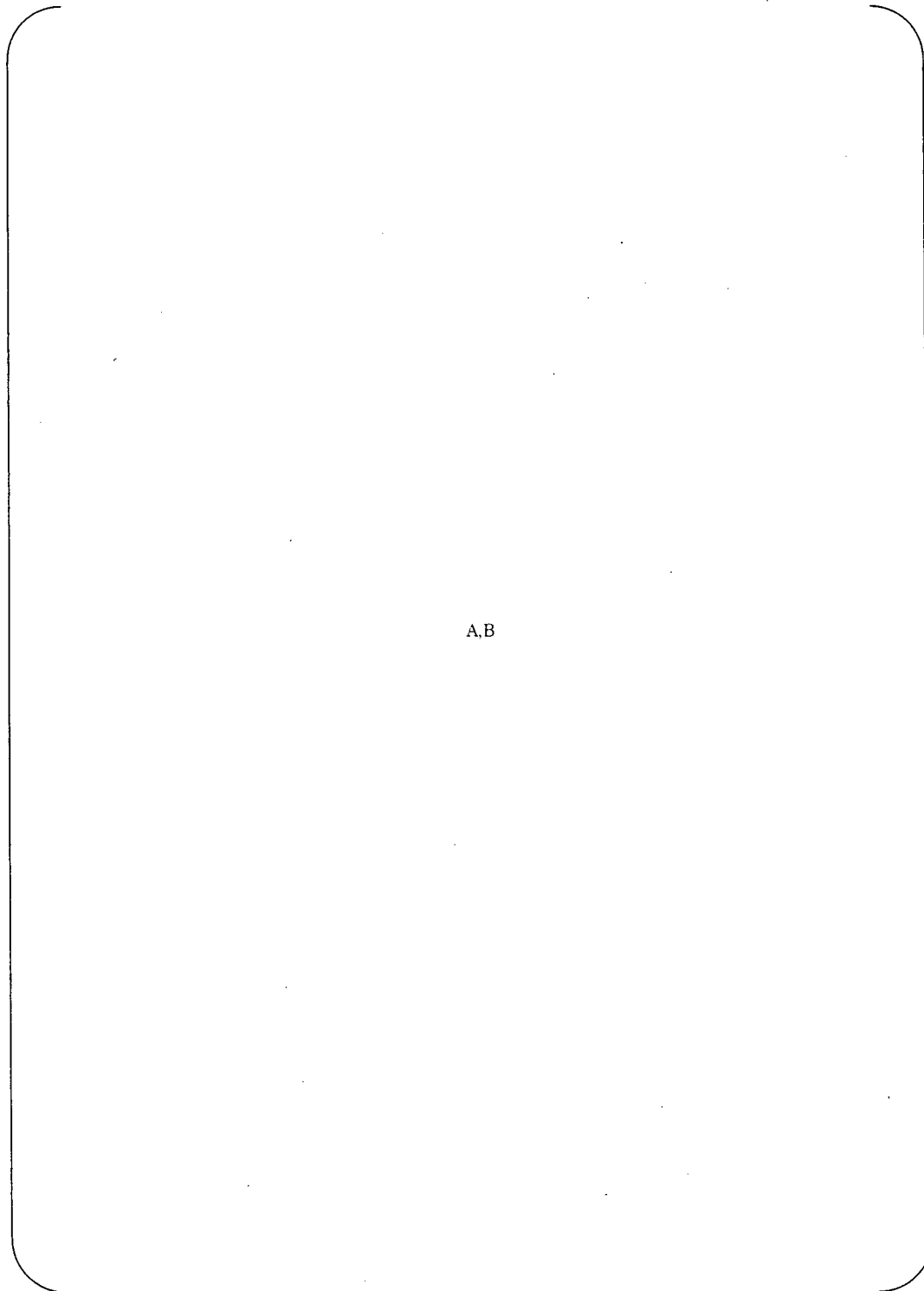
The hardness of 152 buttering very near fusion boundary is from HV(0.002){ A,B }.

The hardness of LAS very near fusion boundary is from HV(0.002){ A,B }. There is large scattering of hardness very near fusion boundary.



A,B

Fig.C.21 Macro-structure observation



A,B

Fig.C.22 Micro-structure observation



A,B

Fig. C.23 Result of Vickers hardness measurement



8. High hardness in the heat affected zone

Hardness tests were conducted using mockup. Conclusion is as follows.

1. Hardened depths of mockups are the same between the grooves prepared by machining and gouging to remove ESW stainless steel clad.
2. Hardened depth observed in boat samples is similar to the mockups that have ESW stainless steel clad and the removal of it is as explained in item 1 above.
3. Mockup that does not have ESW stainless steel clad and buttered zones to gouged surface does not have hardened area like mockups in item 1 above.
4. Hardened depth by gouging is the same as the depth of heat affected zone observed by macro-structure, which varies from [A,B].

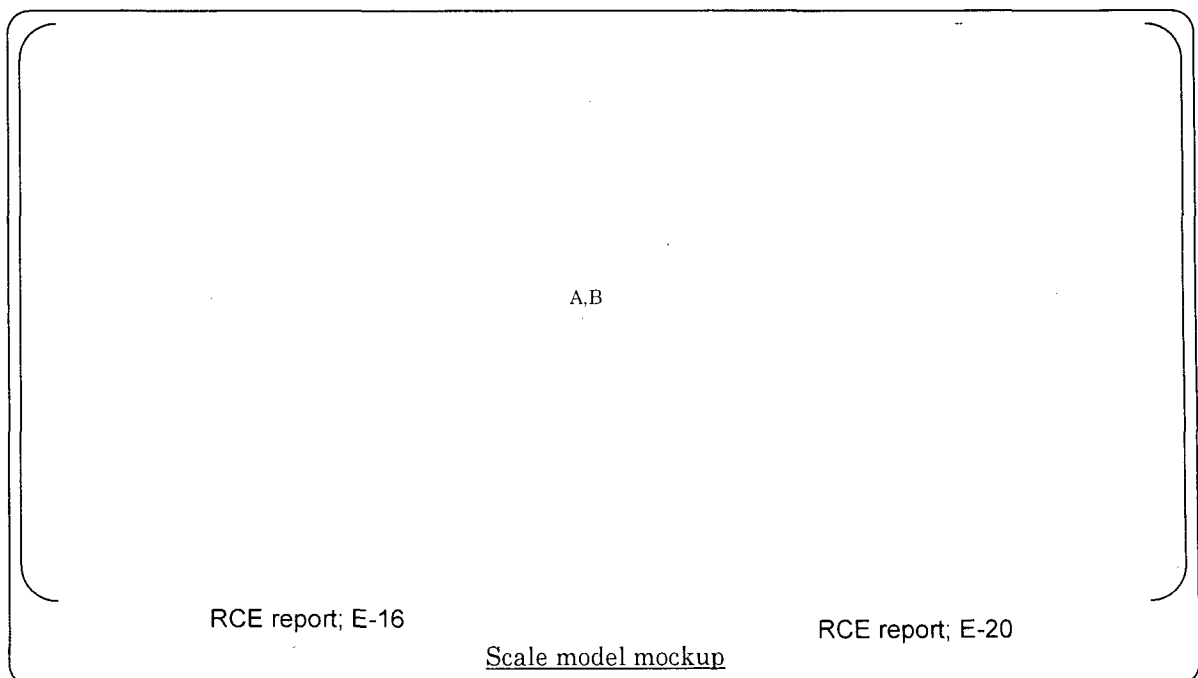
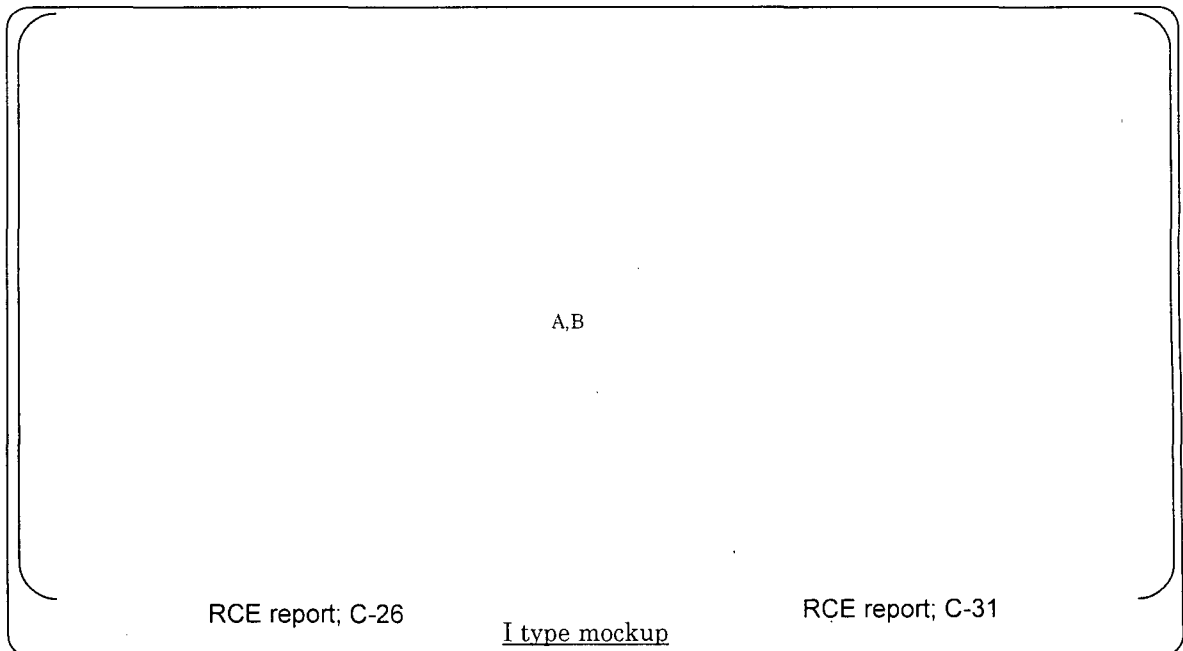


(1) Manufacturing process simulated mockup

Mockup is prepared with full of manufacturing process simulation. That is,

- Stainless steel cladding by ESW process
- PWHT
- Remove clad by machining (simulate u2) or gouging/grinding (simulate u3)
- Alloy 152 buttering by SMAW process
- Joint weld of divider plate

According to these mockups, hardened depth ($H_v > 200$) and peak value are almost the same

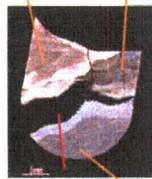




Reference: Hardness of heat affected zone of the boat samples

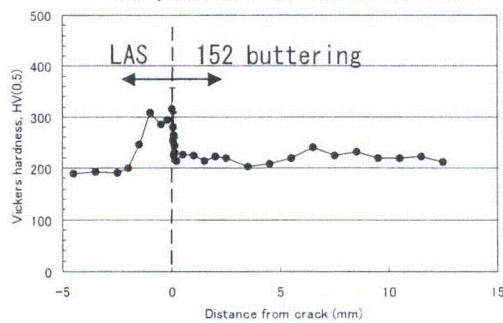
152 buttering

SS clad



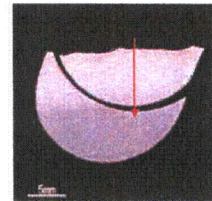
LAS

The position of hardness test

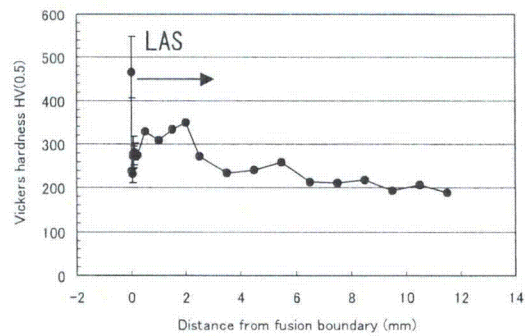


Boat sample A

RCE report A-32

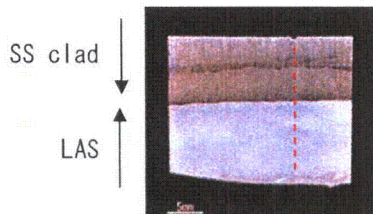


Measurement line of hardness

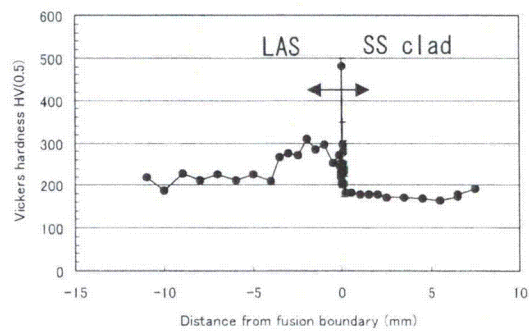


Boat sample B

RCE report A-50



Position of hardness test



Boat sample C

RCE report A-64

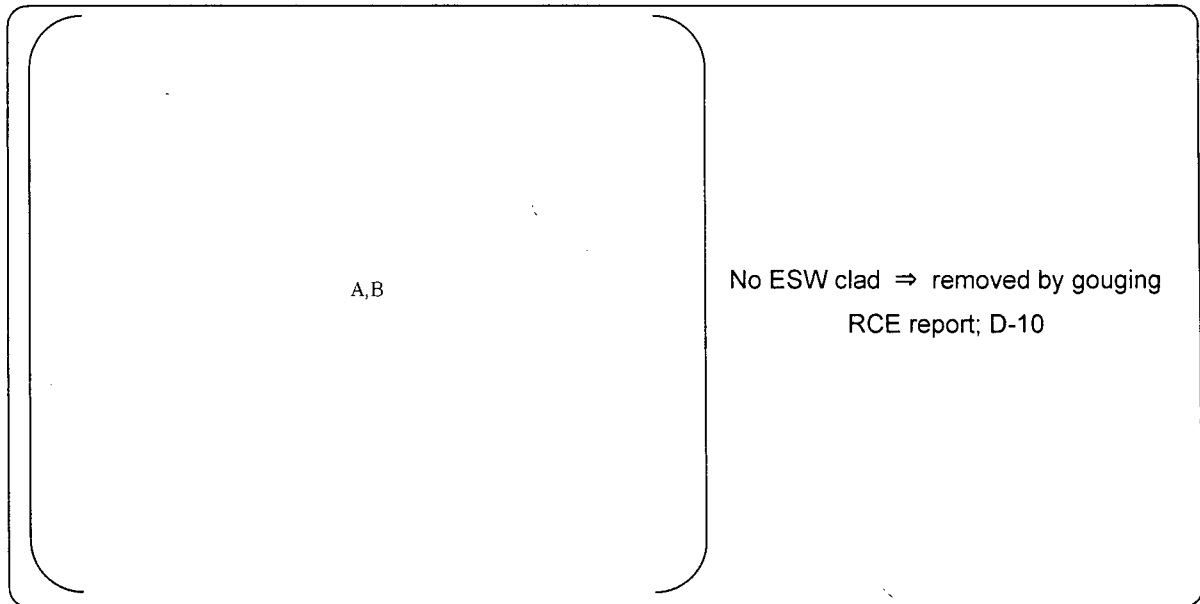


(2) Mockup without ESW

Mockup is prepared without ESW stainless steel clad and without finishing after gouging. That is,

- Remove low alloy steel by gouging and no grinding or buffing is applied to finish gouged surface.
- Alloy 152 buttering by SMAW process on as gouged surface.
- Joint weld of divider plate

According to this mockup, hardness is similar to that of base material and is much lower than that of HAZ in test (1) above.





Attachment-D
Additional I-Type Test



1. Purpose

The purpose of this test is to obtain metallurgical feature and tensile strength of fusion boundary of the weld which was welded on the gouged surface without grinding.

2. Outline of test

The mockup (I type model) was fabricated where 152 butter was welded on LAS after gouging without grinding.

Metallurgical examination of the mockup was conducted and smooth and notched tensile specimens were machined from it. Then, tensile tests and fracture surface observation were conducted at room temperature.

3. Test method

3.1 Mockup (I type model)

The fabrication flow chart of mockup (I type model) is shown in Fig. D.1. Alloy 152 clad was welded on the gouged surface without grinding and the mockup was fabricated.

For the reason that carbon included in arc electrode might remain when 152 butter was welded on LAS after gouging without grinding, the hardening near fusion boundary could occur and the susceptibility of low temperature cracking could increase, FSR was done 48 hours after post-heating to provide enough time for cold cracking to appear.

The configuration of mockups is shown in Fig. D.2.

3.2 Tensile specimen

Two types of tensile specimens were tested. One was typical smooth specimen and the other was notched specimen which radius of notch root was 4mm. The specimens were machined from mockups to make the longitudinal direction of specimens parallel to the height direction of mockups. The fusion boundary of weld was set at the center of smooth specimen or the root of notched specimen.

3.3 Tensile test

Tensile tests were conducted at room temperature condition with 10tonf(98kN) universal test machine. The test procedure was according to JIS Z 2241(98).



4. Test results

4.1 Tensile test

The results of all tensile tests are shown in table D.1 and Photographs of specimen and fracture surface were shown in Fig. D.4 and D.5.

As shown in Fig.D.4, smooth specimens were broken at LAS base metal and fracture at boundary between LAS and 152 buttering did not occur. As shown in Fig.D.5, notched specimens were broken at notch but all fracture surfaces showed ductile feature and brittle fracture surface which was observed in the actual SG was not observed.

The tensile strength was equivalent to that of mockup with grinding after gouging.

The difference of fracture location, 152 buttering in the specimen of mockup with grinding after gouging and LAS in the specimen of mockup without grinding after gouging, was observed. The reason for this difference is assumed that there was small difference of hardness (strength) between LAS and 152 buttering and the small difference of strength caused the differences in fracture location.

4.2 Metallurgical examination

The results of metallurgical examination (macro structure, micro structure, hardness measurement and surface etching) on mockups are shown in Fig. D.6, D.7 and D.8.

- (1) Indication of the presence of remaining carbon that was included in arc electrode and it affects to the metallurgical structure was not observed and the metallurgical structure near fusion boundary was almost the same as that of the mockup with grinding after gouging.
- (2) Hardness near the fusion boundary was equivalent to that of the mockup with grinding after gouging although high hardness region was observed.

5. Summary

Welding 152 butter on LAS after gouging without grinding did not affect the metallurgical feature and tensile strength of fusion boundary.

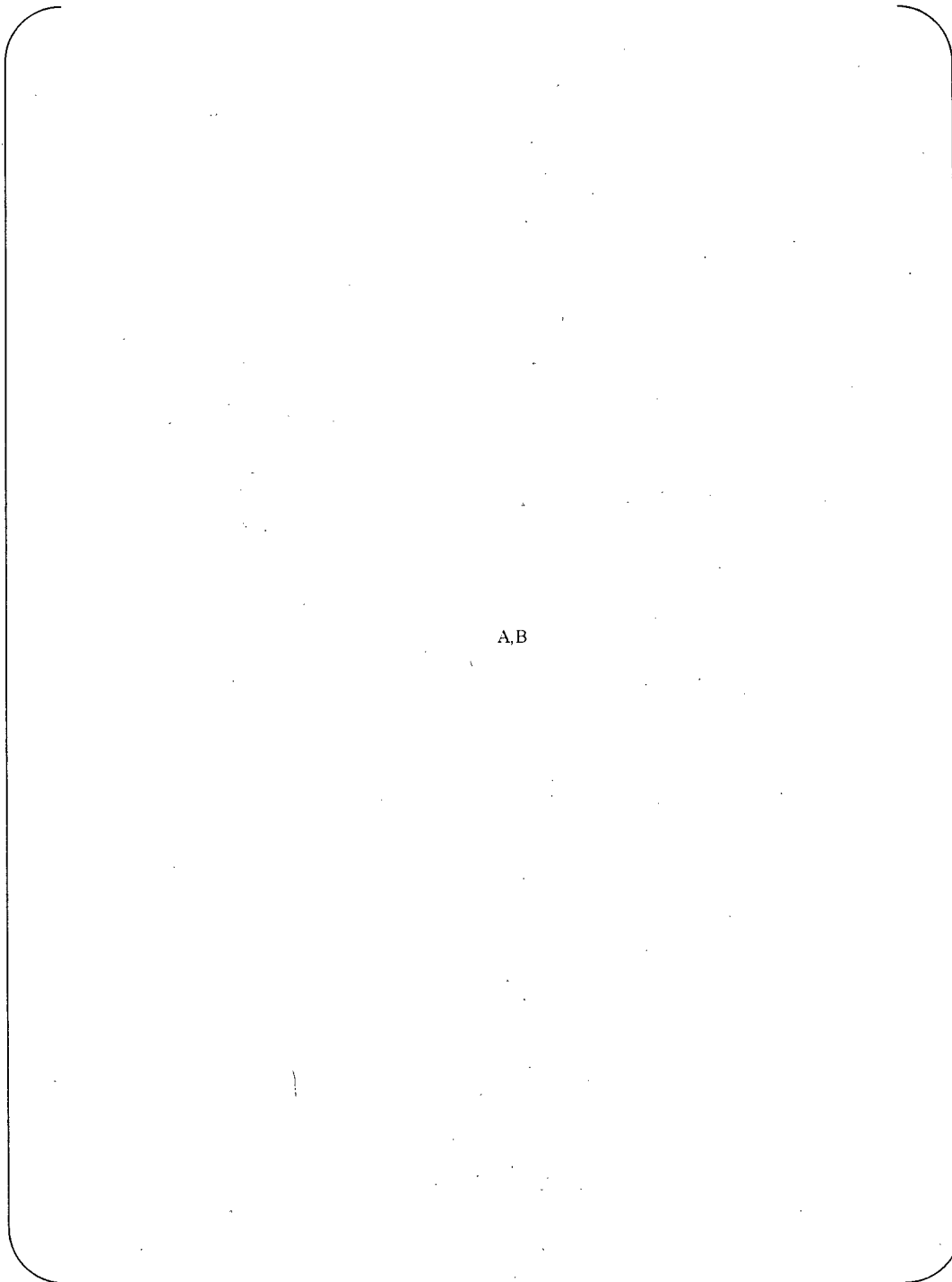
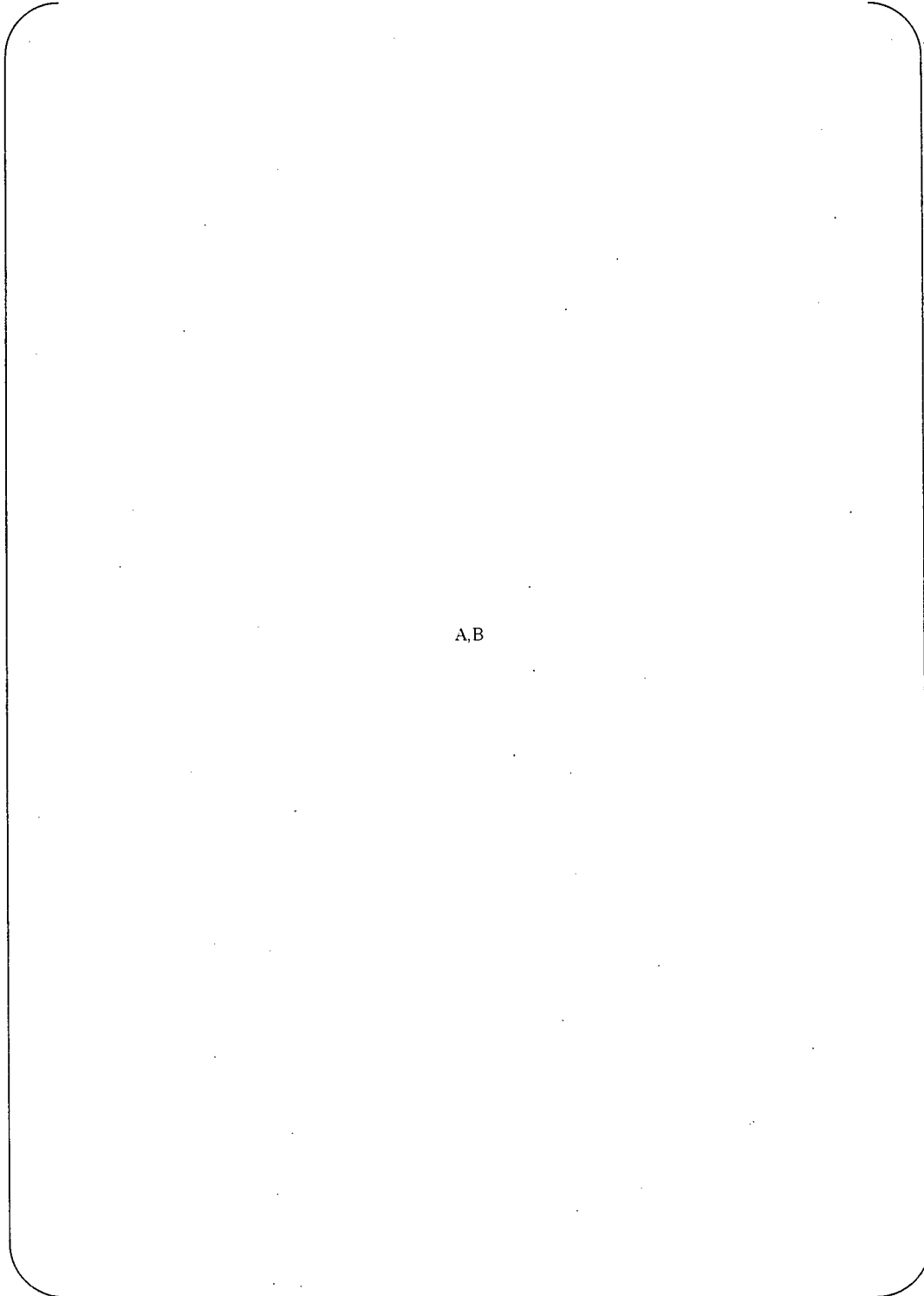


Fig. D.1 Flow chart of manufacturing I type mockup



A,B

Fig.D.3 Tensile test specimen



Table D.1 Result of Tension Test

A.B

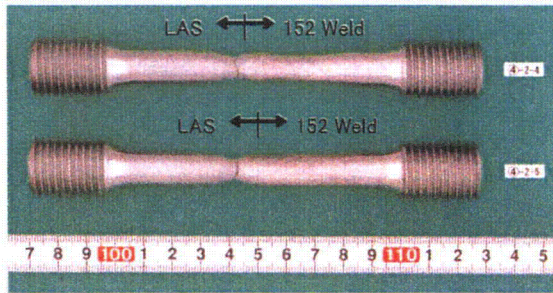
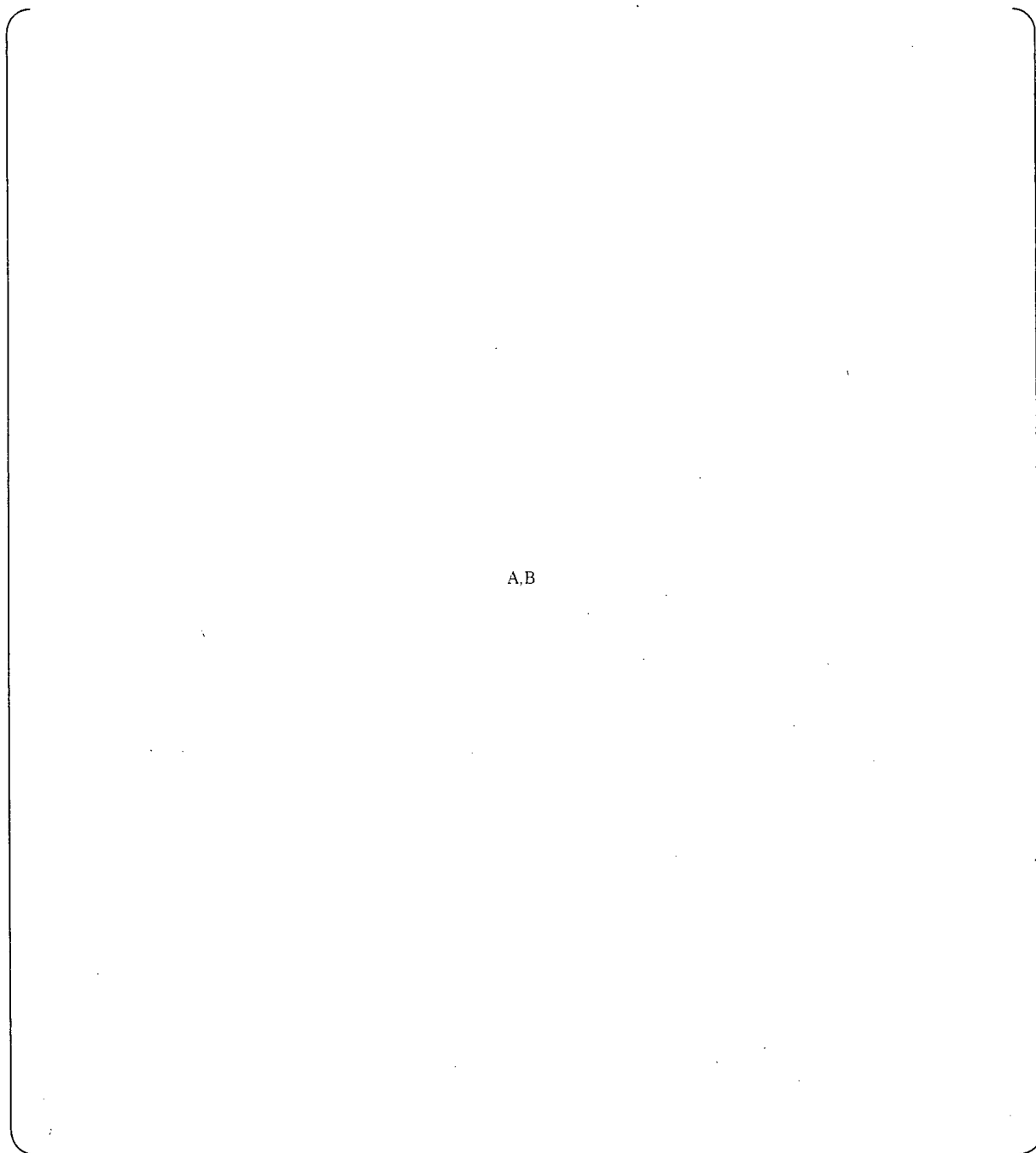
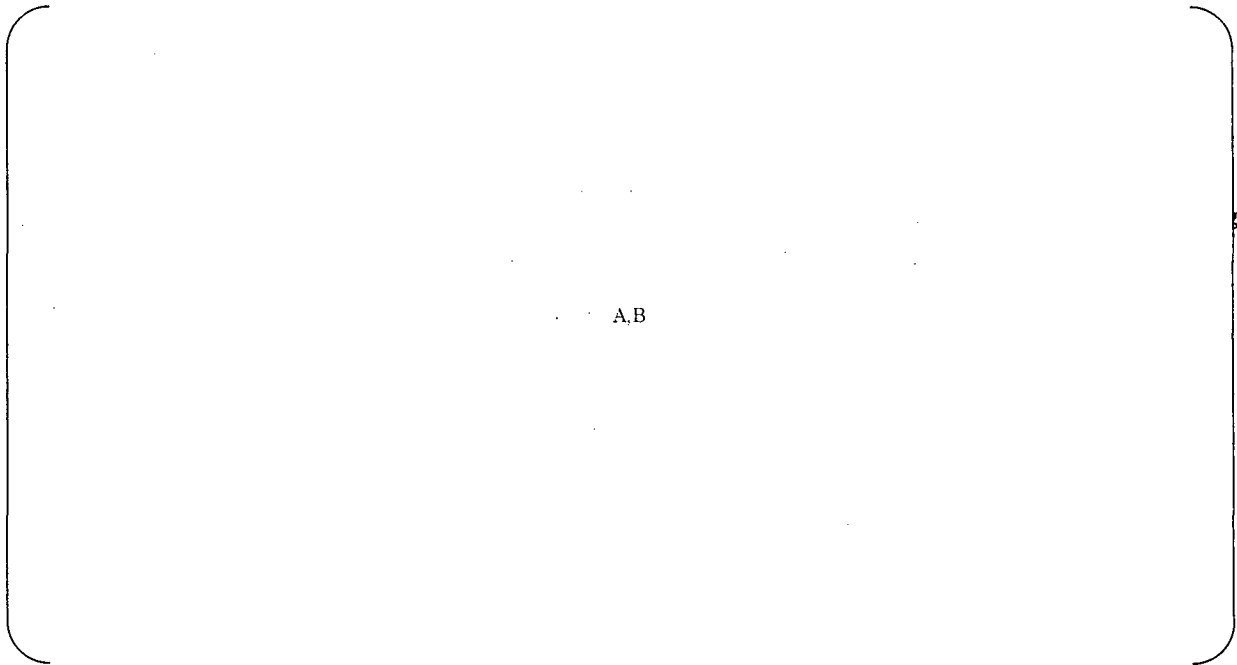
Spec	Test.No	Specimen Type	Appearance
Effect of gouging	④-2-4	JIS 4	
	④-2-5		

Fig.D.4 Photograph of smooth specimen after test (Sample ④-2)



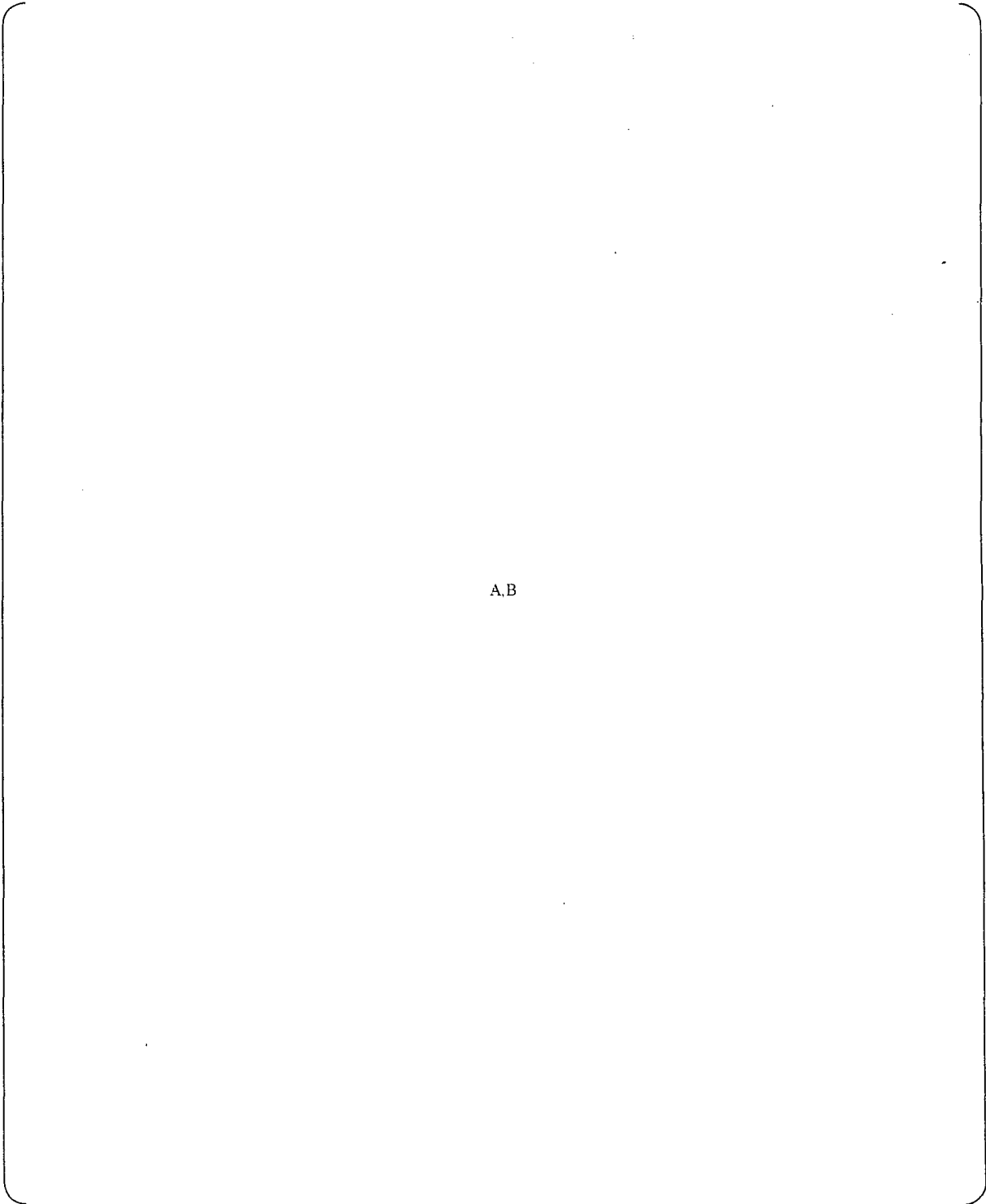
A,B

Fig.D.5 Photograph of fracture surface (Sample ④-2)



A,B

Fig.D.6 Macro-structure observation



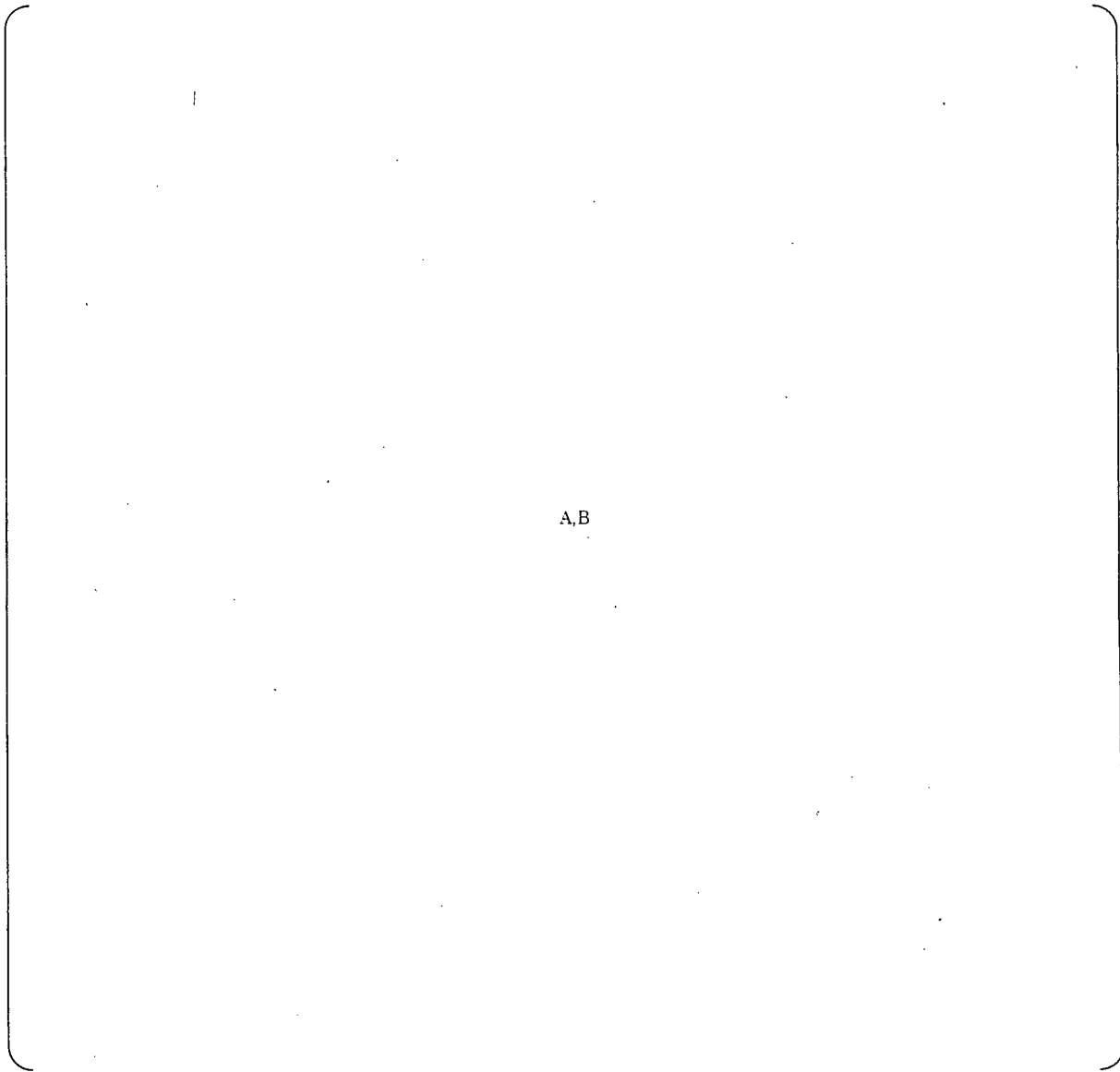
A.B

Fig. D.7 Micro-structure observation



A,B

Fig. D.8(1) Result of Vickers hardness measurement



A,B

Fig. D.8(2) Result of Vickers hardness measurement



Attachment-E

T-Type Test



Attachment-E Scale model test report

1. Purpose

Purposes of the scale model test are shown below.

- (1) To confirm whether the fracture stress of the scale model test is almost equal to the stress due to hydrostatic test.
- (2) To confirm whether the differences between gouging and machining affects fracture (location where fracture occurs, fracture load) of the welding joint between divider plate and channel head.

2. Outline of the scale model test

Two test pieces, which simulates the welding joint between divider plate and channel head, were manufactured. Gouging process was applied to one of the test pieces (TYPE-A) to simulate unit 3, machining process was applied to the other test piece (TYPE-B) to simulate unit 2. Tension load due to hydrostatic test was applied to the test pieces until the test pieces were fractured.

The applied load was measured during the test. After the tests, the location of fracture was confirmed and metallurgical examination (macro-structure, micro-structure and hardness measurement) was performed.

3. Scale model test specimen

3.1 Limited condition for design of the test specimen

Limited conditions, which have to be considered for design of the test specimen, are shown below.

(1) Load capacity of test machine

Maximum load capacity of the available test machine is 5500 kN (=1237 lbf). Therefore, the maximum load of each test has to be smaller than 5500 kN (= 1237 lbf).

(2) Maximum stress at the cross section of the divider plate

If fracture does not occur at the fusion boundary between Alloy 152 buttering and channel head (low alloy steel), fracture will occur at the divider plate because the ultimate stress of the divider plate is lower and it has to sustain higher stresses.

Therefore, stress at the divider plate caused by the maximum load of the test machine set to be equal to the ultimate stress of the divider plate.



(3) Thickness of the divider plate

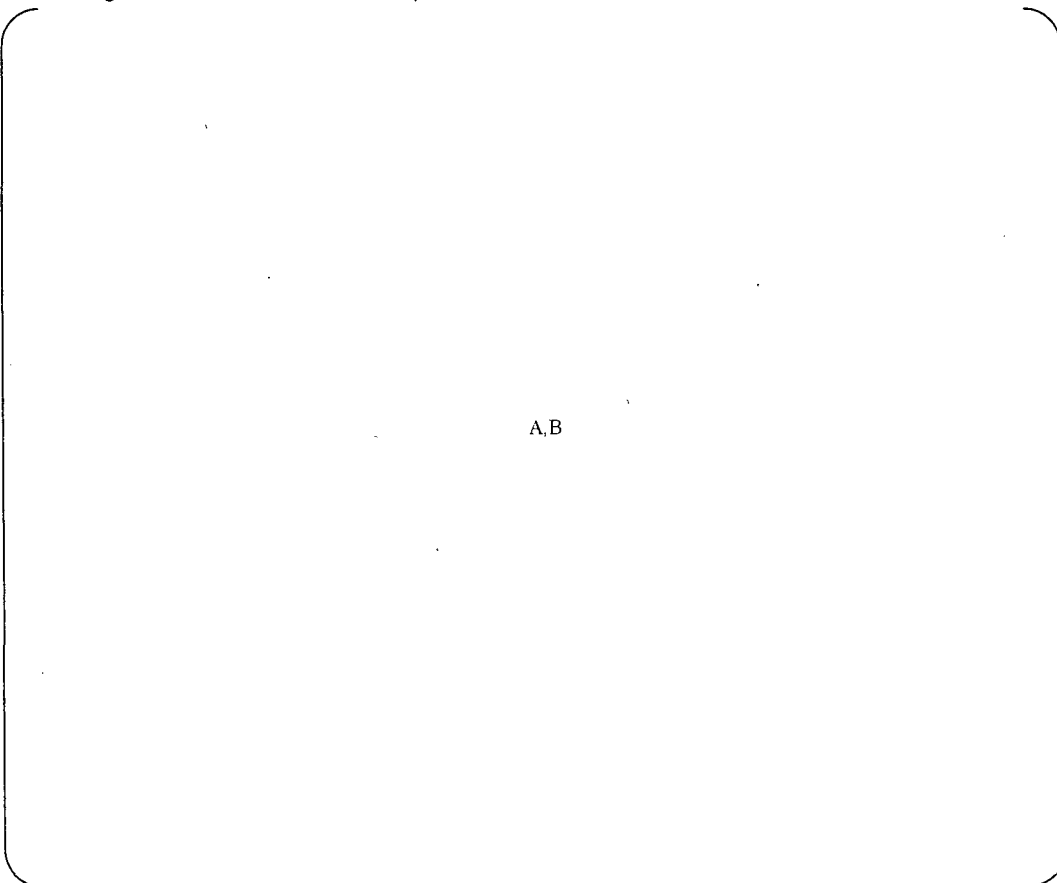
The thickness of the divider plate of the scale model test specimen is [A,B] which is the thickness of the actual divider plate.

(4) Material of the divider plate

Alloy 690 plate whose thickness was [A,B] was not available, low alloy steel plate was used as the divider plate instead of alloy 690 plate. Since the purpose of this test is to evaluate fracture at the fusion boundary between alloy 152 buttering and low alloy steel and the divider plate is just jig to transmit the load, it is considered that to use the divider plate of low alloy steel does not affect the fracture load at the fusion boundary between alloy 152 buttering and low alloy steel.

Validity of using the low alloy steel plate is also confirmed in comparison of stress distributions calculated by FE analysis. This FE analysis result is described in section 3.3.

3.2 Design of the scale model test specimen



A,B



A,B

3.3 Stress distribution of the scale model test specimen

In order to confirm the stress distribution of the test specimen near the boundary between alloy 152 buttering and low alloy steel is almost equal to that of the Unit 3, FE analyses are performed and the stress distribution of the test specimen is compared with that of unit 3. FigureE.3 shows the comparison of both stress distributions. From FigureE.3, because the stress distribution of the test specimen is almost equal to that of unit 3, it can be seen that the test specimen can simulate the stress distribution that resembles the stress distribution of unit 3.

3.4 Manufacturing process of the test specimen

FigureE.4 shows flow of the manufacturing process of the test specimen.

Two test specimens were manufactured to perform fracture test.

One is the test specimen which simulates unit3 and it is called "TYPE-A", the other is the test specimen which simulates unit2 and it is called "TYPE-B".

The only difference between TYPE-A and TYPE-B is removal method of stainless steel cladding on low alloy steel. The removal method of stainless steel cladding of TYPE-A is gouging and grinding, while for TYPE-B is machining.

4. Test method

4.1 Test machine

Photo and sketch of the test machine which set the test specimen and jig are shown in FigureE.5.

Tension load is applies to two pins which are shown in FigureE.5 until the test specimen is broken.

4.2 Measurement

(1) Load(Strain)

As shown in FigureE.6, strains are measured using four strain gauges on the section of the divider plate. Load which is applied to the test specimen is calculated using the measured strains.



(2) Fracture location(point)

From the video image and fractured test piece, fracture location (point) is evaluated.

(3) Metallurgical examination (macro-structure, micro-structure and hardness measurement)

Metallurgical examination (macro-structure, micro-structure and hardness measurement) are performed near the fusion boundary between alloy 152 buttering and low alloy steel.

5. Test result

(1) TYPE-A (simulated unit3)

a. Location (point) where fracture occurred

Photo of TYPE-A after test is shown in FigureE.7.

From FigureE.7, location (point) where fracture occurred is the divider plate simulated by alloy 152 buttering.

b. Maximum load

FigureE.8 shows relationship between load and time. From FigureE.8, the maximum load is [A,B].

c. Metallurgical examination (macro-structure, micro-structure and hardness measurement)

Figures E.9 to 11 show the results of macro-structure observation, micro-structure observation and hardness measurement.

Metallurgical structure observed near the fusion boundary of TYPE-A was similar to that observed near the fusion boundary of Unit 3.

From metallurgical structure observed near the fusion boundary of TYPE-A, crack did not occur at the fusion boundary.

Hardness near fusion boundary was [A,B]

(2) TYPE-B (simulated unit2)

a. Location (point) where fracture occurred

Photo of TYPE-A after test is shown in FigureE.12.

From FigureE.12, fracture location (point) is the divider plate simulated by alloy 152 buttering.

b. Maximum load

FigureE.13 shows relationship between load and time. From FigureE.13, the maximum load



is { A,B }.

c. Metallurgical examination (macro-structure, micro-structure and hardness measurement)
Figures E.14 to 16 show the results of macro-structure observation, micro-structure observation and hardness measurement.

Metallurgical structure observed near the fusion boundary of TYPE-B was similar to that observed near the fusion boundary of Unit 3.

From metallurgical structure observed near the fusion boundary of TYPE-B crack did not occur at the fusion boundary.

Hardness near fusion boundary was { A,B }

6. Summary

- Two test pieces which simulated the welding joint between divider plate and channel head were made and tension load due to hydrostatic test was applied to the test piece until the test piece is fractured.
- Gouging process was applied to one test piece (TYPE-A) to simulate unit 3 while machining process was applied to the other test piece (TYPE-B) to simulate unit 2.
- Both test specimens fractured at the divider plate simulated by alloy 152 buttering and did not fracture at the boundary between the alloy 152 buttering and low alloy steel of channel head.
- Metallurgical structure observed near the fusion boundary of TYPE-A was similar to that observed near the fusion boundary of Unit 3.



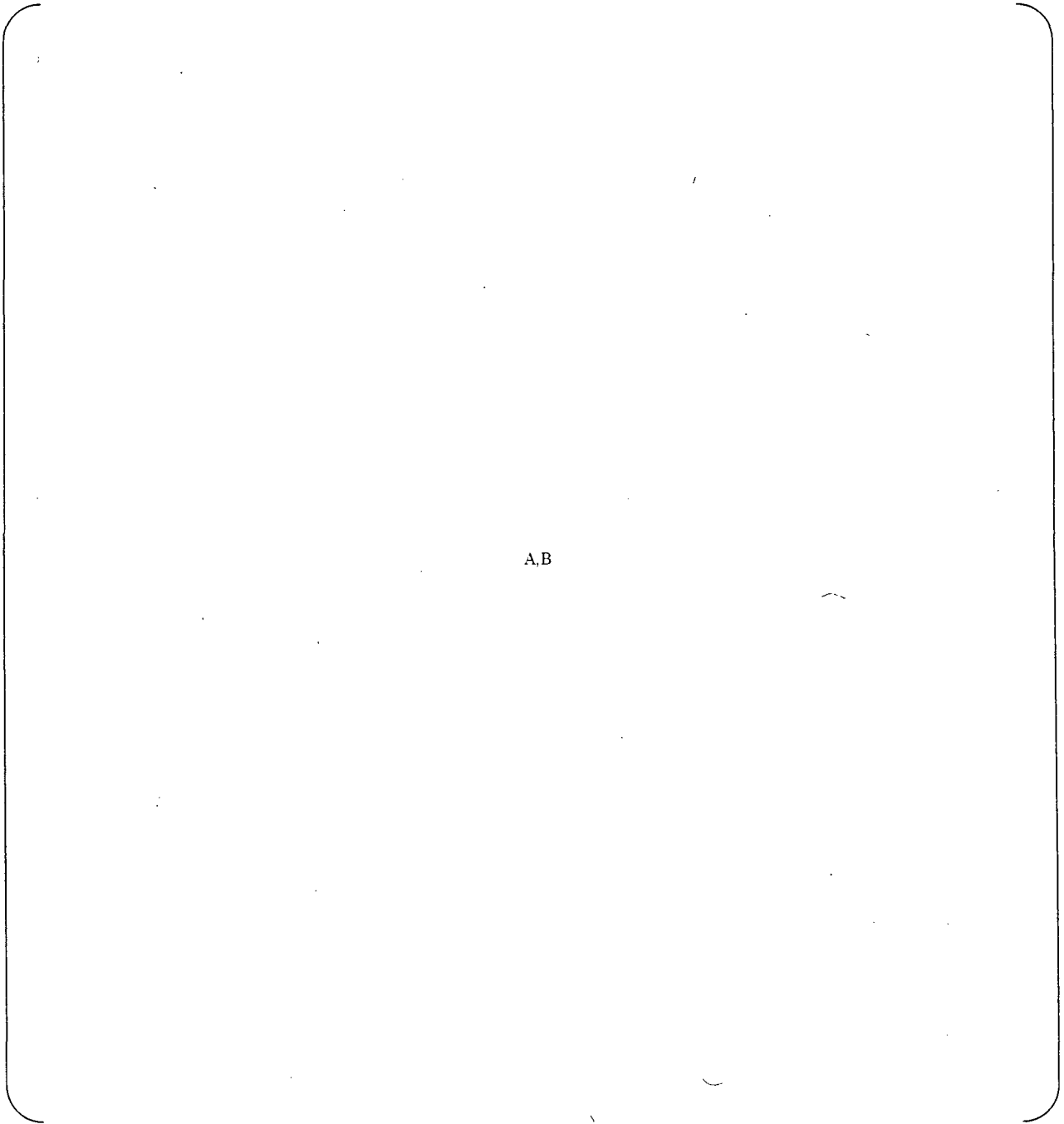
A,B

FigureE.1 Sketch of configurations of the scale model test specimen

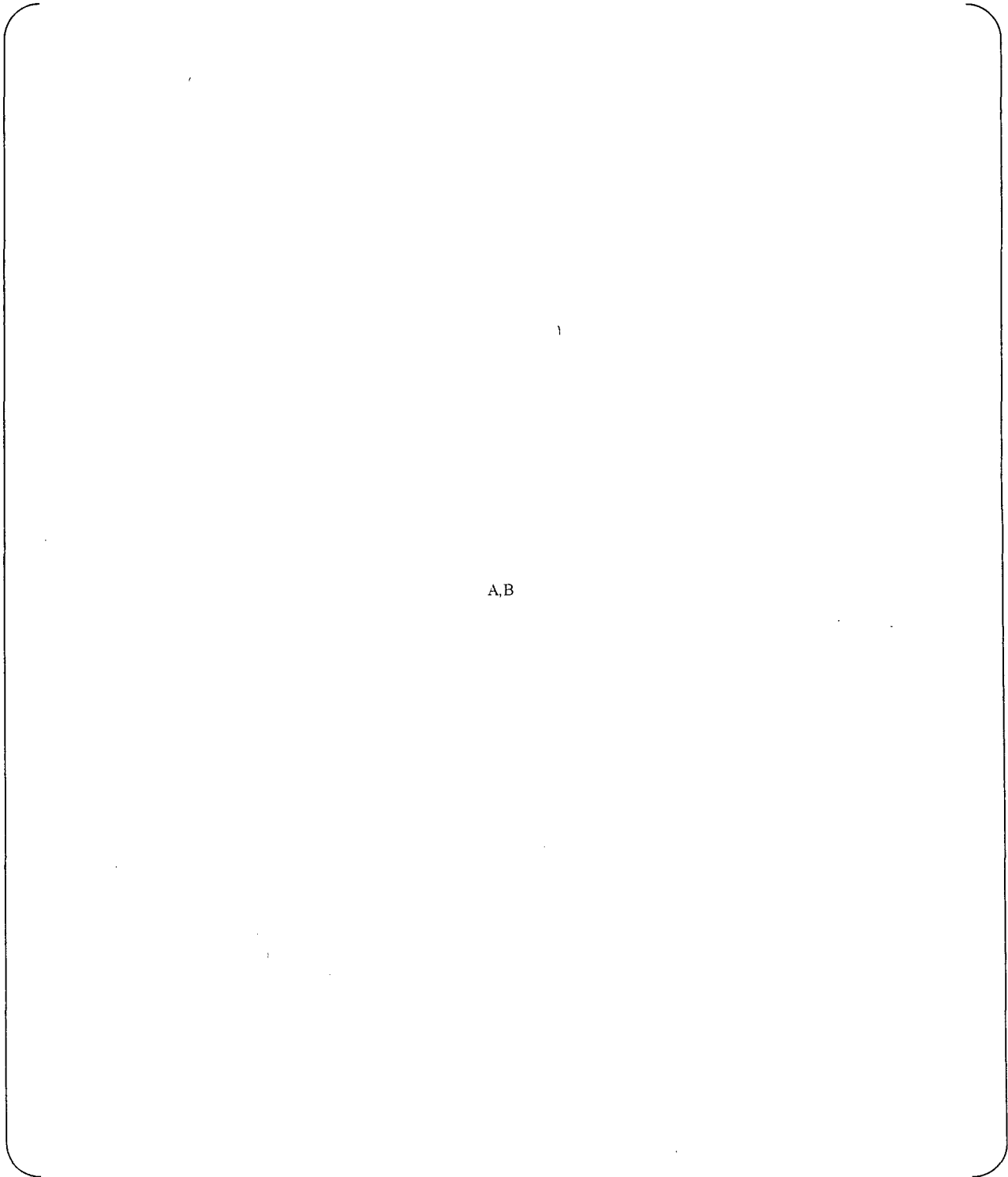


A,B

FigureE.2 Sketch and photo of the jig and the test specimen

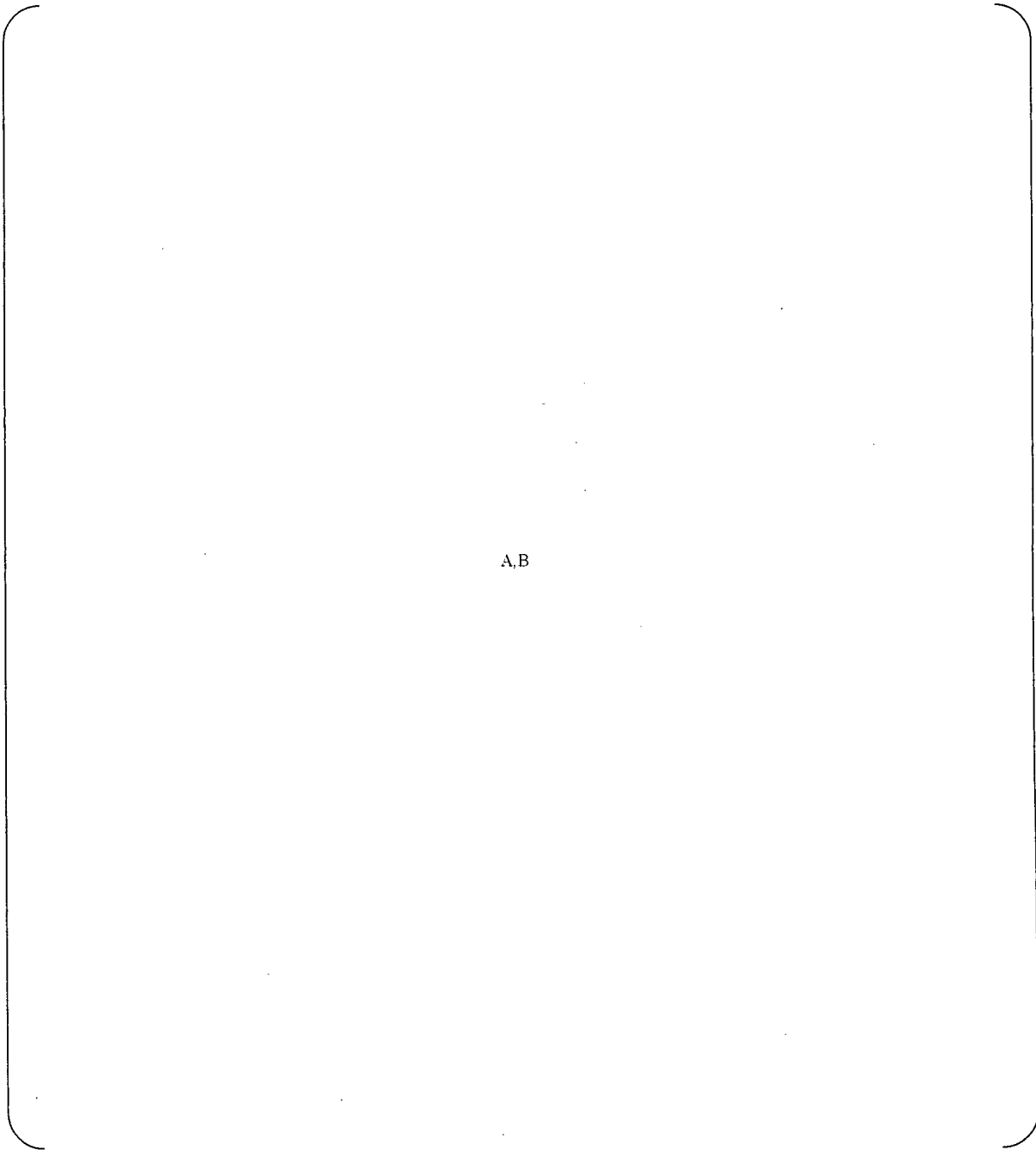


FigureE.3 Comparison of stress distributions of vertical direction(X-direction)



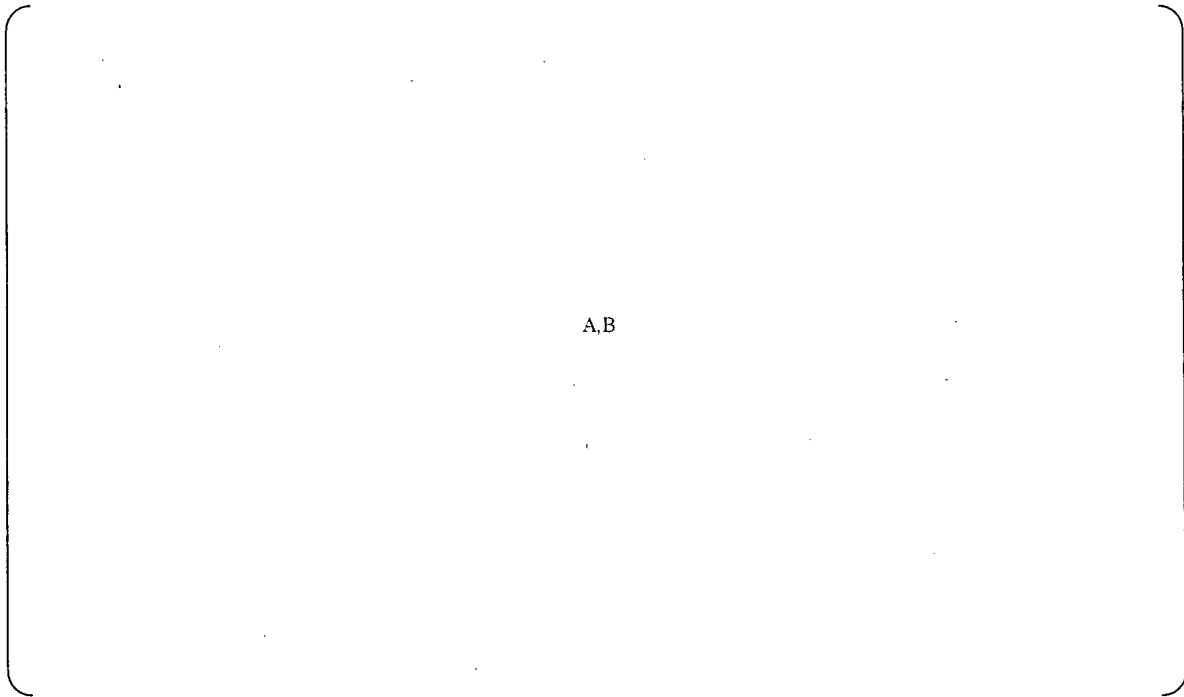
A,B

FigureE.4 Flow of the manufacturing process of the test specimen



A,B

FigureE.5 Photo and sketch of the test machine which set the test specimen and jig



A,B

Figure E.6 Strain gauge to measure load



A,B

FigureE.8 Relationship between load and time



A,B

Fig. E. 9 Macro-structure observation (type-A)



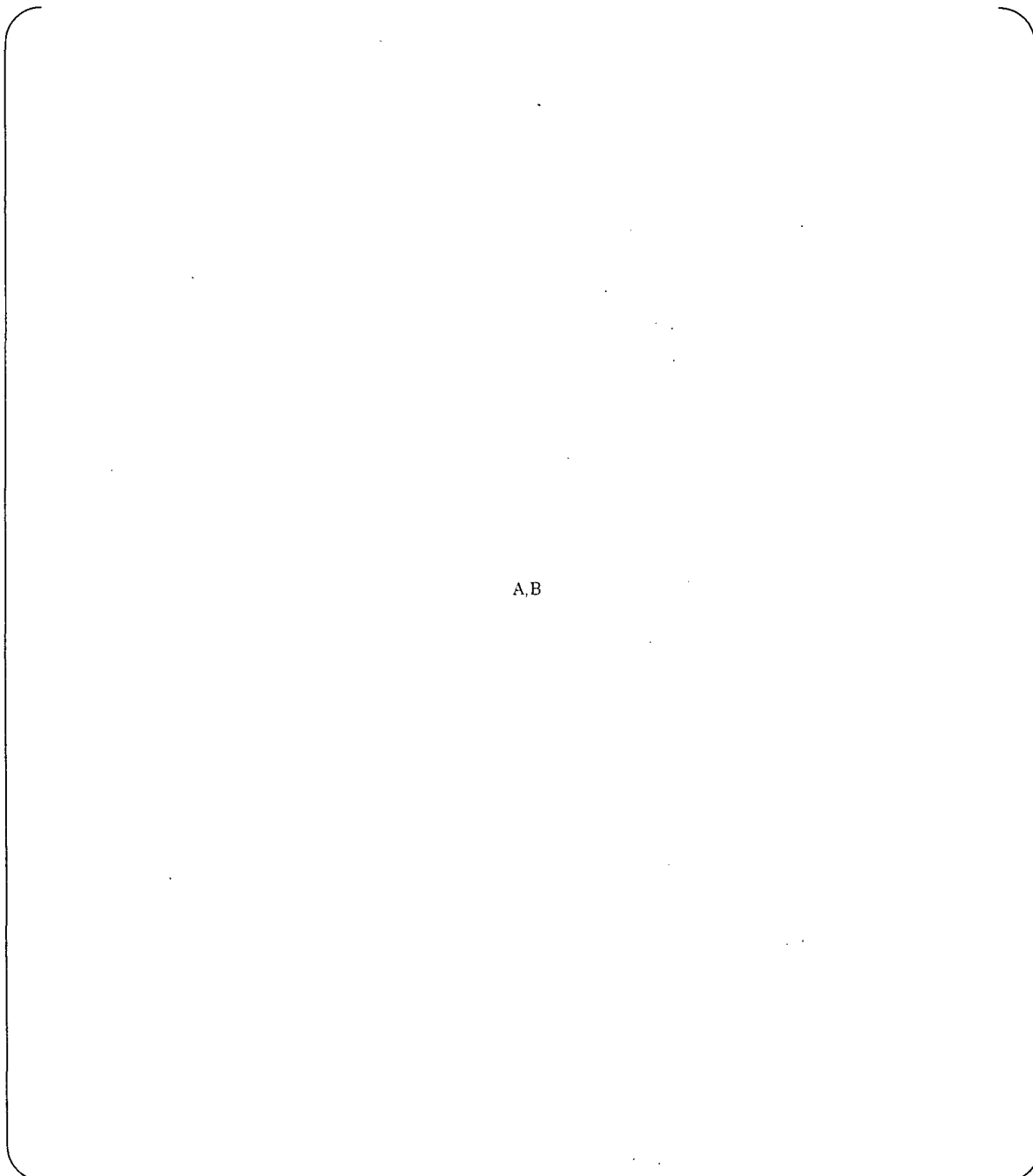
A,B

Fig.E.10 Micro-structure observation (type-A)



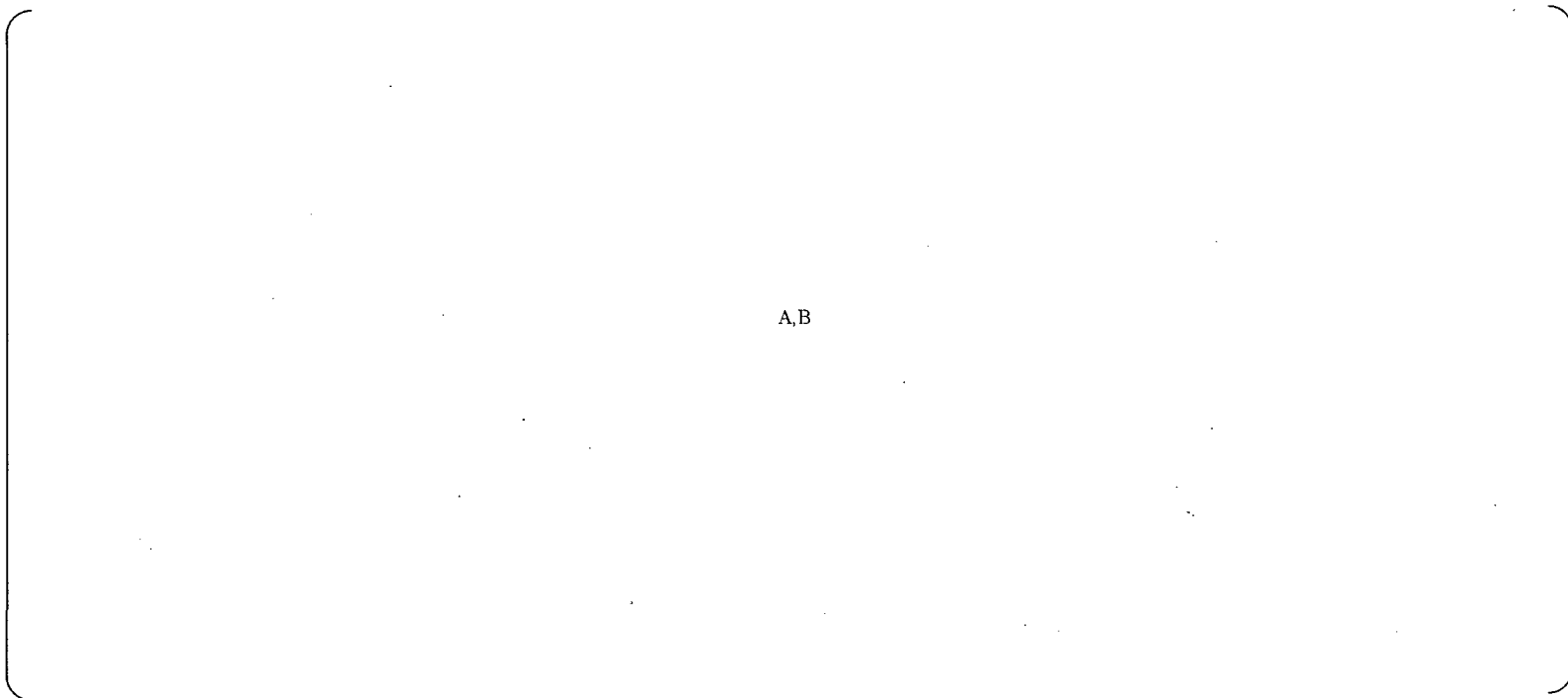
A,B

Fig.E.11 Result of hardness measurement (type-A)



A,B

FigureE.13 Relationship between load and time



A,B

Fig.E.14 Macro-structure observation (Type-B)





A,B

Fig.E.15 Micro-structure observation (Type-B)



A,B

Fig.E.16 Result of hardness measurement (Type-B)



Attachment-F
Fracture Toughness Test



1. Purpose

The purpose of fracture toughness test is to reproduce the fracture along fusion boundary of weld occurred in Unit 3 RSGs, to obtain the necessary data for fracture evaluation and to confirm the effects of the differences between gouging and machining on fracture along the fusion boundary.

2. Outline of test

The mockup which simulated the fractured weld between LAS and 152 alloy was fabricated. Two types of methods to remove stainless steel cladding were employed. One was gouging which was applied to Unit 3 RSGs and the other was machining which was applied to Unit 2 RSGs.

Fracture toughness specimens were machined from these mockups and fracture toughness tests and fracture surface observations were conducted at room temperature. Parts of the tests were conducted after hydrogen charge to examine the effect of hydrogen on the fracture along fusion boundary.

3. Test method

3.1 Mockup

The fabrication flow chart of mockup is shown in Fig. F.1. The manufacturing procedure for the actual SG was reproduced including heat treatment and inspection.

3.2 Fracture toughness test specimen

The location and direction of specimens and the configuration of specimen were shown in Fig.F.1 and F.2 respectively. The specimen was machined to make the direction of crack propagation parallel (S-L) and perpendicular (S-T) to welding direction. The slit of specimen was set at fusion boundary of weld. The configuration of specimen was referred to ASTM E1820, but the side groove was not introduced for both side of the specimen.

The specimens without fatigue pre-crack, those with about [A,B] fatigue pre-crack and those with pre-crack which was introduced after hydrogen charge to introduce pre-crack along fusion boundary were tested.

3.3 Fracture toughness test

The condition of fracture toughness test is shown in Table F.1. Parts of tests were conducted right after hydrogen charge.

Fracture toughness tests were conducted in room temperature air with 10tonf (98 k N) universal test machine. The test procedure was according to ASTM E1820.

Fracture toughness was evaluated according to ASTM E1820. The following values which



are averages of LAS and 152 weld metal were used for fracture toughness evaluation.

Young modulus: 200300MPa

Yield stress: 481MPa

Tensile stress: 620MPa

Poisson ratio: 0.38

4. Test results

4.1 Fracture toughness test

Photographs of specimen are shown in Fig. F.4, F.5 and appendix-2, results of SEM observation on some fracture surface are shown in Fig.F.6.

Load and load-line displacement curves during tests are shown in appendix 1.

(1) Specimens with hydrogen pre-charge

The fracture surface of both gouging (G-1) and machining (M-1) is uneven and macroscopically brittle surface which shows the aspect of fusion boundary crack observed in Unit 3 as shown in Fig. F.4.

Flat fracture surface with grain boundary like feature, quasi-cleavage fracture surface and ductile fracture surface were observed in Fig. F.6 which were observed in Unit 3.

(2) Specimens with fatigue pre-crack

Ductile fracture occurred in 152 buttering and fracture along fusion boundary did not occur.

(3) Specimens without pre-crack and hydrogen pre-charge

Ductile fracture occurred in 152 buttering and fracture along fusion boundary did not occur.

(4) Specimens with hydrogen crack

The fractured surface of both gouging (G-6) and machining (M-6) which propagates due to the tensile load applied after hydrogen charge is uneven and macroscopically brittle surface as shown in Fig. F.5. The fractured surface of those which propagated due to the tensile load applied after heat treatment undergone ductile fracture in 152 buttering and fractures along the fusion boundary did not occurred. The fracture surfaced which propagates before heat treatment was colored with light brown by the heat at { A,B }.

(5) Fracture toughness

From the above test results, fracture along fusion boundary did not occur and fracture toughness cannot be obtained under hydrogen free condition.

J-R curve obtained in tests after hydrogen pre-charge (G-1, G-6, M-1, M-6) is shown in Fig.F.7. There are no large differences of the J-R curve between gouging and machining.

Although the exact fracture toughness according to ASTM E1820 cannot be obtained, the



fracture toughness of { A,B } was estimated as the cross point of J-R curve and 0.2mm off set line. This value corresponds stress intensity factor K of { A,B } by below equation.

$$K = \sqrt{E \cdot J / (1 - \nu^2)}$$

4.2 Metallurgical examination of mockup

The results of macro-structure observation, micro-structure observation, and hardness measurement of mockup G and M are shown in appendix-3.

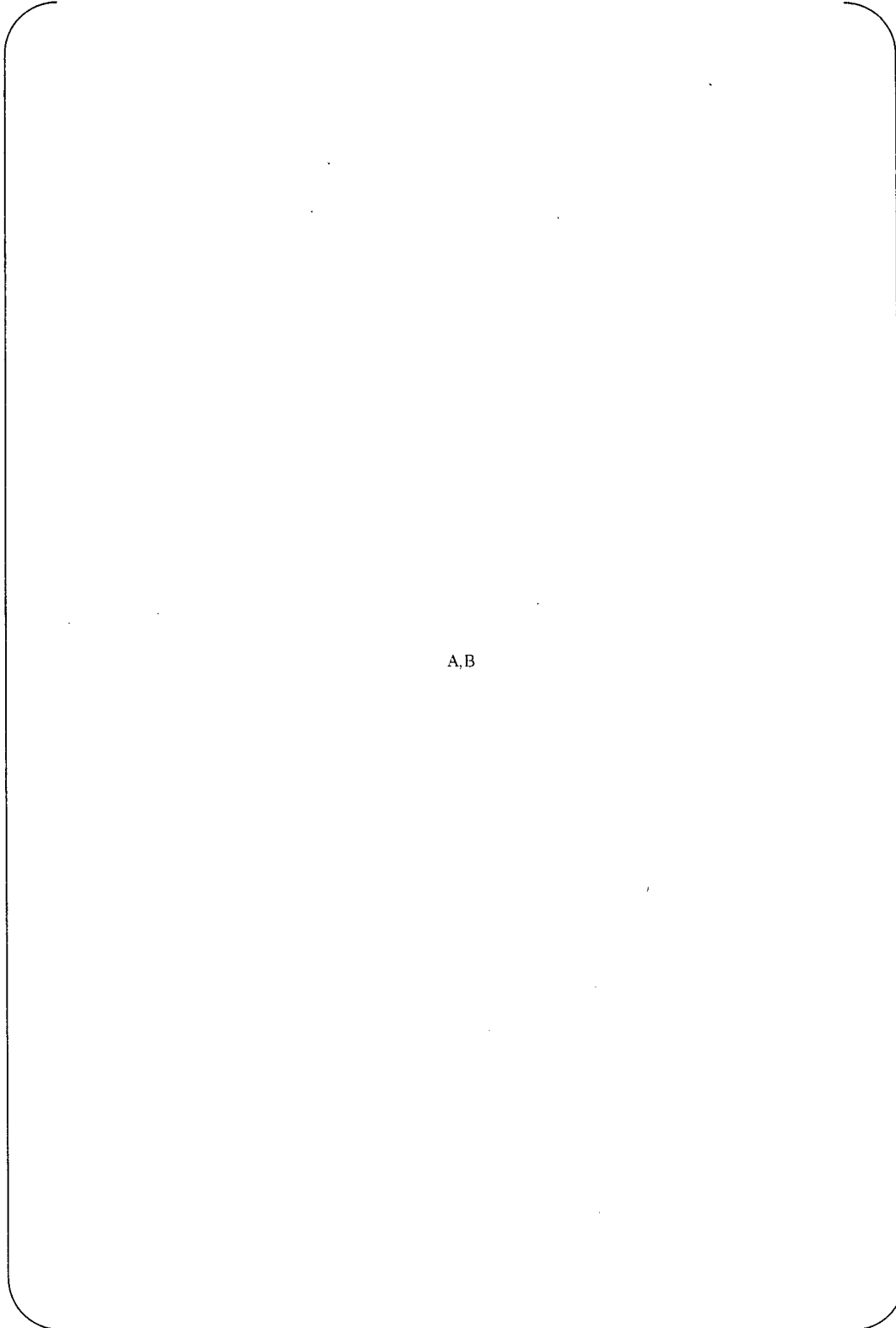
The results of macro-structure observation, micro-structure observation, and hardness measurement of specimen G-1 after test are shown in appendix-4.

The below results are obtained.

- (1) The metallurgical structure observed near the fusion boundary of mockup G (gouging) was similar to that observed near the fusion boundary of Unit 3, but the color of grain boundary near the fusion boundary of specimen G-1 was different from the other location. The reason of this difference may be related to the effect of hydrogen charge.
- (2) There are no large differences of metallurgical structure near the fusion boundary between the mockup G (gouging) and M (machining).
- (3) The hardness near fusion boundary of mockup G, specimen G-1 and mockup M was { A,B }, { A,B } and { A,B }, respectively, but higher hardness beyond { A,B } was observed at the other point. Therefore, it is supposed there is not large difference of hardness among the mockups and specimens.

5. Summary

- (1) Fracture along fusion boundary occurred after hydrogen charge but fracture toughness did not occur under hydrogen free condition.
- (2) There are no large differences of fracture resistance of fusion boundary (J-R curve) between the mockup G (gouging) and M (machining).



A,B

Fig. F.1 Flow chart of manufacturing I type mockup



A.B

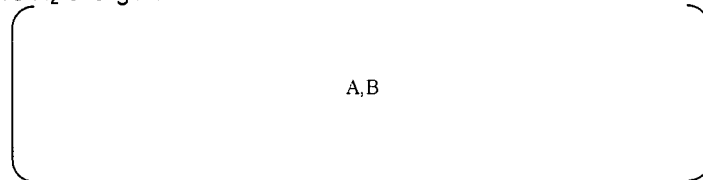
Fig.F.3 1T Compact Tension Specimen



Table F.1 Test matrix

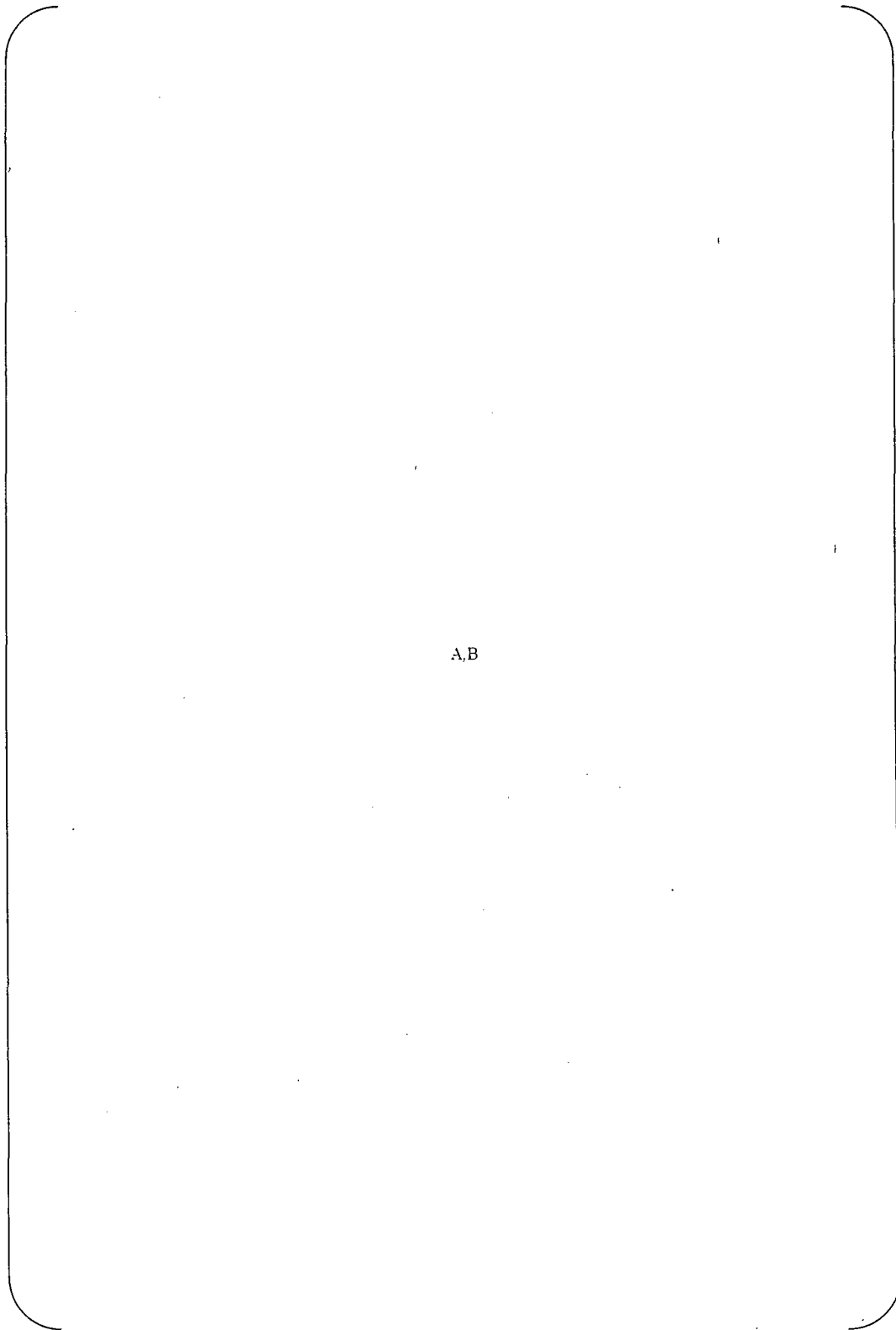
Pre-crack	Pre H ₂ Charge *1	Orientation of crack	Fracture Test No.	
			Machining	Gouging
No	Yes	S-L	M-1	G-1
Fatigue crack	No	S-L	M-2	G-2
		S-T	M-3	G-3
No	No	S-L	M-4	G-4
		S-T	M-5	G-5
Hydrogen crack *2	No *3	S-L	M-6	G-6

*1: Pre H₂ charge condition before fracture test



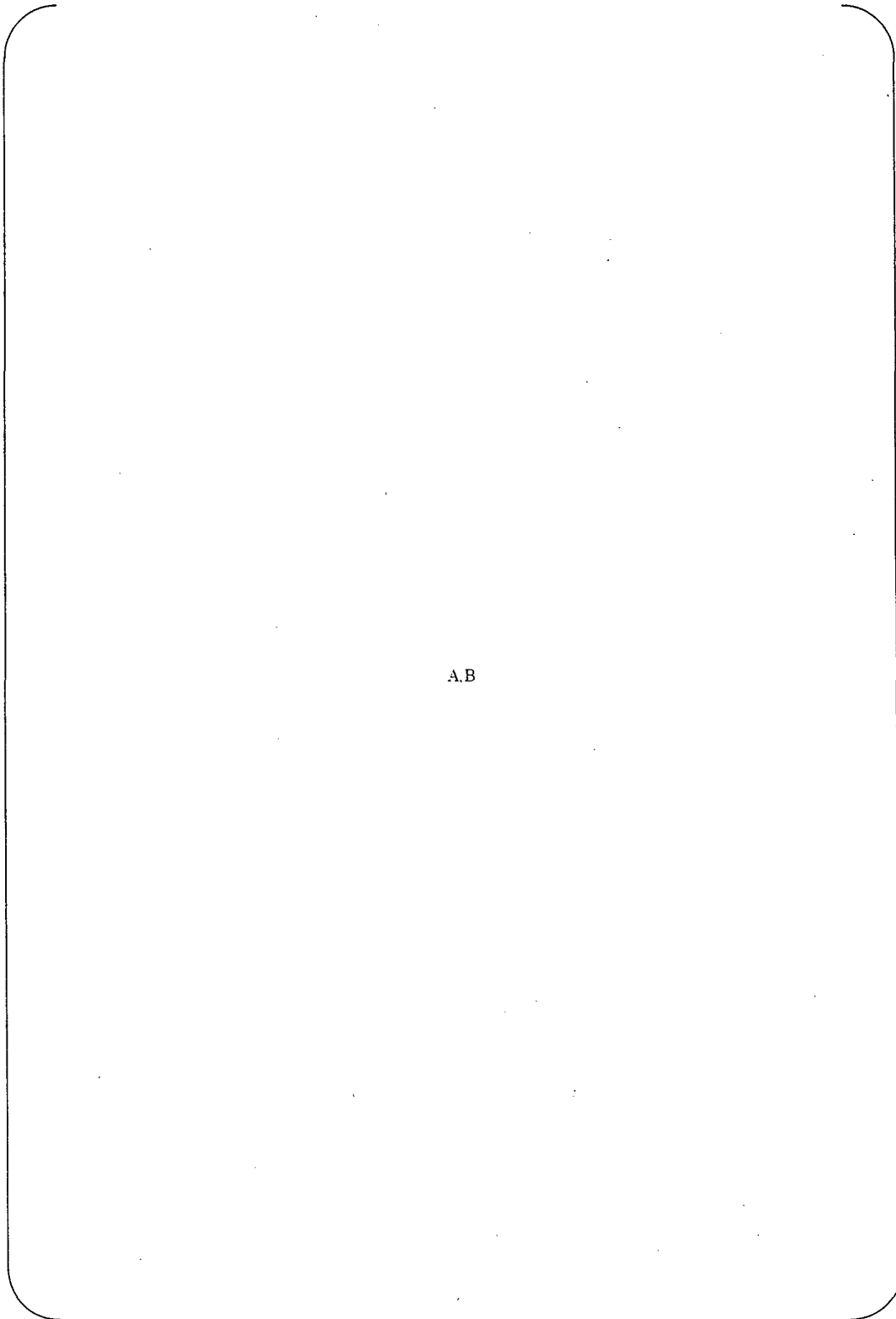
*2: Hydrogen crack is introduced at the same condition of M-1 and G-1 tests.

*3: Heat treatment to remove hydrogen from the specimen is conducted after hydrogen pre-cracking at 400°C for 4 hours.



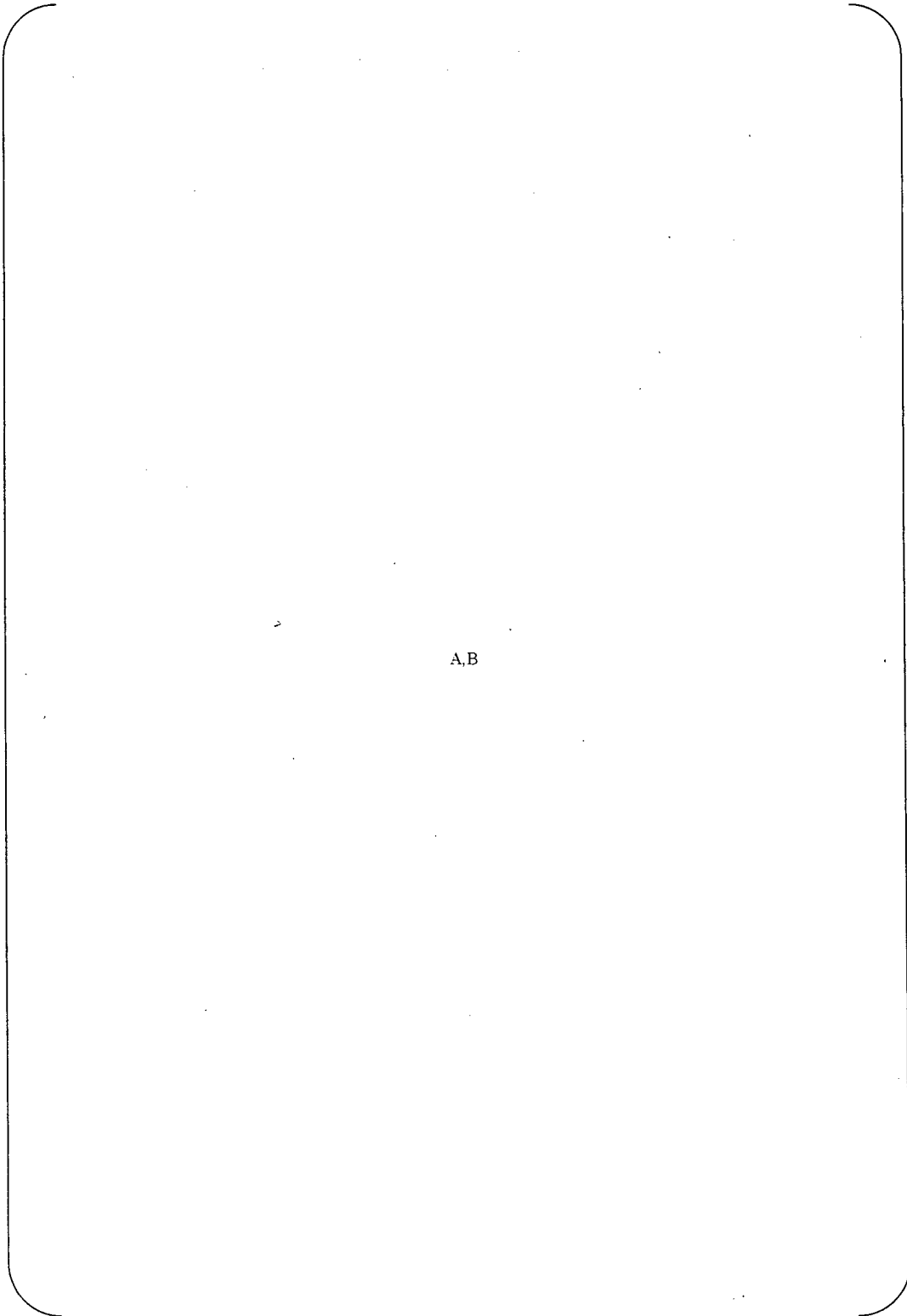
A,B

Fig.F.4-1 Photograph of fracture surface (M-1)



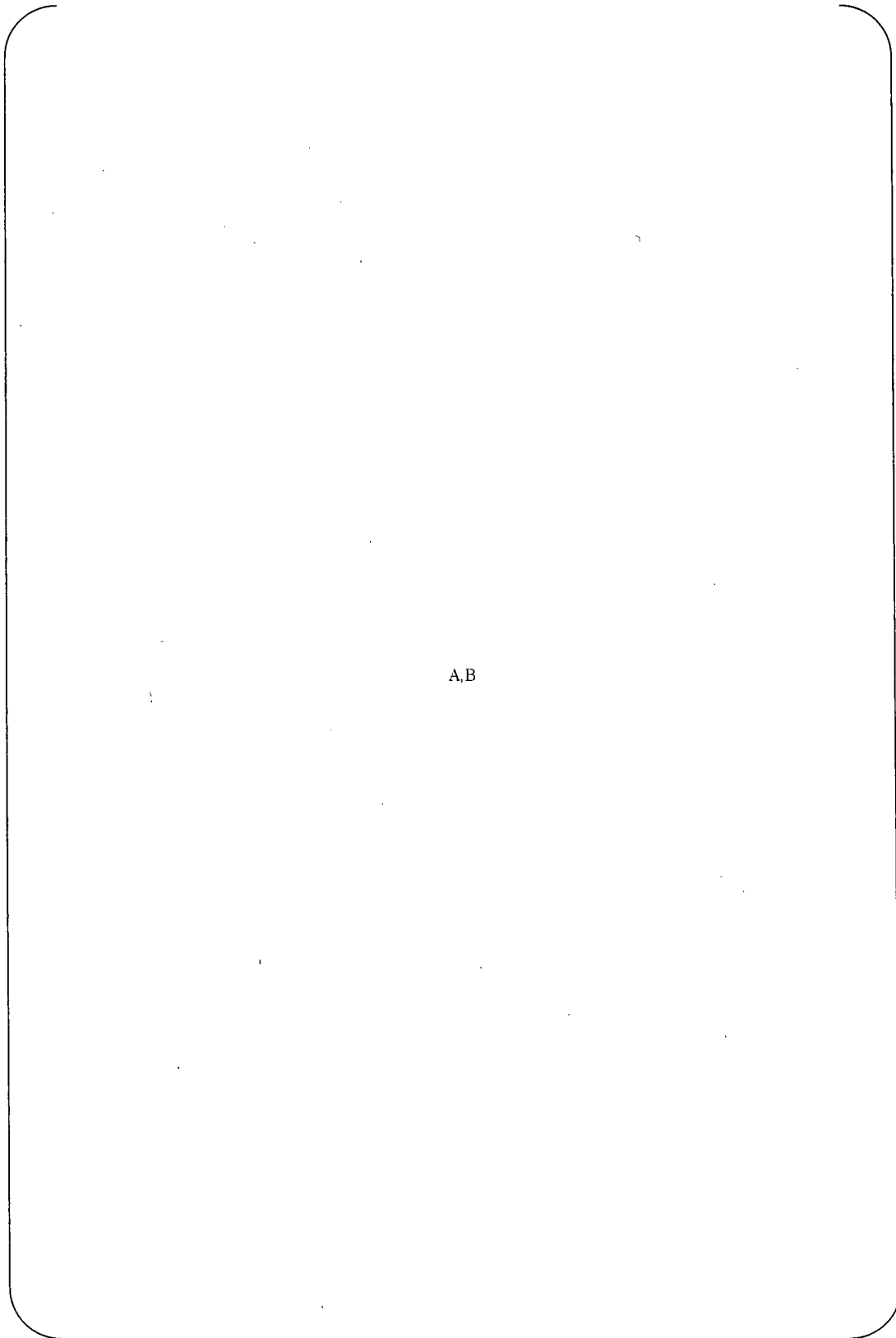
A.B

Fig.F.4-2 Photograph of fracture surface (G-1)



A,B

Fig.F.5-1 Photograph of fracture surface (M-6)



A,B

Fig.F.5-2 Photograph of fracture surface (G-6)



A,B

Fig.F.6-1 SEM observation of fracture surface of M-1



A,B

Fig.F.6-2 SEM observation of fracture surface of M-1



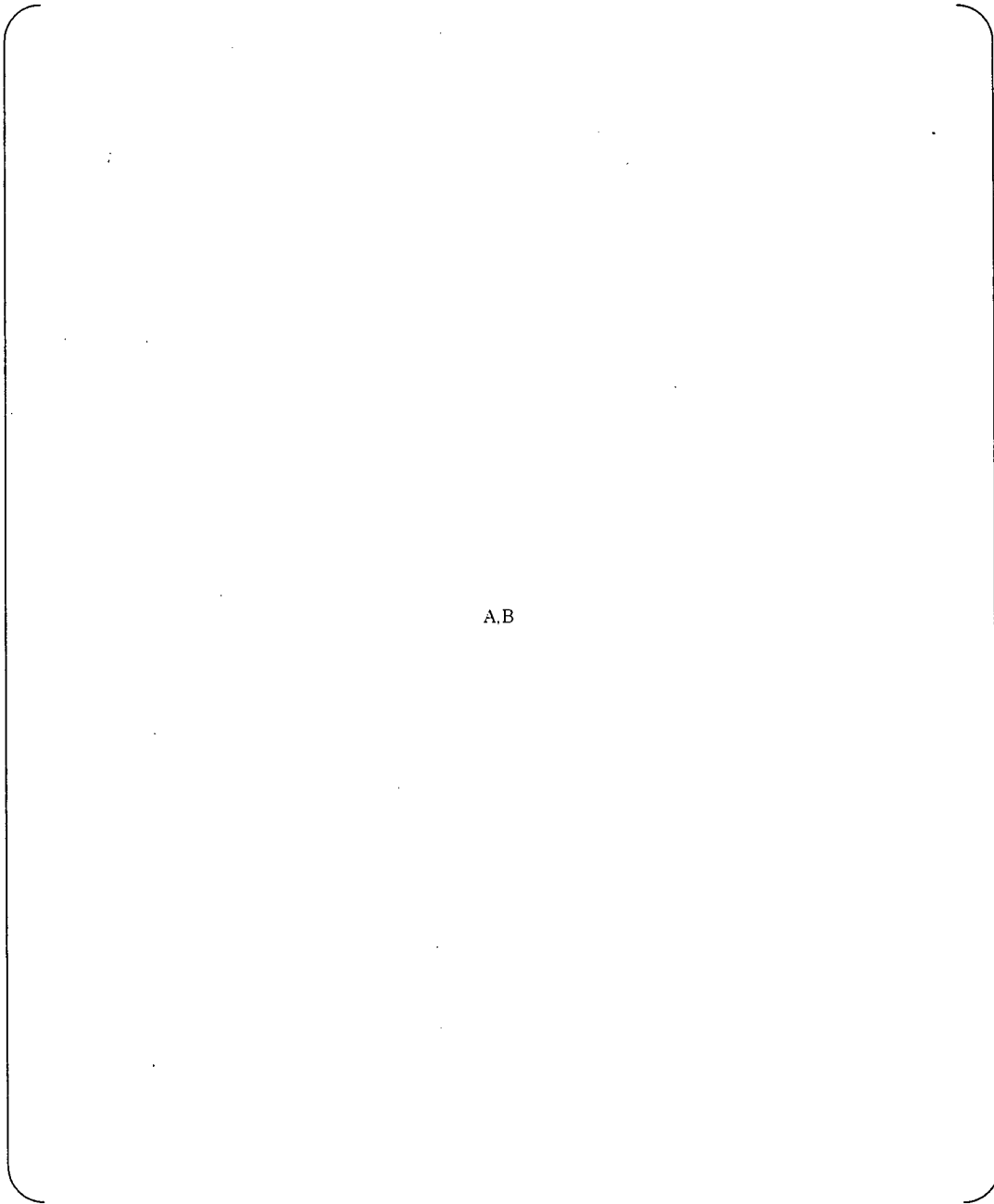
A,B

Fig.F.6-3 SEM observation of fracture surface of G-1



A,B

Fig.F.6-4 . SEM observation of fracture surface of G-1

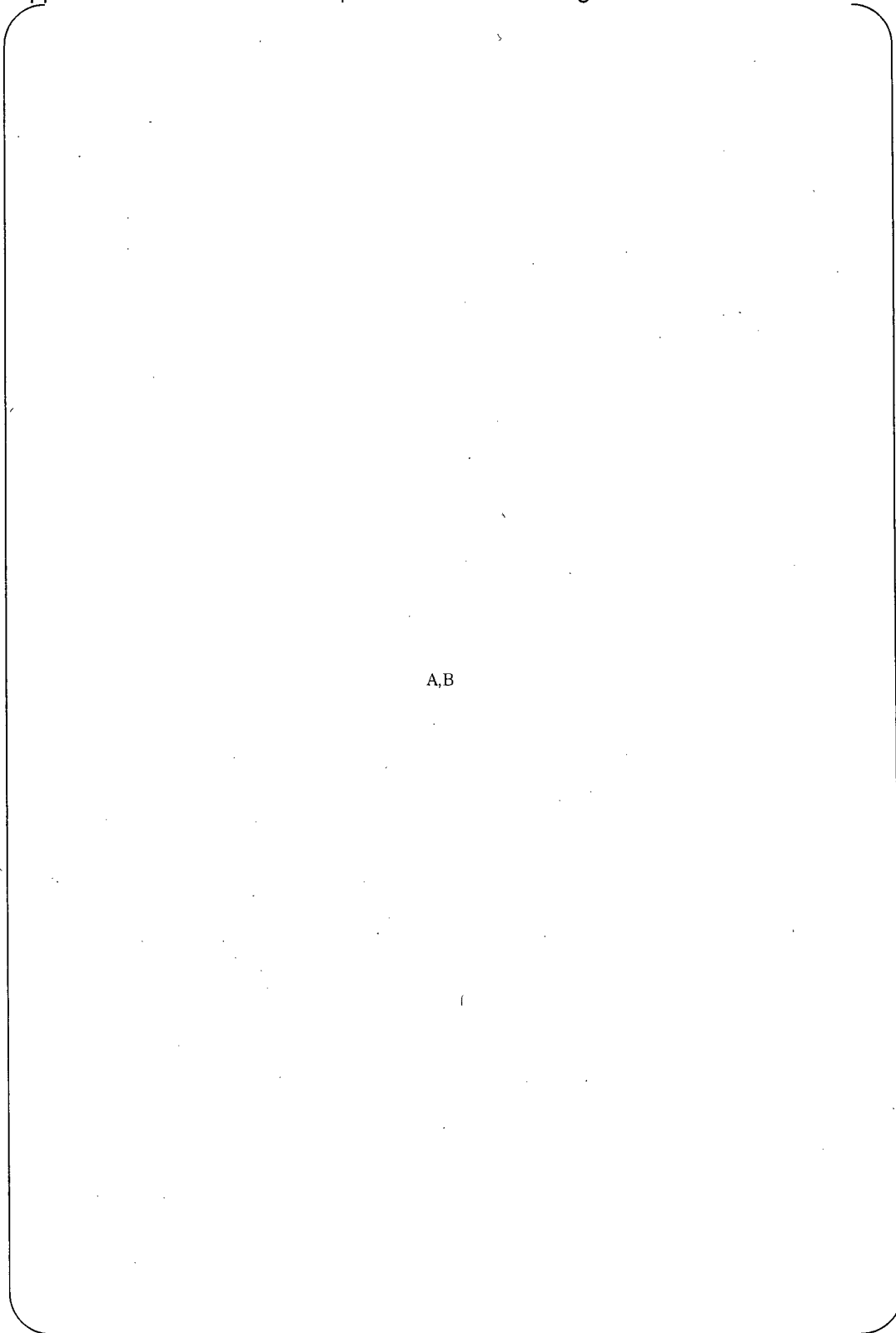


A.B

Fig.F.7 J-R curve of specimens after hydrogen pre-charge



Appendix-1 Load-Load line displacement curve during test



A,B

Fig.F.8 Load-Load line displacement curve

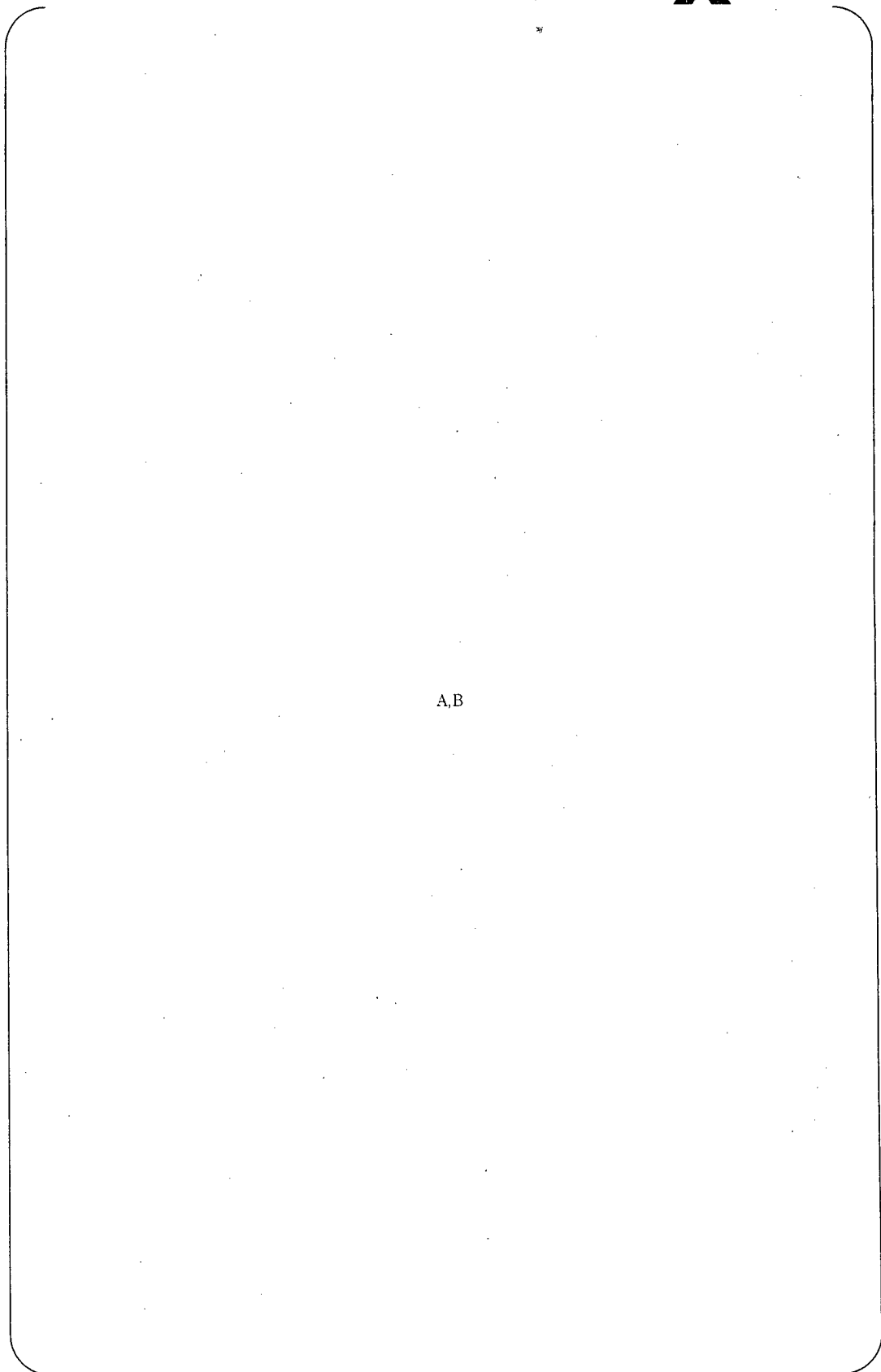
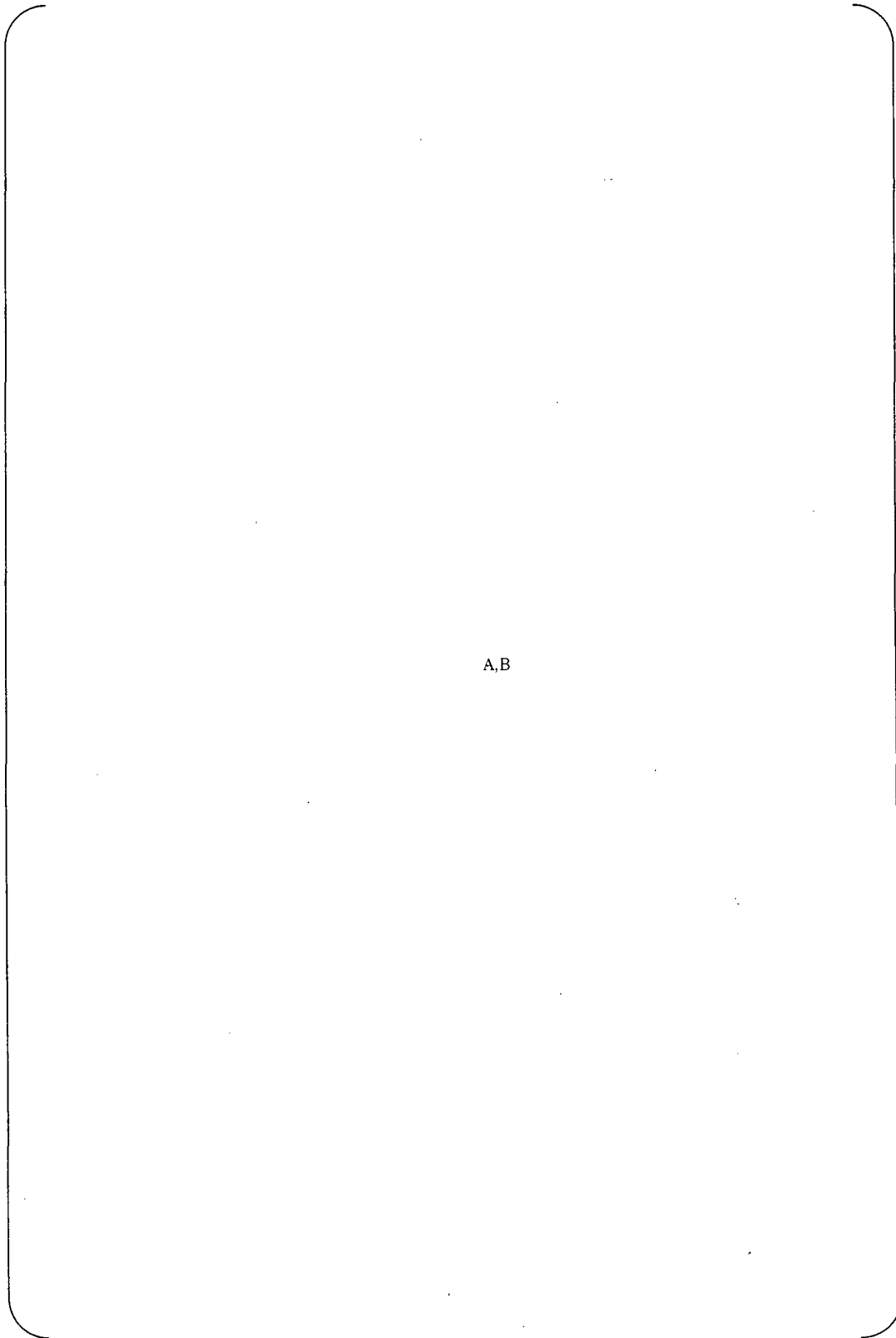


Fig.F.9 Load-Load line displacement curve



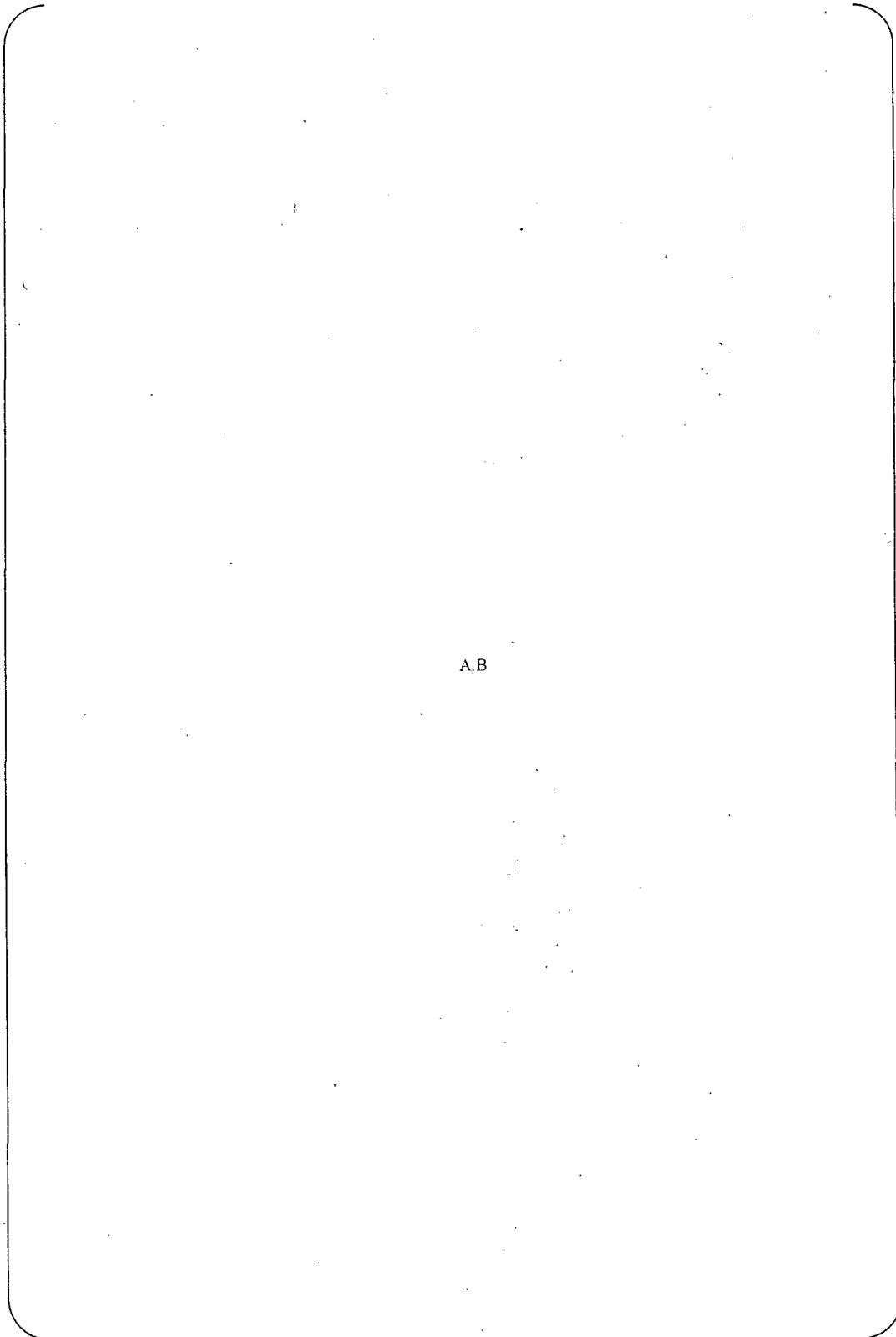
A,B

Fig.F.10 Load-Load line displacement curve



A,B

Fig.F.11 Load-Load line displacement curve



A,B

Fig.F.12 Load-Load line displacement curve



A,B

Fig.F.13 Load-Load line displacement curve (After remove hydrogen)

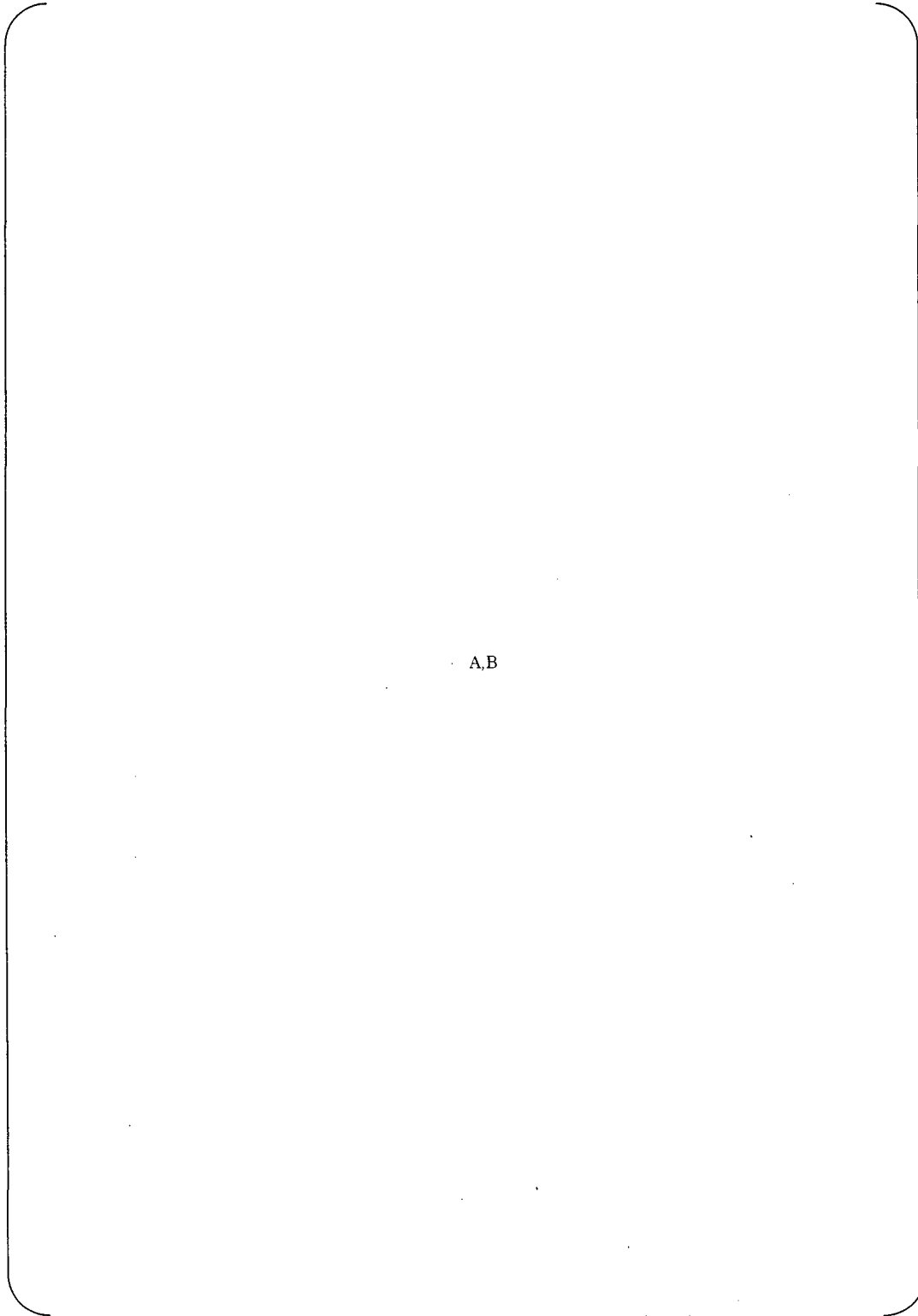


A,B

Fig.F.14 Load-Load line displacement curve (hydrogen crack test)

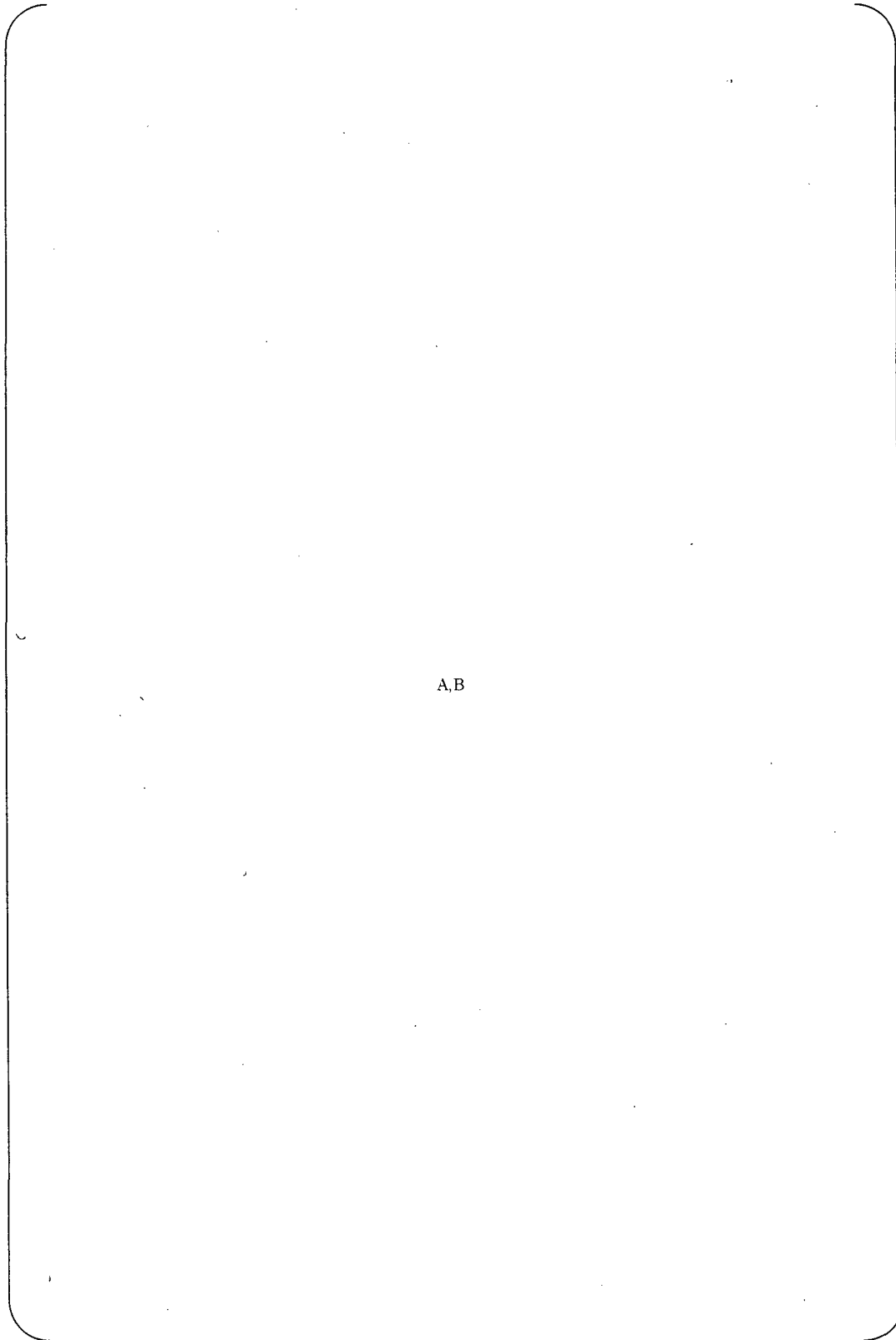


Appendix-2 Photograph of fracture surface



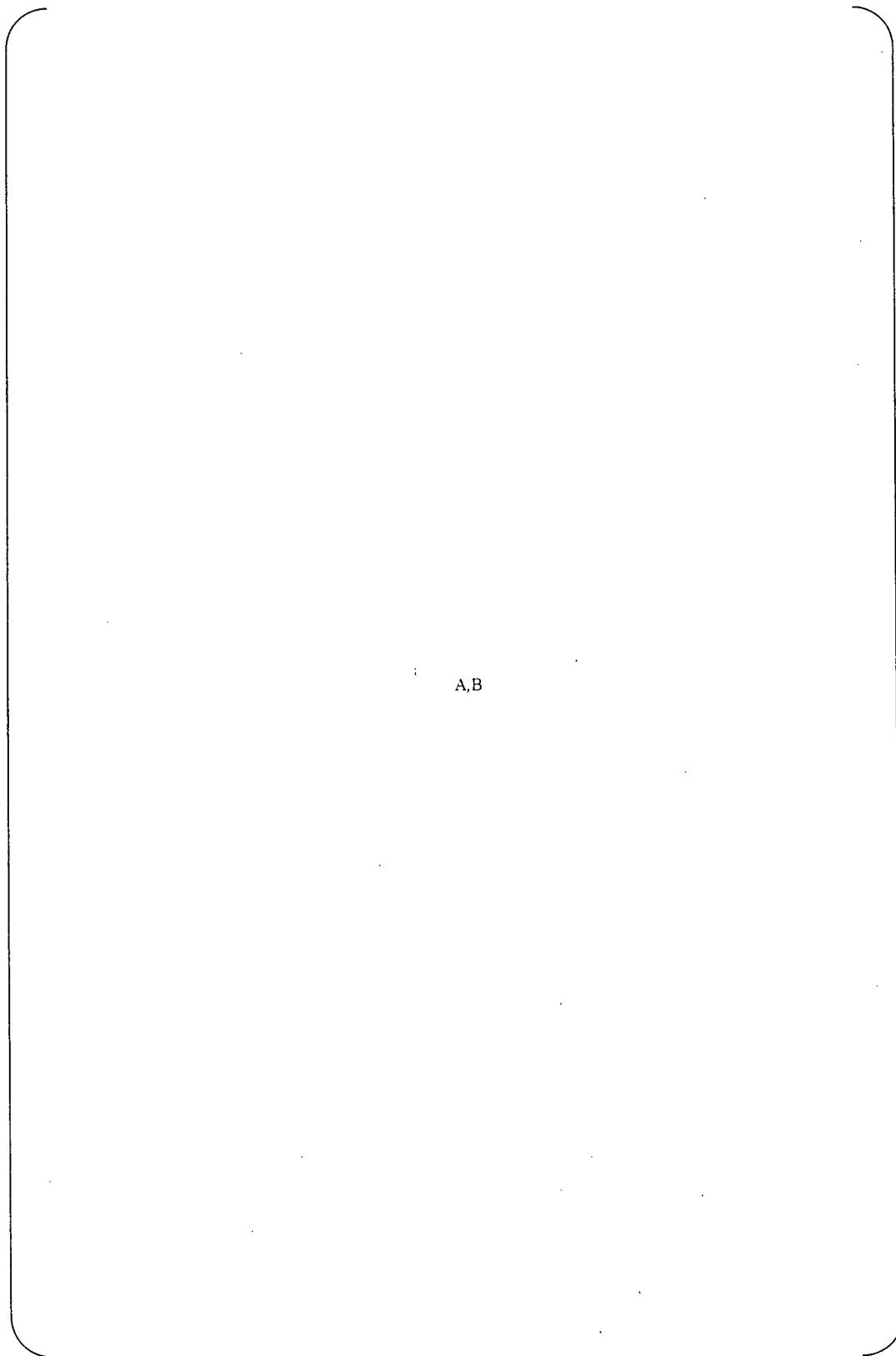
A,B

Fig.F.15-1 Photograph of fracture surface (M-2)



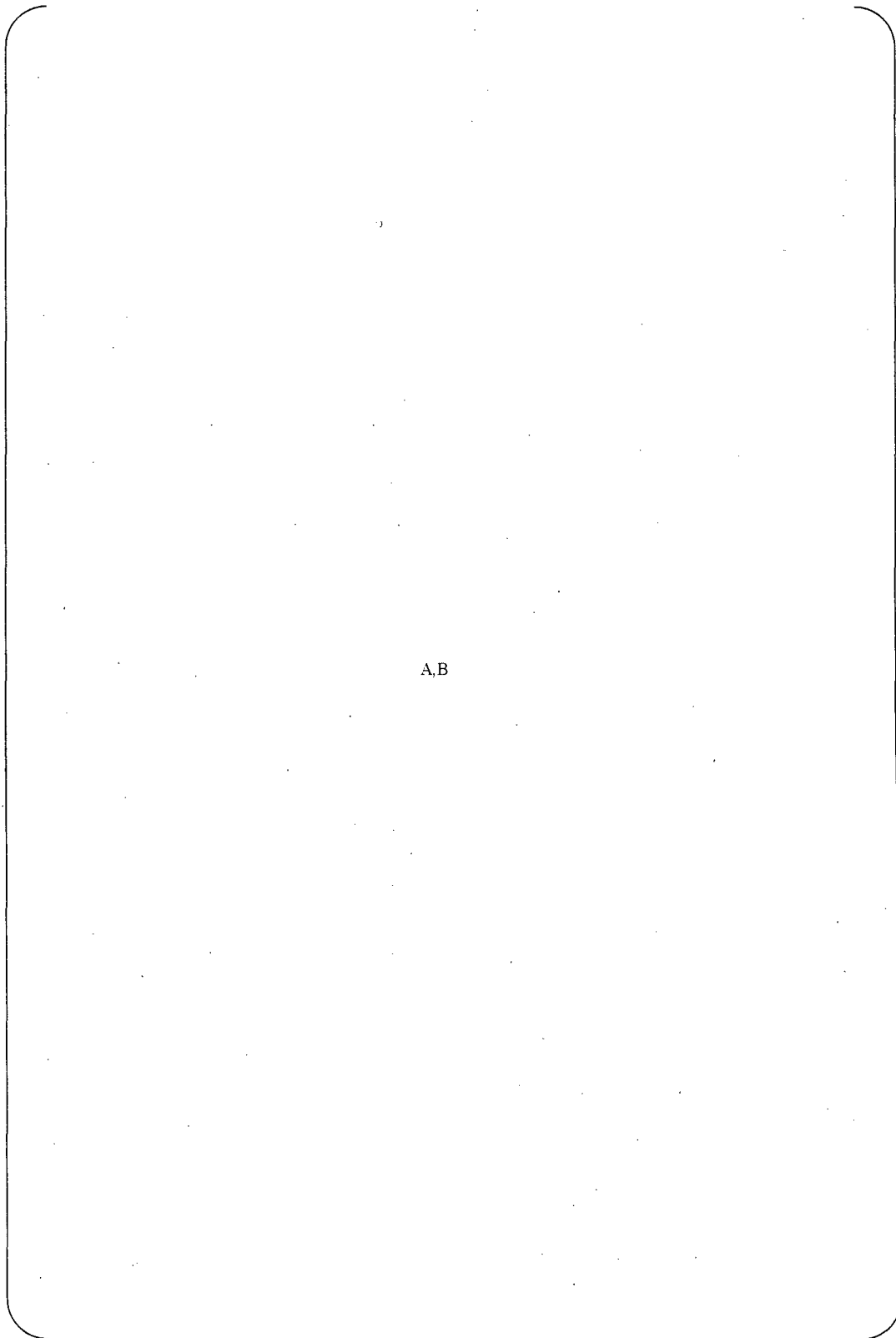
A,B

Fig.F.15-2 Photograph of fracture surface (G-2)



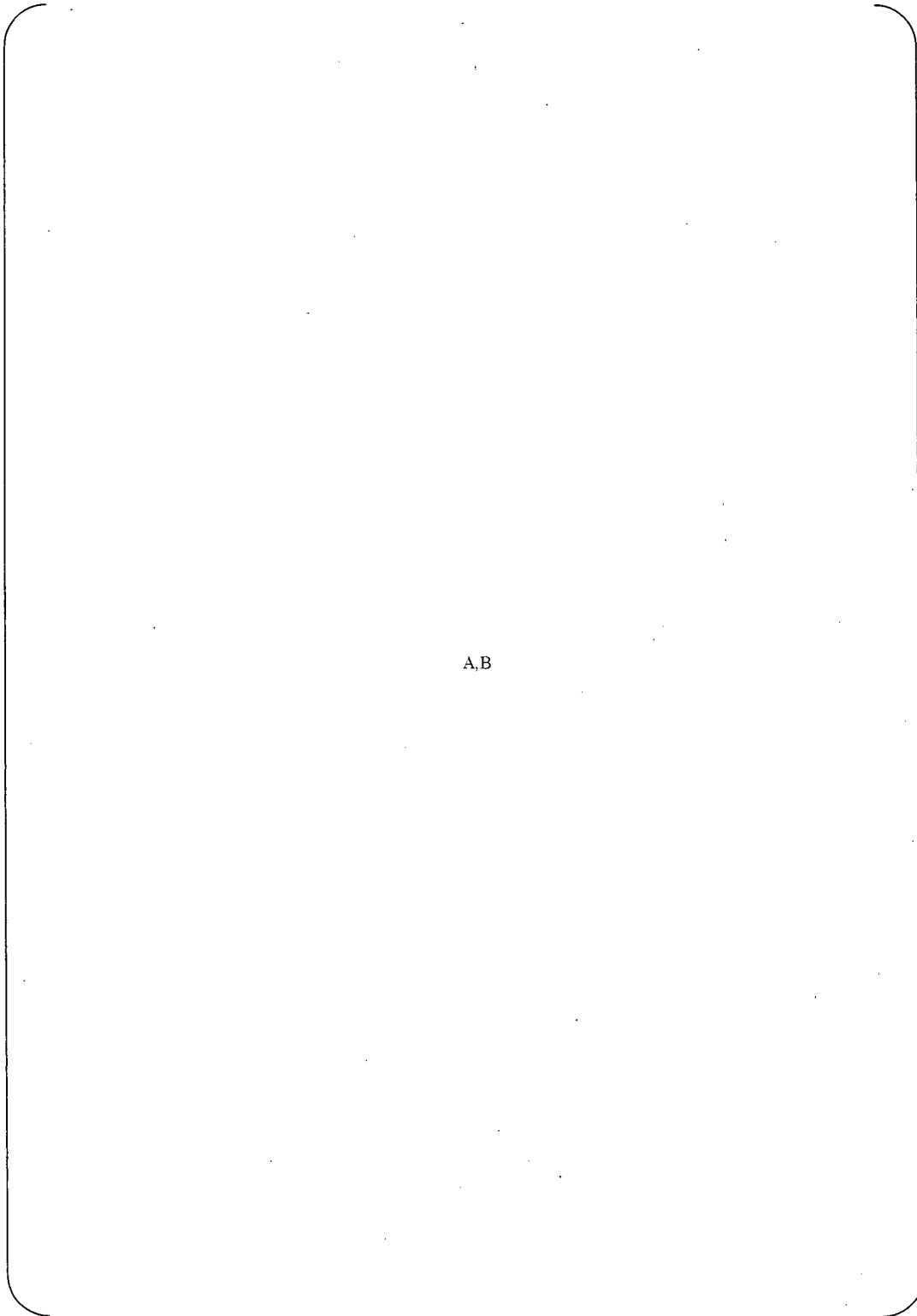
A,B

Fig.F.15-3 Photograph of fracture surface (M-3)



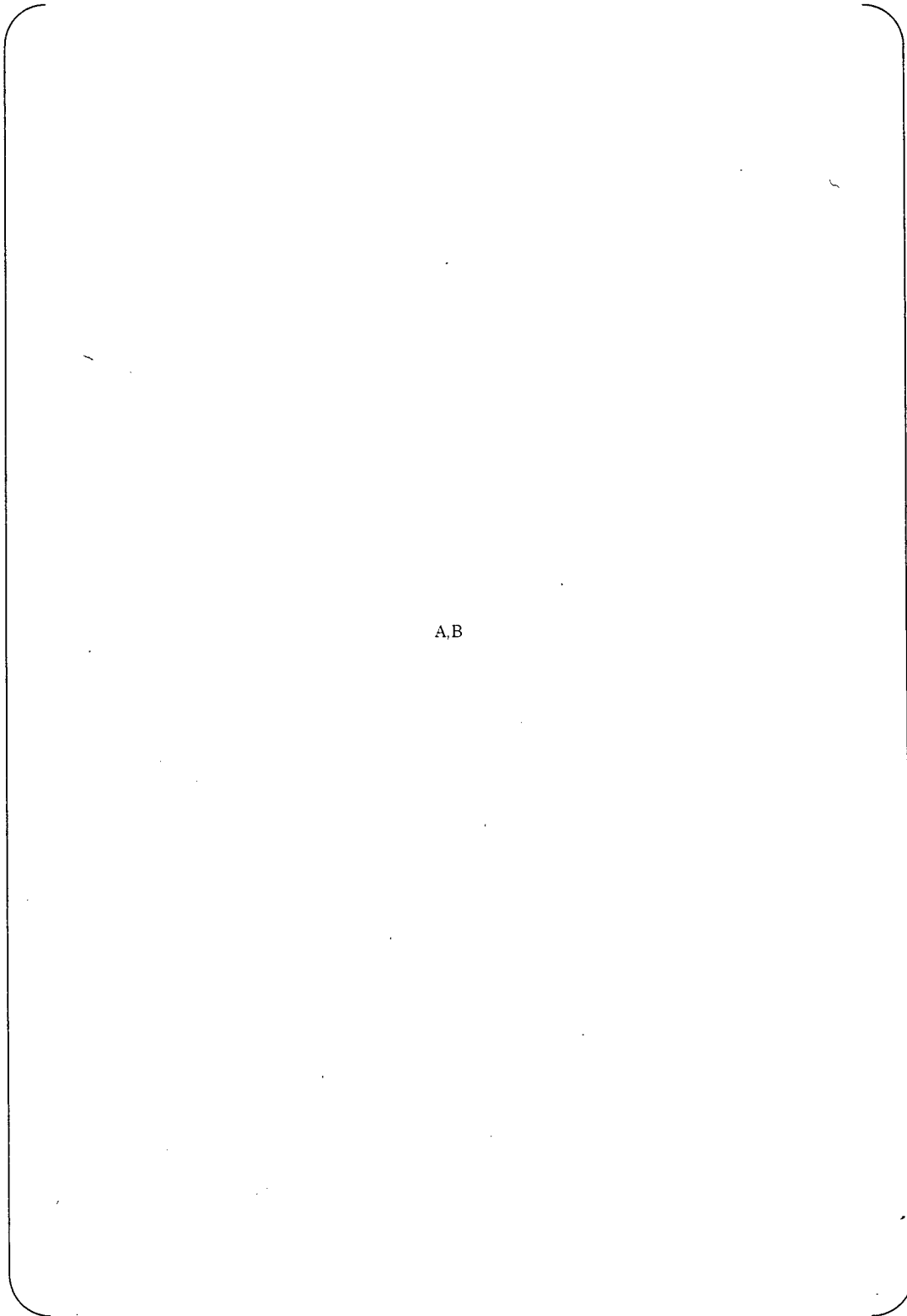
A,B

Fig.F.15-4 Photograph of fracture surface (G-3)



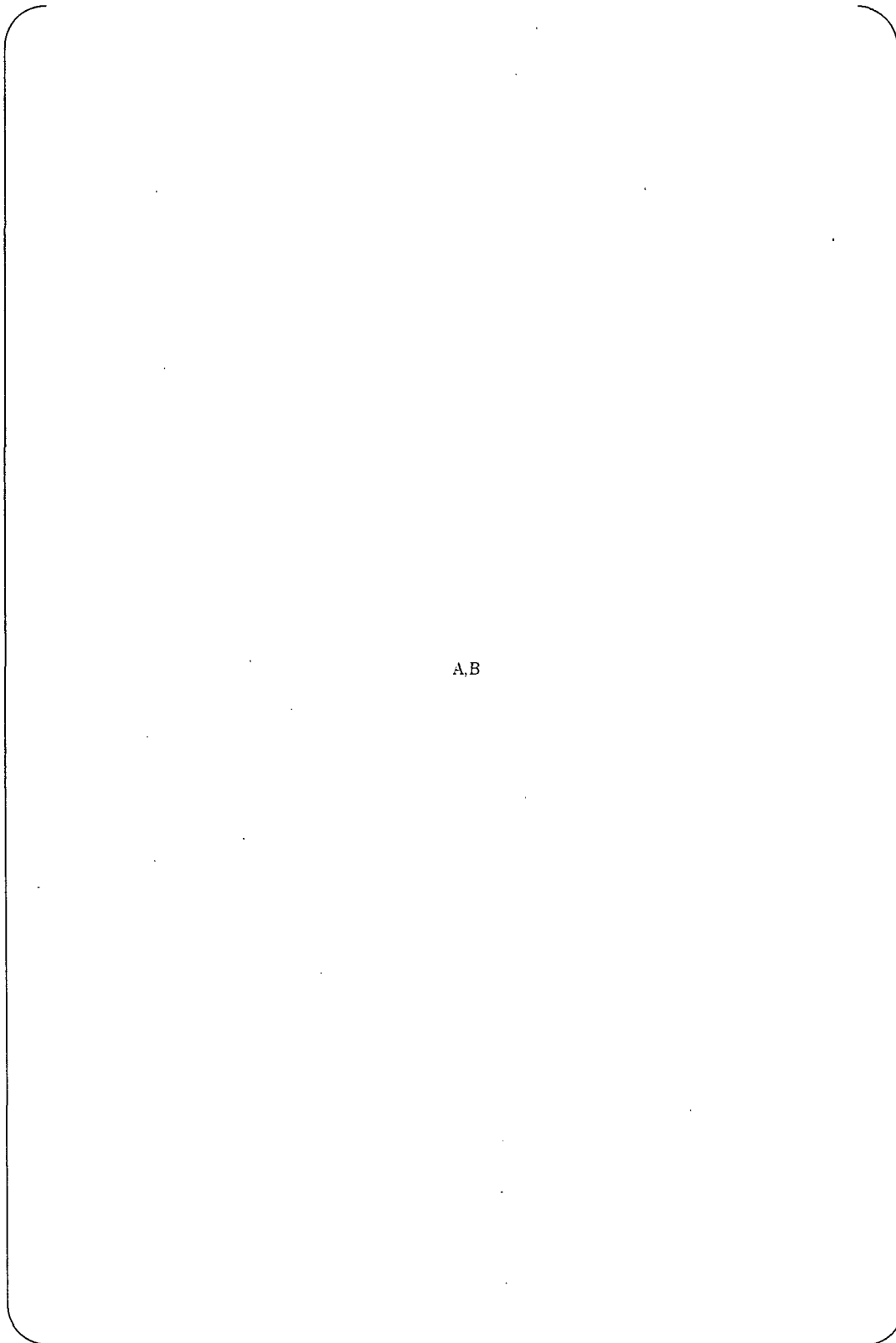
A,B

Fig.F.16-1 Photograph of fracture surface (M-4)



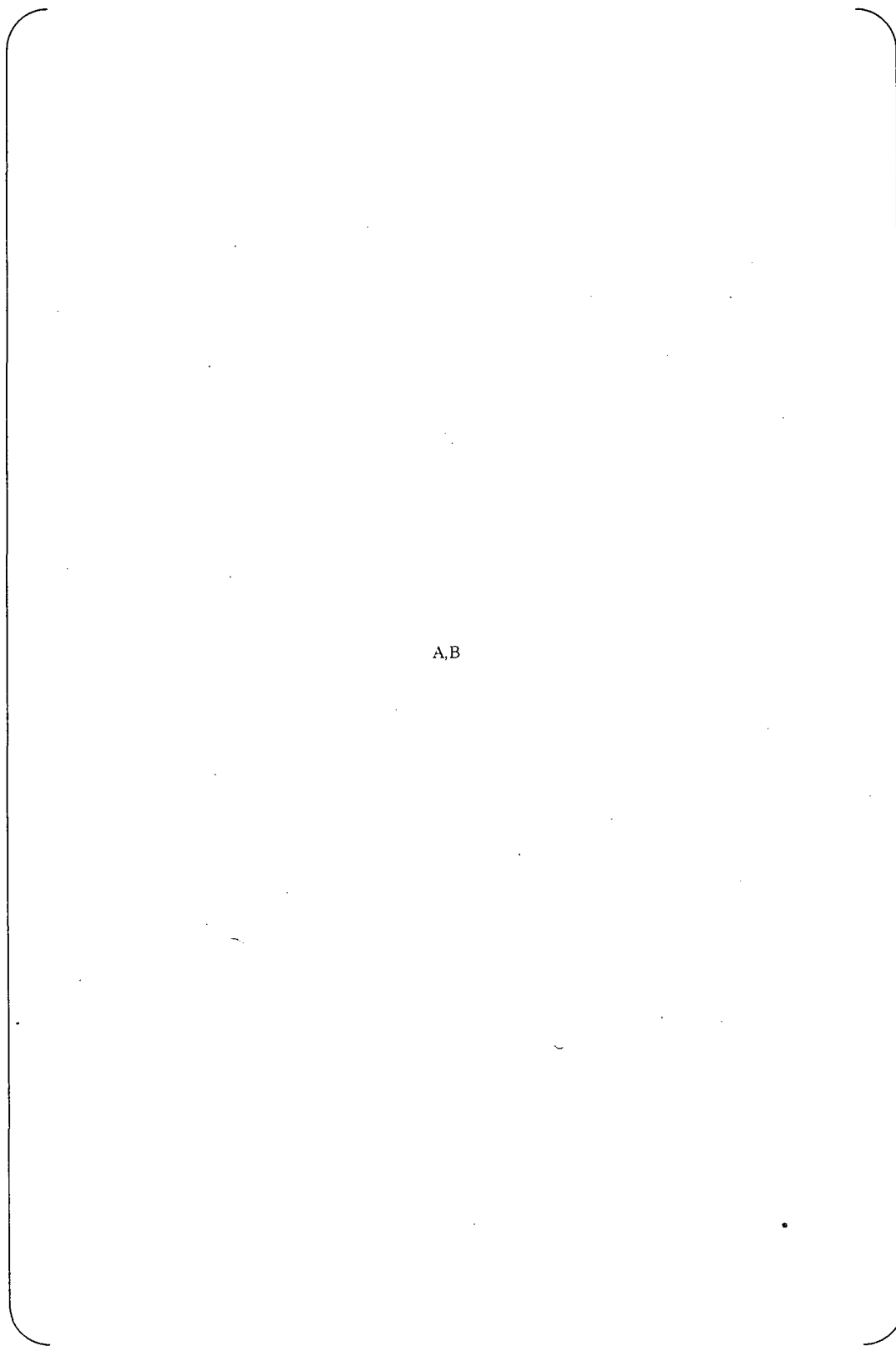
A,B

Fig.F.16-2 Photograph of fracture surface (G-4)



A,B

Fig. F.16-3 Photograph of fracture surface (M-5)

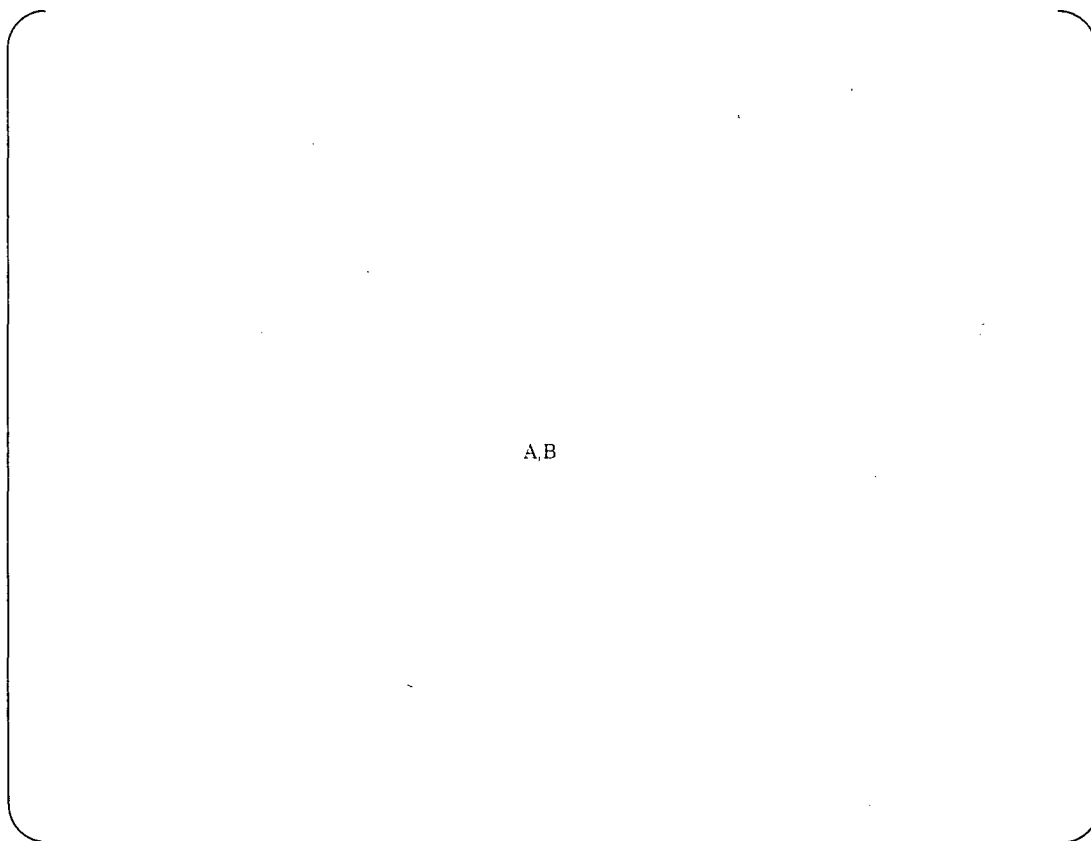


A,B

Fig.F.16-4 Photograph of fracture surface (G-5)

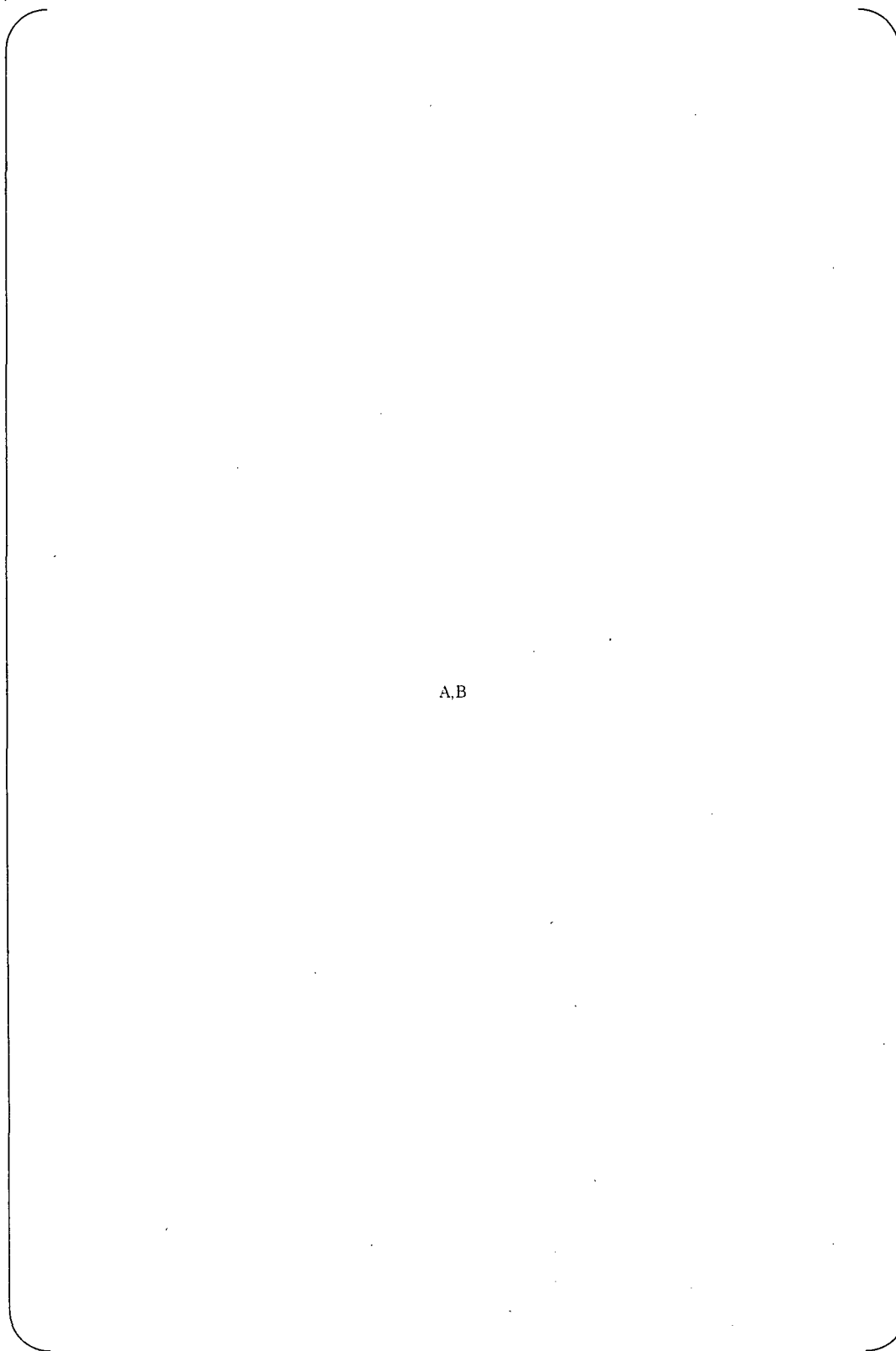


Appendix-3 Metallurgical examination of mockups



A,B

Fig .F.17 Macro-structure observation



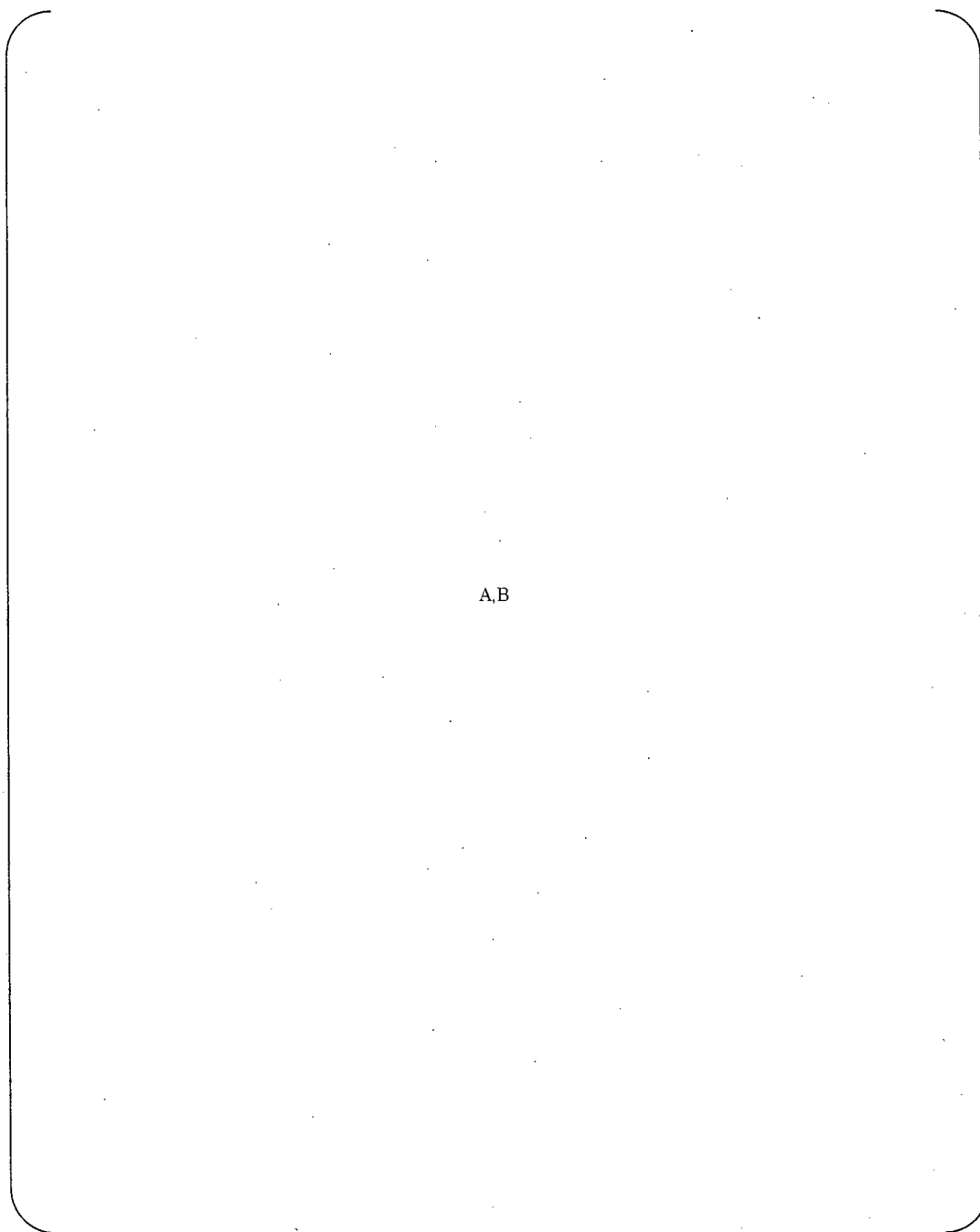
A,B

Fig. F.18 Micro-structure observation



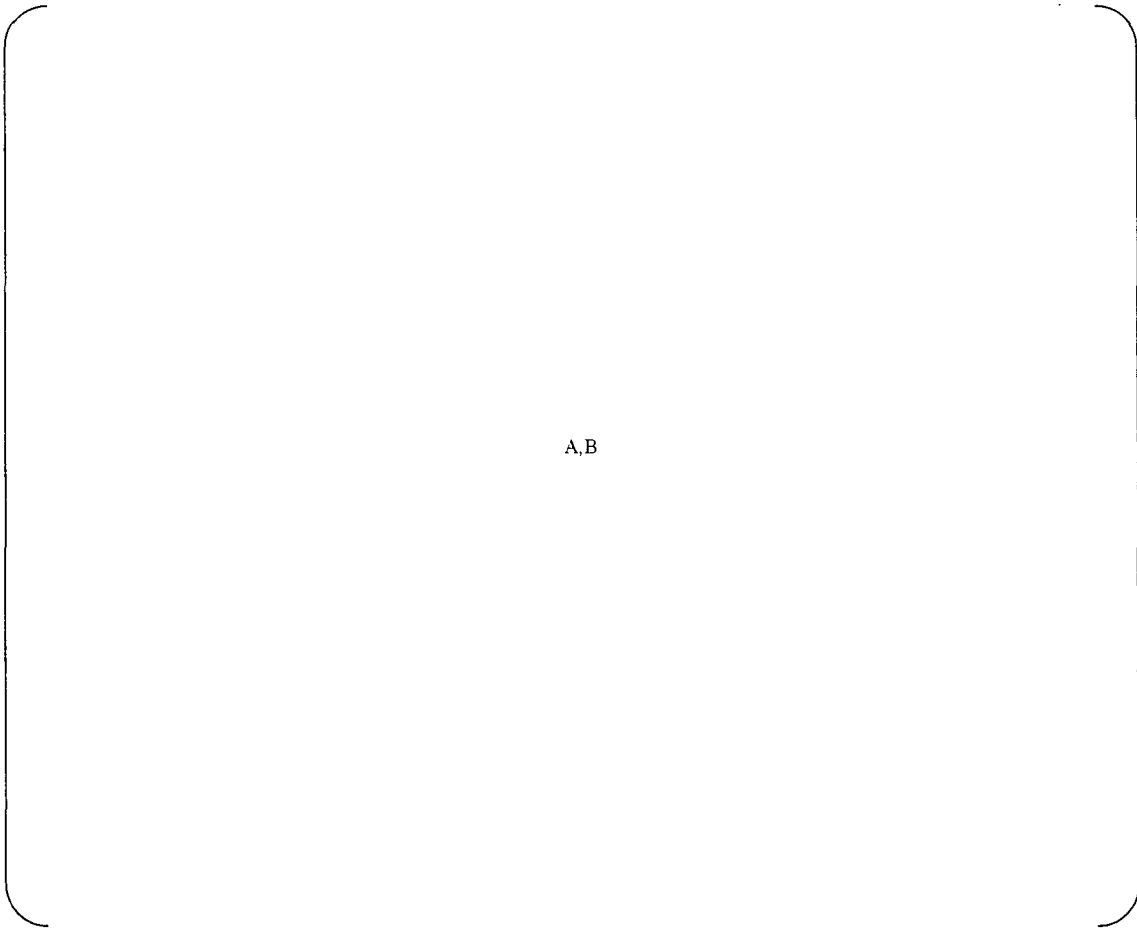
A,B

Fig. F.19-1 Result of Vickers hardness measurement



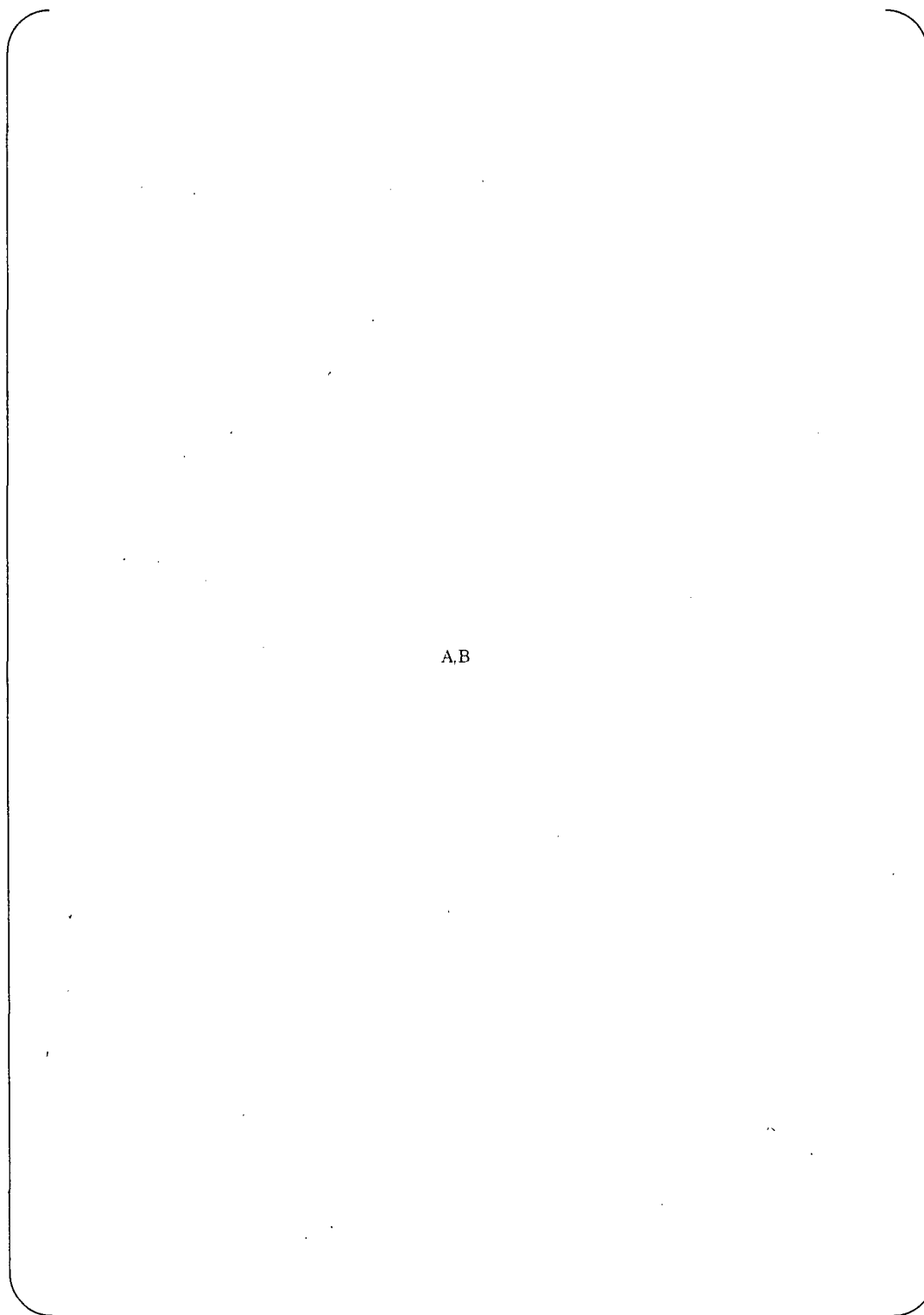
A,B

Fig. F.19-2 Result of Vickers hardness measurement



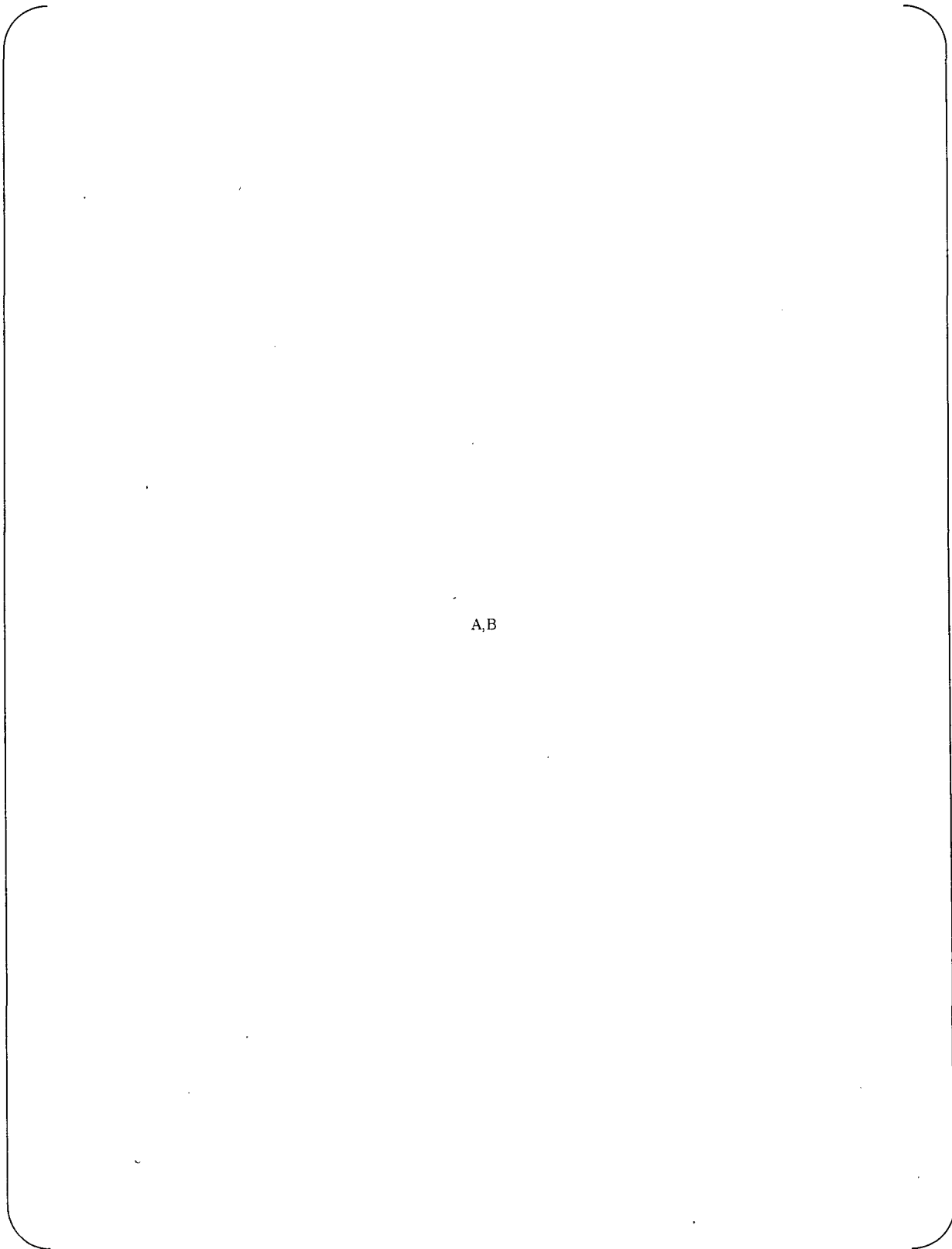
A,B

Fig .F.20 Macro-structure observation



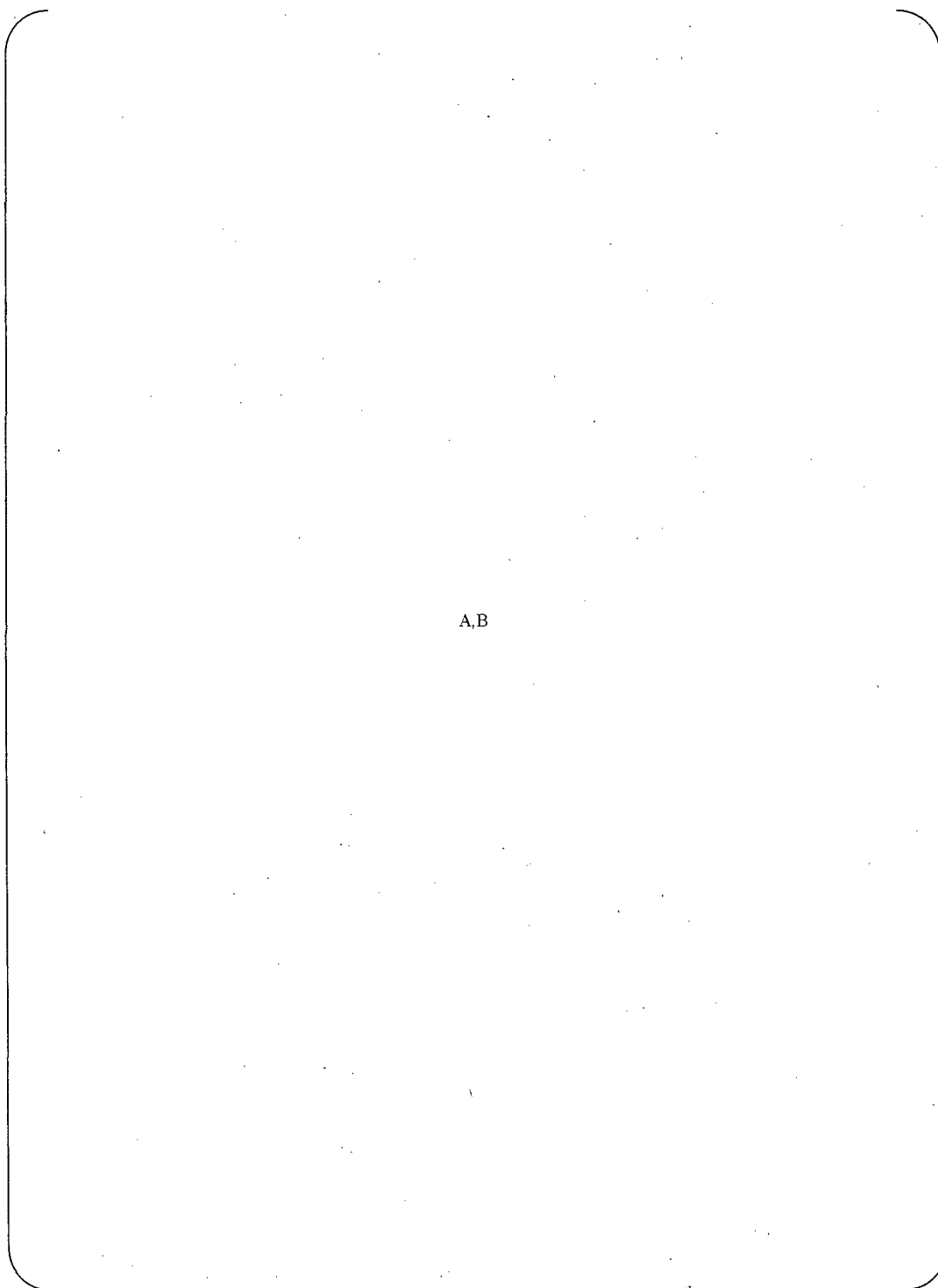
A.B

Fig. F.21 Micro-structure observation



A,B

Fig. F.22-1 Result of Vickers hardness measurement

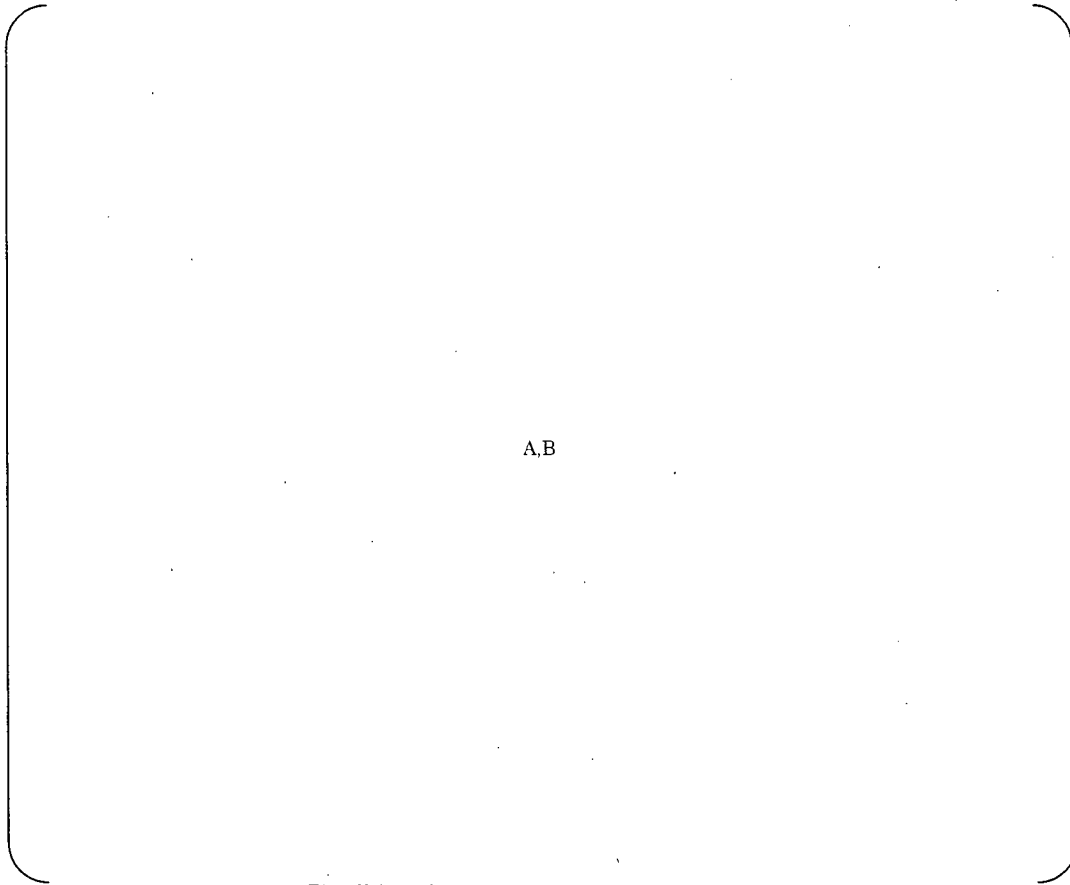


A,B

Fig. F.22-2 Result of Vickers hardness measurement



Appendix-4 Metallurgical examination of tested specimen



A,B

Fig. F.23 Macro-structure observation



A,B

Fig. F.24-1 Micro-structure observation



A,B

Fig. F.24-2 Micro-structure observation



A,B

Fig. F.25-1 Result of Vickers hardness measurement



A,B

Fig. F.25-2 Result of Vickers hardness measurement



Attachment-G

Buttering Mock Up Test



1. Purpose

The purpose of this report is to provide the investigation results of test coupons which are welded by using coated electrode with moisture absorption for hydrogen cracking.

2. Test coupon

Schematic illustrations of the test coupons are shown in Figure G.1. The stainless steel clad by ESW was removed by gouging and grinding (TC H-G) or machining (TC H-M). 152 buttering was performed by SMAW using coated electrode with moisture absorption. Moisture absorption condition and welding condition is shown in Table G.1.

3. Investigation Methodology

The investigation methodology matrix of test coupon was summarized in Table G.2

4. Results of investigation

Table G.3 shows the result of ultrasonic inspection of test coupons. Any significant indications were not inspected in both coupons.

Figures G.2 show macro-structure of cross section of test coupons. Any significant cracks or defects were not observed in both test coupons.

Figure G.3 shows micro-structure of cross section of test coupons. Any significant difference between the coupons was not observed in microstructure. There is no abnormality in microstructure of 152 buttering and LAS base metal.

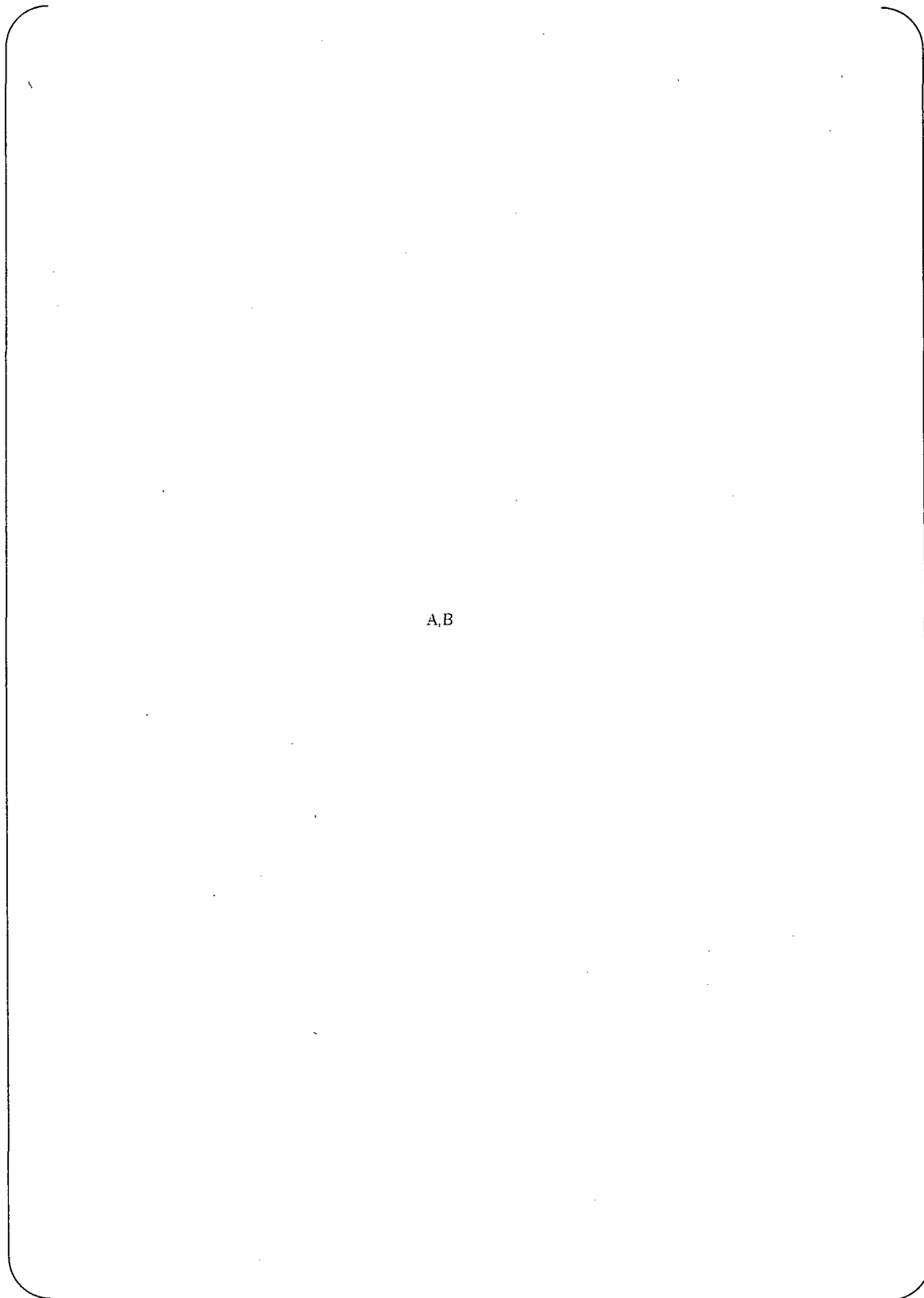
Figure G.4 shows the results of Vickers hardness test. Any significant difference between the coupons was not confirmed in hardness distribution. There is no abnormality in hardness of 152 buttering and LAS base metal.

5. Summaries of the investigation

1) Hydrogen cracking was not observed in ultrasonic inspection test and macrostructure observation in this test (T-5).

2) Any significant differences in microstructure and hardness were not confirmed between the test coupons.

3) There is no abnormality in microstructure and hardness in test coupons.



A,B

Figure G.1 Schematic illustration of test coupons.

A, B

[illegible]

Table G.2 Investigation Methodology of test coupon

Item	Method	Purpose
Ultrasonic inspection	Ultrasonic inspection from surface	Inspect the crack occurrence
Macro-structure	Visual examination of the cross-section at low magnification after etching	Evaluate the macro-structure of the materials and crack occurrence
Micro-structure	Visual examination of the cross-section at high magnification after etching	Evaluate the micro-structure of near the fusion boundary
Hardness	Measure Vickers hardness	Evaluate the hardness distribution near the fusion boundary and HAZ



Table G.3 The results of ultrasonic inspection test

Test coupon No	Removal process for stainless steel clad	Results of ultrasonic inspection	
		After buttering	48Hr later
H-G	Gouging and grinding	No indication	No indication
H-M	Machining	No indication	No indication



A,B

Figure G.2(1) Macro-structure of cross section of test coupon (Gouging and grinding)



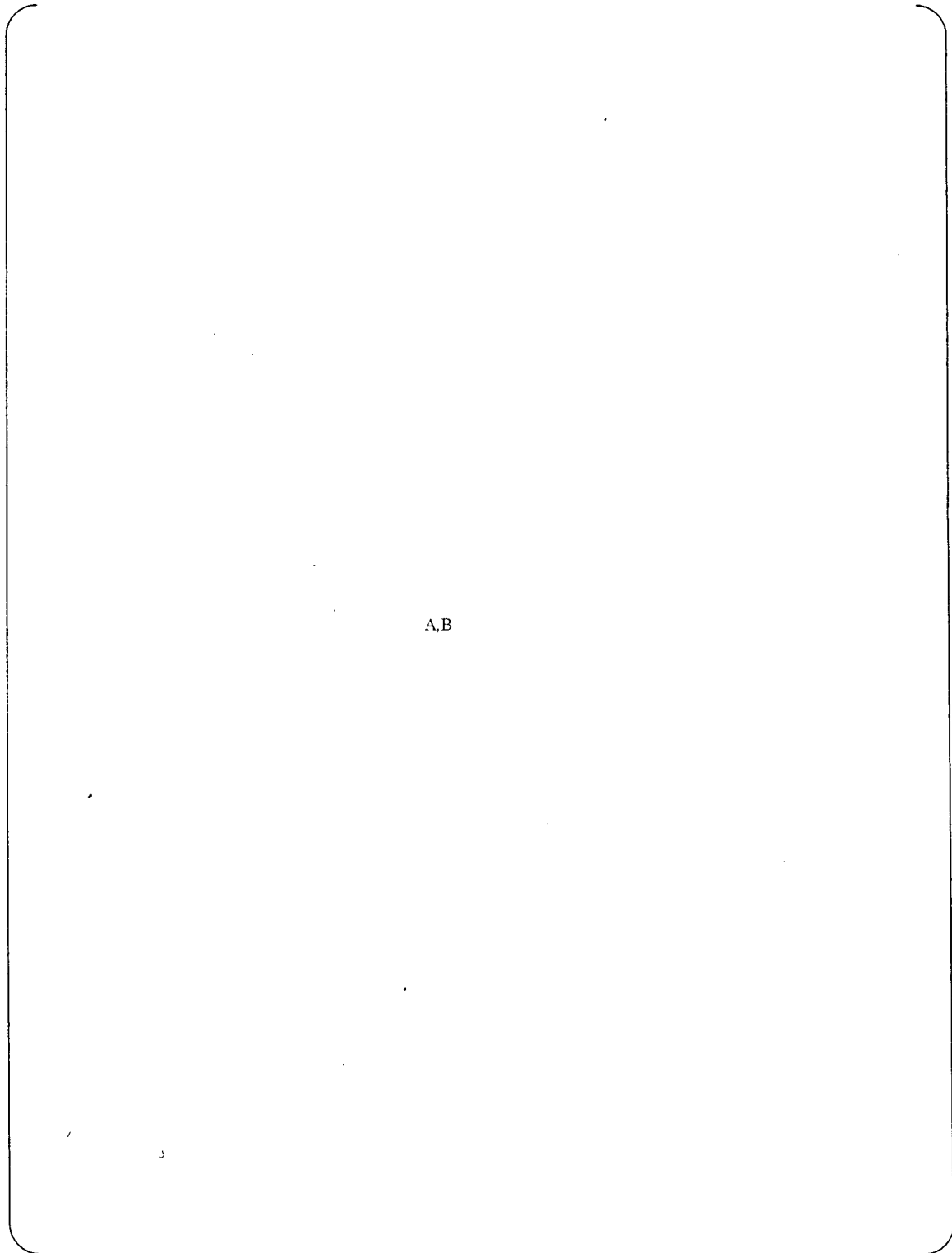
A,B

Figure G.2(2) Macro-structure of cross section of test coupon (Machining)



A,B

Figure G.3 Micro-structure of cross section of test coupons



A,B

Figure G.4 Vickers hardness of cross section of test coupons



Attachment-H

Tensile Restraint Cracking Test



1. Purpose

The purpose of this report is to provide the investigation results of tensile restraint cracking (TRC) test.

2. Testing procedure

Figure H.1 shows appearance of TRC testing machine. The load was applied and held by oil hydraulic cylinder. Figure H.2 shows shape of TRC test piece. Tensile load was applied on test piece immediately after welding. Moisture absorption condition of electrode and welding condition and loading condition were shown in Table H.2. Gouging condition was shown in Table H.3.

3. Investigation Methodology

The investigation methodology matrix of test pieces after testing was summarized in Table H.1

Table H.1 Investigation Methodology

Item	Method	Purpose
Fracture surface	Visual examination at low magnification	Evaluate the macro-structure of the fracture surface
Separation surface	SEM (Scanning Electron Microscope) examination at high magnification	Evaluate the micro-structure of the fracture surface
Micro-structure	Optical microscopic observation of the cross-section at high magnification after etching	Evaluate the micro-structure near the fracture surface

4. Results of testing

Figure H.3 shows results of TRC test. In normal groove type, with decreasing load, rupture time became longer. Rupture did not occur below certain load.

It seemed that the carbon addition and gouging of groove surface accelerates the rupture occurrence. It was assumed that the hardening in transition zone, which was caused by carbon addition and remained carbon by gouging as shown in Attachment J "Carbon Residue Influence on Fusion Boundary Hardness", affects the rupture behavior.

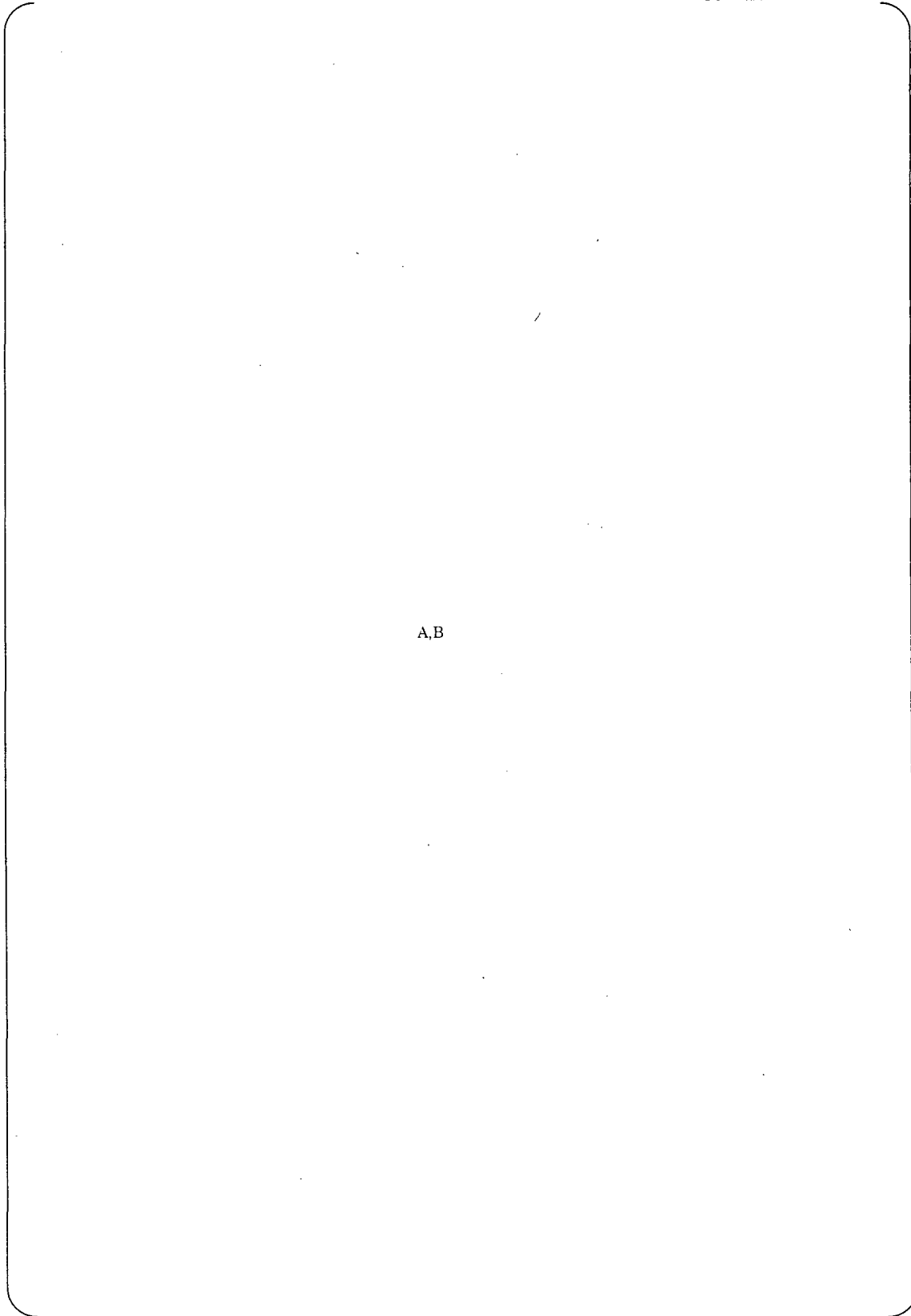
Figure H.4 shows SEM pictures of fracture surface of TRC test piece. The fracture surface revealed relatively flat fracture morphology similar to the separation observed in boat samples collected from Unit 3 RSG as shown in Attachment A "Unit 3 As-Built Sample Investigation". The fracture surface revealed quasi-cleavage fracture surface as observed in boat samples.



Figure H.5 shows micro-structure of cross section of test piece ruptured. It was observed that the rupture had been occurred adjacent to fusion boundary between 152 weld metal and LAS base metal as observed in boat samples collected from Unit 3 RSG. It was supposed that the separation which occurred in Unit 3 was reproduced by TRC test.

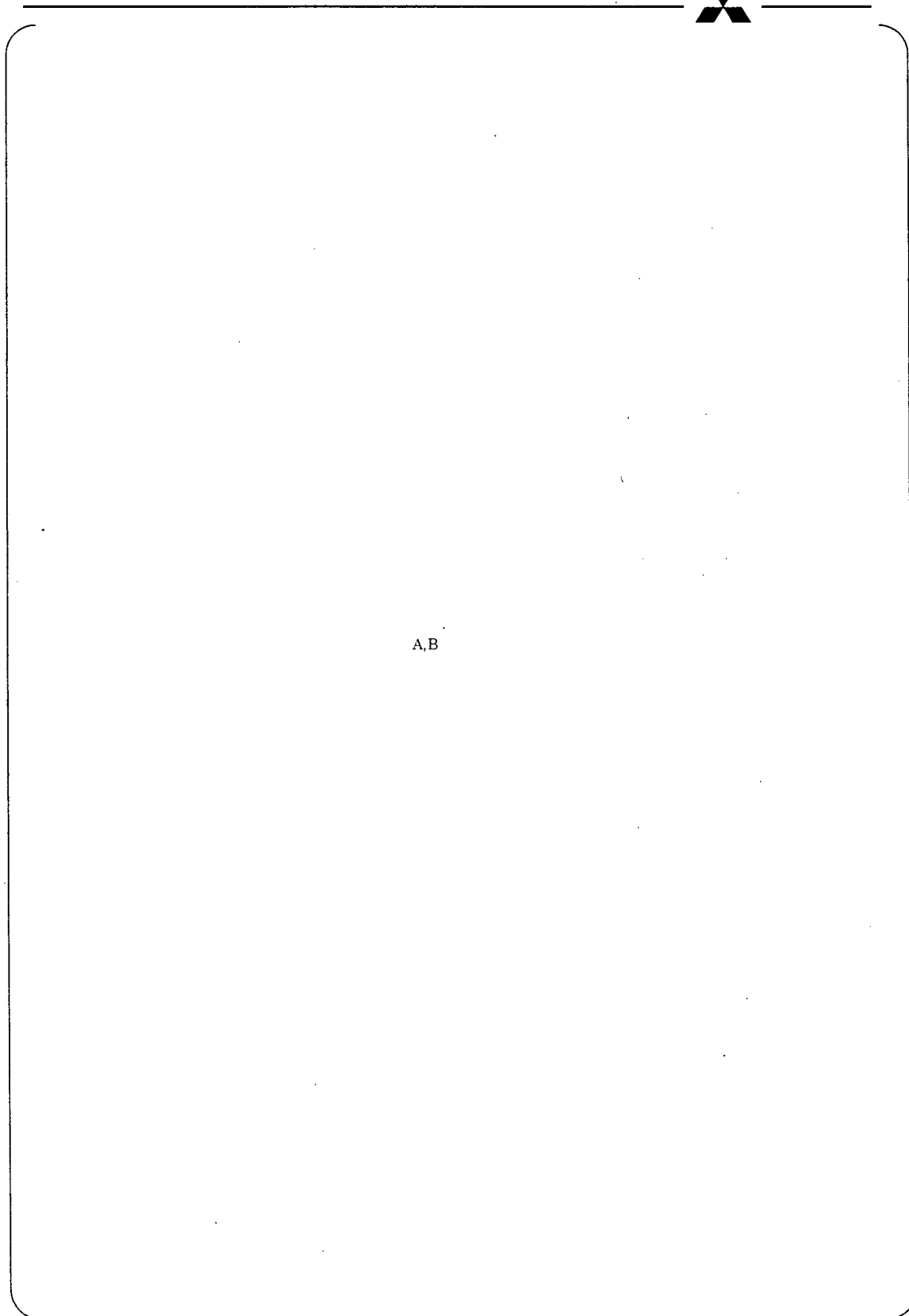
5. Summaries of the investigation

- 1) It was presumed that the separation occurred in Unit 3 RSG was reproduced by TRC test.
- 2) It seems that the carbon addition and gouging of groove surface affect the possibility for occurrence of separation.



A,B

Figure H.1 Appearance of TRC testing machine.



A,B

Figure H.2 Shape of TRC test piece

A,B

A,B

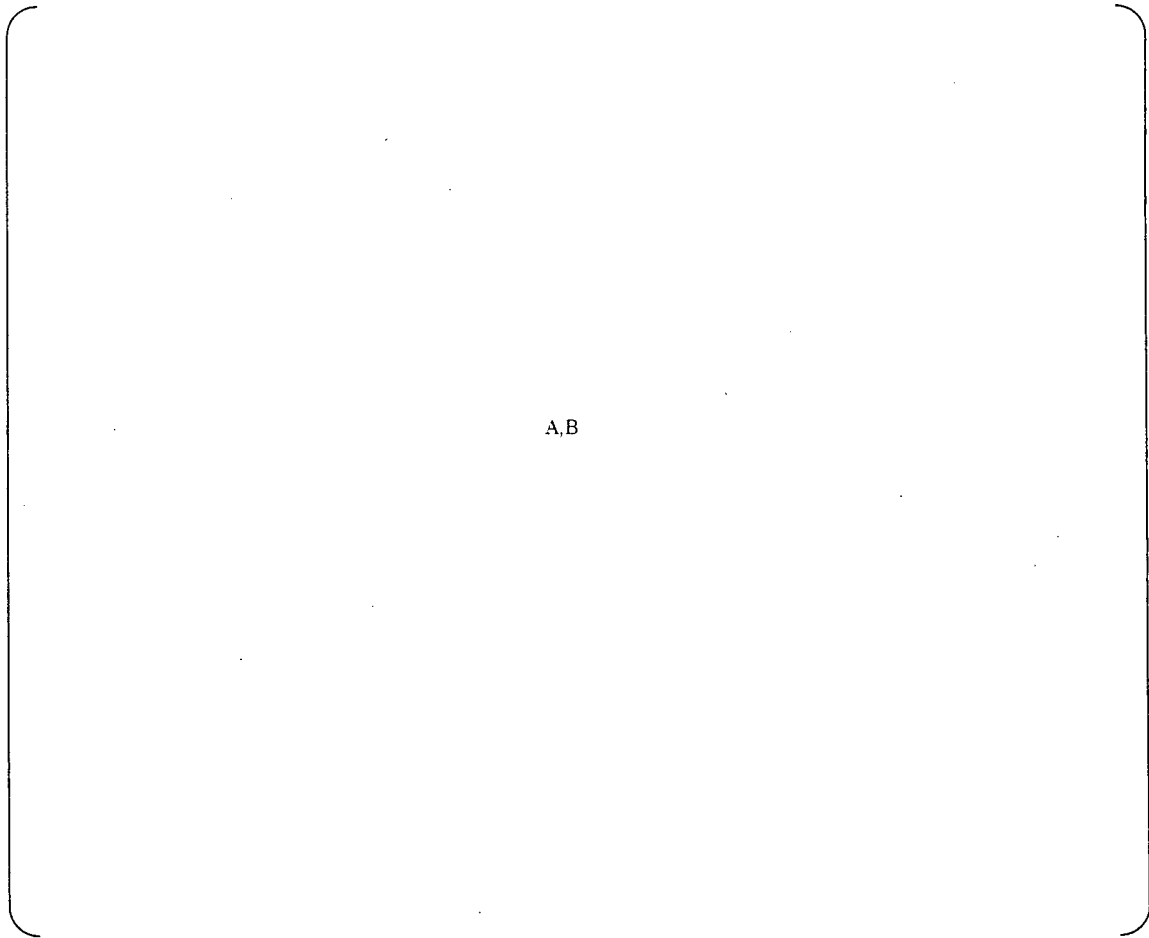


Figure H.3 Results of TRC test

A,B

Figure H.4 Fracture surface of TRC test piece ruptured
(Normal groove type, applied stress:425MPa)

A,B

Figure H.5 Microstructure of cross section of TRC test piece ruptured
(Normal groove type, applied stress:425MPa)



Attachment-I

Measurement of Residual Hydrogen



Measurement of Residual Hydrogen Concentration

1. Purpose

The purpose of this report is to confirm the influence on residual hydrogen by the heat-treatment conditions of the mockups by simulating alloy 152 buttering of Unit-2A, 2B and 3A/3B RSGs, and to measure the residual hydrogen at welded part (alloy 152 buttering and stainless steel clad) by using the samples obtained from Unit-3A RSG.

2. Conclusion

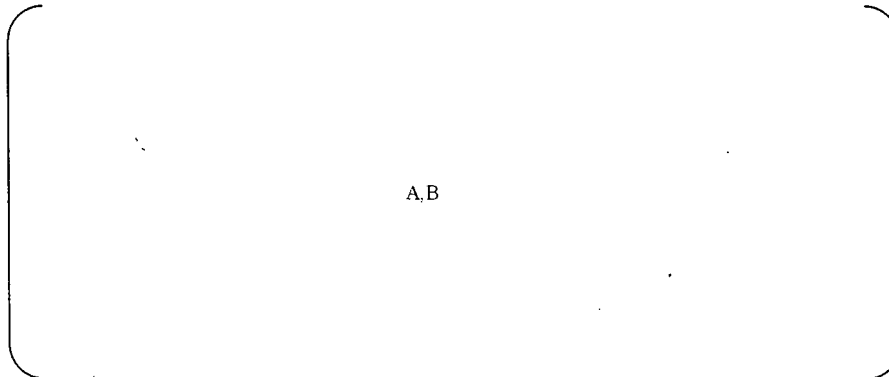
- Concentration of trapped hydrogen was confirmed to be about [A,B] in the mockups. This result is the equivalent of the established value.
- As for the influence on residual hydrogen by the post-heat, no significant difference in the mockups was observed, though the heat treatment conditions such as temperature for Unit-2 and 3 were different.
- Hydrogen remained in alloy 152 buttering and stainless steel cladding at Unit-3A RSG.

The hydrogen concentration was approximately 3 ppm in alloy 152 buttering and stainless steel cladding (SMAW), and approximately 2 ppm in stainless steel cladding (ESW).

3. Methods and Procedures

(1) Mockups

The following is the specifications for the mockups used in the experiment.



(2) Conditions for Measurement

The conditions for the test pieces of residual hydrogen concentration measurement are presented on Table I.1. Figure I.1 (a) shows the initial shape of the test pieces. For post heating, the test pieces were cut into the shape shown in Figure I.1 (b). Figure I.2 shows the selected parts of the test pieces (from Unit-3A RSG) for hydrogen concentration measurement. The mockups and the samples were cut into the shape of a



cube of approximately [A,B] for hydrogen concentration measurement. As for simulated heat treatment timeline which is recorded for reference, it is shown in Figure I.3.

Table I.1 The conditions of Test pieces

Case	Condition		No. of Measurement
A1	pre-heated and not post-heated (Basis of P1,P2 & P3)		3
P1	add post-heat to A1	simulate Unit-2A RSG	3
P2		simulate Unit-2B RSG	3
P3		simulate Unit-3A/3B RSGs	3
R1	Sample (Unit-3A RSG) Alloy 152 buttering		3
R2	Sample (Unit-3A RSG) Stainless steel cladding/SMAW		3
R3	Sample (Unit-3A RSG) Stainless steel cladding/ESW		3

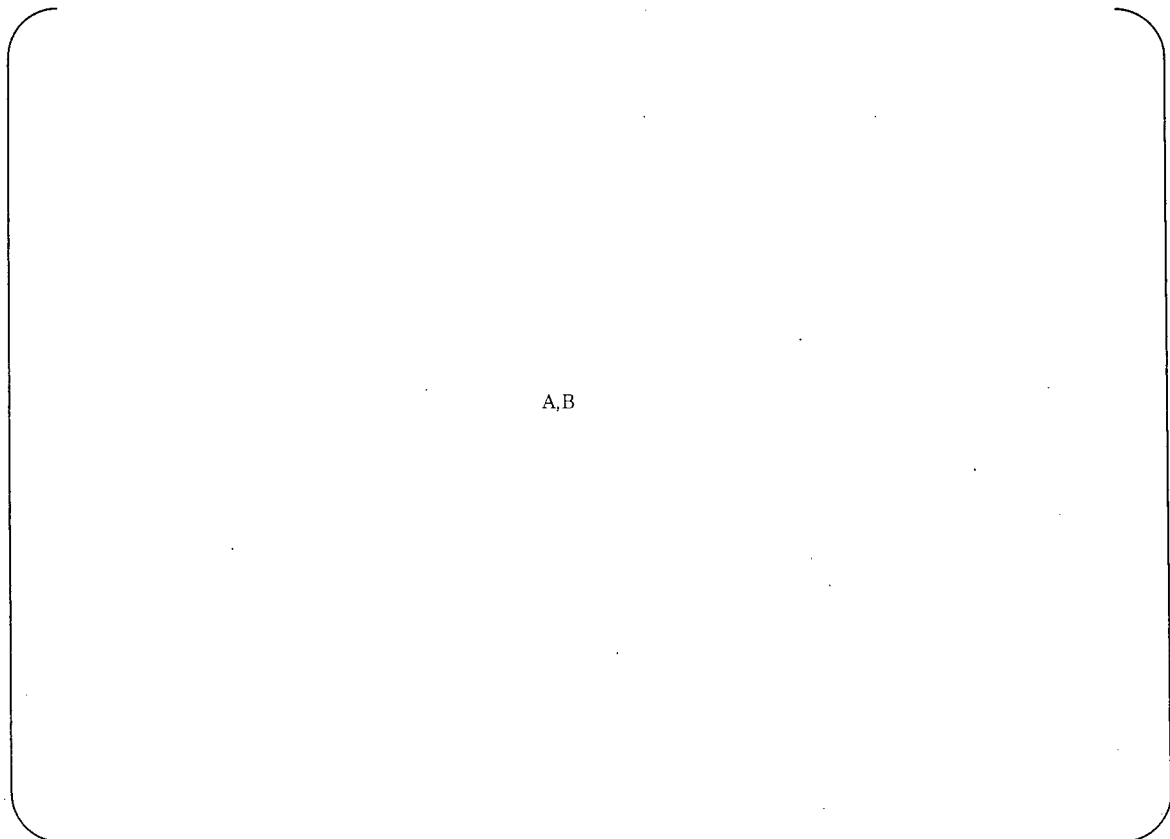


Figure I.1 Shape of test pieces for measurement of hydrogen concentration

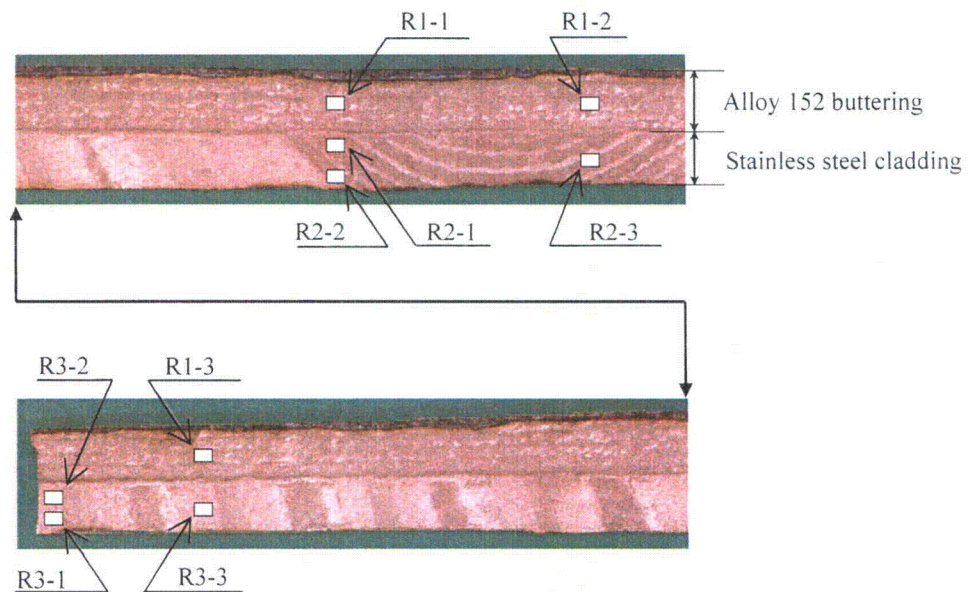
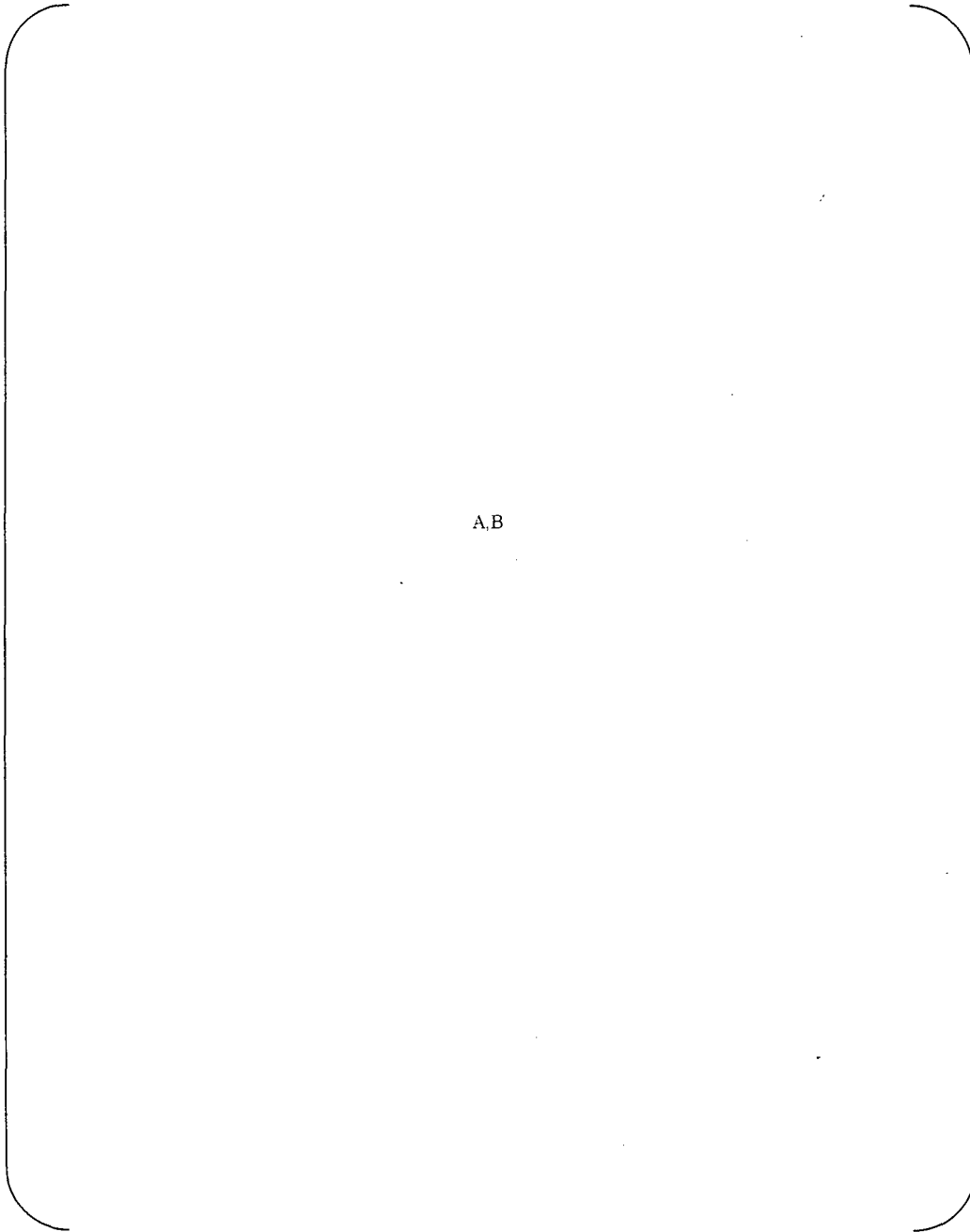


Figure I.2 Locations of samples obtained from Unit-3A RSG



A,B

Figure I.3 Heat-treatment condition of mockups



(3) Measurement Methodology

By using a gas chromatograph, the amount of hydrogen released from the specimen when it is heated until the melting point was measured.

For reference, Appendix-1 shows the data of released hydrogen at each temperature when Alloy 152 weld metal was heated up gradually in the previous test.

(4) Results of Measurement

Table I.2 Results of Measurement

Case	Condition		Hydrogen Concentration (ppm)			
			Sample 1	Sample 2	Sample 3	Average
A-1	Pre-heat and not Post-heat (Basis of P1,P2 & P3)					
P-1	With Post-heat	Simulate Unit-2A RSG				
P-2		Simulate Unit-2B RSG				
P-3		Simulate Unit-3A/3B RSGs				
R-1	Sample (Unit-3A RSG) Alloy 152 buttering		3.6	3.4	3.3	3.4
R-2	Sample (Unit-3A RSG) Stainless steel cladding/SMAW		3.3	3.3	3.6	3.4
R-3	Sample (Unit-3A RSG) Stainless steel cladding/ESW		1.8	1.9	1.8	1.8

A,B

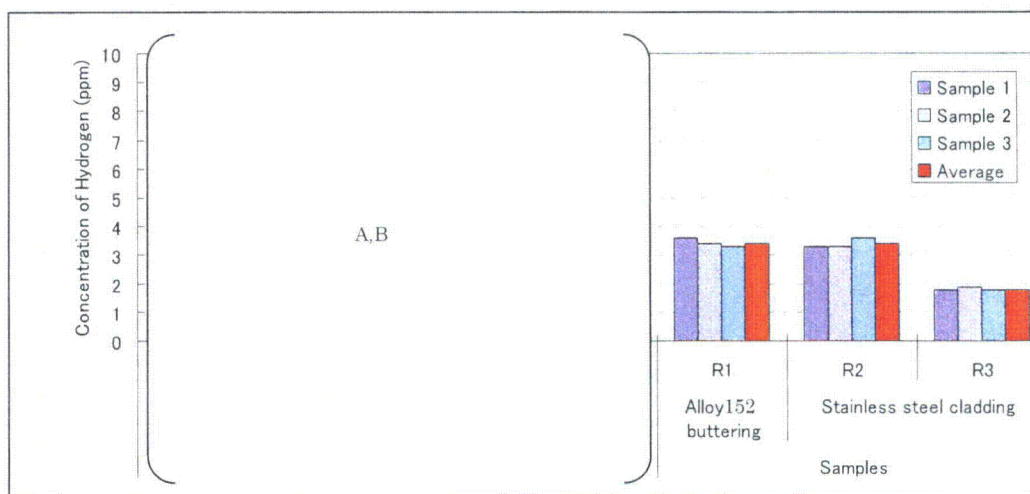


Figure I.4 Results of Measurement



Appendix-I

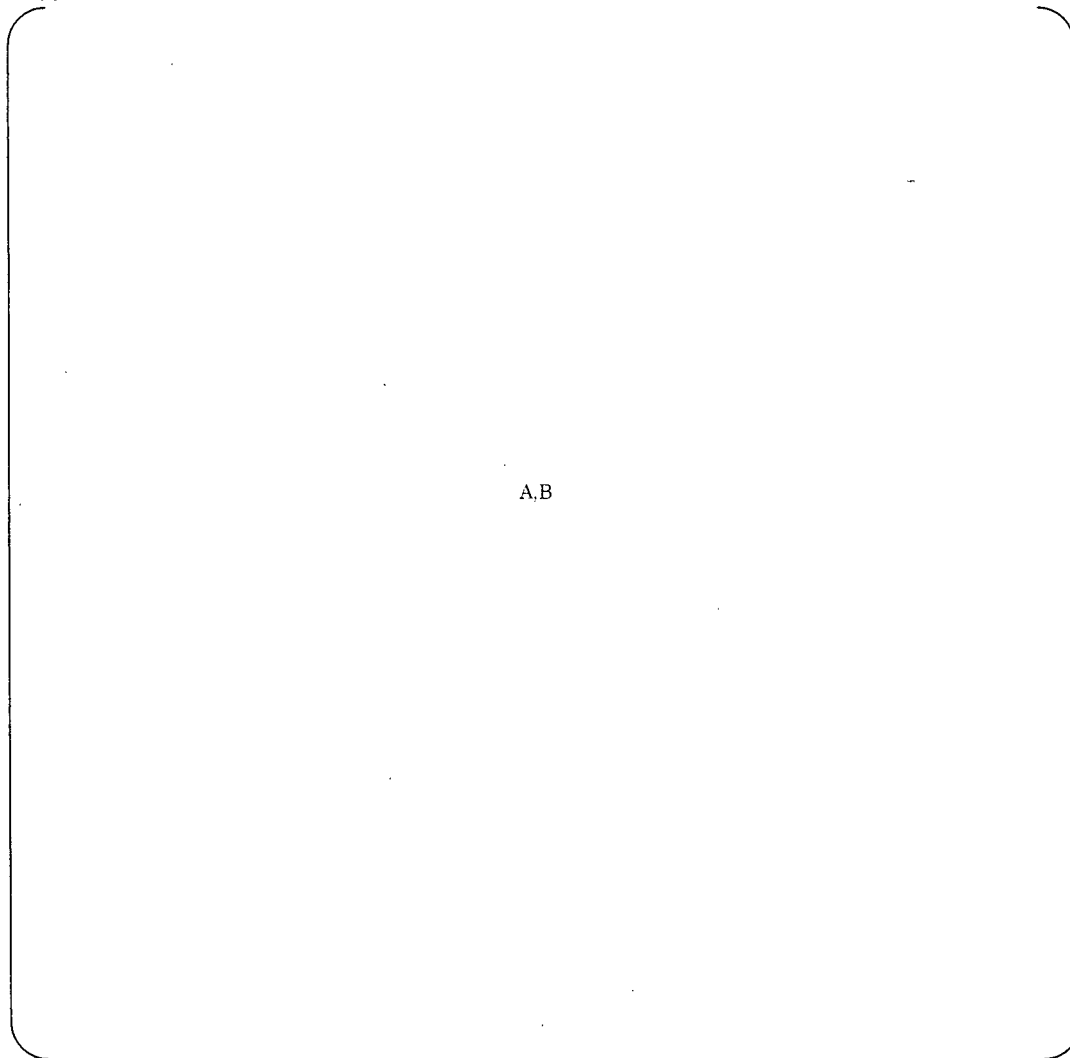


Figure I.5 Results of Thermal Desorption Spectrometry of hydrogen gas



Attachment-J

Carbon Residue Influence on Fusion Boundary Hardness



1. Purpose

The purpose of this report is to provide the investigation results of remained carbon by gouging.

2. Test coupon

Two test coupons were prepared for the investigation. Schematic illustrations of the test coupons were shown in Figure J.1. Gouging was performed on test coupon A to produce residual carbon on the surface. Then, welding was performed over the residual carbon. Gouging condition and welding condition were shown in Table J.2.

In the test coupon B, welding was performed on the thin groove with mashed carbon electrode of gouging. Welding condition of test coupon B was shown in Table J.3.

3. Investigation Methodology

The investigation methodology matrix of test coupon was summarized in Table J.1

Table J.1 Investigation Methodology of test coupon A and B

Item	Method	Purpose
Macro-structure	Visual examination of the cross-section at low magnification after etching	Evaluate the macro-structure of the materials
Micro-structure	Optical microscopic observation of the cross-section at high magnification after etching	Evaluate the micro-structure near the fusion boundary
Hardness	Measure Vickers hardness	Evaluate the hardness distribution near the fusion boundary

4. Results of investigation

4.1 Test coupon A (welding after gouging)

Figure J.2-1 shows the appearance of test coupon. The remaining carbon on the surface in the gouged condition was observed (remained carbon was indicated by arrow in Figure J.2-1).

Figure J.2-2 shows the macro-structure of cross section of test coupon. Some defects were observed near the fusion boundary in cross section of test coupon.

Figure J.2-3 shows the micro-structure of cross section of test coupon. The remaining carbon, which was surrounded by weld metal, resulted by the defects was observed. The light etched zone and deep etched zone were observed in the transition zone adjacent to the carbon in the defect. It is assumed that carburization which was caused by the remaining carbon affects the optical microstructure in transition zone.



Figure J.2-4 shows results of Vickers hardness test. High hardness was measured in transition zone adjacent to the carbon around the defect. It is assumed that carburization caused by the remaining carbon affects the hardness in transition zone.

Figure J.2-5 shows the micro-structure of the cross section of the test piece shown in Figure J.2-3 after additional polishing to remove the defect. The light etched zone which corresponds to the transition zone was still observed at the position where the defect had been located.

Figure J.2-6 shows the results of Vickers hardness test in the cross section shown in Figure J.2-5. High hardness value was obtained in transition zone. It was assumed that carburization which was caused by removed carbon affects the hardness in transition zone.

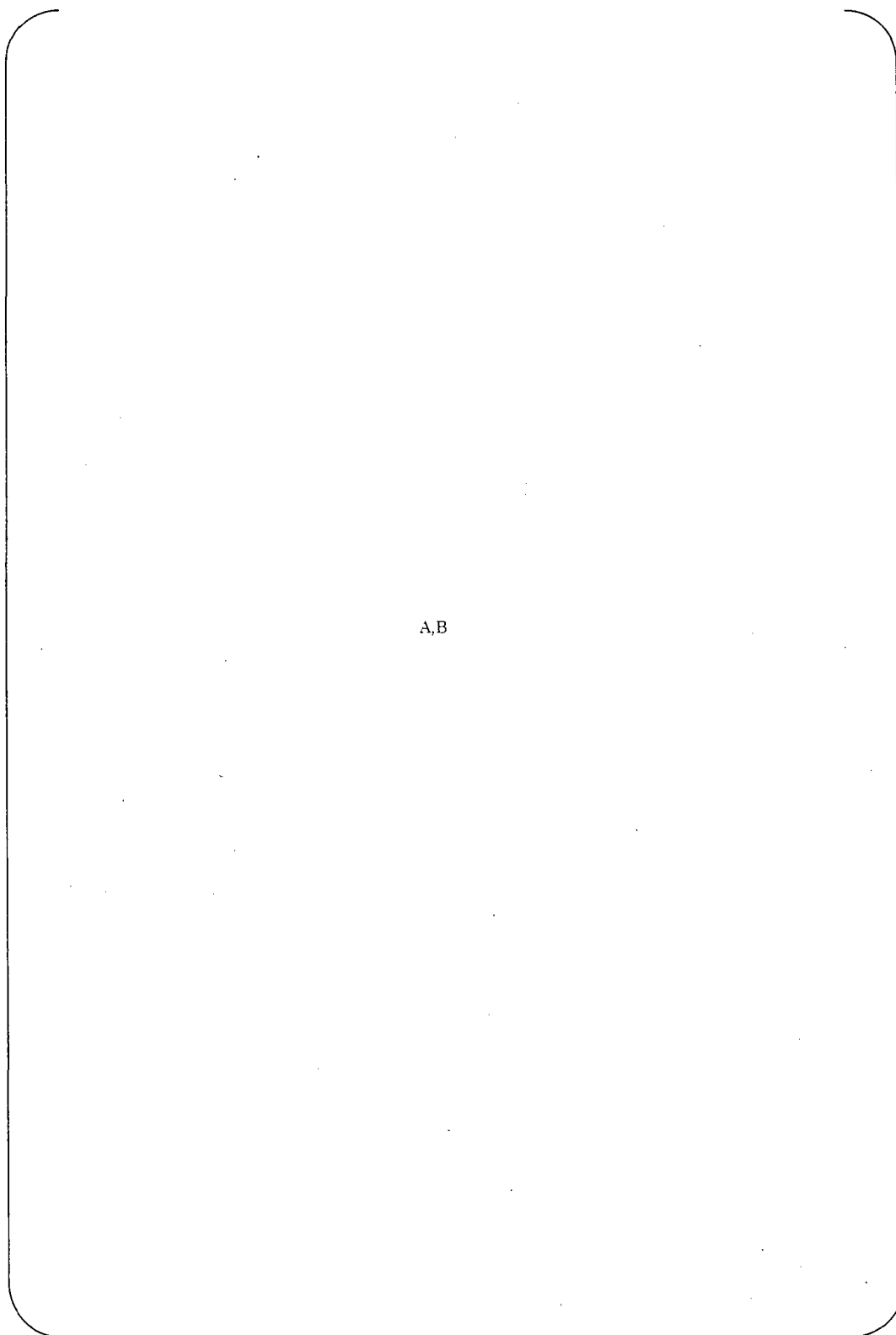
4.2 Test coupon B (welding on the mashed carbon electrode)

Figures J.3-1 show macro-structure and micro-structure of cross section of test coupon. Any significant defects or carbon remained were not observed in the cross section of test coupon. The abnormal micro structure was also not observed. Light colored zone adjacent to the fusion boundary was observed.

Figure J.3-2 shows reference of hardness distribution in transition zone in samples with or without carbon added. It is assumed that carbon addition affects the hardening of transition zone.

5. Summaries of the investigation

- 1) Welding on gouged surface with remaining carbon leads to carburization in transition zone.
- 2) Adding carbon results in high hardness in transition zone.



A,B

Figure J.1 Schematic illustration of test coupons.

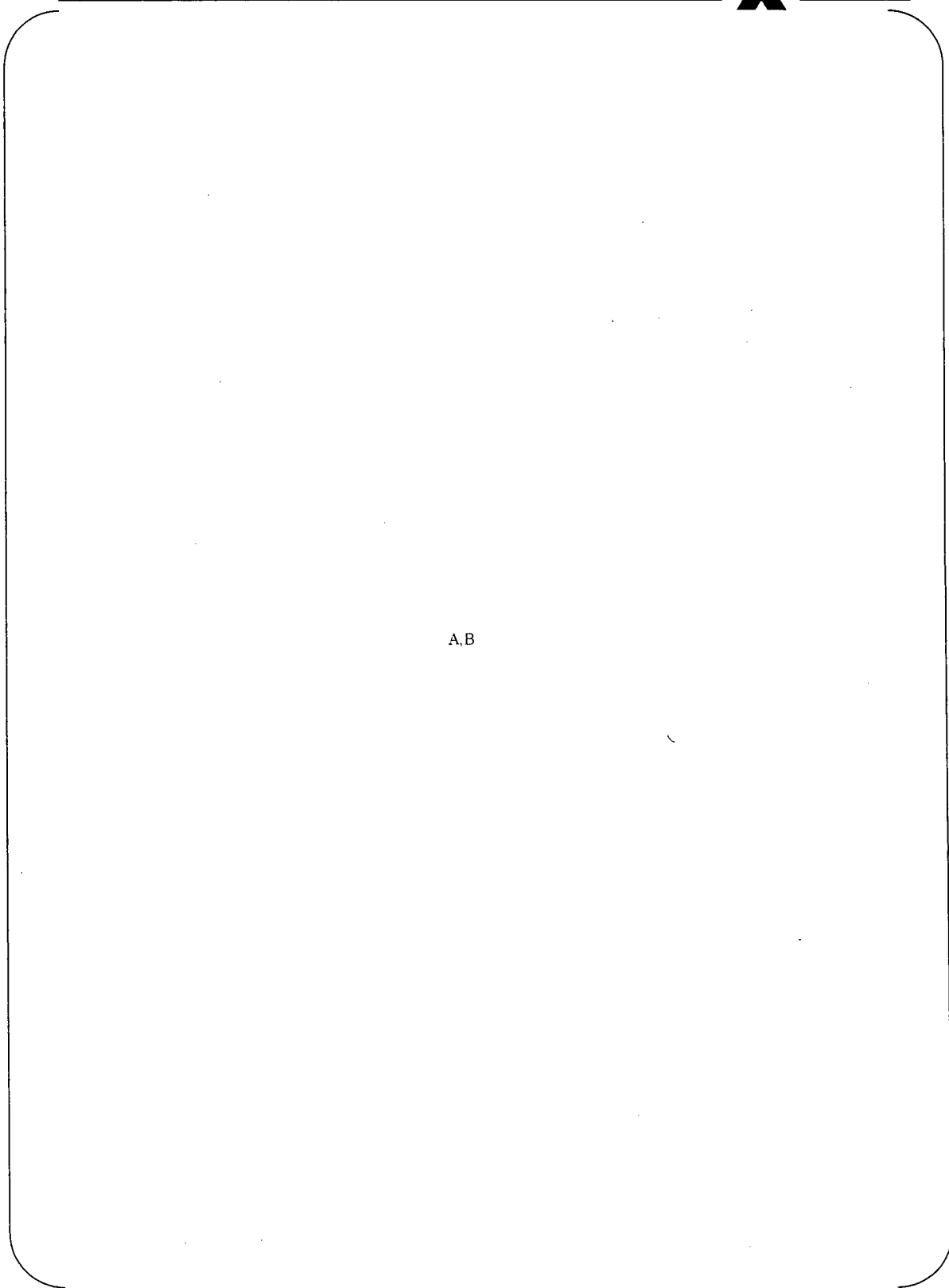


Table J.2 Gouging condition and welding condition of test coupon A

A,B

Table J.3 Welding condition of test coupon B

A,B



A,B

Figure J.2-1 Appearance of test coupon A



A,B

Figure J.2-2 Macro-structure of cross sections of test coupon A



A,B

Figure J.2-3 Micro-structure of cross section of test coupon A (Location E)

A,B

Figure J.2-4 The results of Vickers hardness test of cross section (Location E)



A,B

Figure J.2-5 Micro-structure of cross section of test coupon A after additional polishing



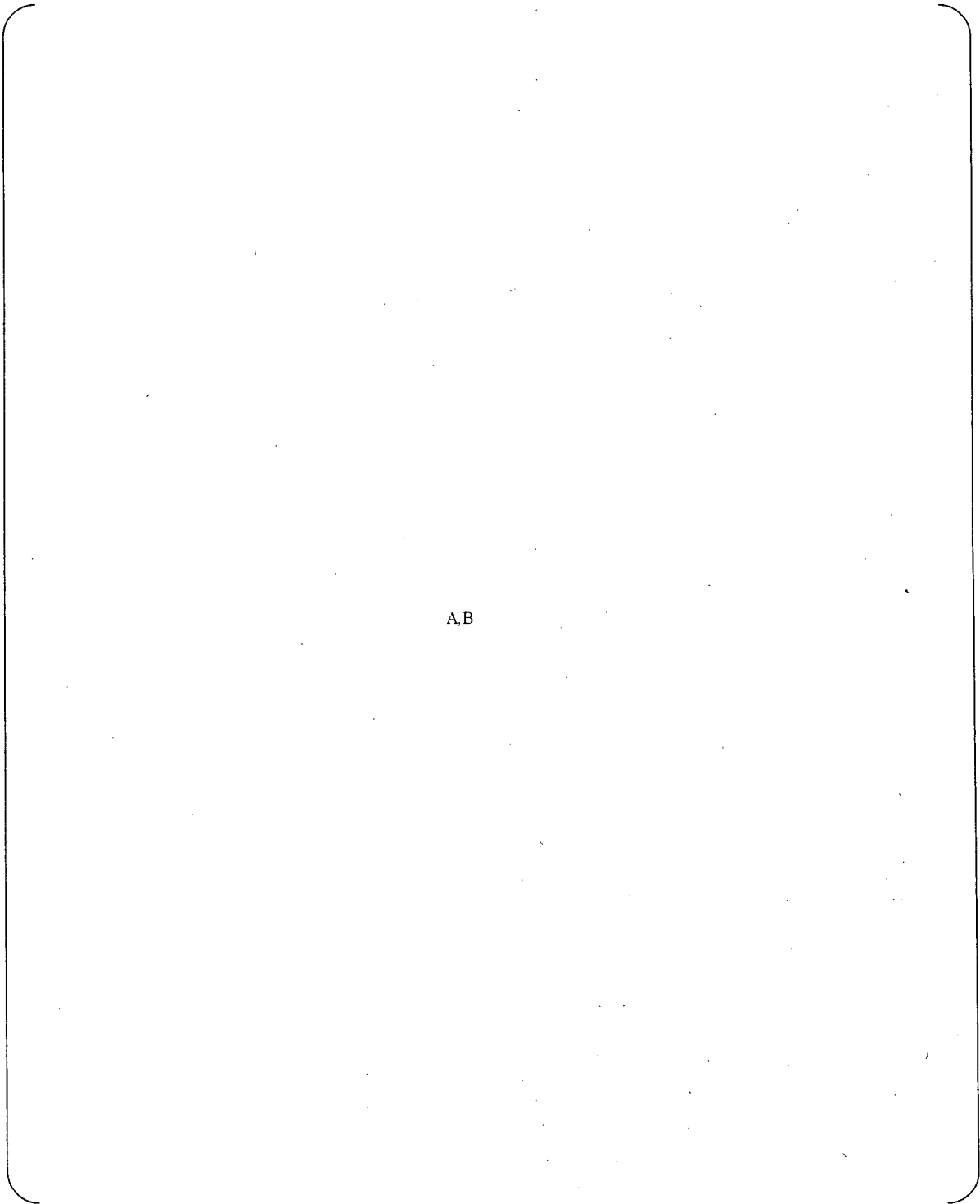
A,B

Figure J.2-6 The results of Vickers hardness test of cross section of test coupon A after additional polishing



A,B

Figure J.3-1 Macro-structure and micro structure of cross section of test coupon



A,B

Figure J.3-2 Reference of hardness distribution in transition zone in samples with or without carbon addition

(K-1)

Document No.L5-04GA440 (0)



Attachment-K

Attachment-K

Reheat Cracking Investigation

MITSUBISHI HEAVY INDUSTRIES, LTD.



1. Purpose

The purpose of this investigation is to determine whether heat input during gouging could initiate reheat cracking.

2. Outline of investigation

The mockup which simulated the weld between LAS and 152 alloy was fabricated. Two types of welding methods were employed. One was SMAW which was applied to the center of channel head bottom and the other is ESW which was applied to the other area of channel head. After that, the gouging was applied to remove the clad. After gouging, alloy 152 joint weld was performed on the mockup.

The test specimens were machined from the mockup and metallographic investigation and tensile test were performed on them.

Detail investigation methodology is discussed in Section 3.



3. Investigation Methodology

Figure K.1 shows schematic illustration of test coupon and specimens for metallographic investigation and tensile test. The detail conditions of specimens were shown in Table K.1 and K.2.

Table K.1 Detail condition of specimens for metallographic investigation

A,B

Table K.2 Detail condition of specimens for tensile test

A,B



The investigation methodology was summarized in Table K.3.

Table K.3 Investigation Methodology

Item	Method	Purpose
Macro-structure	Visual examination of the cross-section at low magnification after etching	Evaluate the macro-structure of the materials
Micro-structure	Visual examination of the cross-section at high magnification after etching	Evaluate the micro-structure around the fusion boundary Examine the existence of micro-cracking in low alloy steel (LAS) Measure the grain size of HAZ
Hardness	Measurement for Vickers hardness	Evaluate the hardness distribution of heat affected zone (HAZ)
Tensile Test	Tensile Test on the Round Bar Specimen	Evaluate whether the reheat cracking initiation occurs on the welding boundary area

Grain size in HAZ of LAS was measured with comparison method: some photographs of micro structure of the cross section were compared to figures of JIS G0551:2005 standard grain size number.

Grain size number G is described by equation 1 using m: number of grains per 1mm² in cross section. The grain size D is obtained by equation 2.

$$m = 8 \times 2^G \quad (\text{eq. 1})$$

$$D = 1/\sqrt{m} = 1/\sqrt{8 \times 2^G} \quad (\text{eq. 2})$$



4. Investigation Results

4.1 Results of metallographic investigation

Figure K.2 shows macro structure of cross section of test coupon. HAZ of ESW was observed in specimens that stainless steel clad was welded by ESW. Neither cracks nor defects were observed in macro structure observation.

Figures K.3 shows micro structure of cross section of test coupons. Neither micro-cracking nor defects were observed in HAZ in cross section. There is no abnormality in microstructure of 152 buttering and LAS base metal.

Table K.4 shows the results of the grain size measurement in HAZ. No significant difference was confirmed in grain size distribution in specimens whose clad were welded by ESW or SMAW. The grain size in those specimens was consistent with the results in boat samples and mock-ups already reported.

Figure K.4 shows results of Vickers hardness test. No significant difference between specimens was confirmed in hardness distribution. There is no abnormality in hardness of 152 buttering and LAS base metal.

4.2 Results of tensile tests

Figure K.5 shows the test specimens after tensile test. The tensile test samples fractured within the base metal. These tests did not produce reheat cracking and the sample fracture surface characteristics did not duplicate those present in the samples collected from the Unit-3 RSGs.

5. Summaries of the investigation

- 1) No micro-cracking or defect were observed in HAZ in cross section.
- 2) Any significant difference was not confirmed in grain size distribution in specimens whose clad were welded by ESW or SMAW.
- 3) There is no abnormality in hardness of 152 buttering and LAS base metal.
- 4) No cracking were observed on the fusion boundary between LAS and alloy 152 in the tensile test specimens.



A,B

Figure K.1 Schematic illustration of test coupon.



A,B

Figure K.2 Macro structure of cross section of test coupons



A,B

Figure K.3(1) Micro structure of cross section of test coupon (clad was welded by ESW)



A,B

Figure K.3(2) Micro structure of cross section of test coupon (clad was welded by ESW)



A,B

Figure K.3(3) Micro structure of cross section of test coupon (clad was welded by SMAW)



A,B

Figure K.3(4) Micro structure of cross section of test coupon (clad was welded by SMAW)



Table K.4 The results of grain size measurement in HAZ of test coupon

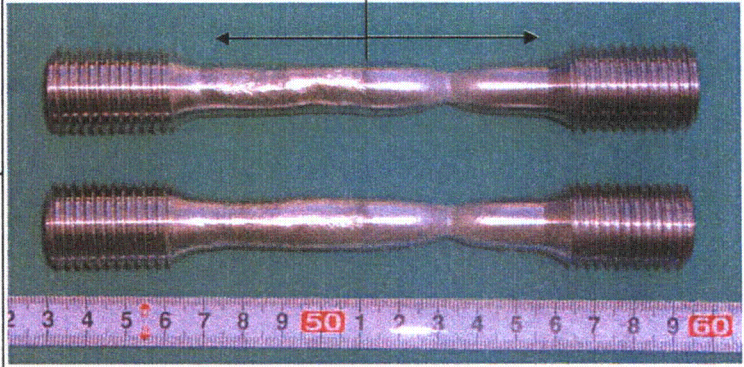
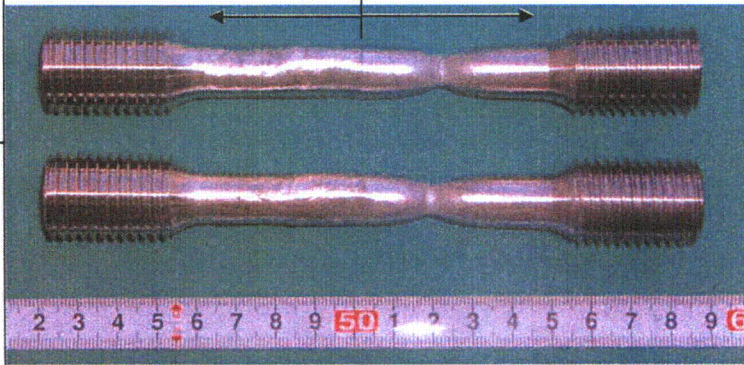
A,B



A,B

Figure K.4 Vickers hardness of cross section of test coupons



Cladding process	Test.No	Appearance
ESW	ET1	
	ET2	
SMAW	ST1	
	ST2	

Unit:mm

Figure K.5 Photograph of specimen after tensile test

(L-1)

Document No.L5-04GA440 (0)



Attachment-L

Attachment-L

Alloy 152 Butter Residual Stresses Analysis

MITSUBISHI HEAVY INDUSTRIES, LTD.



Residual stress evaluation of the channel head after Alloy 152 buttering was performed

1. Purpose

The purpose of this evaluation is to demonstrate the qualitative differences of residual stress due to the differences of buttering configuration between Unit2 and Unit3 after 152 buttering was performed on the channel heads.

2. Outline of analysis

After stainless steel cladding was performed on the low alloy steel with the same thickness as the channel head flat bottom region, the cladding near the center of the plate is removed. After that, alloy 152 buttering is performed on the area where the stainless steel cladding was removed.

Figure L.1 shows the sequence of manufacturing process from stainless steel cladding process to alloy 152 buttering process. In the analysis, three manufacturing processes in Figure L.1 are simulated and stress distributions of Unit3 and Unit2 are compared to evaluate the qualitative difference of the residual stress due to the difference of buttering configuration.



A,B

Figure L.1 Manufacture process



3. Analysis model

Figure L.2 shows the dimensions of the stainless steel cladding and alloy 152 buttering of Unit2A, Unit2B, Unit3A and Unit3B. Since the dimension of Unit3A is almost equal to that of Unit3B, the same analysis model is used for analyses of Unit3A and Unit3B and it is written in Figure L.2 as "Unit3AB".

As shown in Figure L.2, the difference between Unit2A and Unit2B is the length of the flat bottom of alloy152 buttering (L1). Unit2B is more similar to Unit3AB compared to Unit2A in regards of L1.

Since the purpose of this evaluation is to demonstrate the qualitative differences of residual stress due to the differences of buttering configuration between Unit2 and Unit3, Unit2B which is more similar to Unit3AB is selected for comparison with Unit3AB. Therefore, two kinds of analyses, which are CASE-3AB and CASE2B, are performed.

As shown in Figure L.3, the analysis model is three-dimensional model with unit thickness. In Figure L.4, three kinds of material properties are shown. The material properties used in the analyses are shown from Figure L.5 through Figure L.7. The material of the channel head in actual plant is low alloy steel, but carbon steel is used in the analysis because carbon steel can be selected in [A,B] and its property is similar to low alloy steel. Four different phases, which are "ferrite", "bainite", "martensite" and "austenite", are set in the material property of carbon steel because carbon steel and low alloy steel have phase transformation.

The boundary condition is shown in Figure L.8. Figure L.9 and Figure L.10 show welding passes used in this analysis. Figure L.11 and Figure L.12 show welding sequences used in this analysis. Heat input of welding passes is shown in Figure L.13. From the macro photograph of cross section of I type mockup specimen, melted length due to welding is set to [A,B].

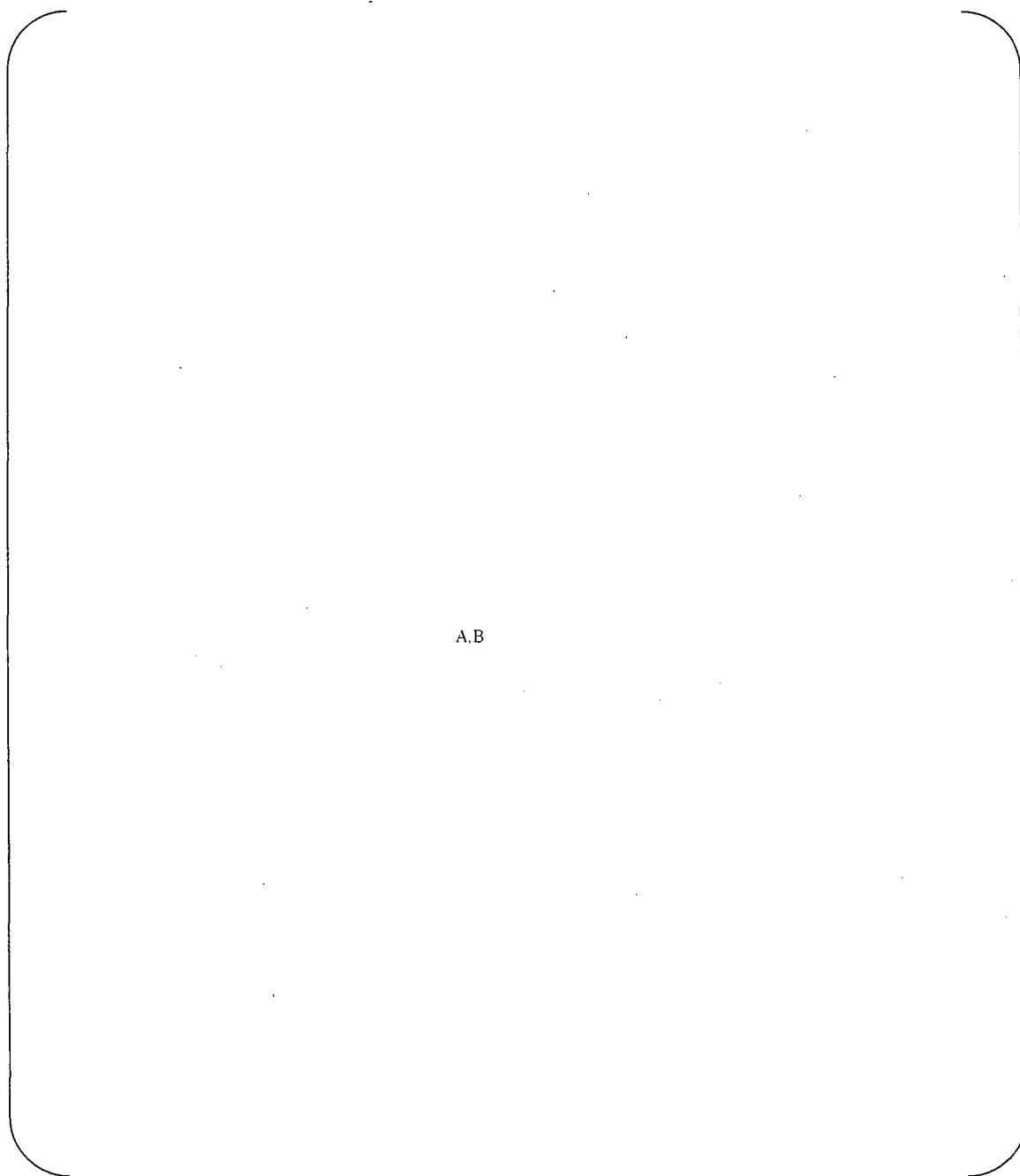


Figure L.2 Dimension of stainless steel cladding and alloy152 buttering



A,B

Figure L.4 Material properties



A,B

Figure L.5 Material properties of channel head
(Carbon steel: SCM420(20MoCr4_022C))



A,B

Figure L.8 Boundary condition



A,B

Figure L.10 Welding passes of alloy152 buttering



A,B

Figure L.12 Welding passes of alloy152 buttering

— MITSUBISHI HEAVY INDUSTRIES, LTD. —



A,B

Figure L.13 Heat input of welding passes



4. Analysis result

Figure L.14 shows the residual stress distribution after the 3rd process. The 3rd process refers to the process where alloy 152 buttering is performed on the area where the stainless steel cladding was removed. From Figure L.14, the stress at each direction of Unit3AB and Unit2B shows the almost same tendency.

For the residual stress after the 3rd process, stress at the x direction is higher because of the restraint of X-direction at both sides of the area where alloy152 buttering was performed.

Since the occurrence of defect at the boundary between alloy152 buttering and low alloy steel depends on the stress at the boundary, normal stresses at the boundary between alloy152 buttering and low alloy steel of Unit3AB and Unit2B are evaluated as shown in Figure L.15. From Figure L.15, for stress on where distance from the center of alloy152 buttering is $[A, B]$, stress of Unit3AB is higher than that of Unit2B because of the difference of the shape of the boundary between alloy152 buttering and low alloy steel.

As shown in Figure L.15, the angle between the boundary of alloy152 buttering and low alloy steel and X-direction is defined as "TH1". Since the angle of Unit3AB is larger than that of Unit2B as shown in Figure L.2, the direction of the normal stress at the boundary of Unit3AB is closer to the X-direction than that of Unit2B. Therefore, for stress on where the distance from the center of alloy152 buttering is $[A, B]$, it is considered that the normal stress at the boundary of Unit3AB is higher than that of Unit2B.



A,B

Figure L.14 Stress contour after 3rd process

MITSUBISHI HEAVY INDUSTRIES, LTD.



A,B

Figure L.15 Normal stress distribution to the boundary between Alloy152 buttering and carbon steel(channel head)



Attachment-M

2D Analysis to Evaluate the Effect of the Divider Plate Offset



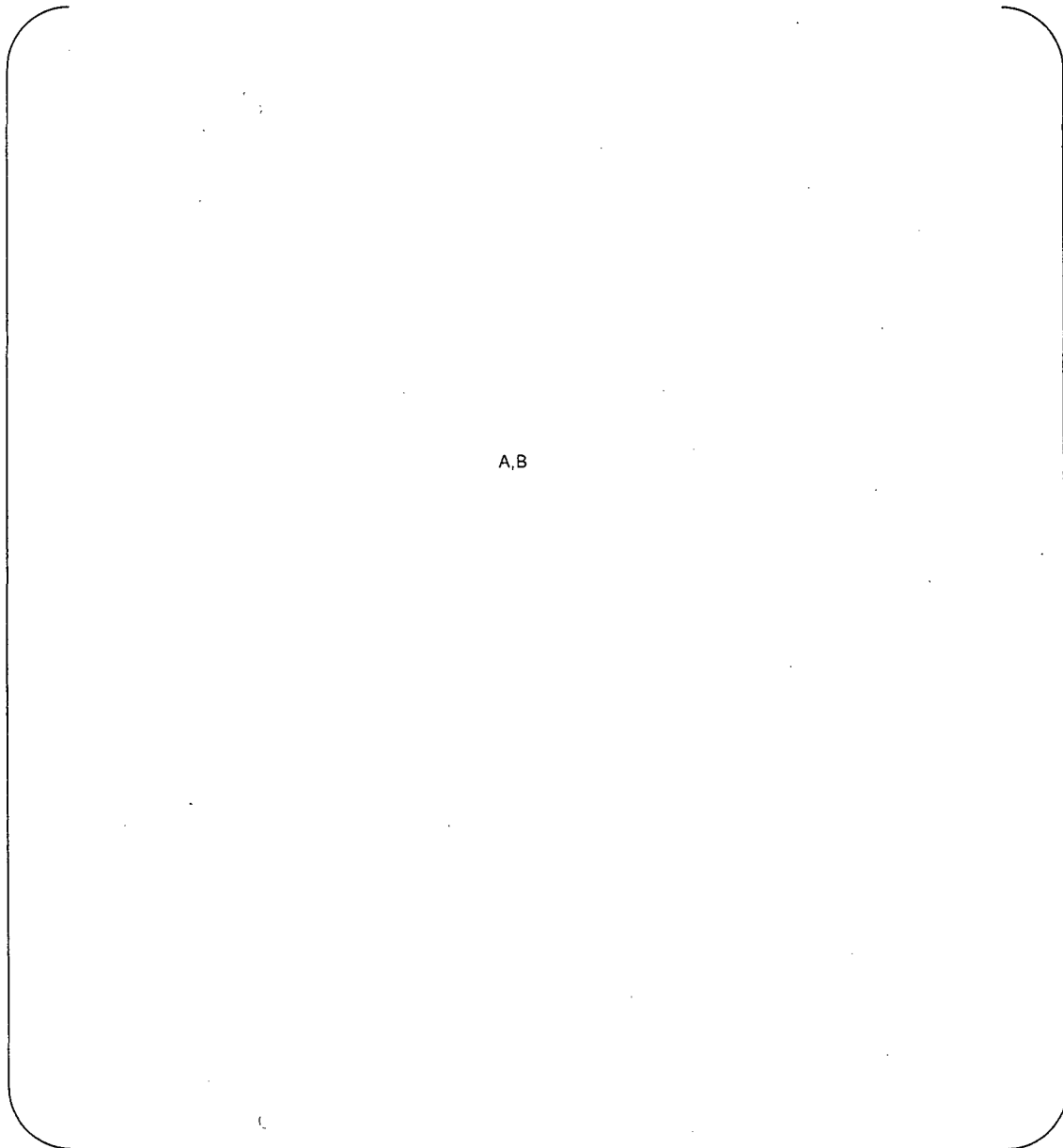
FE Analysis

The FE model is shown in Figure M.1. Load and boundary condition are shown Figure M.2.

Each material is shown in Figure M.3 and the material properties (S-S curve) used in the analyses are shown in Table M.1.

The deformation and the stress contours due to elastic analysis are shown in Figure M.4-1 through Figure M.4-4.

The deformation and the stress/strain contours due to elastic-plastic analysis are shown in Figure M.5-1 through Figure M.5-7.



A,B

Figure M.1 Analysis Model



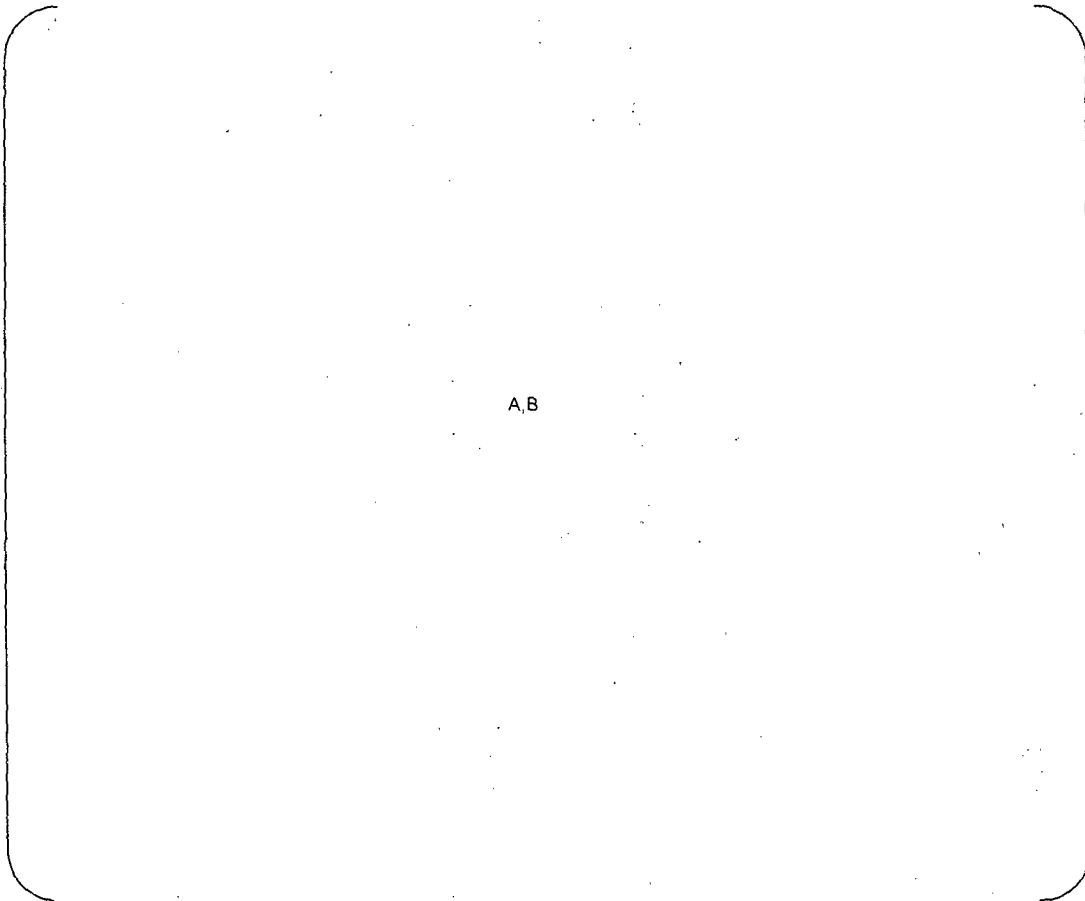
A,B

Figure M.3 Material



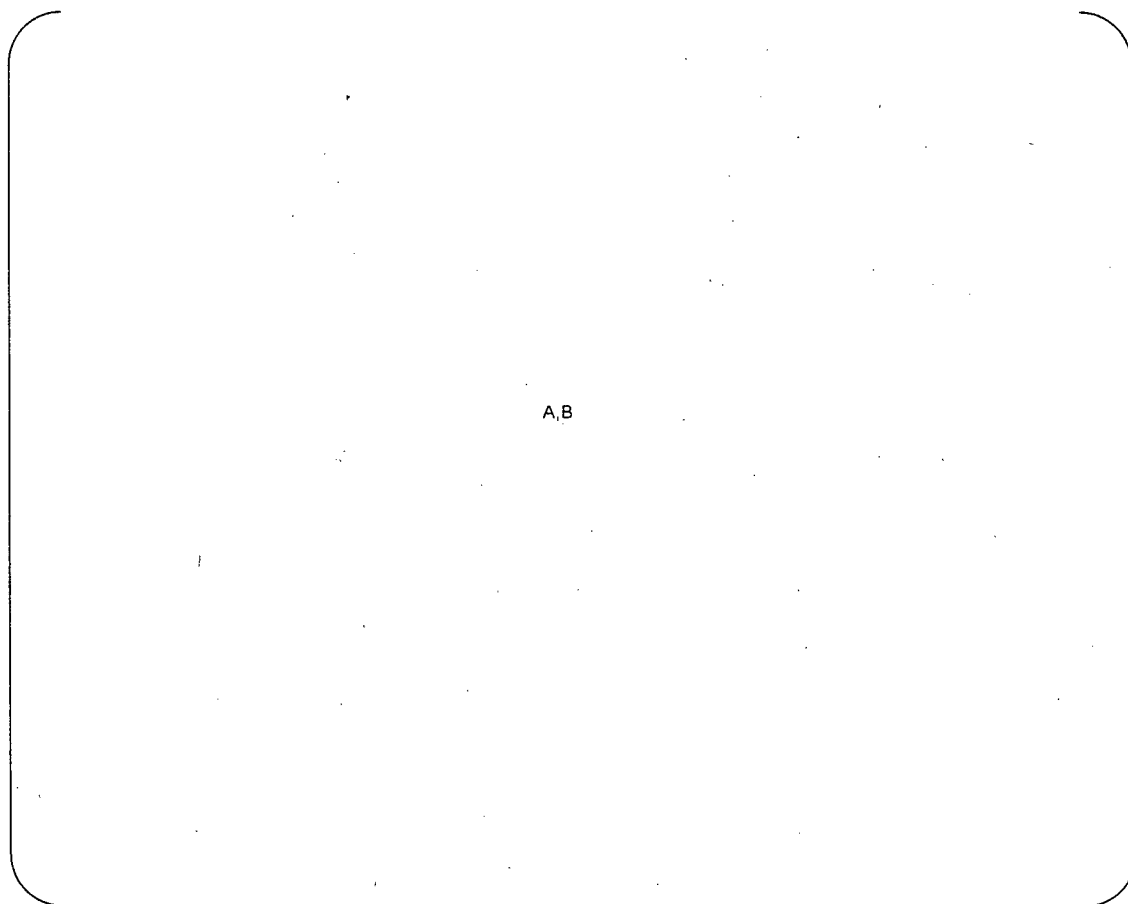
Table M.1 Material Properties

A,B	
-----	--



A,B

Figure M.4-1 Displacement (Elastic Analysis)



A,B

Figure M.4-2 (1/3) Stress Contour [Mises] (Elastic Analysis)

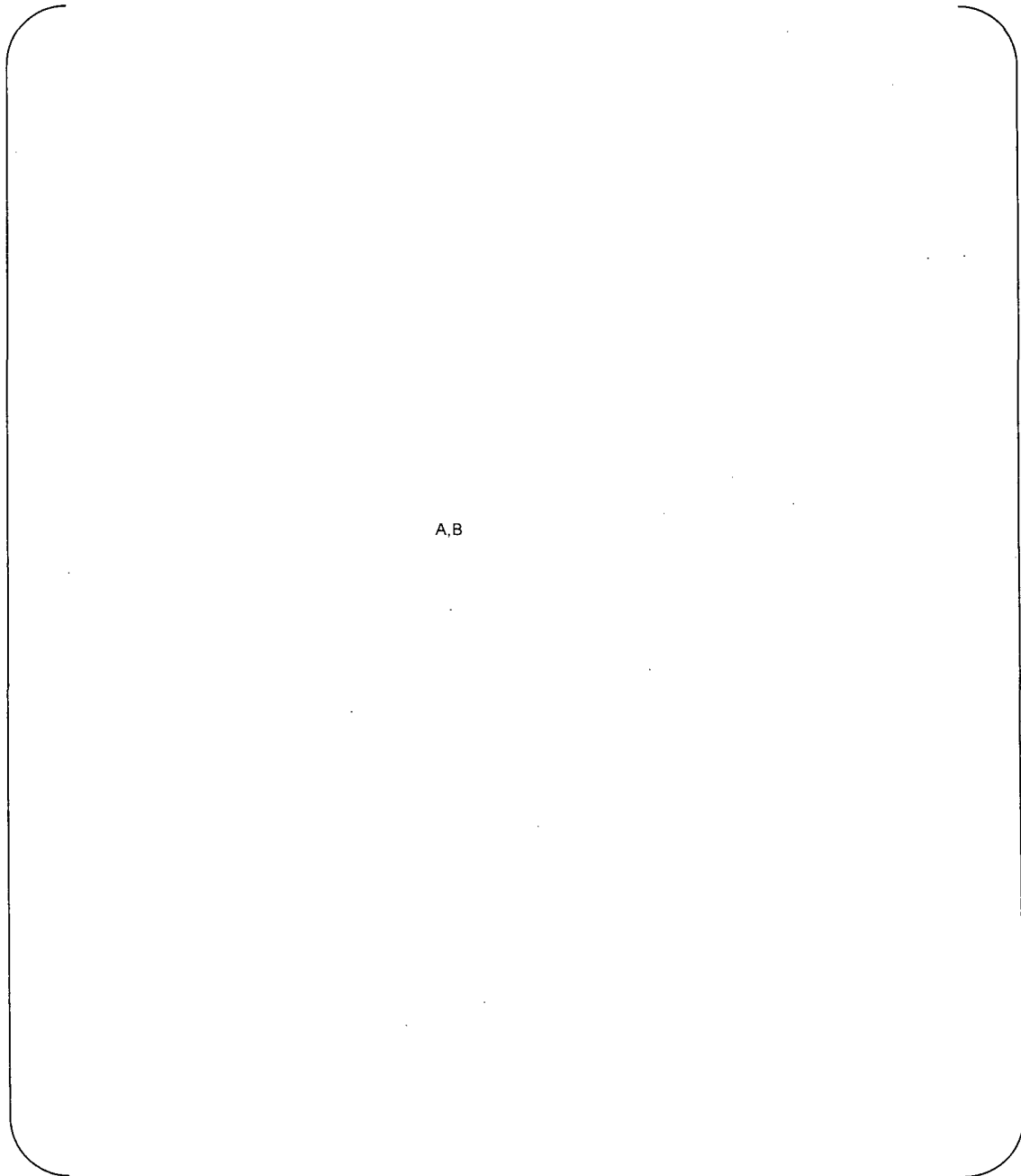
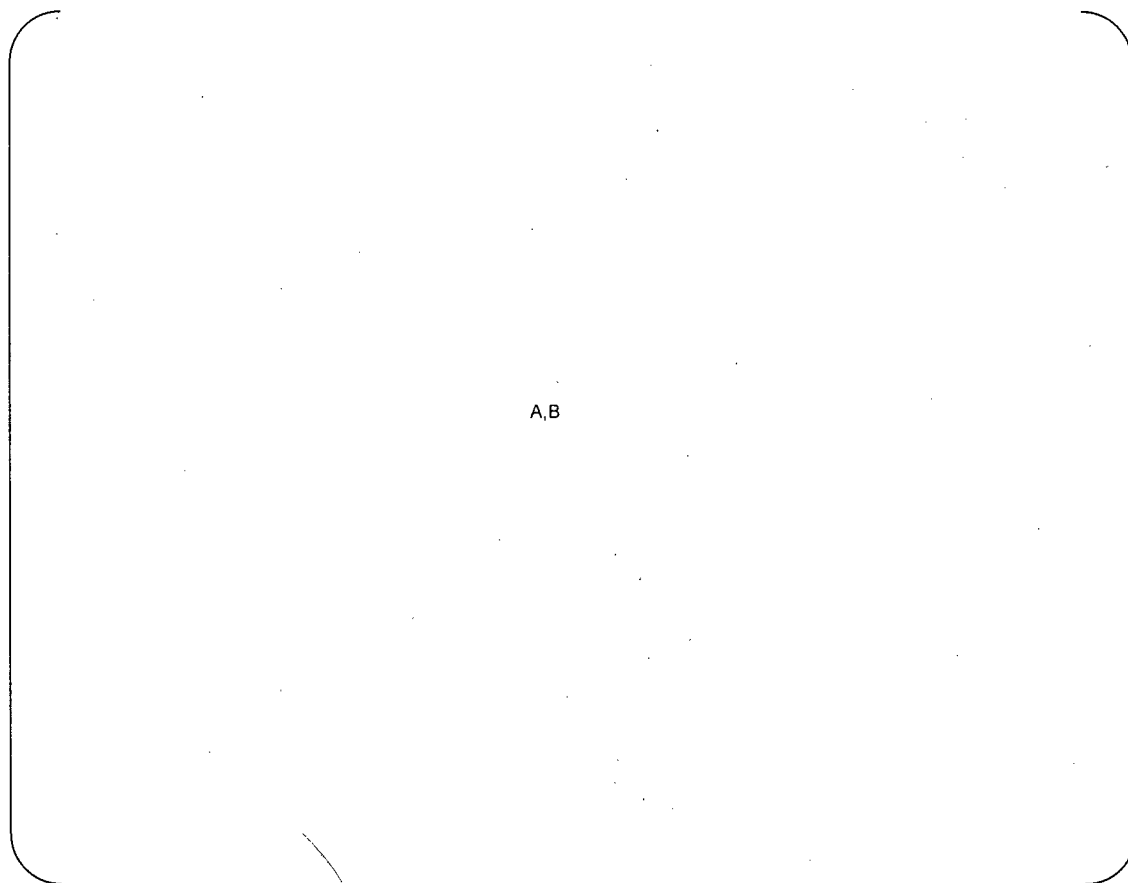
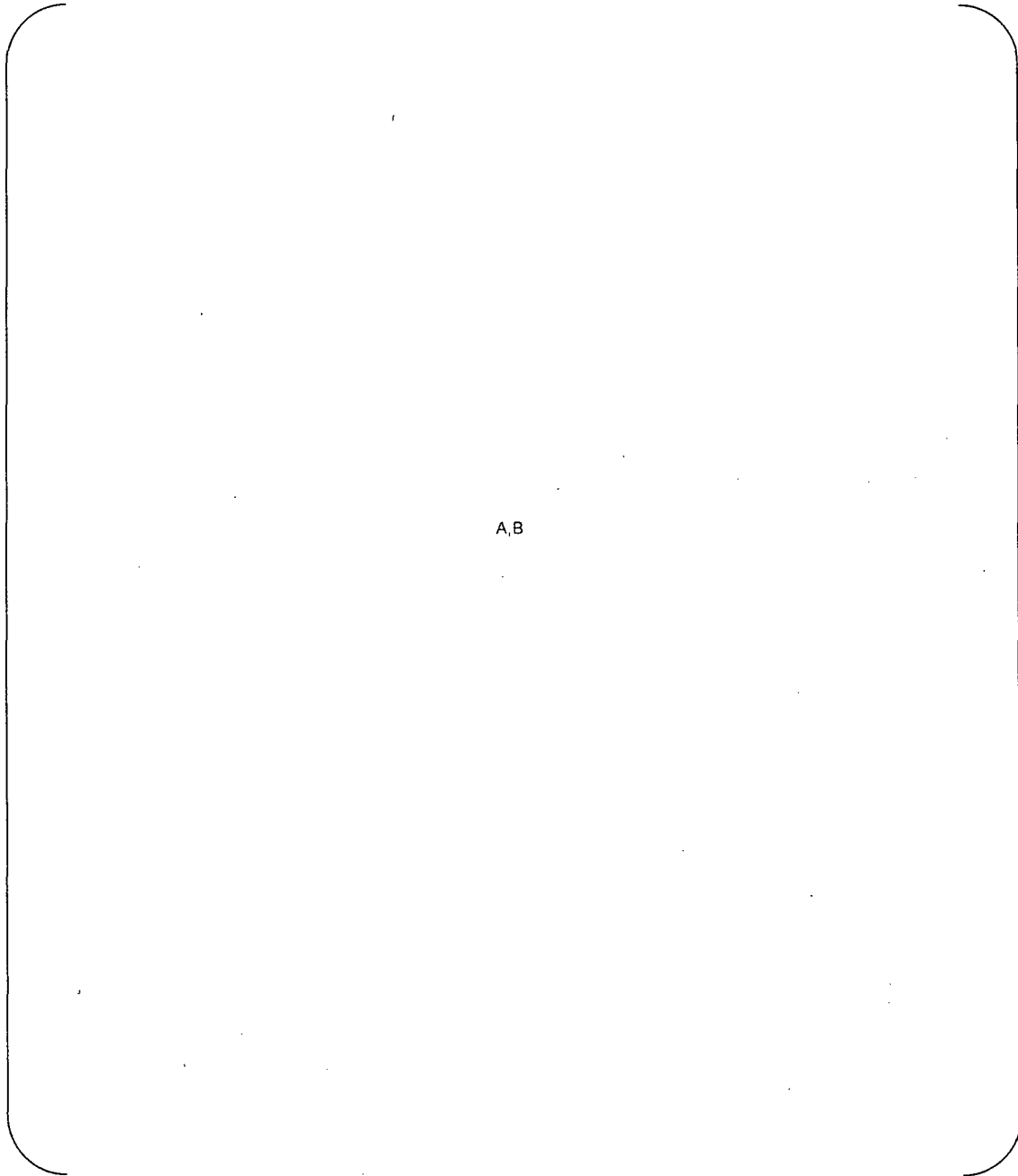


Figure M.4-2 (3/3) Stress Contour <Part-2> [Mises] (Elastic Analysis)



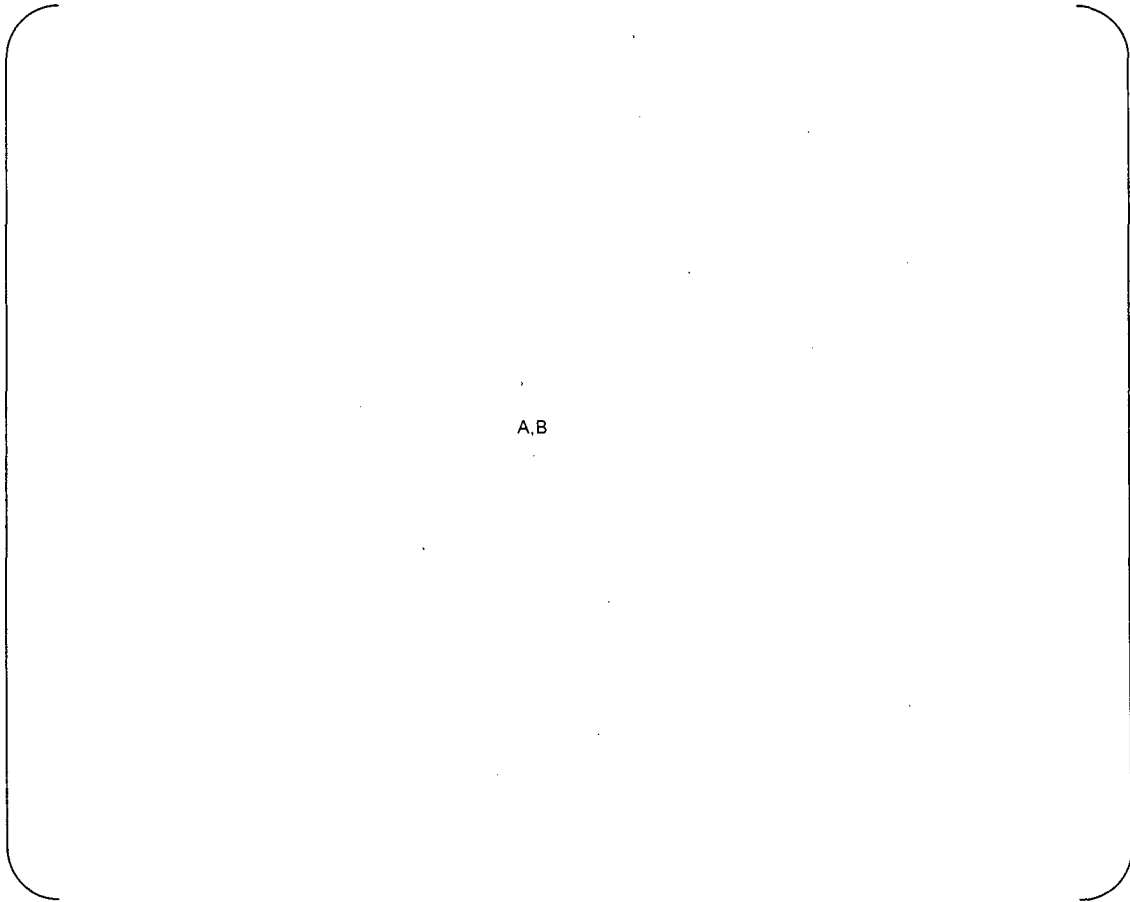
A,B

Figure M.4-3 (1/3) Stress Contour [σ_X] (Elastic Analysis)



A,B

Figure M.4-3 (3/3) Stress Contour <Part-2> [σ_X] (Elastic Analysis)



A,B

Figure M.4-4 (1/3) Stress Contour [σ_Y] (Elastic Analysis)

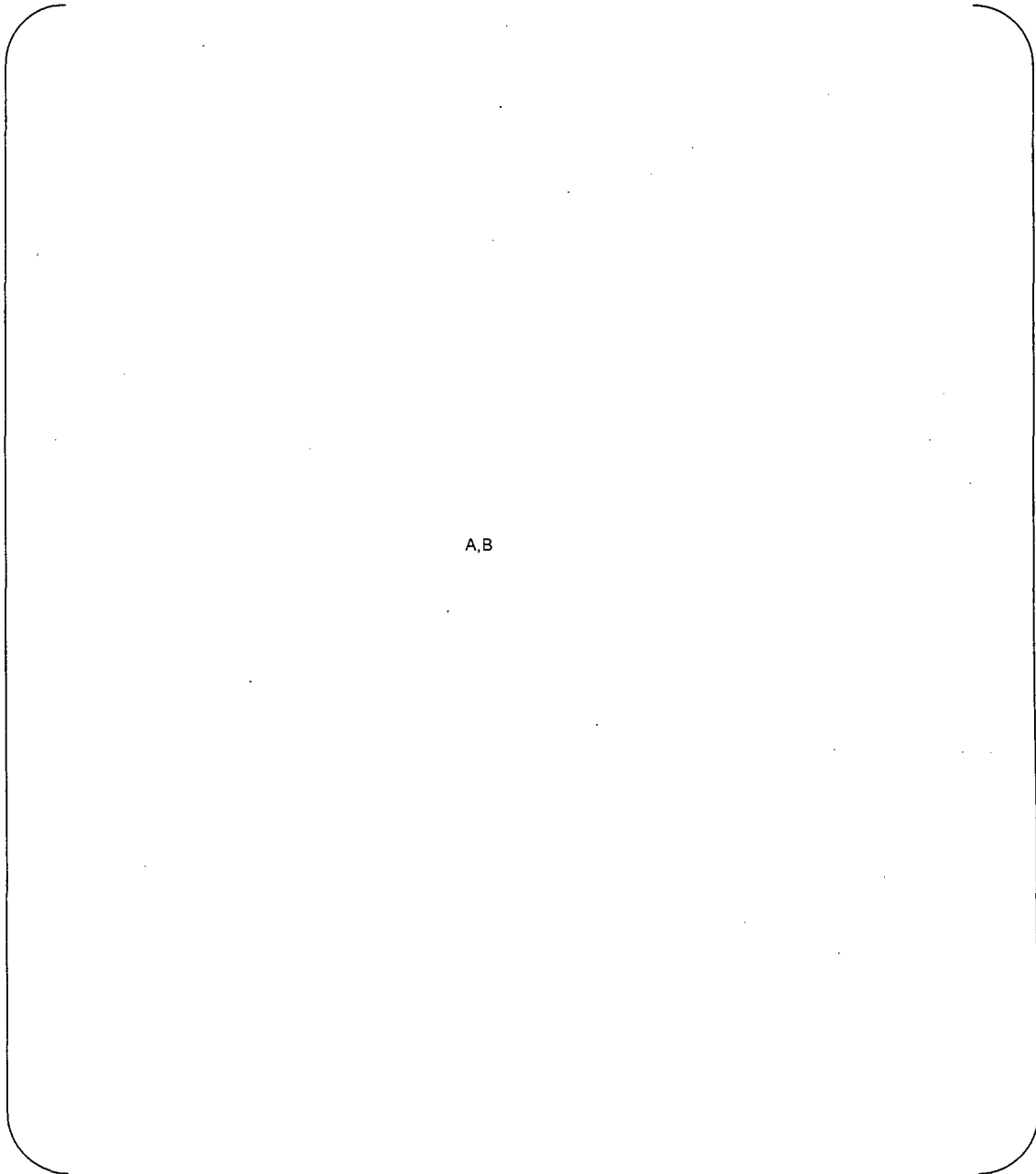
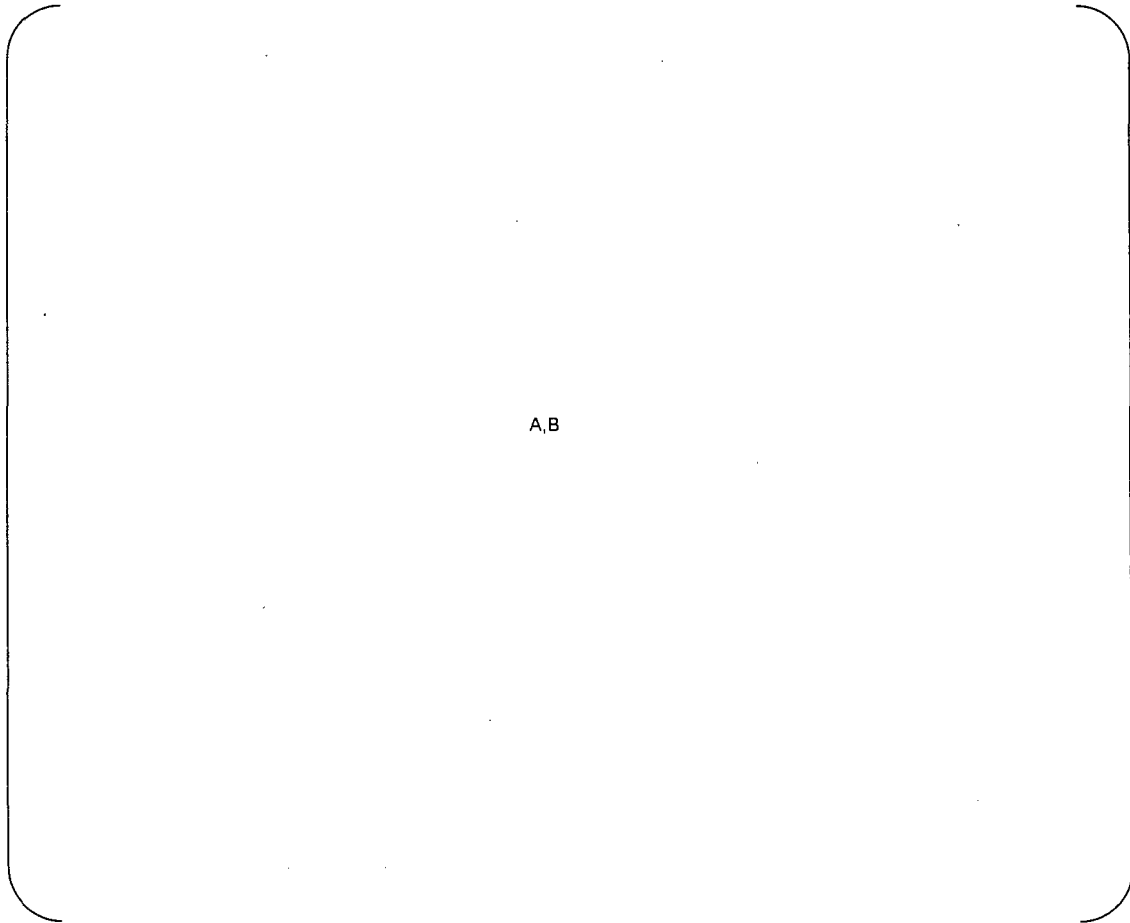


Figure M.4-4 (3/3) Stress Contour <Part-2> [σ_Y] (Elastic Analysis)



A,B

Figure M.5-1 Displacement (Elastic-Plastic Analysis)

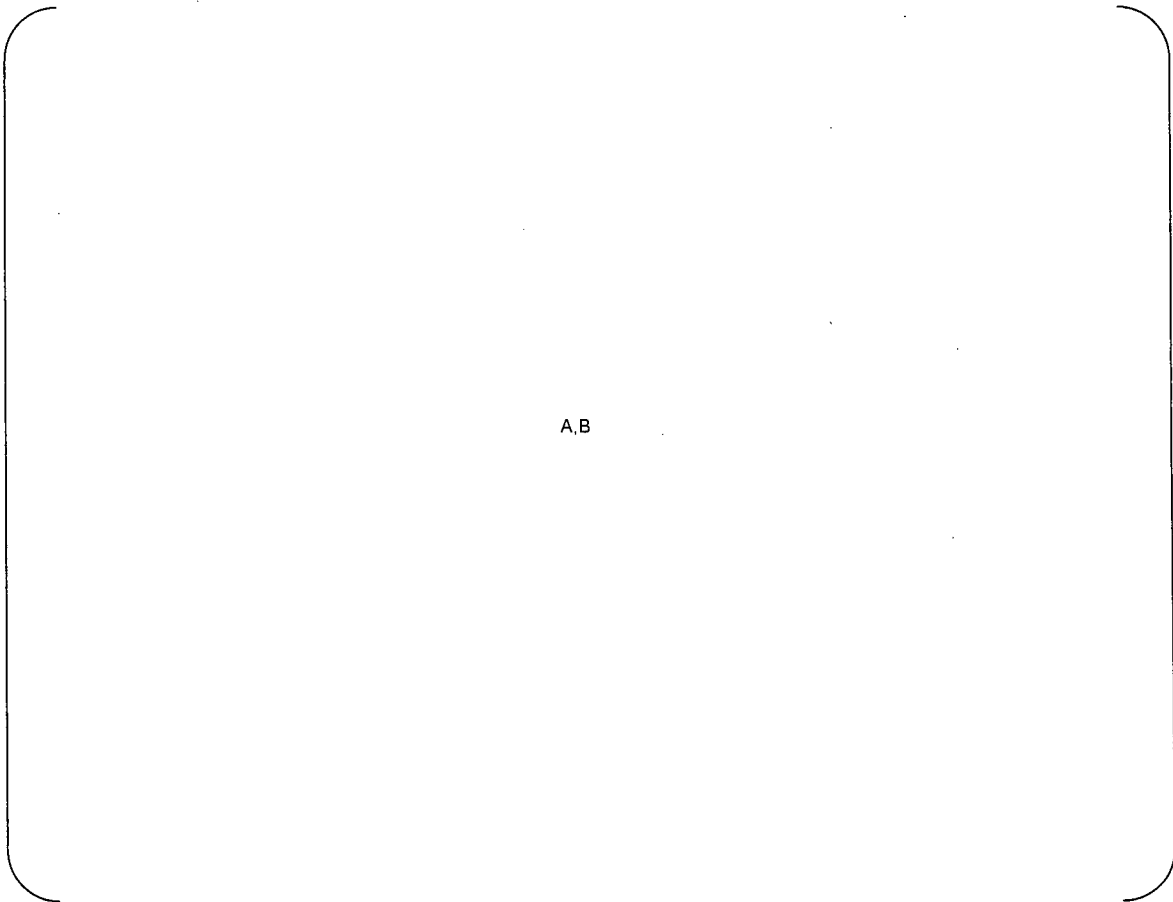
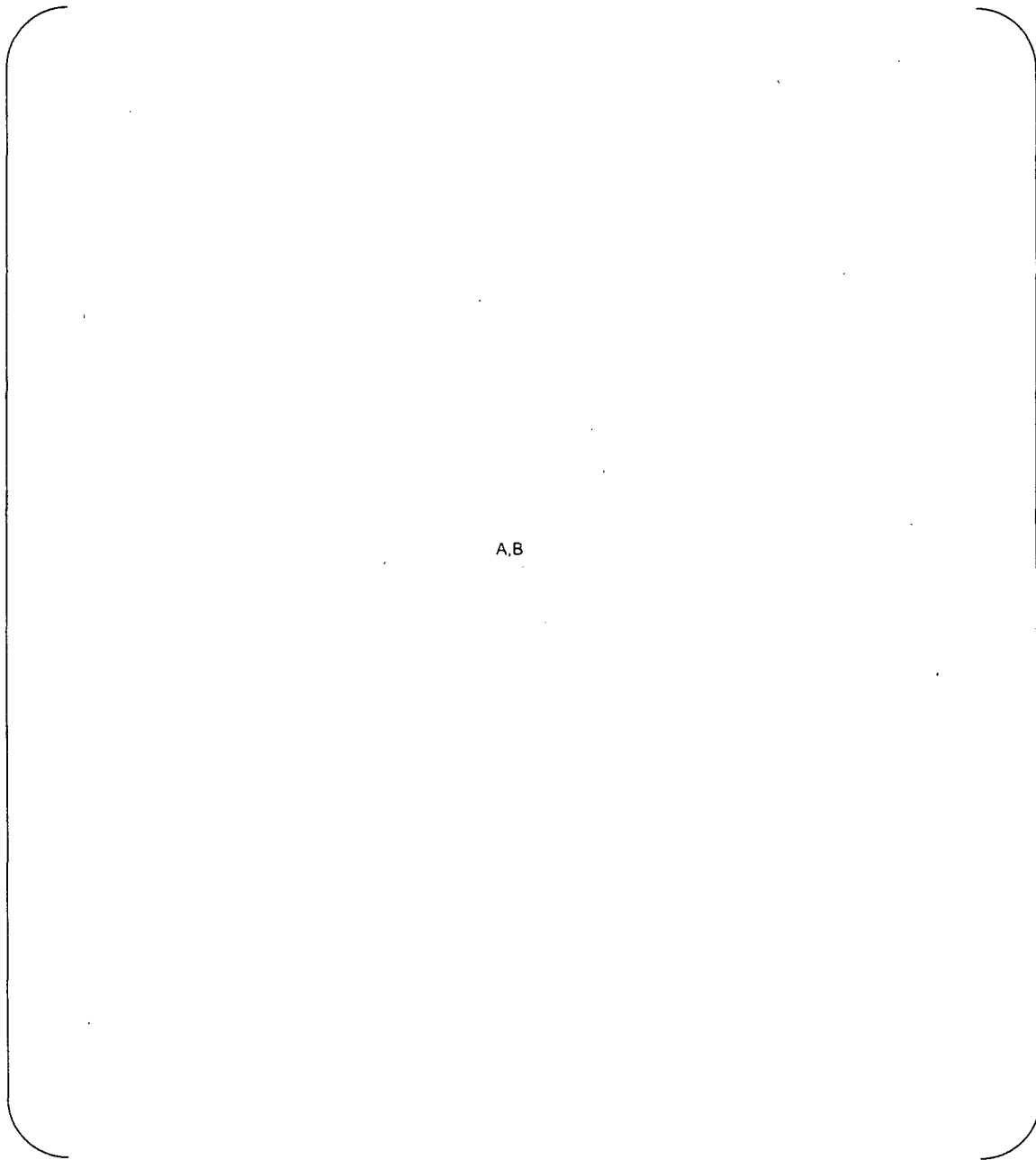


Figure M.5-2 (1/3) Stress Contour [Mises] (Elastic-Plastic Analysis)



A,B

Figure M.5-2 (3/3) Stress Contour <Part-2> [Mises] (Elastic-Plastic Analysis)

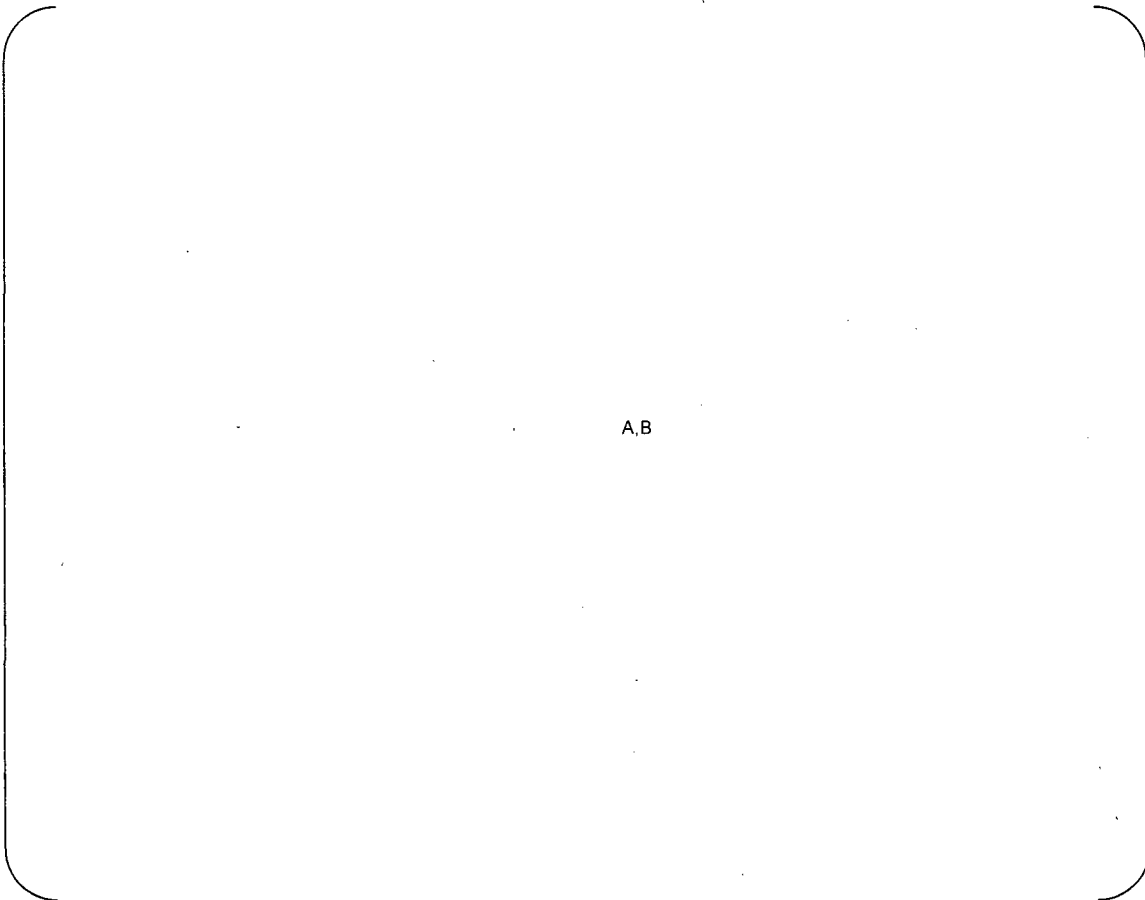
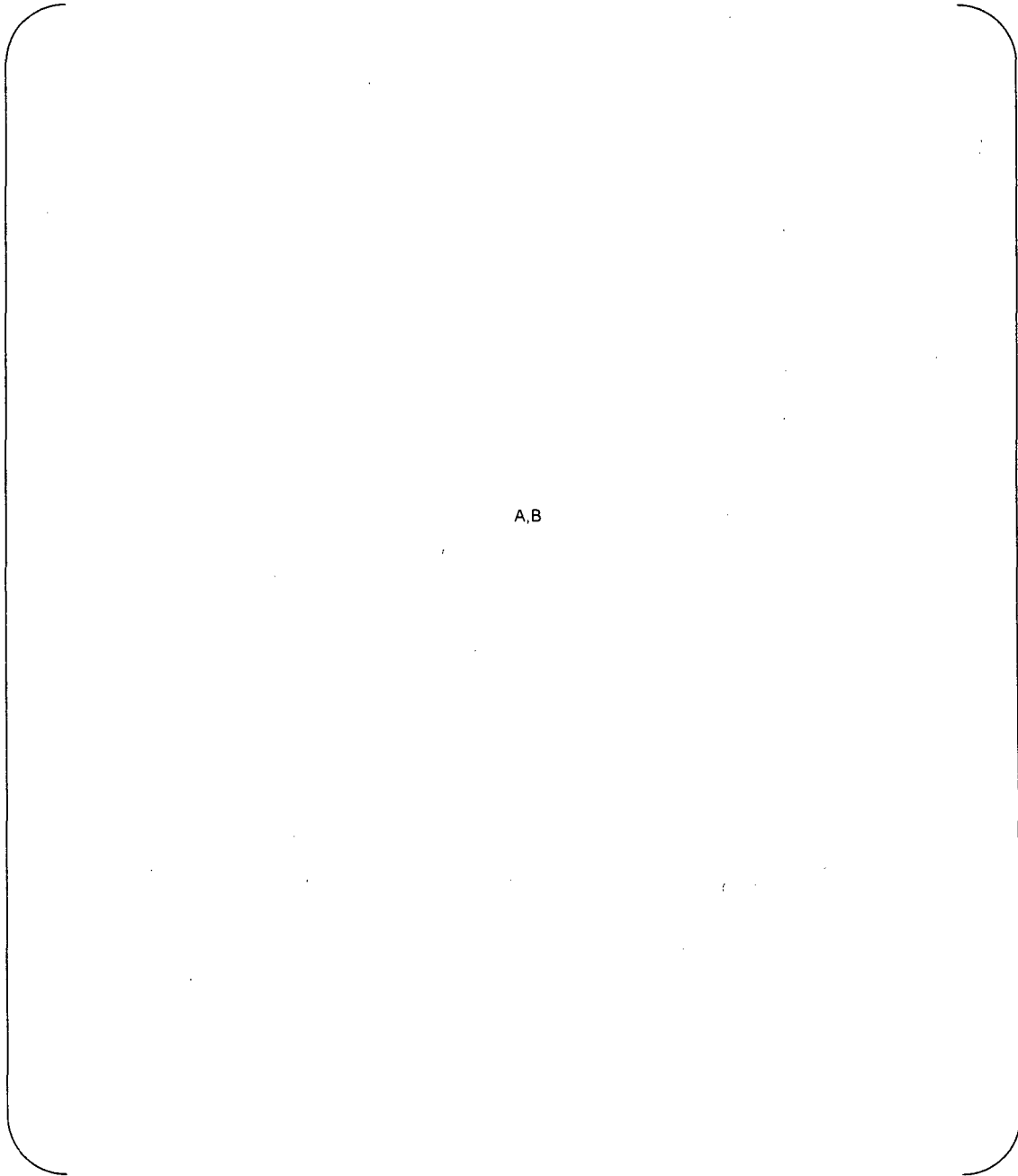


Figure M.5-3 (1/3) Stress Contour [σ_X] (Elastic-Plastic Analysis)

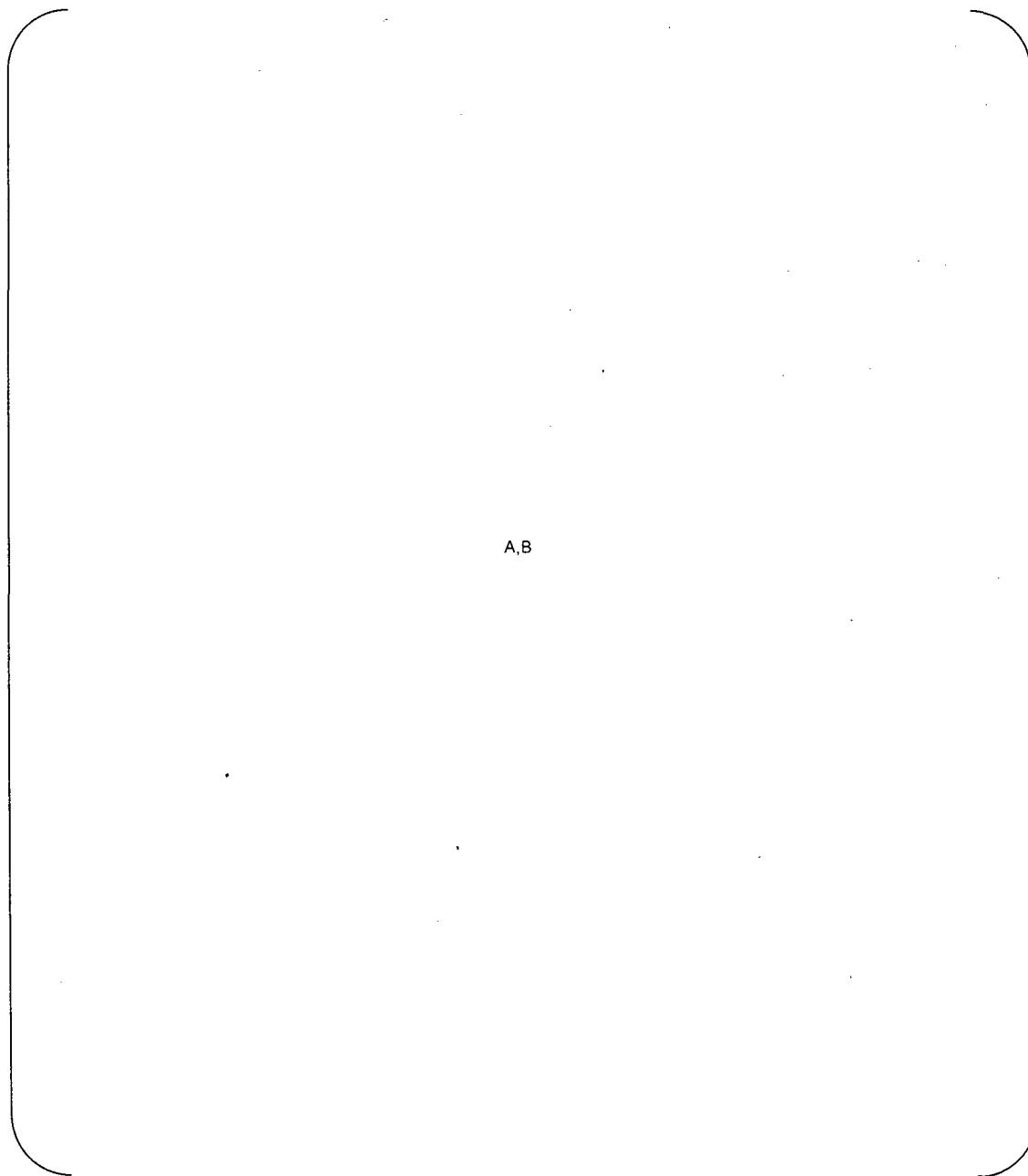


A,B

Figure M.5-3 (3/3) Stress Contour <Part-2> [σ_X] (Elastic-Plastic Analysis)



Figure M.5-4 (1/3) Stress Contour [σ_Y] (Elastic-Plastic Analysis)



A,B

Figure M.5-4 (3/3) Stress Contour <Part-2> [σ_Y] (Elastic-Plastic Analysis)

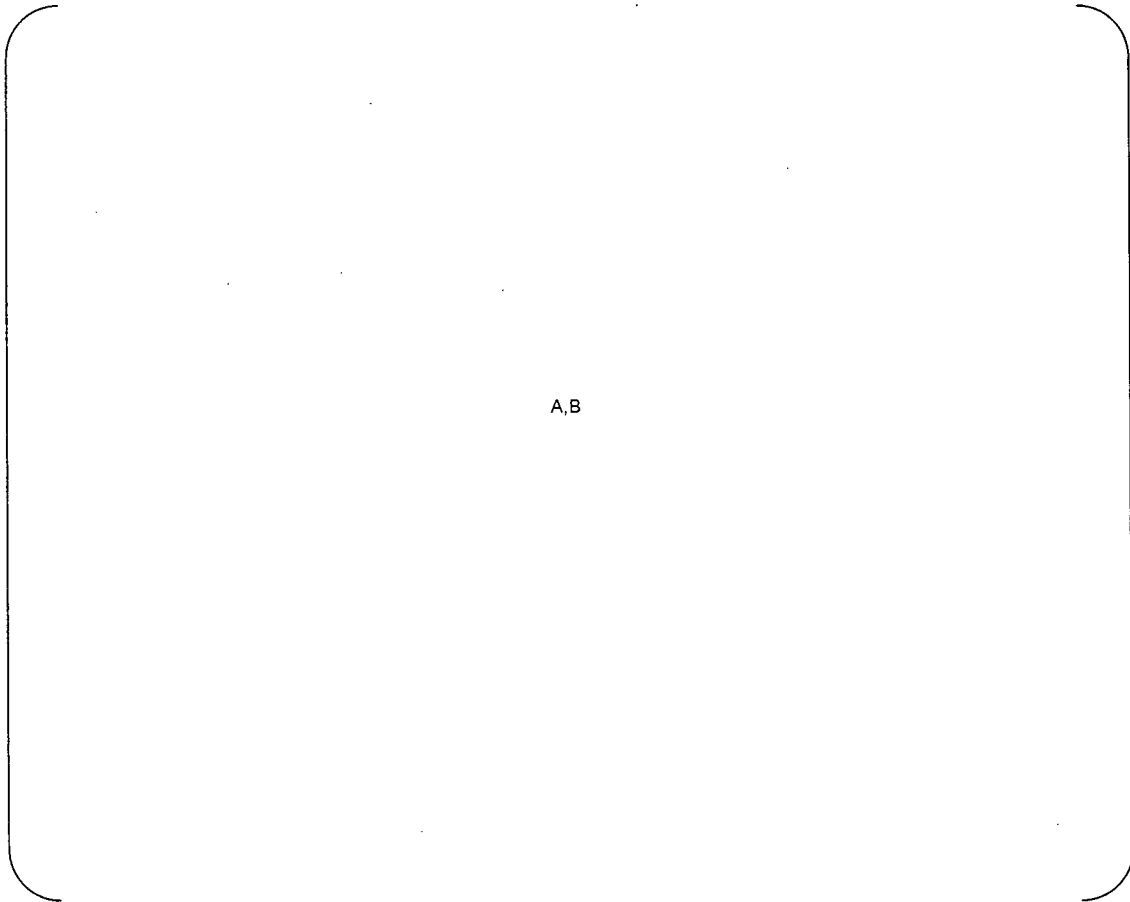
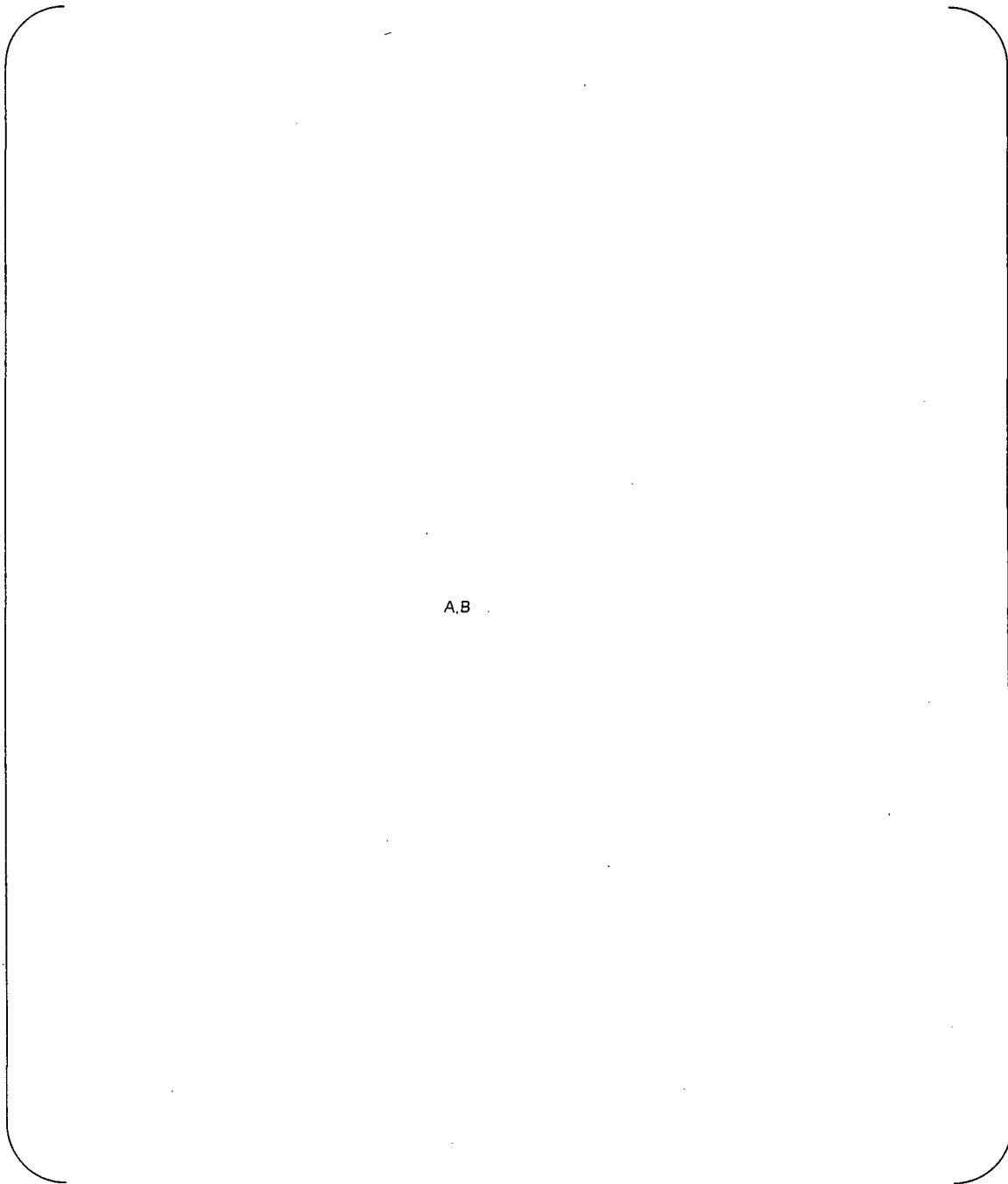
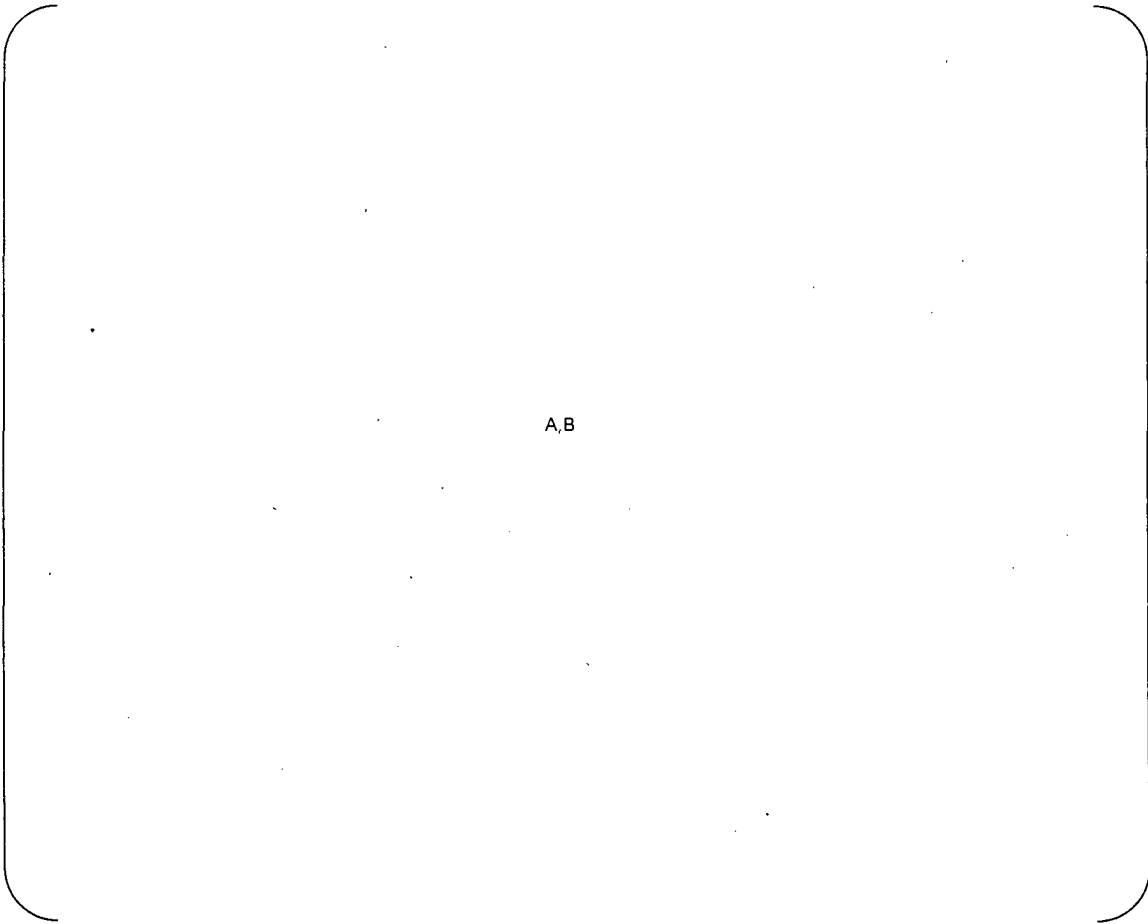


Figure M.5-5 (1/3) Strain Contour [equivalent plastic strain] (Elastic-Plastic Analysis)



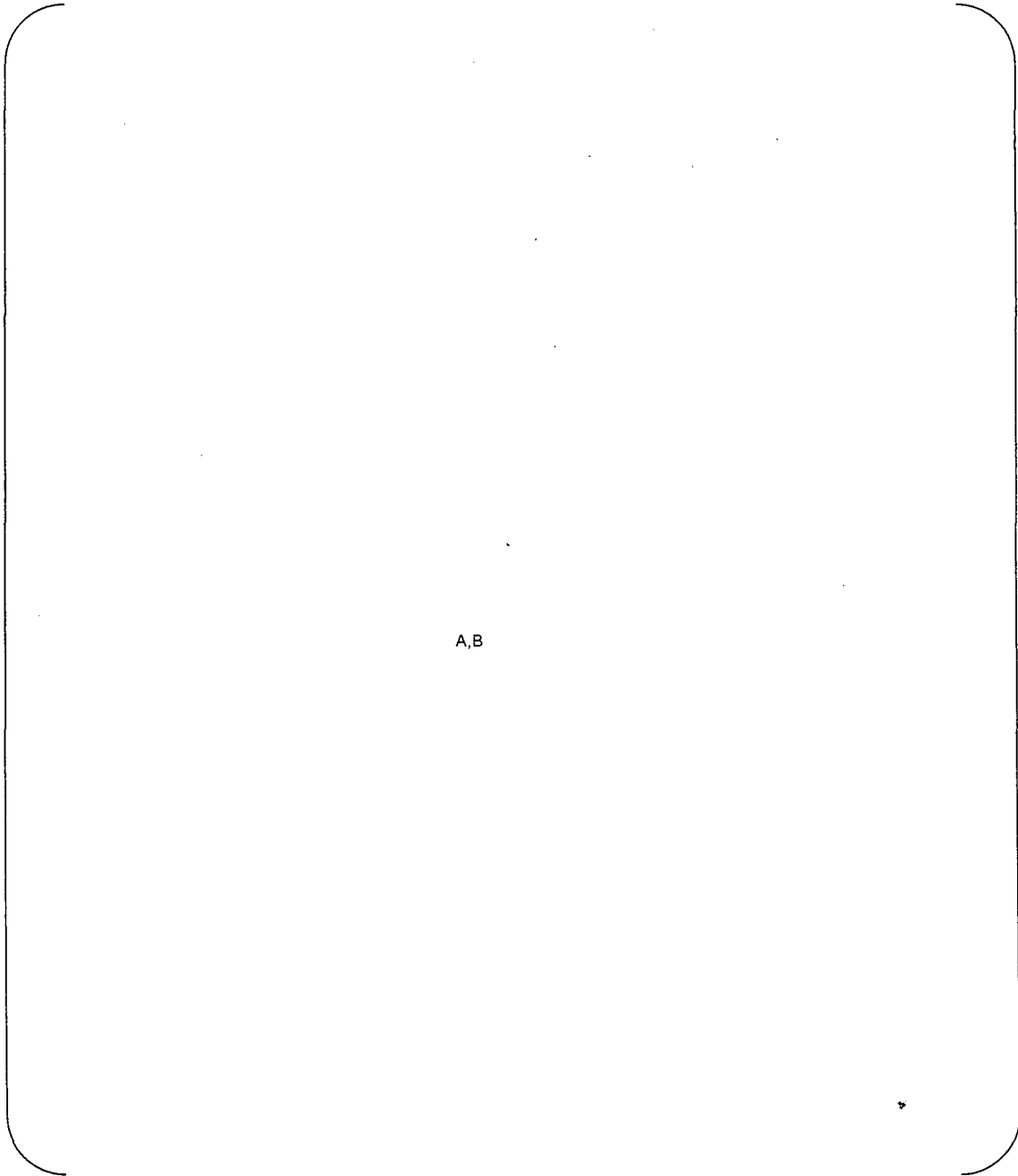
A,B

Figure M.5-5 (3/3) Strain Contour <Part-2> [equivalent plastic strain] (Elastic-Plastic Analysis)



A,B

Figure M.5-6 (1/3) Strain Contour [plastic strain : ϵ_X] (Elastic-Plastic Analysis)



A,B

Figure M.5-6 (3/3) Strain Contour <Part-2> [plastic strain : ϵ_X] (Elastic-Plastic Analysis)

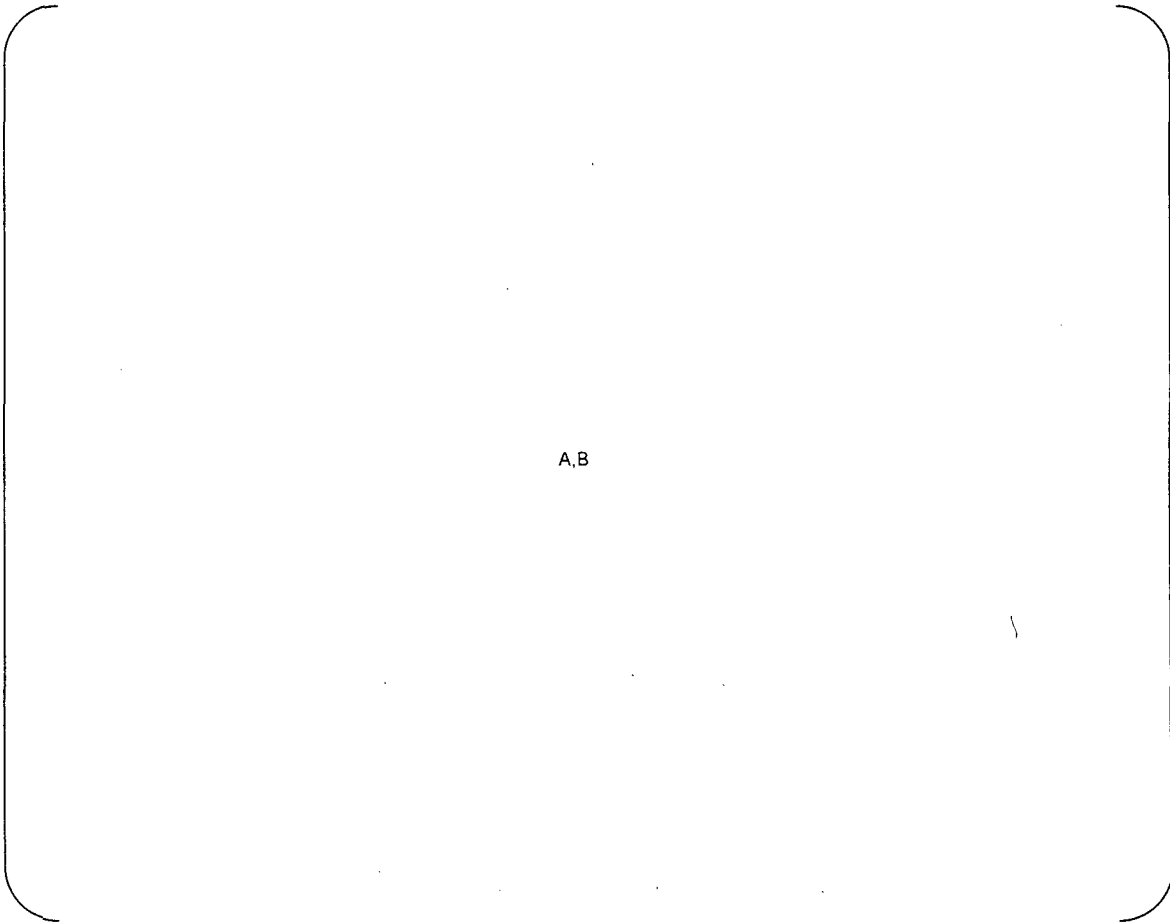
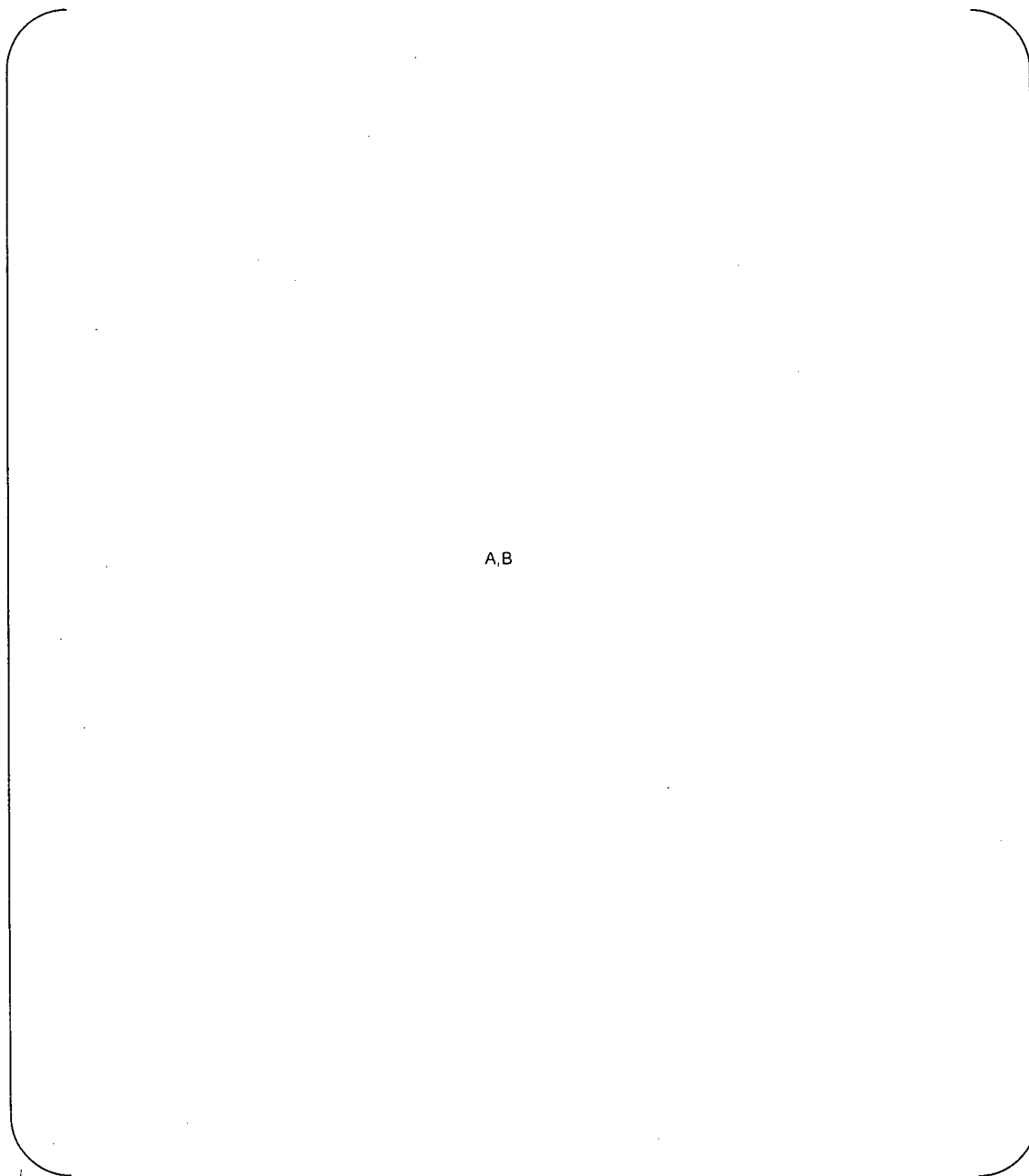


Figure M.5-7 (1/3) Strain Contour [plastic strain : ϵ_Y] (Elastic-Plastic Analysis)



A,B

Figure M.5-7 (3/3) Strain Contour <Part-2> [plastic strain : ϵ_Y] (Elastic-Plastic Analysis)



Attachment-N

**3D Analysis to Evaluate the Channel Head-to-Tubesheet Weld
Shrinkage**

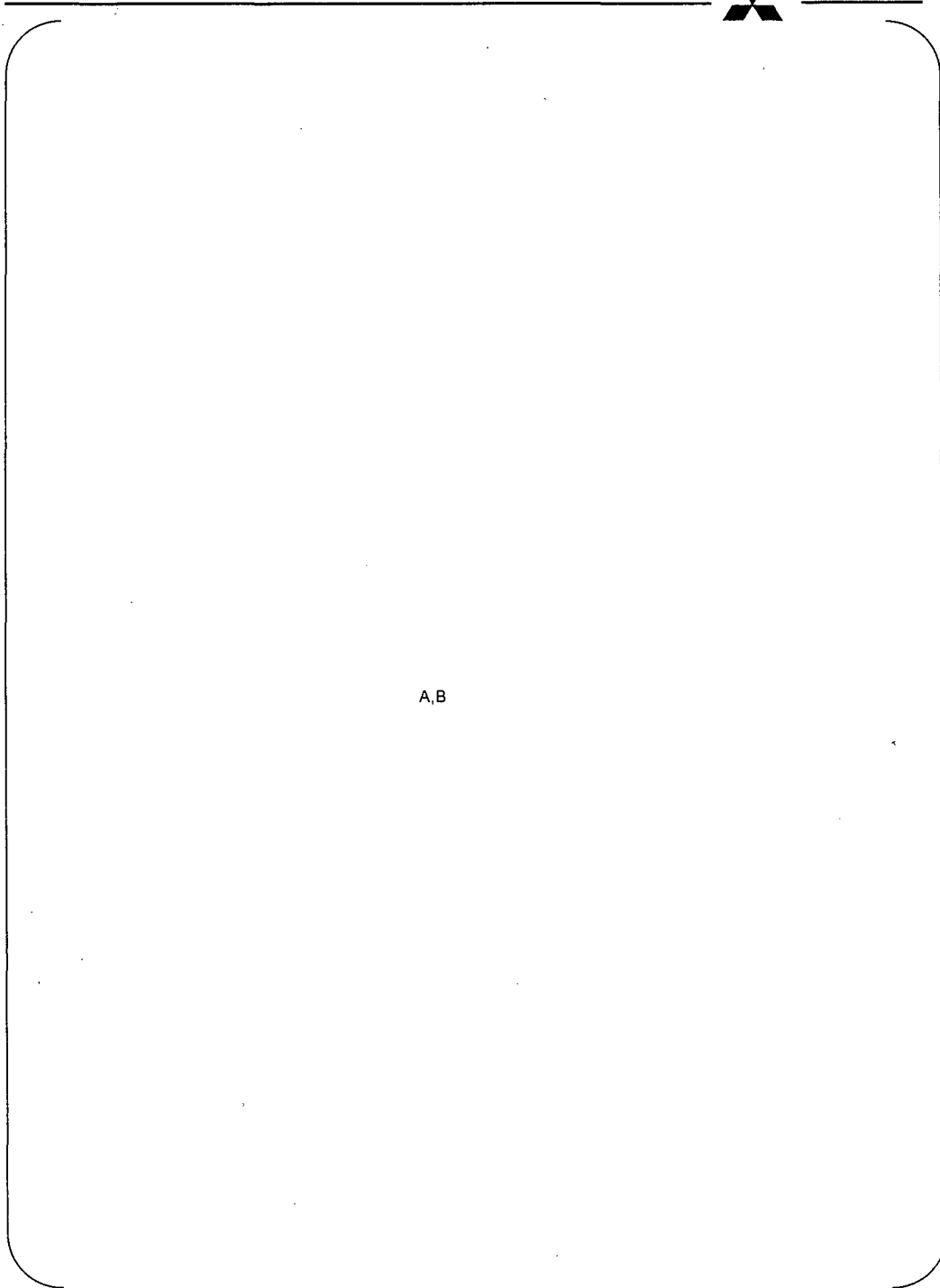


FE Analysis

Load condition is shown in Figure N.1 in the Tubesheet-to-Channel Head welding.
($\Delta T = [A, B]$)

The materials and the material properties are the same as the ones in “Design Report of the Tubesheet Region” (L5-04GA401).

The deformation and the stress/strain contours are shown in Figure N.2 and Figure N.3.



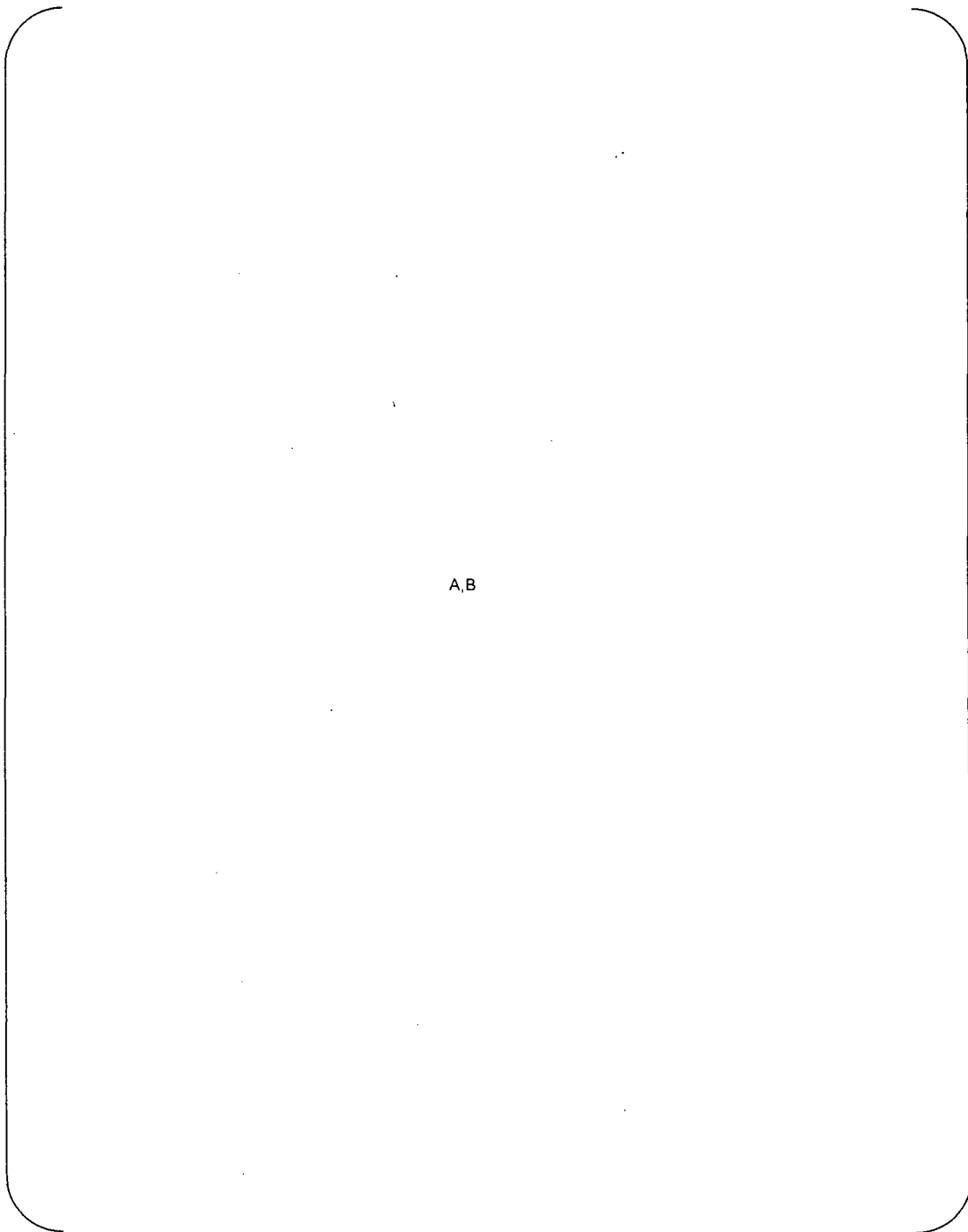
A,B

Figure N.1 Analysis Conditions



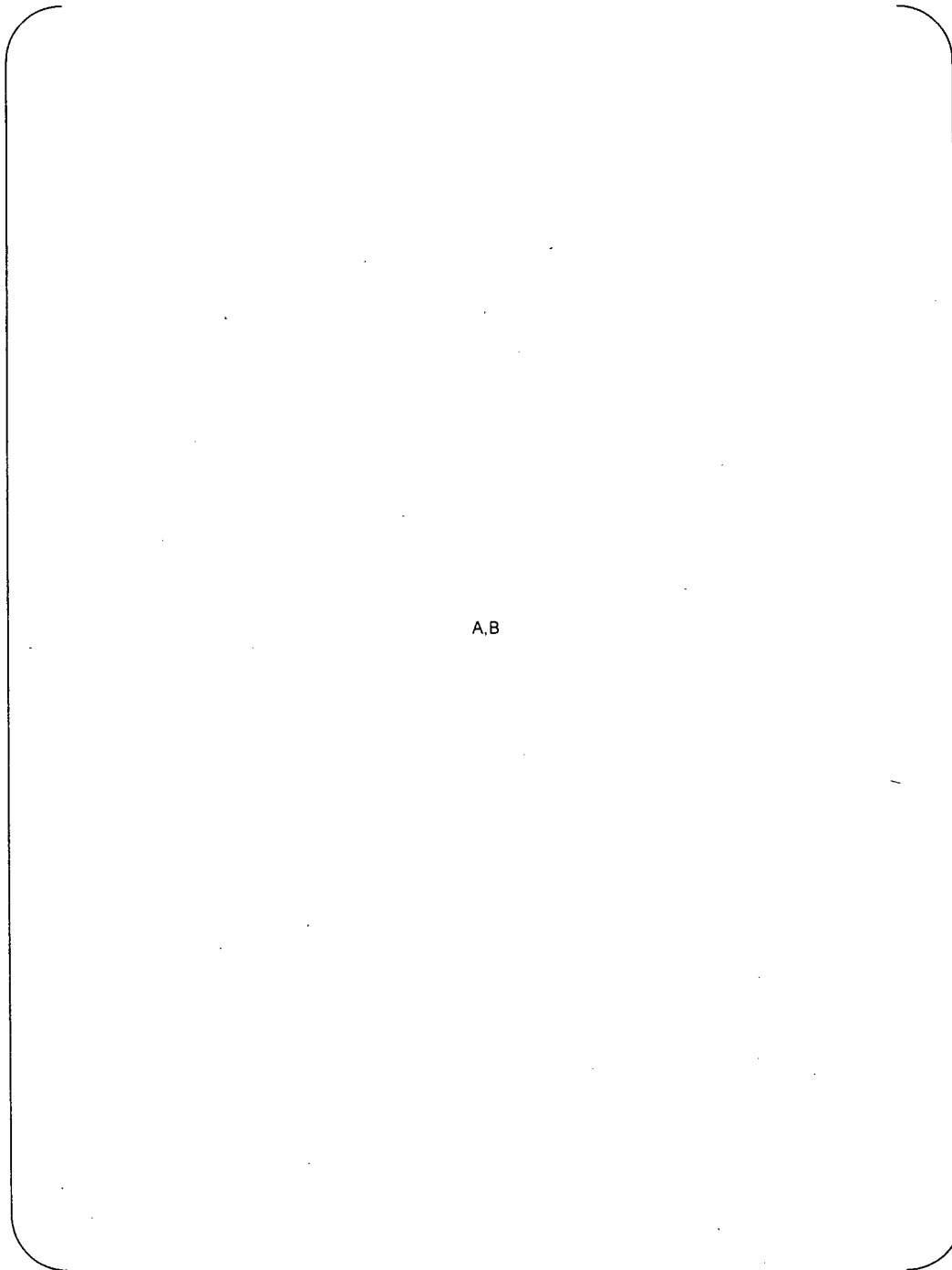
A,B

Figure N.2 Contour of Strain [Tubesheet Weld]



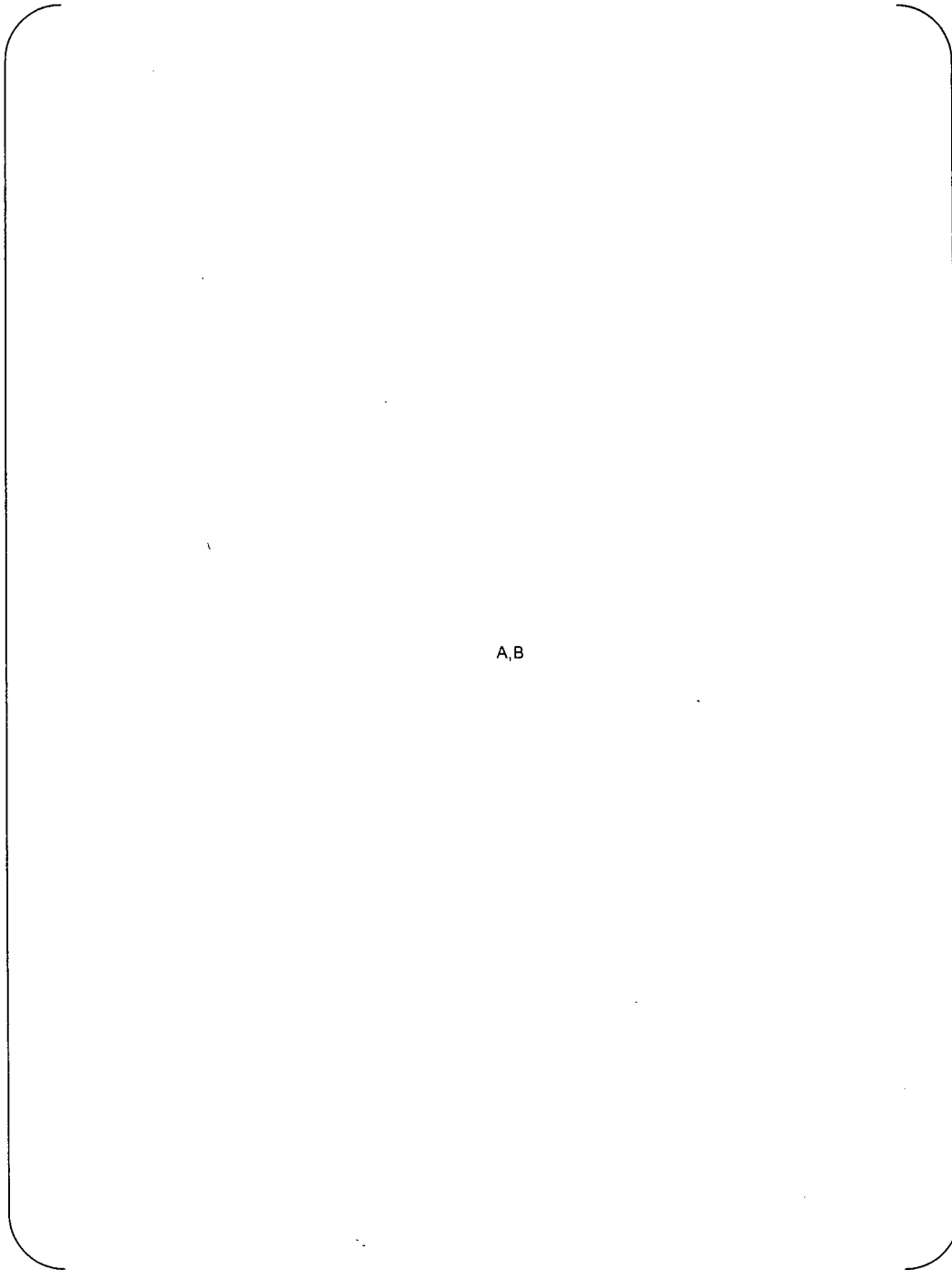
A,B

Figure N.3 (1/3) Contour of Mises Stress [Tubesheet Weld]



A,B

Figure N.3 (2/3) Contour of Mises Stress [Tubesheet Weld]



A,B

Figure N.3 (3/3) Contour of Mises Stress [Tubesheet Weld]



Attachment-O

3D Analysis to Evaluate the Channel Head-to-Tubesheet Weld PWHT



FE Analysis

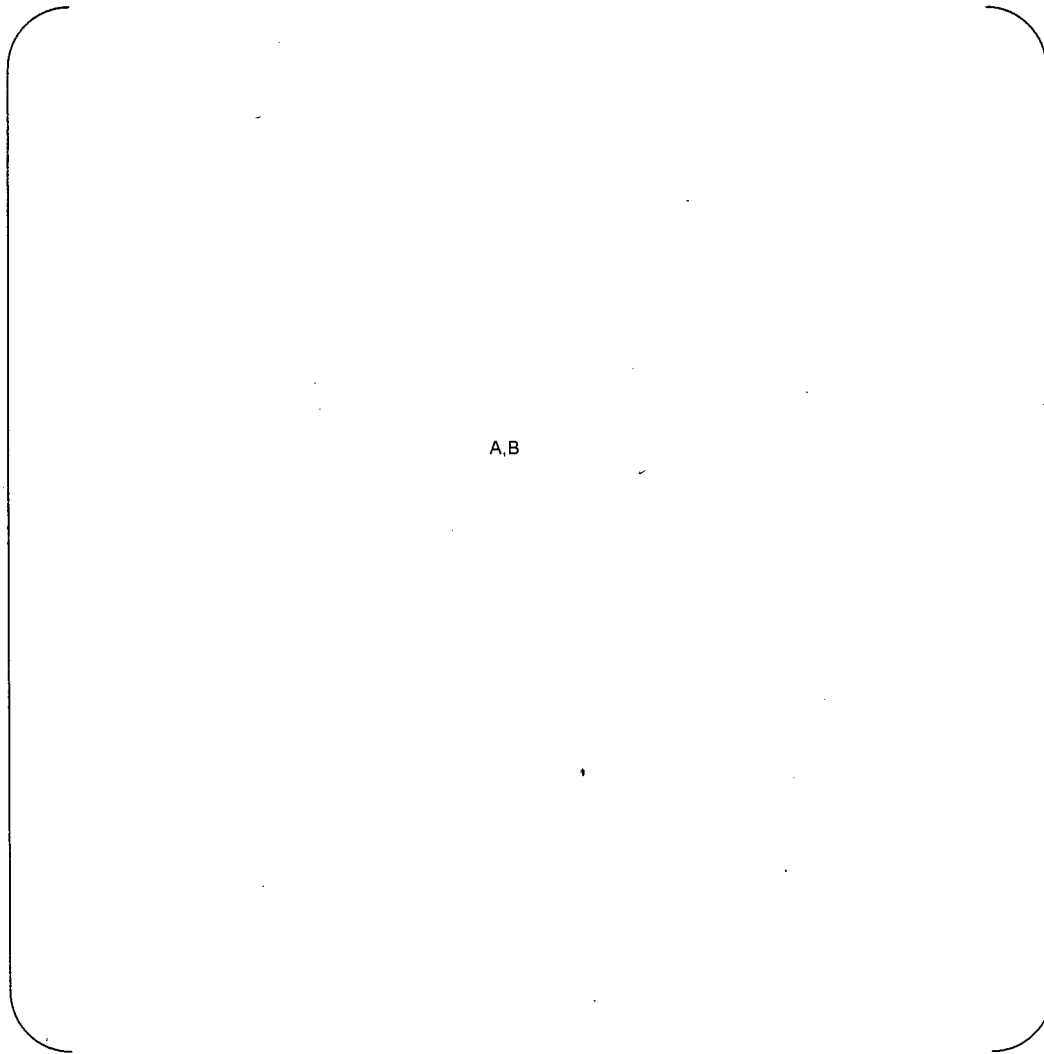
The FE model is shown in Figure O.1. This model is the same as the one in “Design Report of the Tubesheet Region” (L5-04GA401).

Load and boundary conditions are shown in Figure O.2. Nodal temperatures are based on “Thermal Analysis under PWHT” (L5-04GA414).

The material properties used in the analyses are shown in Table O.1.

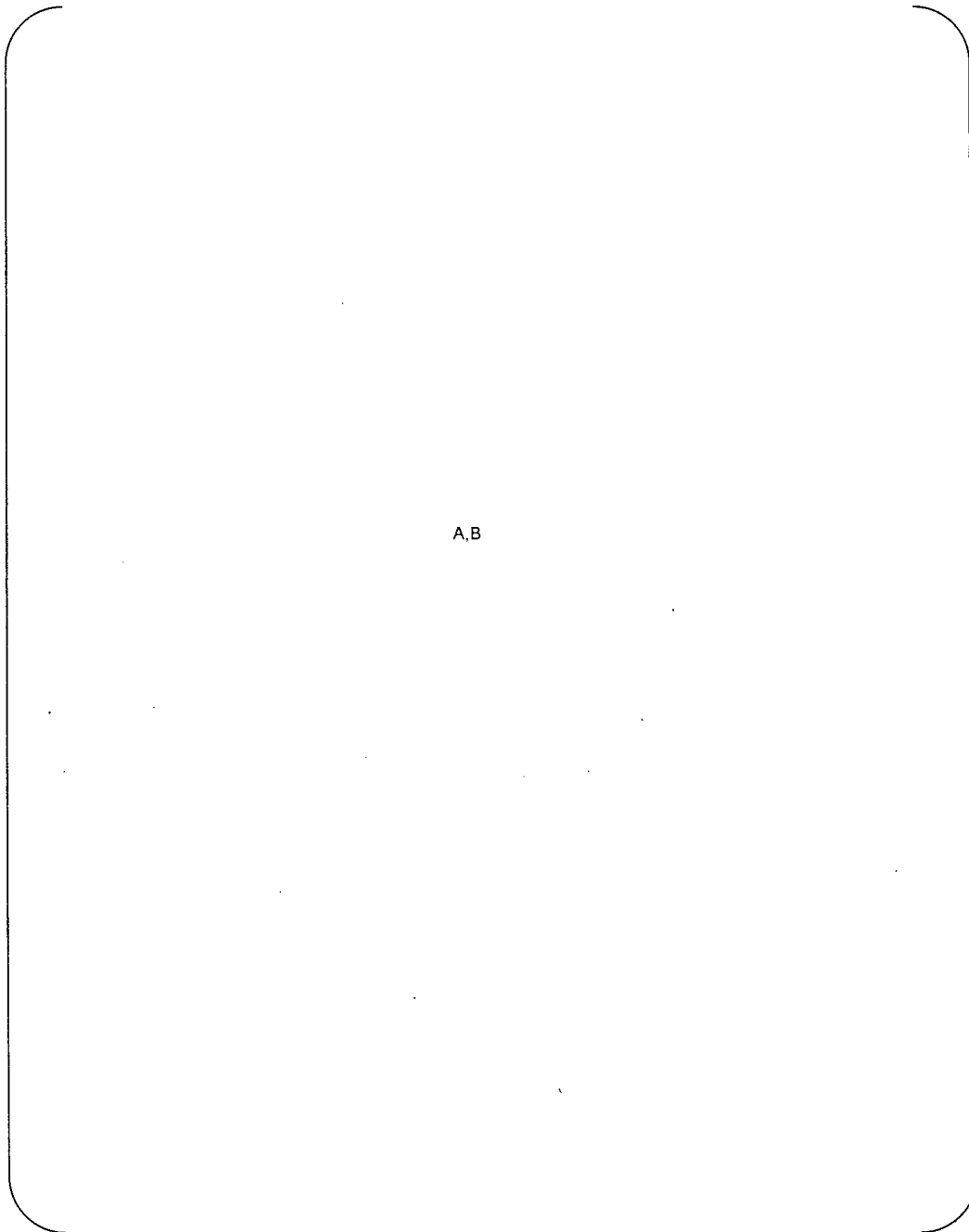
The temperature contours for PWHT are shown in Figure O.3-1. The stress contours are shown in Figure O.3-2 through Figure O.3-4.

Comparison of temperature distribution (End of Heat up Process) of L5-04GA401 and L5-04GA414 is shown in Figure O.3-5.



A,B

Figure O.1 Analysis Model



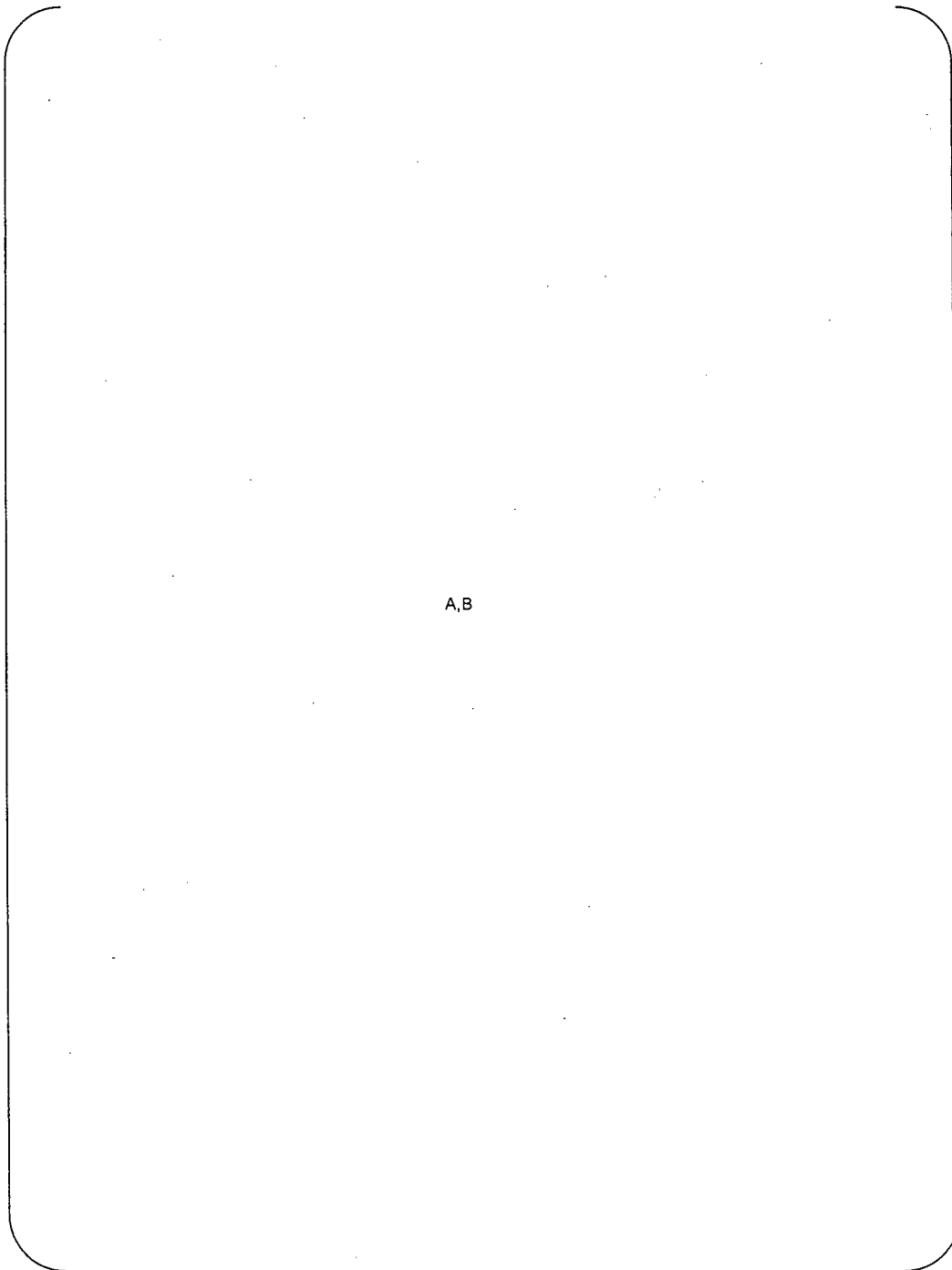
A,B

Figure O.2 Load and Boundary Condition



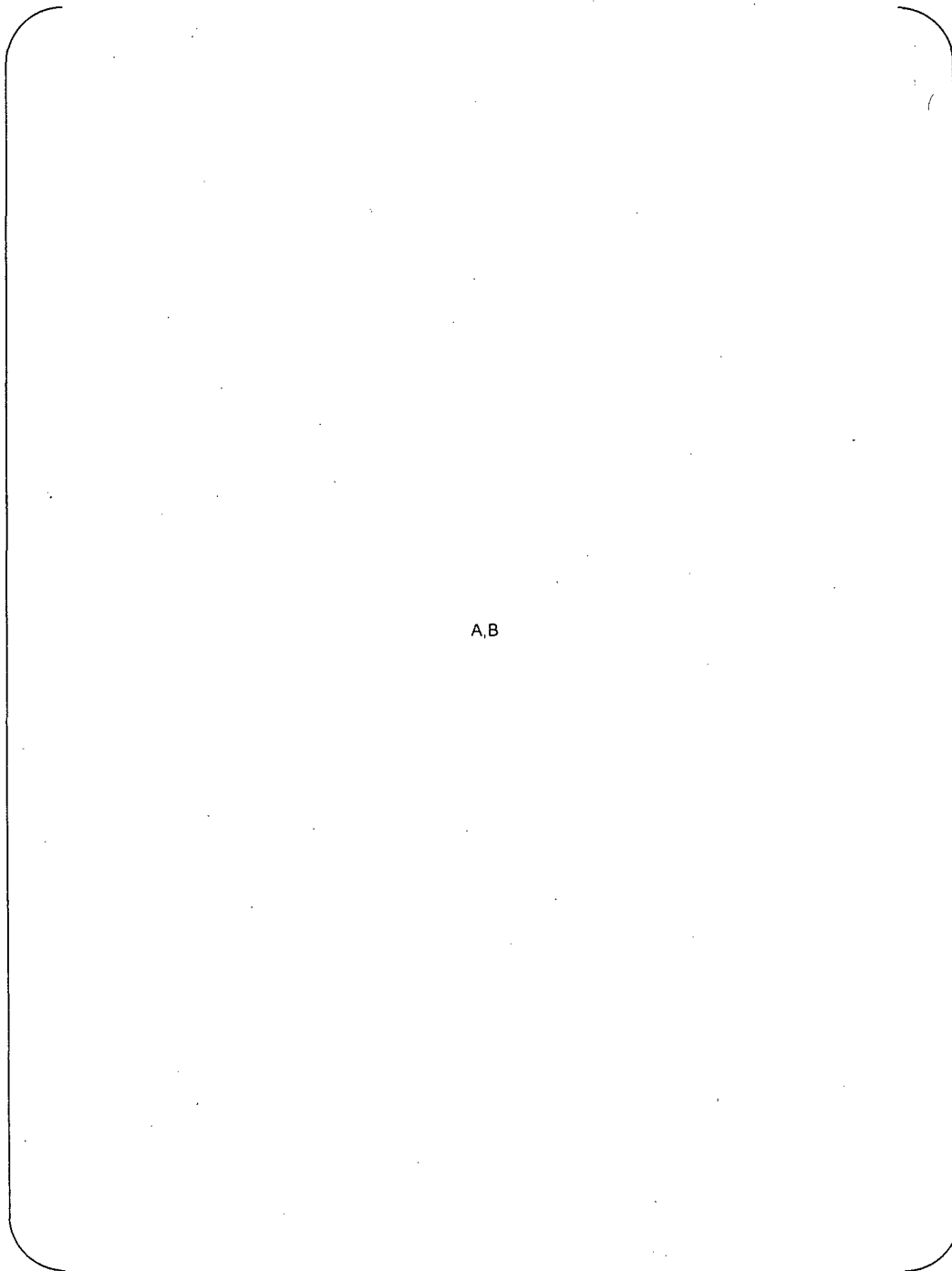
Table O.1 Material Properties

A,B



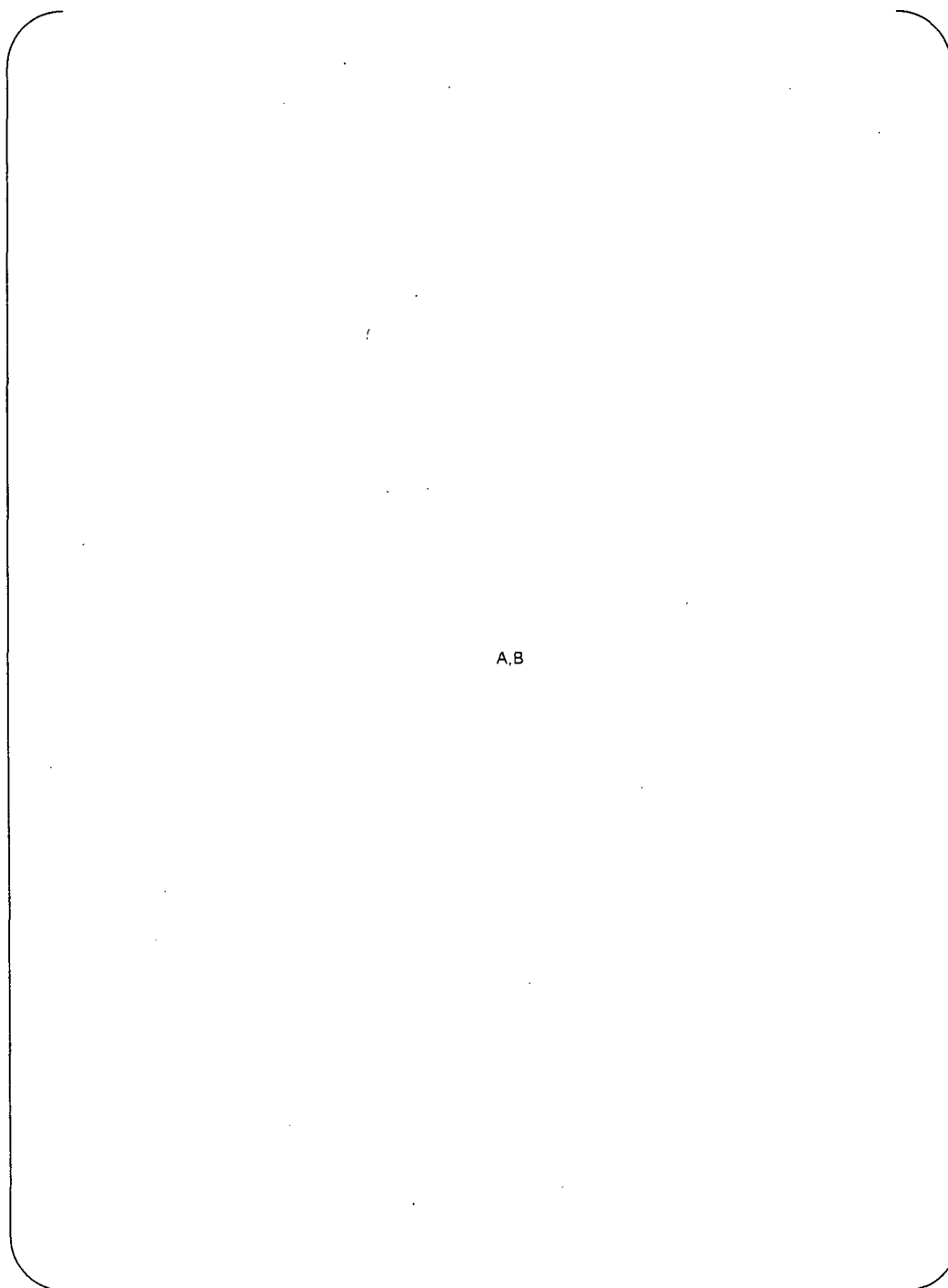
A,B

Figure O.3-1 Temperature Distribution



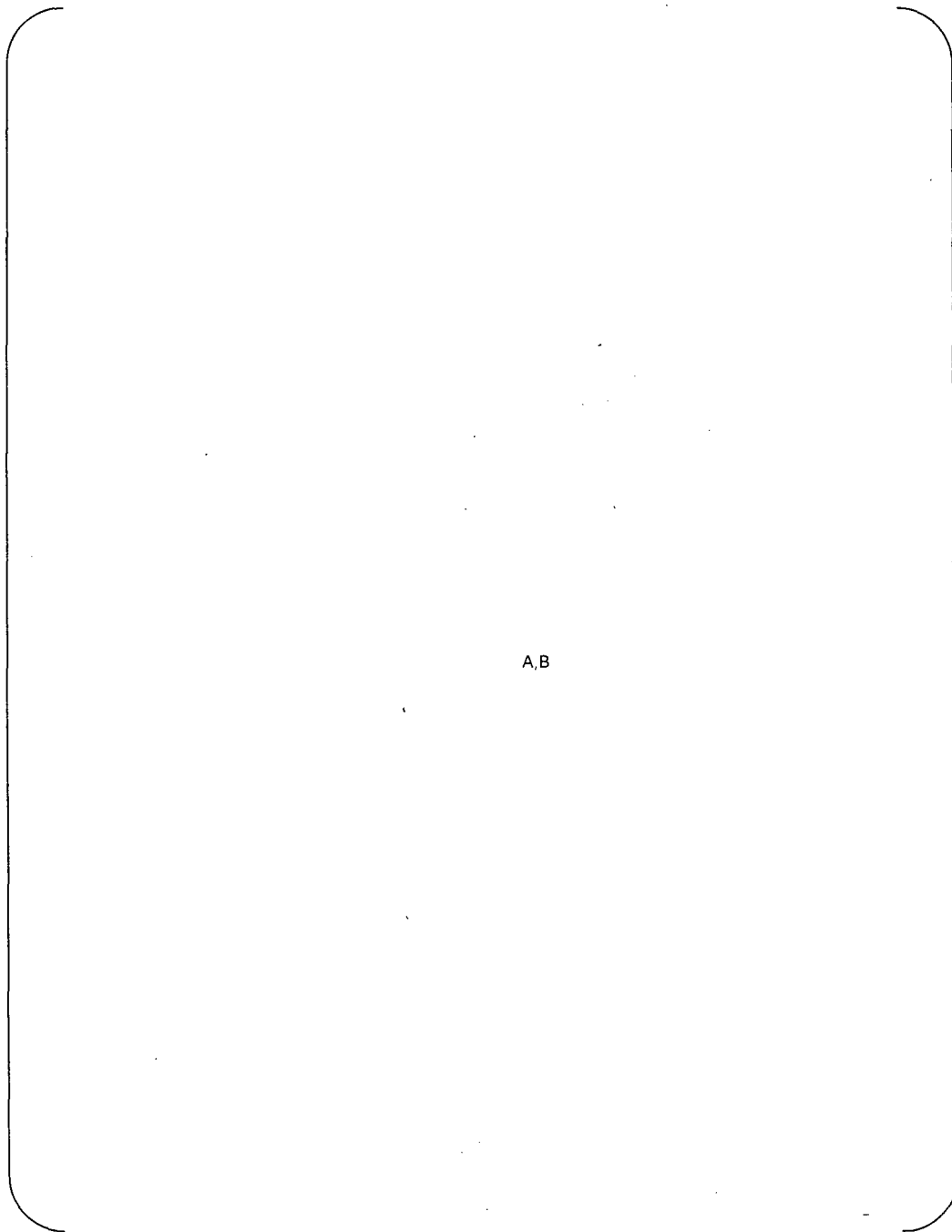
A,B

Figure O.3-2 Stress Contour [Mises] (End of Heat up Process)



A,B

Figure O.3-3 Stress Contour [Mises] (End of Heat up Process)



A,B

Figure O.3-4 Stress Contour [Mises] (End of Heat up Process)



A,B

Figure O.3-5 Comparison of temperature distribution(End of Heat up Process) of L5-04GA414 and L504GA401





Attachment-P

3D Analysis Including the Actual Condition of 3B RSG



FE Analysis

The FE model is shown in Figure P.1. Load and boundary condition are shown Figure P.2.

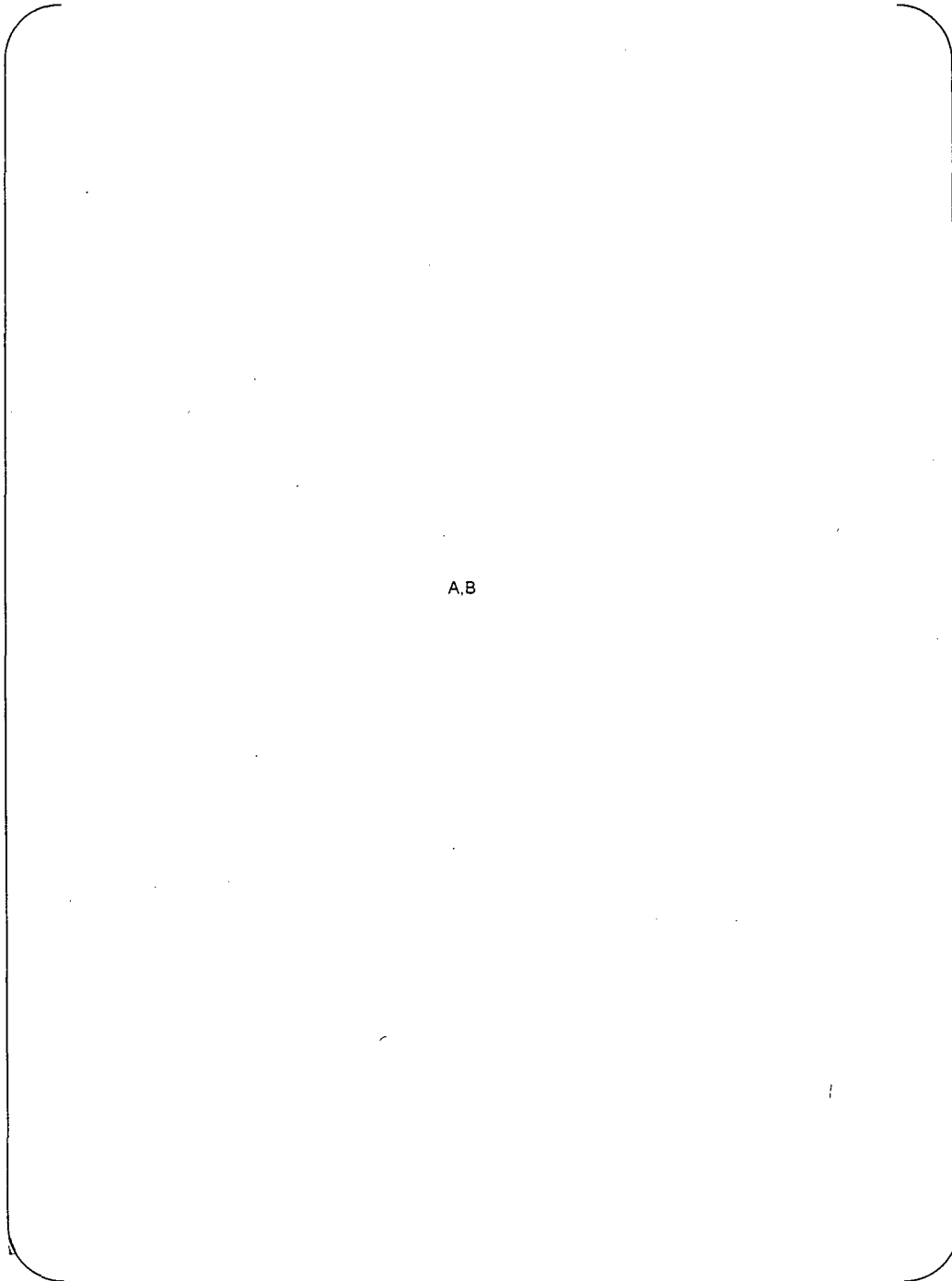
The materials are shown in Figure P.3. The material properties used in the analyses are shown in Table P.1.

Table P.1 Material Properties

A,B

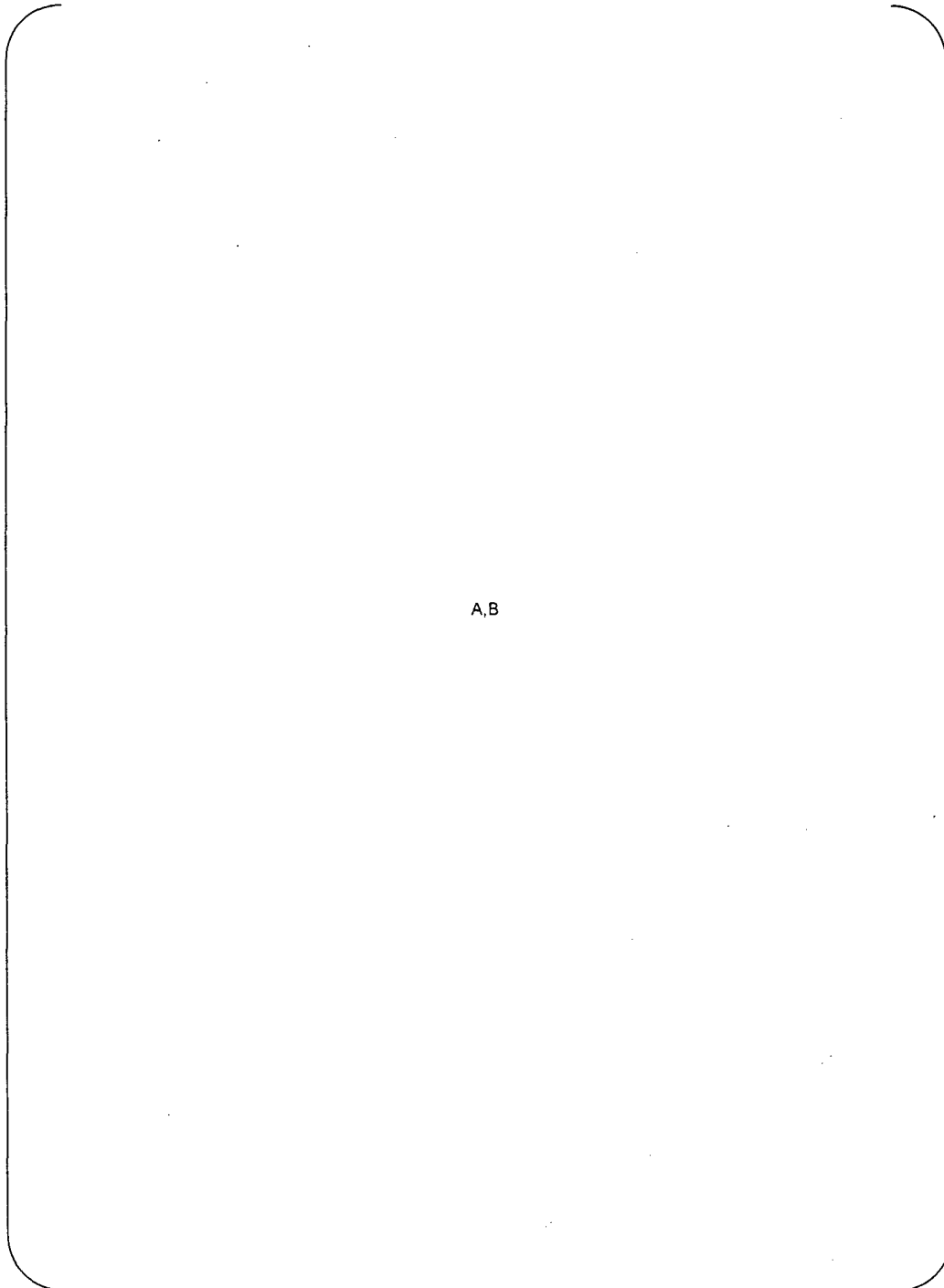
The deformation and the stress contours are shown in Figure P.4 through Figure P.8.

The Stress distribution are shown in Figure P.9.



A,B

Figure P.1 Analysis Model



A,B

Figure P.2 Load and Boundary Condition



A,B

Figure P.3 Material



A,B

Figure P.4 Displacement

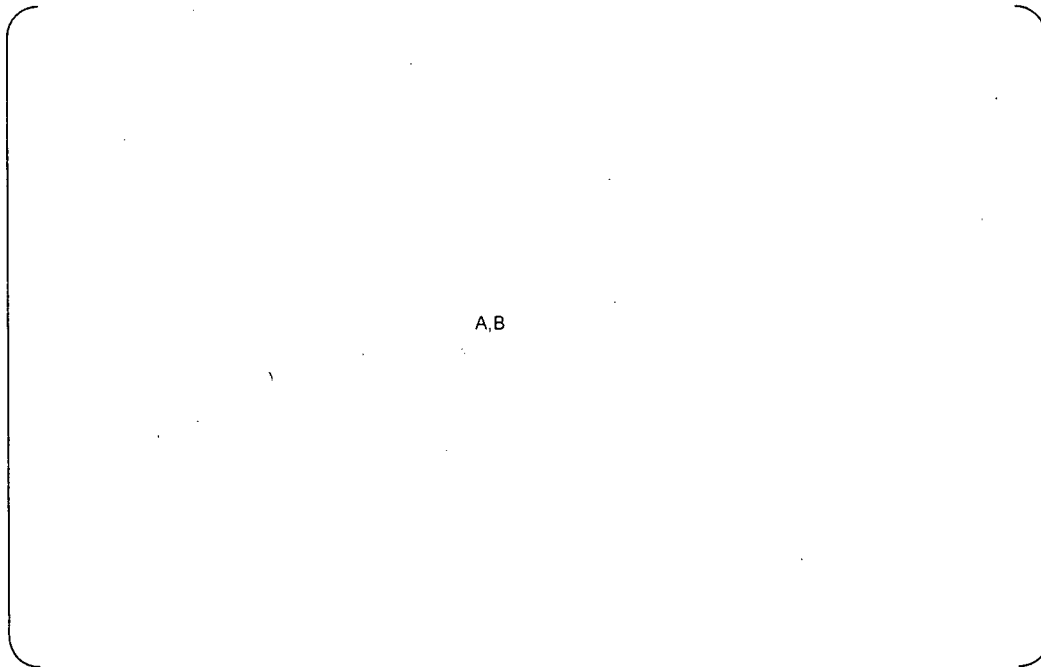


Figure P.5 (1/2) Stress Contour [Mises]

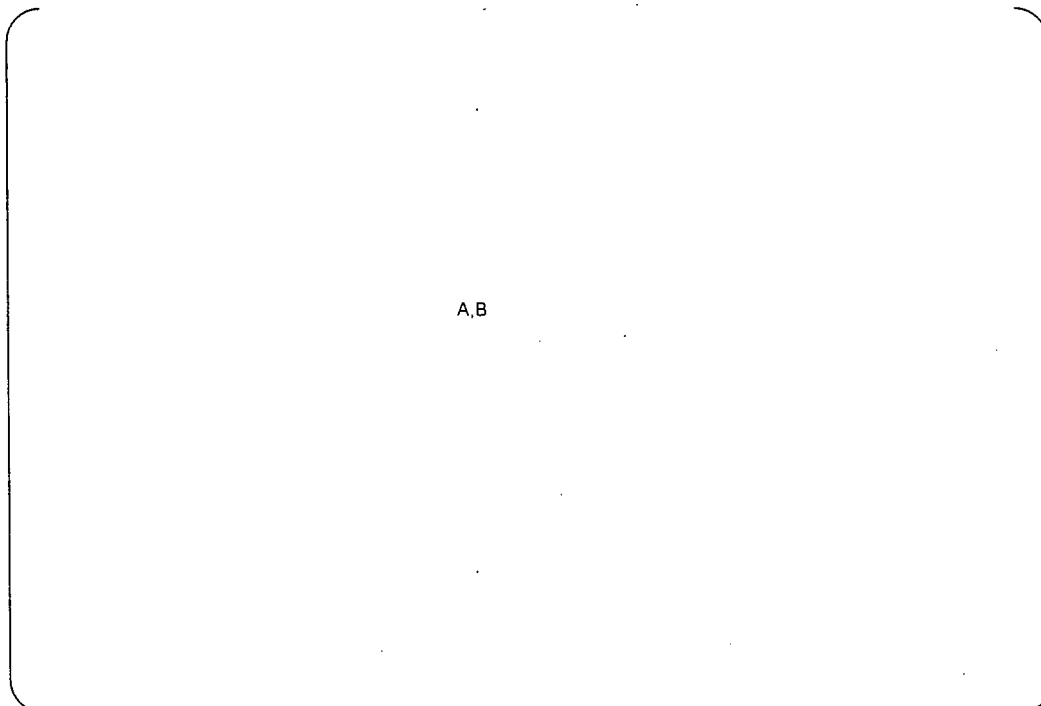


Figure P.5 (2/2) Stress Contour <Part-1> [Mises]

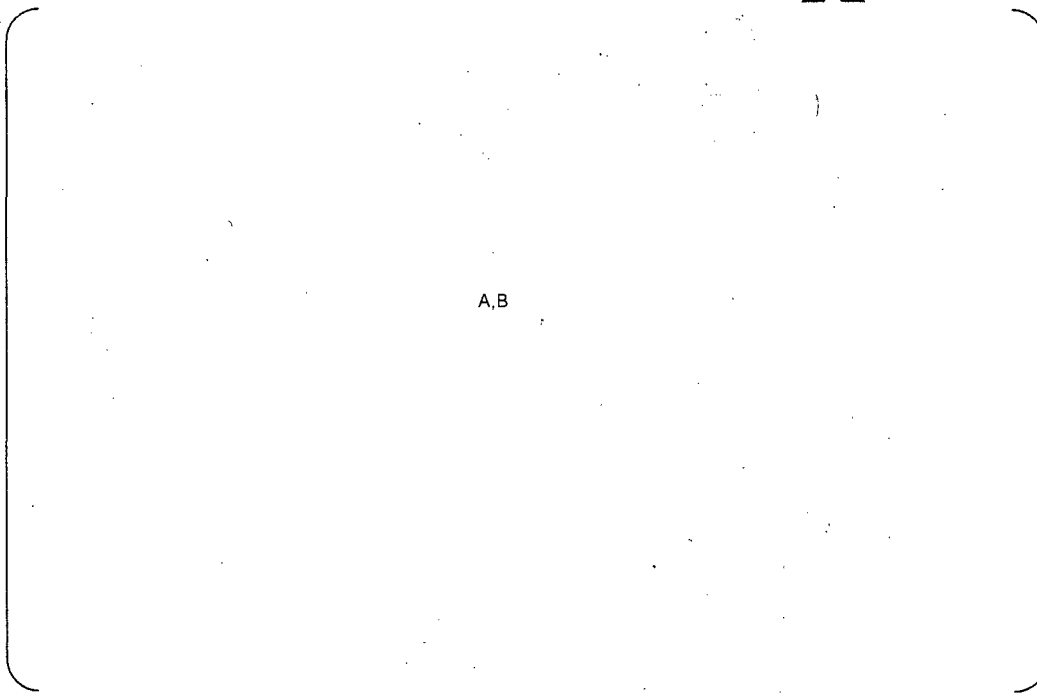


Figure P.6 (1/2) Stress Contour [σ_X]

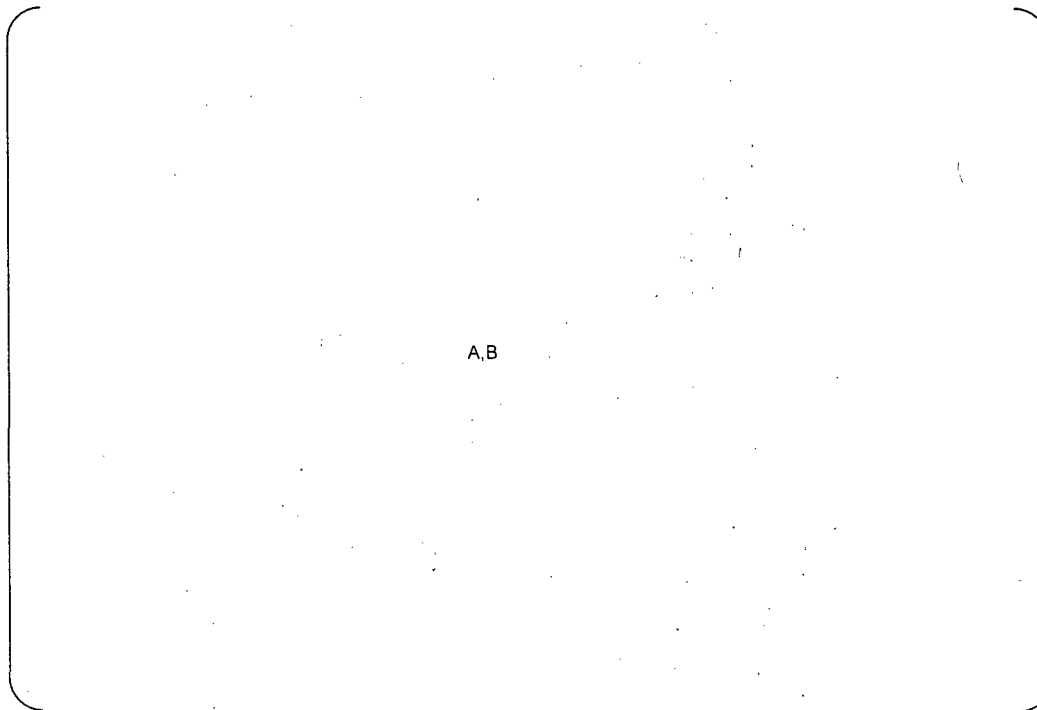


Figure P.6 (2/2) Stress Contour <Part-1> [σ_X] (Elastic Analysis)



Figure P.7 (1/2) Stress Contour [σY]

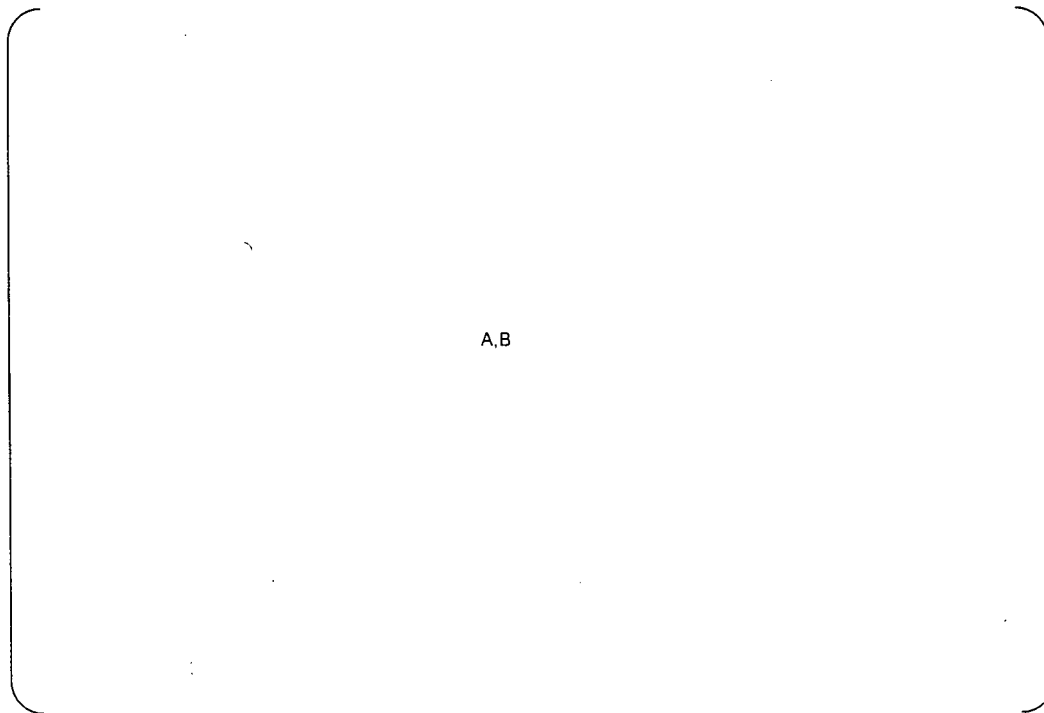


Figure P.7 (2/2) Stress Contour <Part-1> [σY]

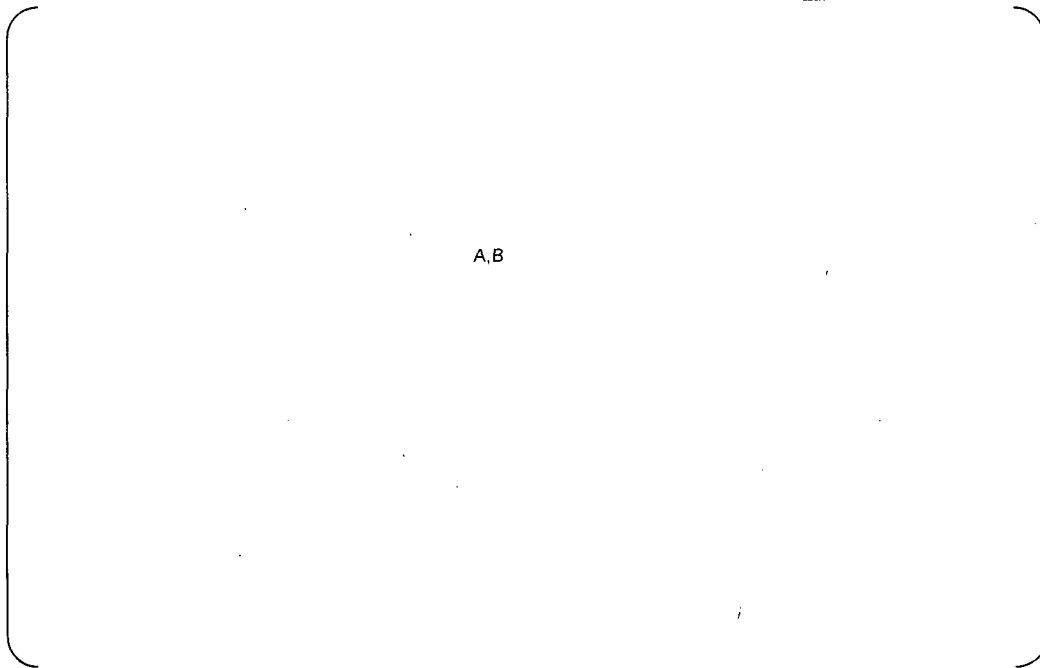


Figure P.8 (1/2) Stress Contour [σ_Z]

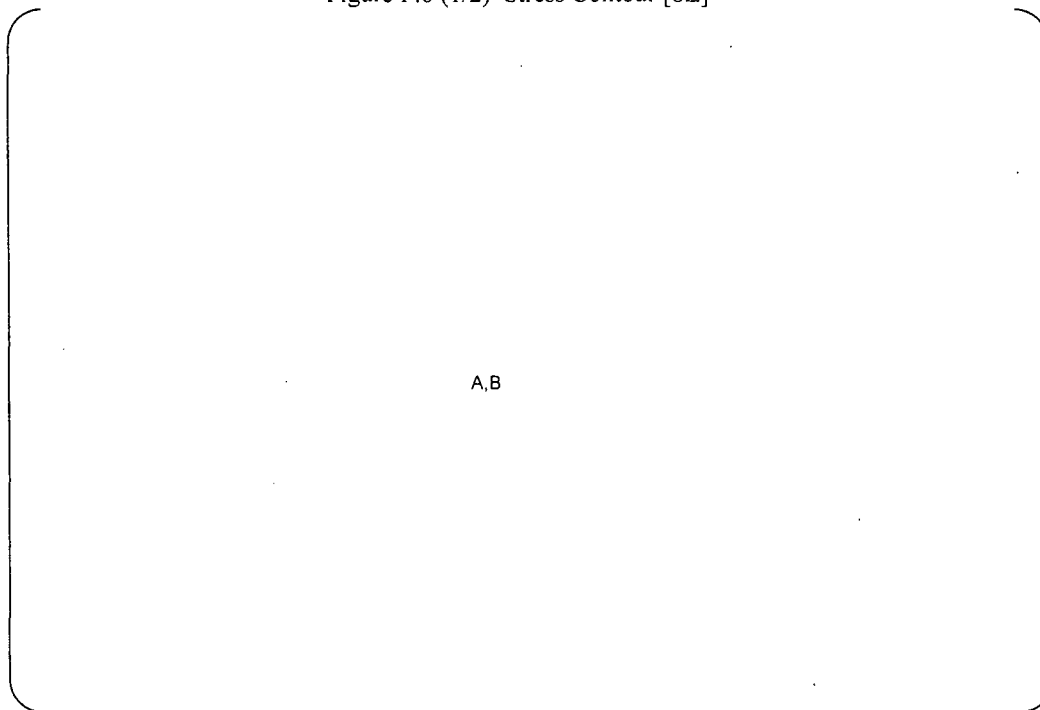
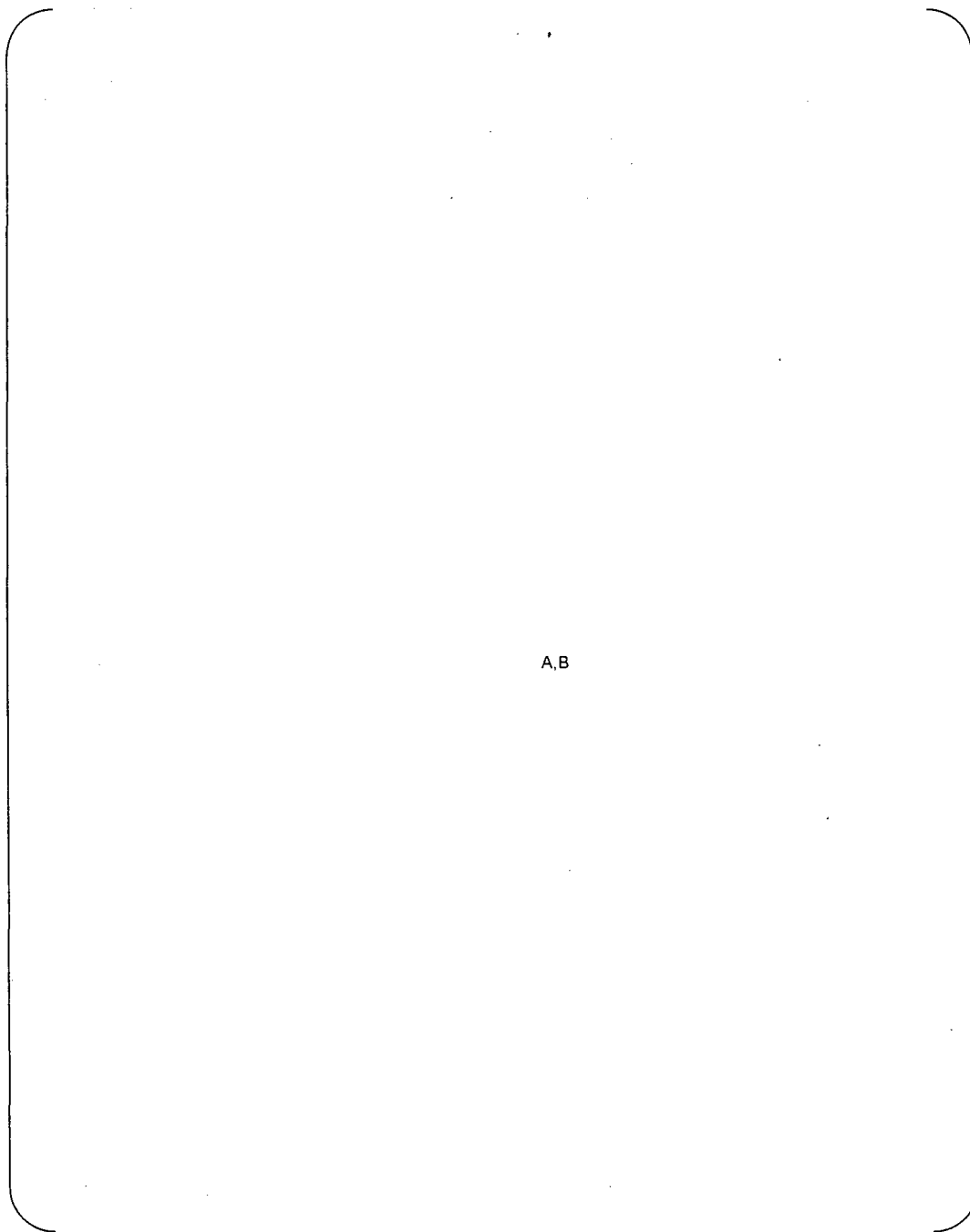


Figure P.8(2/2) Stress Contour <Part-1> [σ_Z]



A,B

Figure P.9 Stress distribution



Attachment-Q

Hydrogen Diffusion Analysis



Hydrogen Diffusion Analysis

1.Purpose

The purpose of this report is to provide the analysis results of hydrogen diffusion behavior in alloy 152 buttering and low-alloy steel (LAS) cladding.

2.Conclusion

(1) As a result of hydrogen diffusion analysis with models simulating the heat treatment conditions of Unit-2B and Unit-3A, the significant difference of residual hydrogen concentration between alloy 152 and LAS after heat treatment was not confirmed although the heat treatment conditions (temperature and time) are different.

(2) In both cases (simulating Unit-2B and Unit-3A), the hydrogen diffusion coefficient within the range of heat treatment for LAS is 100 times smaller or more in comparison with alloy 152. Therefore, the progression of hydrogen concentration from alloy 152 to LAS can be observed near the boundary of alloy 152 and LAS but there was no significant difference in the concentration of hydrogen in alloy 152 after heat treatment.



3. Method of Procedures

(1) Analysis models and Analysis conditions

To simulate hydrogen behavior through-thickness direction, the analysis models are assumed as the configuration shown in Figure Q.1. Table Q.1 shows the heat treatment conditions for hydrogen diffusion analysis based on actual welding record. The graphs of the number of laminated layers of the models by time are presented on Figure Q.2 and Figure Q.3.

Initial hydrogen diffusion in LAS and in alloy 152 is [A,B] and [A,B] each. The hydrogen diffusion coefficients in metal are presented on Apendix-1.

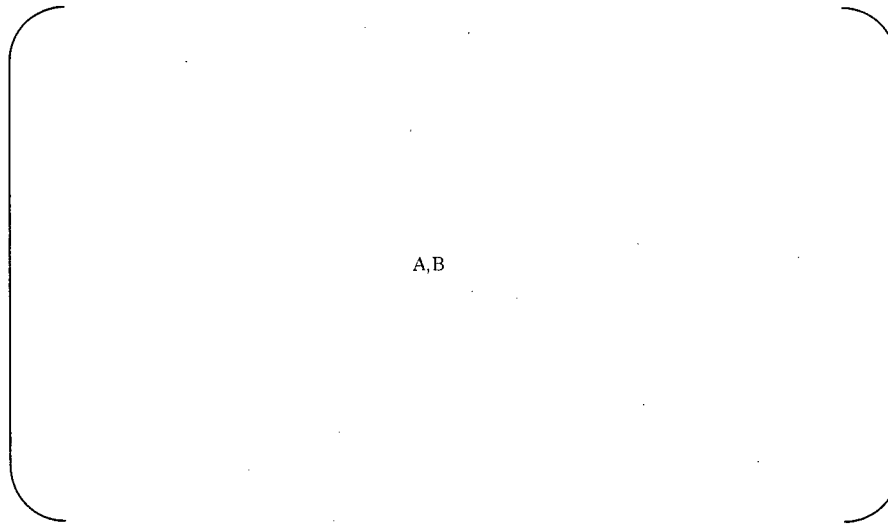
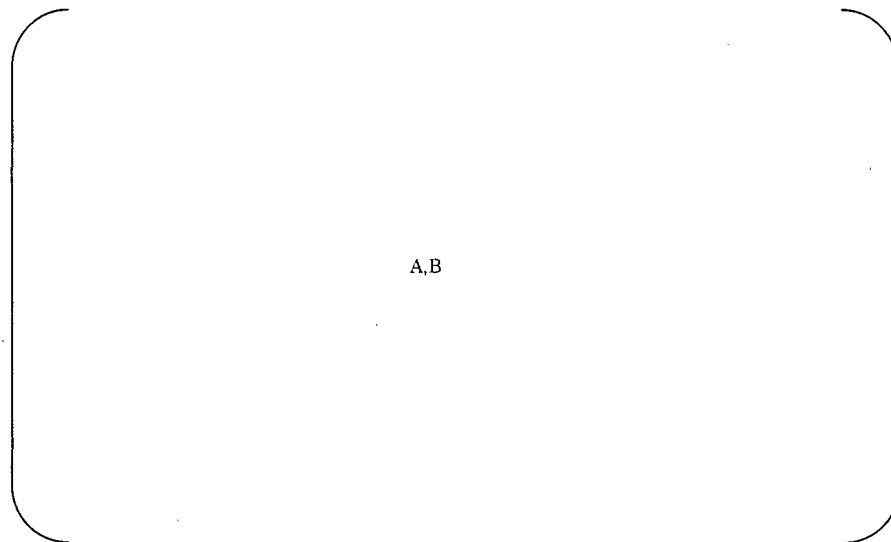


Figure Q.1 Model for hydrogen diffusion analysis

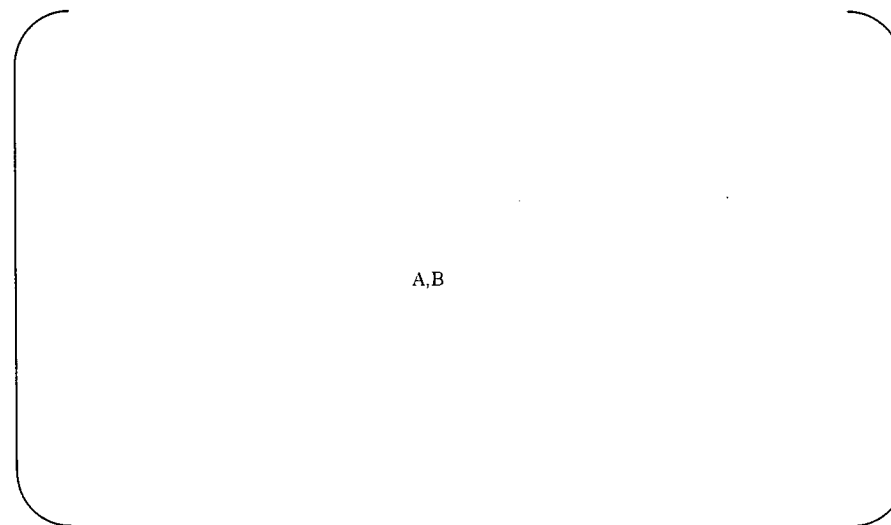
Table Q.1 Heat treatment conditions

A,B



A,B

Figure Q.2 Heat-treatment and Welding condition of Case-1 (U2B-RSG)



A,B

Figure Q.3 Heat-treatment and Welding condition of Case-2 (U3A-RSG)



4. Results of Measurement

For both Case-1 and Case-2, a steep slope of hydrogen concentration is observed and verified at the boundary of alloy 152 and LAS (this happens because the hydrogen diffusion coefficient of alloy 152 and LAS within the range of heat treatment differs 100 times or more), but no significant difference was found between case-1 and case-2 in the following points.

- The depth where hydrogen concentration begins to decrease is less than [A,B] from the boundary of alloy 152 and LAS.
- Hydrogen diffusion value are [A,B] (in case-1), and [A,B] (in case-2) at the boundary of alloy 152 and LAS.

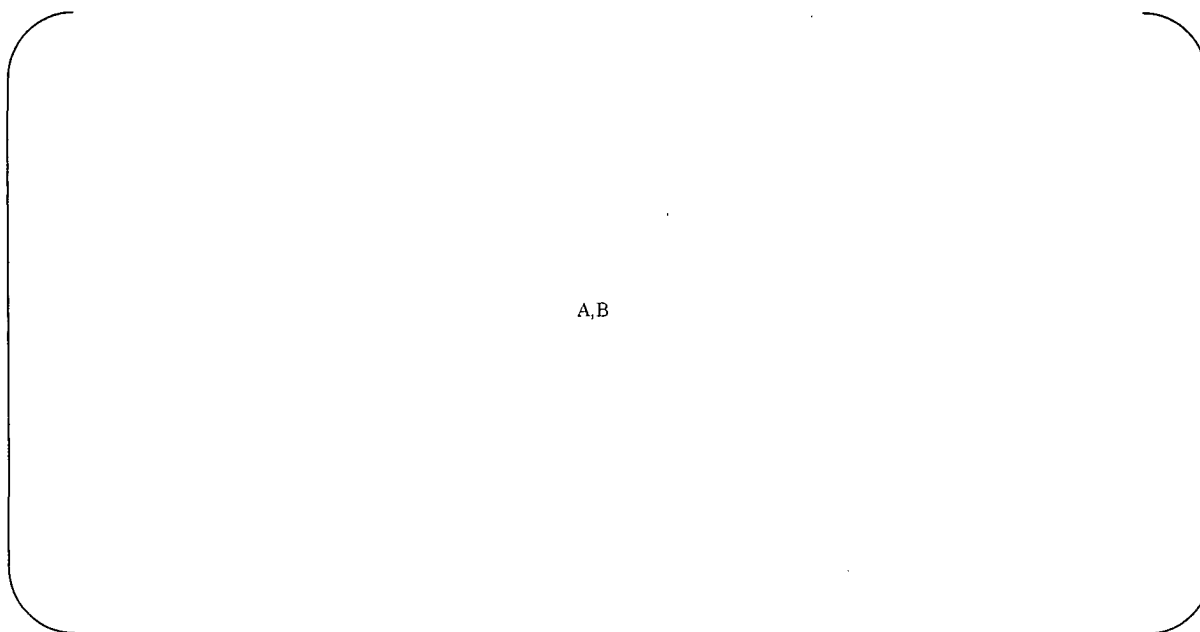


Figure Q.4 Hydrogen Concentration in Alloy 152 buttering

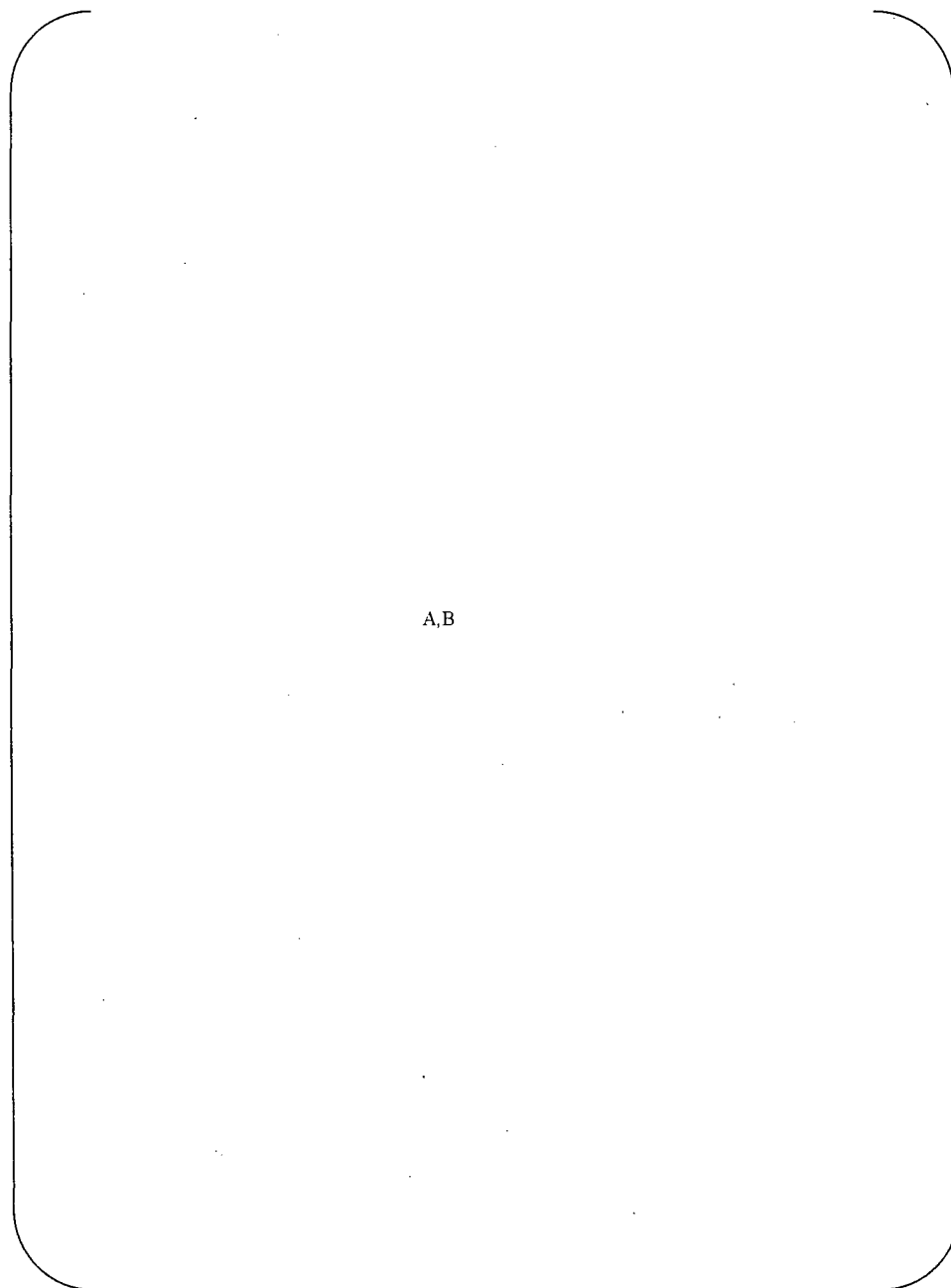


Figure Q.5 Hydrogen Concentration in Low alloy steel
(The under side is the expansion of the upper side.)



Appendix-I

<Hydrogen diffusion coefficient in metals>

A,B



Attachment-R
Fabrication Process Comparison

The Fault Tree Analysis and Investigation Plan shown in Table R.1 is an analysis of the process steps used to produce the channel head assembly. This analysis identifies causes and effects for each process and leads to identification of specific investigations that are intended to reveal the root cause and contributing causes of the divider plate-to-channel head weld separation.



(R-2)
Document No.L5-04GA440 (0)
Attachment-R

[illegible]

A,B

[illegible]

A,B



(R-4)
Document No.L5-04GA440 (0)
Attachment-R

Table R.1 Fault Tree for Analysis & Investigation

A,B

[illegible]

(R-5)
Document No.L5-04GA440 (0)
Attachment-R

A, B

Attachment-R

2 Review of Fabrication History

2.1 Part Materials

Table R.2 Forging Material Properties

2.1.1 Forging Material

A,B.

2.1.2 SS Clad

Table R.3 Chemical Composition of SS Clad (1/2)

A,B



Table R.3 Chemical Composition of SS Clad (2/2)

A,B

2.1.3 Alloy 152 Butter

Table R.4 Chemical Composition of the Alloy 152 Butter

A,B





2.2 Channel Head Cladding Process

The cladding was applied on the channel head bowl by the Electro-Slag Welding process (ESW) except at the center where the Shielded Metal Arc Welding process (SMAW) was used. One of the root causes that could degrade weld quality is "migration of detrimental materials into the base metal, which could lead to degradation of the base metal material properties". Another cause could be improper welding (i.e. exceeding the heat input limit).

Actions taken to address this family of causes include review of the welding records for Units 2 and 3 to confirm that the correct material was used and the welding processes were performed properly.

Table R.5 through 8 lists the welding materials used on the Unit 2 & 3 channel heads. Welding conditions such as current, voltage, speed, preheat / interpass temperature were all found to be within the instructed range. The values for Units 2 and 3 are the same with minor differences. According to the welding record, the cladding materials and processes were applied correctly and it can be concluded that the bond between cladding and channel head are per specification and the base metal contains no detrimental inclusions or degraded cladding.

Table R.5 Weld condition of channel head cladding (SONGS-2A)

[illegible]

A, B

[illegible]

(R-13)
Document No.L5-04GA440 (0)
Attachment-R

A, B

Attachment-K

Table R.6 Weld condition of channel head cladding (SONGS-2B)

A,B

Table R.7 Weld condition of channel head clad weld (SONGS-3A)



Document No.L5-04GA440 (0)
Attachment-R
(R-15)

Table R.7 Weld condition of channel head clad weld (SONGS-3A)

A,B

[illegible]

Table R.8 Weld condition of channel head clad weld (SONGS-3B)

[illegible]

2.3 Clad Removal Process

2.3.1 Unit-2 and 3 Fabrication and Process Comparison

Table R.9 Fabrication Process Comparisons for Unit-2 & 3 RSGs

A,B





2.3.2 Clad Removal Process Prior to Buttering

Machining was used for SONGS-2 and arc-air-gouging was used for SONGS-3. Detail is as follows.

SONGS-2

A,B



SONGS-3

A,B



A,B



2.4 Buttering at Divider Plate Location

Welding record was reviewed in order to confirm that correct material was used and application was performed properly, check if the base metal contains any detrimental inclusions, verify if alloy 152 butter application could degrade the base metal

Pre-heat and post-bake record for SONGS-2A

A,B

Pre-heat and post-bake record for SONGS-2B

A,B



Pre-heat and post-bake record for SONGS-3A

A,B

Pre-heat and post-bake record for SONGS-3B

A,B

A, B

[illegible]

A,B

[illegible][illegible]



A,B

Table R.13 Weld condition of channel head butter weld (SONGS-3A).



A,B

Table R.14 Weld condition of channel head butter weld (SONGS-3B)

Table R.15 Chemical Composition and mechanical property of Welding Materials

A,B





A.B

Figure R.1 Design Drawing Requirement



The welding materials prepared for SONGS-2/3 project were used correctly and welding was performed properly.

Welding condition such as welding current, welding voltage, welding speed and pre-heat/interpass/post-bake temperature were within the instructed condition range. They are almost the same. There are few difference between SONGS-2 and SONGS-3 except number of layer and bead per layer.

In the case of SONGS-2, alloy 152 was buttered [A,B] which is higher than ambient stainless steel clad surface and then ground flush. In the case of SONGS-3, alloy 152 was buttered [A,B] to be the nominal buttering thickness, which resulted [A,B] less than SONGS-2. In SONGS-3B, 5th layer was buttered locally to satisfy the buttering thickness. As a result, buttered thickness of SONGS-3 would be about [A,B] less than that of SONGS-2 including the amount of grinding.

Number of bead per layer would relate to the buttered groove width. (Drawing requirements are shown in Fig.R.1) SONGS-2A has wider groove width so that number of bead is more than that of SONGS-2B. Groove bottom width of SONGS-2B and SONGS-3 are the same. But required corner radius is larger in SONGS-2B. Actual number of weld bead reflects the requirement. As a result, although the drawing requirements are satisfied, groove surface width would be SONGS-2A>SONGS-2B>SONGS-3. This difference may affects to the residual stress difference between SONGS-2 and SONGS-3, but there is no difference in the quality of welded metal.

According to the welding record, there is no potential that the base metal contains any detrimental inclusions and clad welding degraded the base metal.



2.5 Welding of Divider Plate to Channel Head

The processes and sequences used for welding the divider plate to the channel head buttered surface were generally the same for all four RSGs.

Fabrication record was reviewed if alignment accuracy or bracing can increase stress in this weld.

A,B



A,B



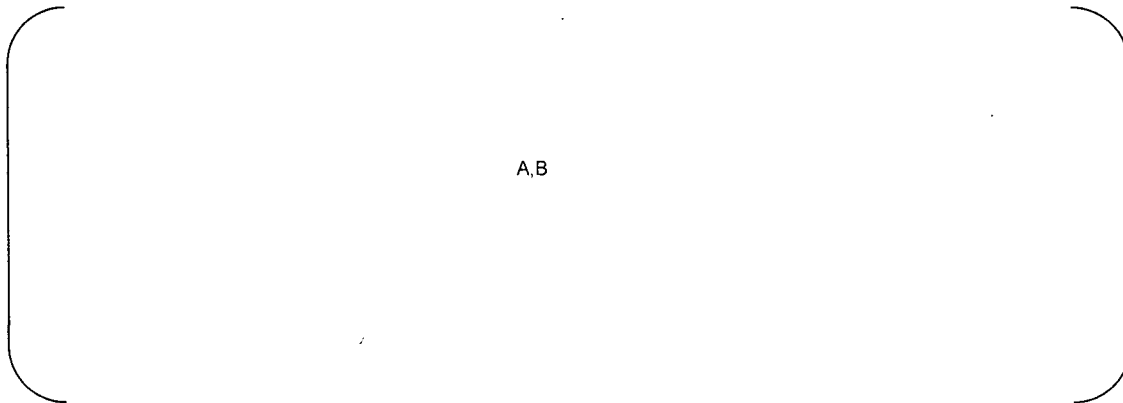
Bracings were applied in order to keep the flatness of divider plate. As shown in the drawings and picture above, bracings were placed in the radial directions at the lip of channel head. Bracings were not applied to prevent shrinkage or deformation of weld in the direction of tubesheet to channel head bottom, which is the concerned direction of the separation.

Another counter measure, welding divider plate to channel head alternatively from hot leg side and cold leg side, was applied so that the weld deformation would be almost equal to both side of the weld.

As a result, flatness of divider plate was good in SONGS-2A and the number of bracings was reduced to two in SONGS-3A and 3B. Flatness of divider plate was not measured during fabrication but measured after the occurrence of this issue.

Applied bracing has least relation to the divider plate separation issue and did not increase or reduce stress in the weld.

Divider plate was welded to channel head and tubesheet by GTAW and SMAW process. In order to minimize weld shrinkage and distortion, welding was applied in accordance with a strict instruction. The same instruction was applied to the four RSGs of SONGS-2A to SONGS-3B.



A,B



A,B



A,B

— MITSUBISHI HEAVY INDUSTRIES, LTD. —



A,B



A.B

A, B

A,B



2.6 Welding of Divider Plate to Tubesheet

The processes and sequences used for welding the divider plate to the tubesheet clad surface were generally the same with the welding to channel head and for all four RSGs.

2.7 Welding of Channel Head to the Tubesheet

The processes and sequences used for welding the channel head to the tubesheet were generally the same for all four RSGs.

2.8 Heat Treatments

The processes and sequences used for heat treating the channel head to the tubesheet welds were generally the same for all four RSGs.

PWHT was applied in accordance with the approved procedure "Post Weld Heat Treatment Procedure" SB-SO-HT-1001 for SONGS-2A/2B/3A/3B channel heads.

Every heat treatment steps designated in FPS (Fabrication Process Sheet) was followed correctly and verified.

PWHT record was confirmed that the heat treatment time and temperature are satisfactory to the procedure and Code requirement.

Difference in the accumulated holding time for each channel head is not large. They are in the order of 2A>3A>2B>3B (">" means longer holding time).

Table R.20 History of PWHT of Channel Head

A,B

[illegible]

(R-44)
Document No.L5-04GA440 (0)
Attachment-R



3 Review of Inspection Record

3.1 Alloy 152 butter and Divider Plate weld Records

Inspections/checks by QC for the Alloy 152 butter under Divider Plate (WF-V116-1) and Divider Plate welds (WA-V116-1) are listed below tables.

As for PT, UT and VT, inspection results were all accepted and there were no recordable UT indications. As for the other QC check, all results were accepted.

Furthermore, the same procedures and instructions were used for each inspection and check, and the same method and acceptance criteria were applied among all RSGs. (Note that verification of removal by etching for Unit-2 were not performed.)

In conclusion, no particular difference between Unit-2 and Unit-3 were identified in the review of inspection record.

Table R.21 History of Inspection and QC check for Divider Plate welds (WF-V116-1)

A,B

Table R.22 History of Inspection and QC check for Divider Plate welds (WA-V116-1)

A,B

3.2 Stainless Steel Clad Records

Inspections for the SS clad (WO-V105-1, 2) are listed below.

PT result of WO-V105-1 on 2A RSG was unacceptable. All locations of unacceptable indications were out of the divider plate attached area, and their indications were appropriately repair-welded in accordance with UGNR-SON2-RSG-071. The PT results for the other RSGs were accepted.



UT result of WO-V105-1 on 3A RSG was unacceptable. Unacceptable indications and acceptable but recordable indications were detected. All locations of indications were out of the divider plate attached area, and unacceptable indications were appropriately repair-welded in accordance with UGNR-SON3-RSG-031. The UT results for the other RSGs were accepted.

UT result of WO-V105-2 on 3A RSG was acceptable, but one recordable indication was identified. This indication was so small that we did not perform repair in accordance with the procedure.

VT results were all accepted.

Table R.23 History of Inspection for stainless steel clad (WO-V105-1, 2)

A,B	
-----	--



3. 3 Hydrostatic Test records

The following table shows all Hydrostatic Tests have been performed for all RSGs. All records were verified that the test pressure were within the proper limits required by the hydrostatic test procedure, and unusual pressure drop/raise was not identified. All hydrostatic tests were properly performed for Unit-2 and Unit-3 RSGs.

TableR.24 Hydrostatic Test Records

A,B	
-----	--



Attachment-S
Additional Investigation of Boat Samples



1. Purpose

The purpose of this report is to provide results of additional investigation of boat samples collected from the U3B RSG.

2. Background

Cracks were discovered on the divider plate-to-channel head weld during the inspection of the tube-to-tube sheet weld after the secondary side hydrostatic test on Unit 3B RSG. The cracks were caused by the separation of the divider plate and the channel head.

3. Investigation Methodology

Boat samples A, B and C which had been collected from U3B RSG were used for additional investigation. Collecting locations of boat samples are shown in Figure S.1.

The investigation methodology matrix is summarized in Table S.1.

Table S.1 Investigation Methodology of boat samples

Item	Method	Purpose
Separation surface	SEM (Scanning Electron Microscope) examination at high magnification (x1500, x2500, x5000)	Evaluate the micro-structure of the separation surface
Chemical analysis	EPMA (Electron Probe Micro Analyzer) analysis	Evaluate chemical composition of the material near the separation and separation surface



4. Results of investigation

Figures S.2 shows the SEM pictures of the fracture surface of sample A, B and C at high magnification.

It was observed that the separation between low alloy steel and 152 buttering reveals indented surface which was like martensitic lath structure at high magnification, though relatively flat fracture surface was observed at low magnification (Figure S.2(1), S.2(2) and S.2(3)). At high magnification, the separation between low alloy steel and 152 buttering appeared with similar fracture surface morphology to hydrogen-induced transgranular cracking in its feature as shown in Figure S.2(5)(a) for reference.

Fracture surface of the separation between low alloy steel and stainless steel clad reveals relatively smooth surface at high magnification (Figure S.2(4)). It is assumed that the separation between low alloy steel and stainless steel clad appeared with similar fracture surface morphology to hydrogen-induced intergranular cracking in its feature at high magnification as shown in Figure S.2(5)(b) for reference.

Figures S.3 shows the results of EPMA line analysis across fusion boundary in the cross section of sample B. Component variations was observed in 152 buttering adjacent to the separation.

Figures S.4 shows the results of compositional mapping by EPMA in the fracture surface of sample B and C. It was observed that there was a certain level of compositional distribution of Fe, Cr and C at the fracture surface.

5. Summary

- 1) At high magnification, the fracture surface of separation between low alloy steel and 152 buttering appeared to be like martensitic lath structure.
- 2) At high magnification, the fracture surface of separation between low alloy steel and stainless steel clad reveals relatively smooth surface.
- 3) Component variations were observed in 152 buttering adjacent to the separation.
- 4) It was observed that there was a certain level of compositional distribution of Fe, Cr and C at the fracture surface.

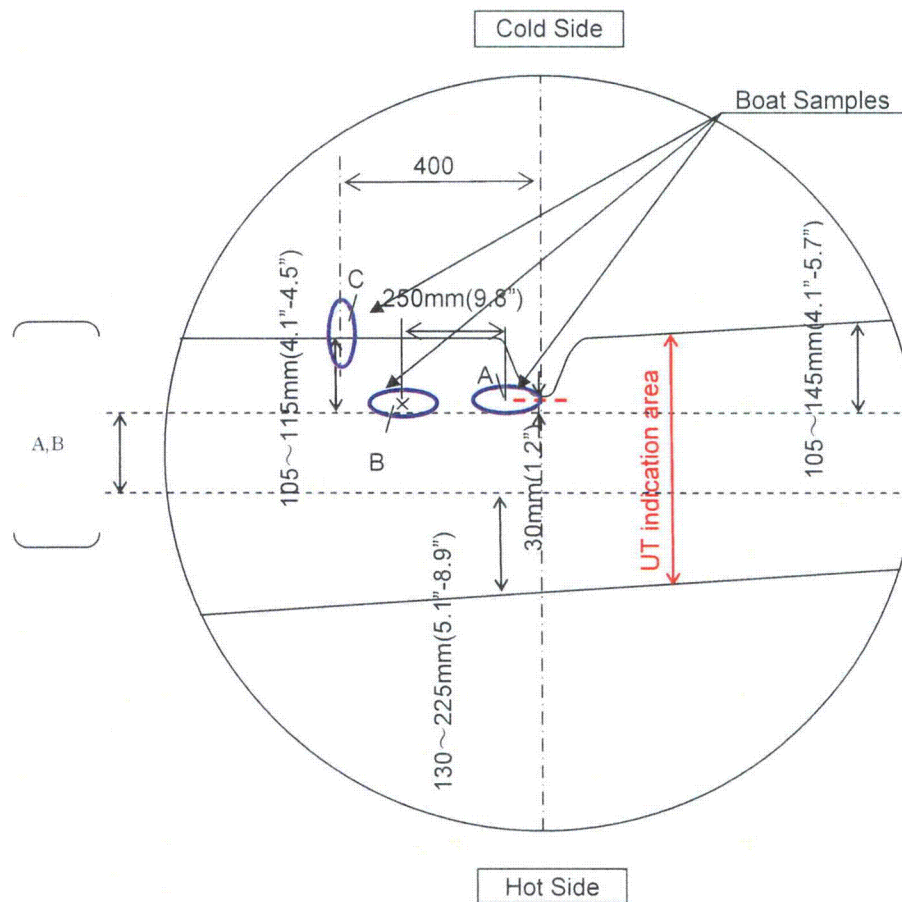
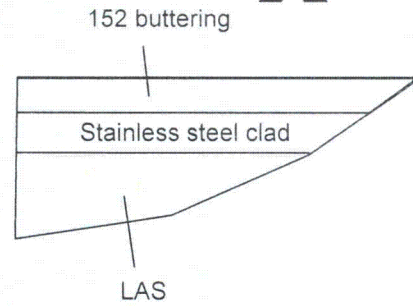
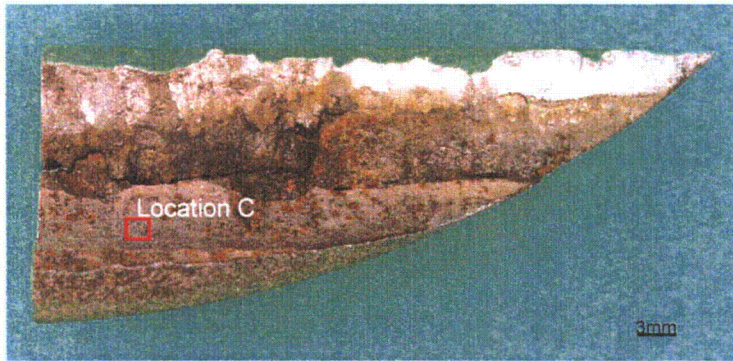
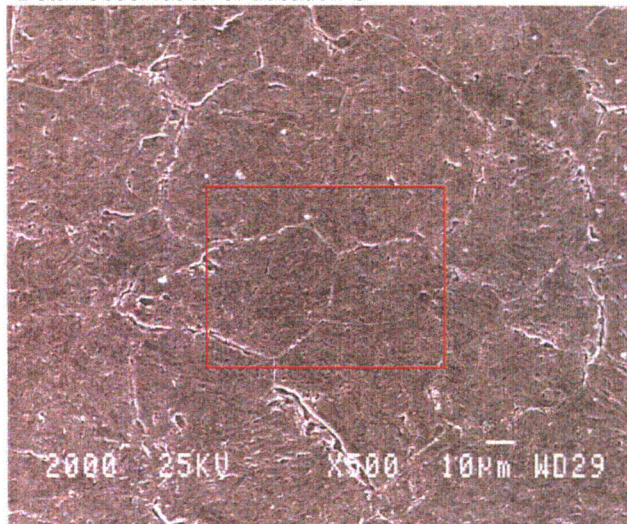


Figure S.1 The collecting locations of boat samples.

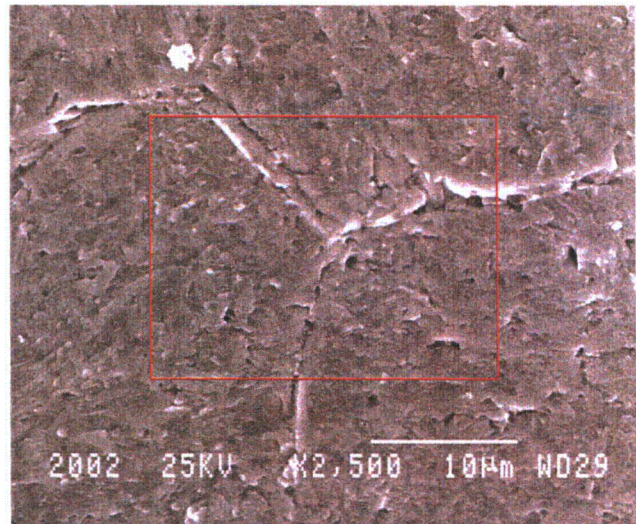


Location of the SEM observation
Detail observation of Location C



Enlarged

Enlarged



Enlarged

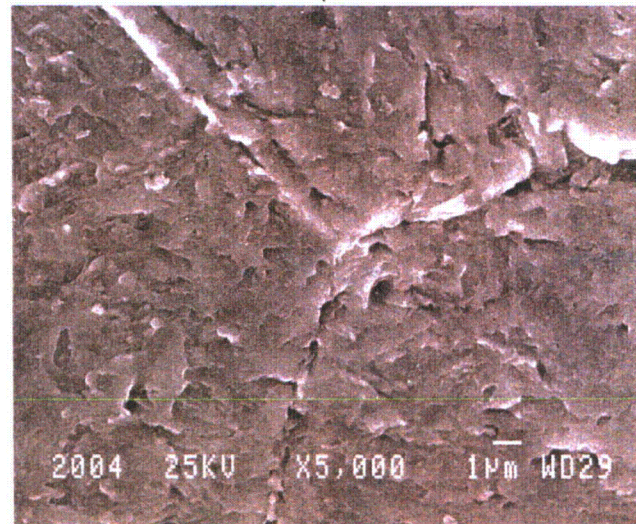
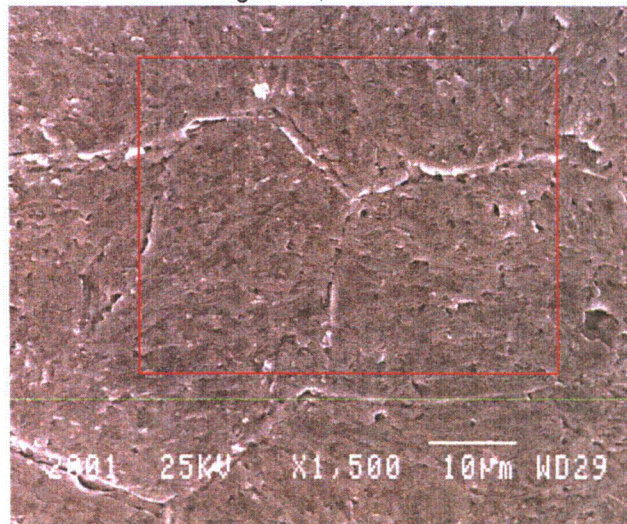
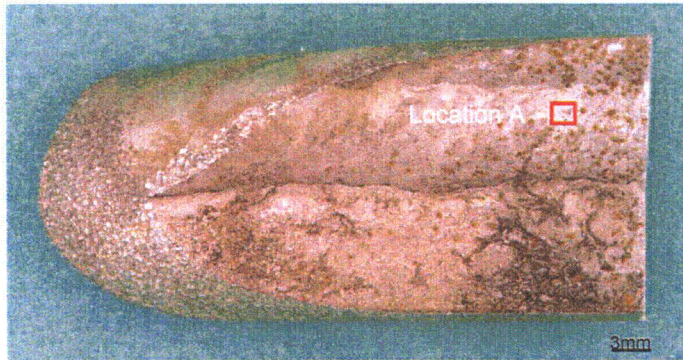
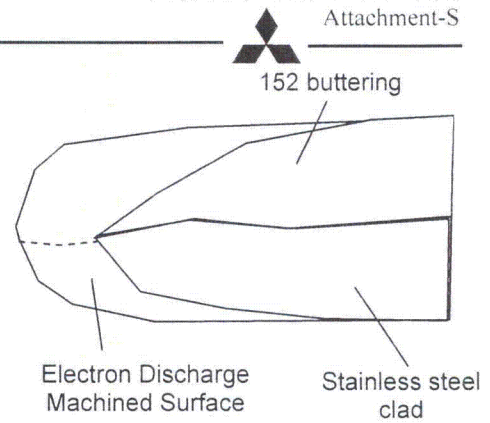


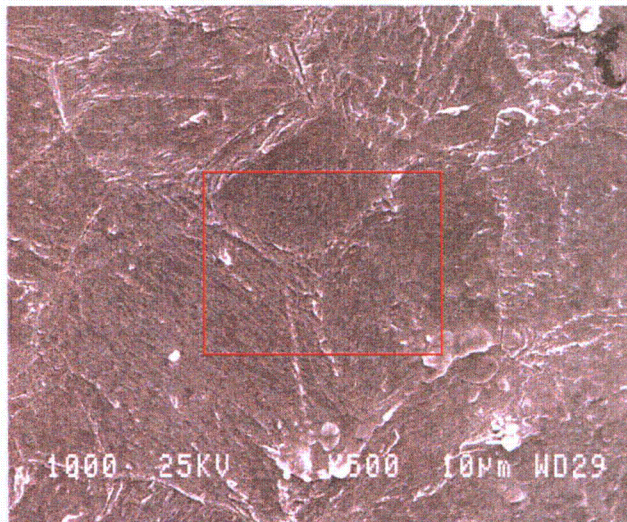
Figure S.2(1) SEM pictures of the fracture surface of the boat sample
(Sample A, TP A-1, location C)



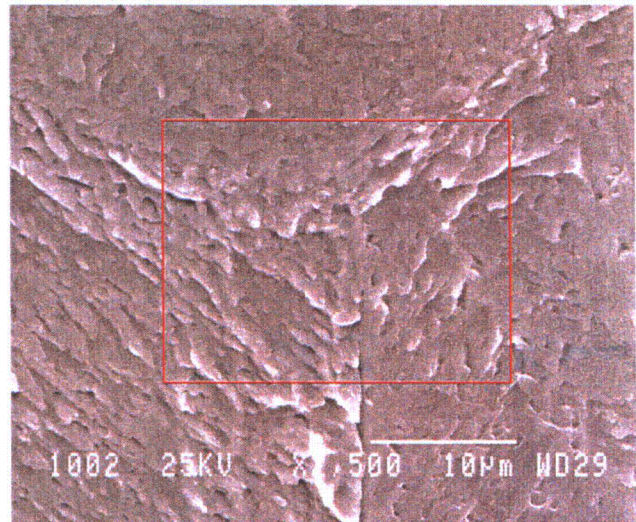
Location of the SEM observation



Detail observation of Location C



Enlarged ↓



Enlarged ↓

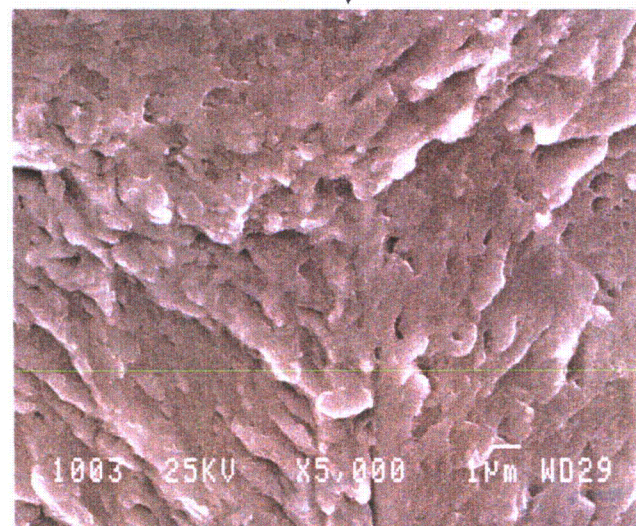
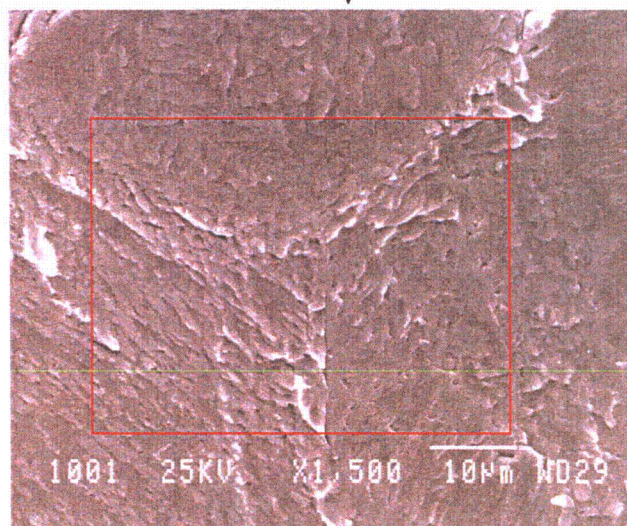
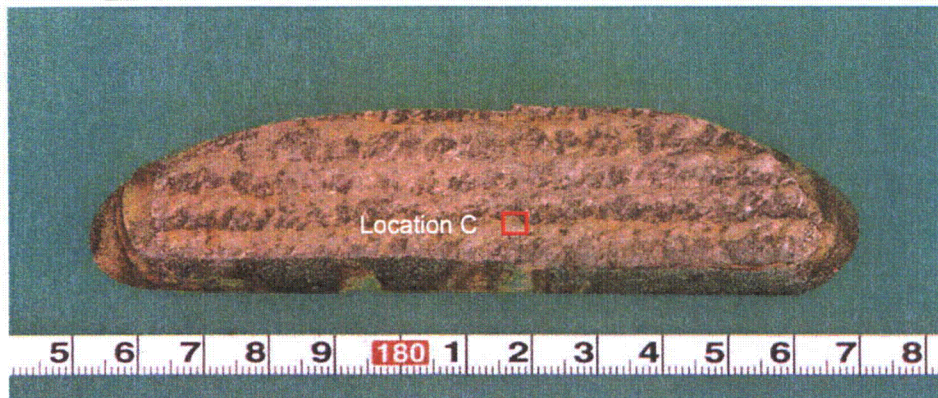
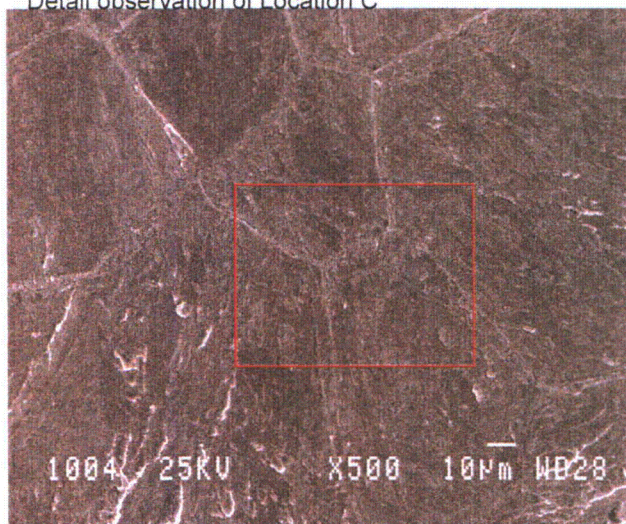


Figure S.2(2) SEM pictures of the fracture surface of the boat sample
(Sample A, TP A-2, location A)



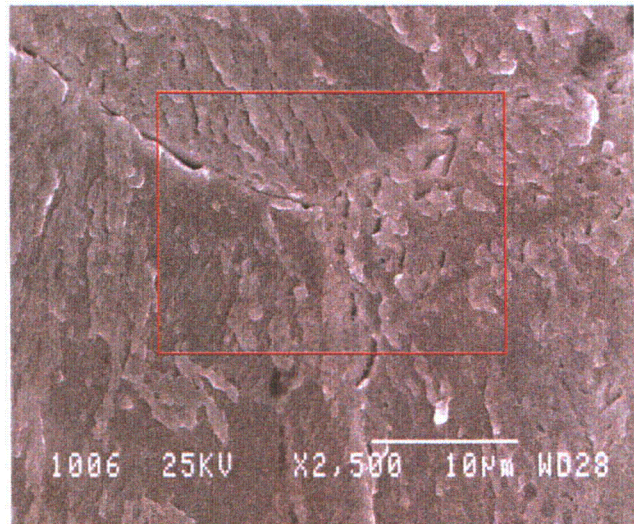
Location of the SEM observation

Detail observation of Location C



Enlarged

Enlarged



Enlarged

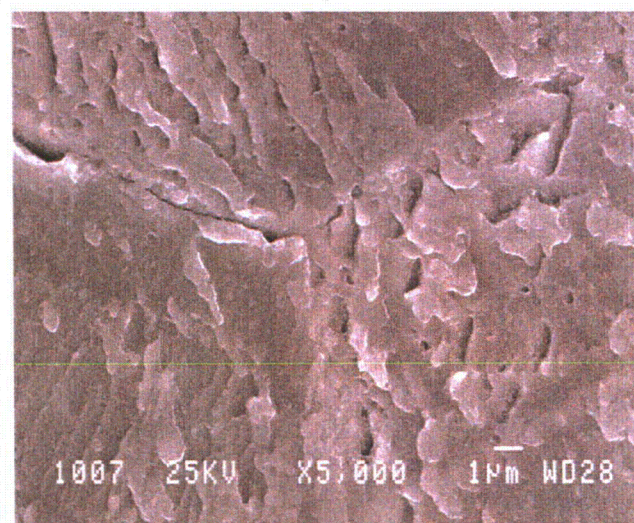
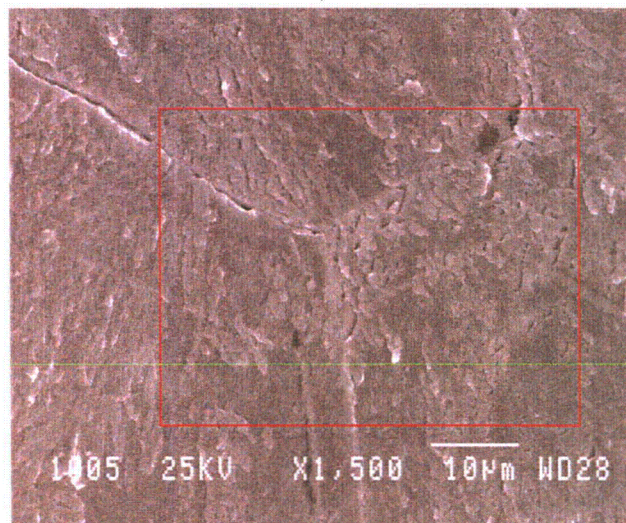
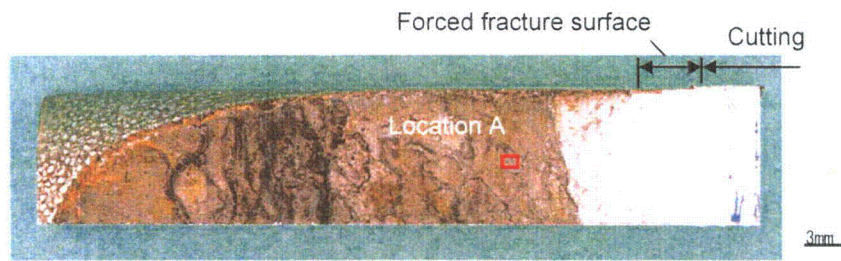


Figure S.2(3) SEM pictures of the fracture surface of the boat sample
(Sample B (152 buttering), location C)



Location of the SEM observation

Detail observation of Location A

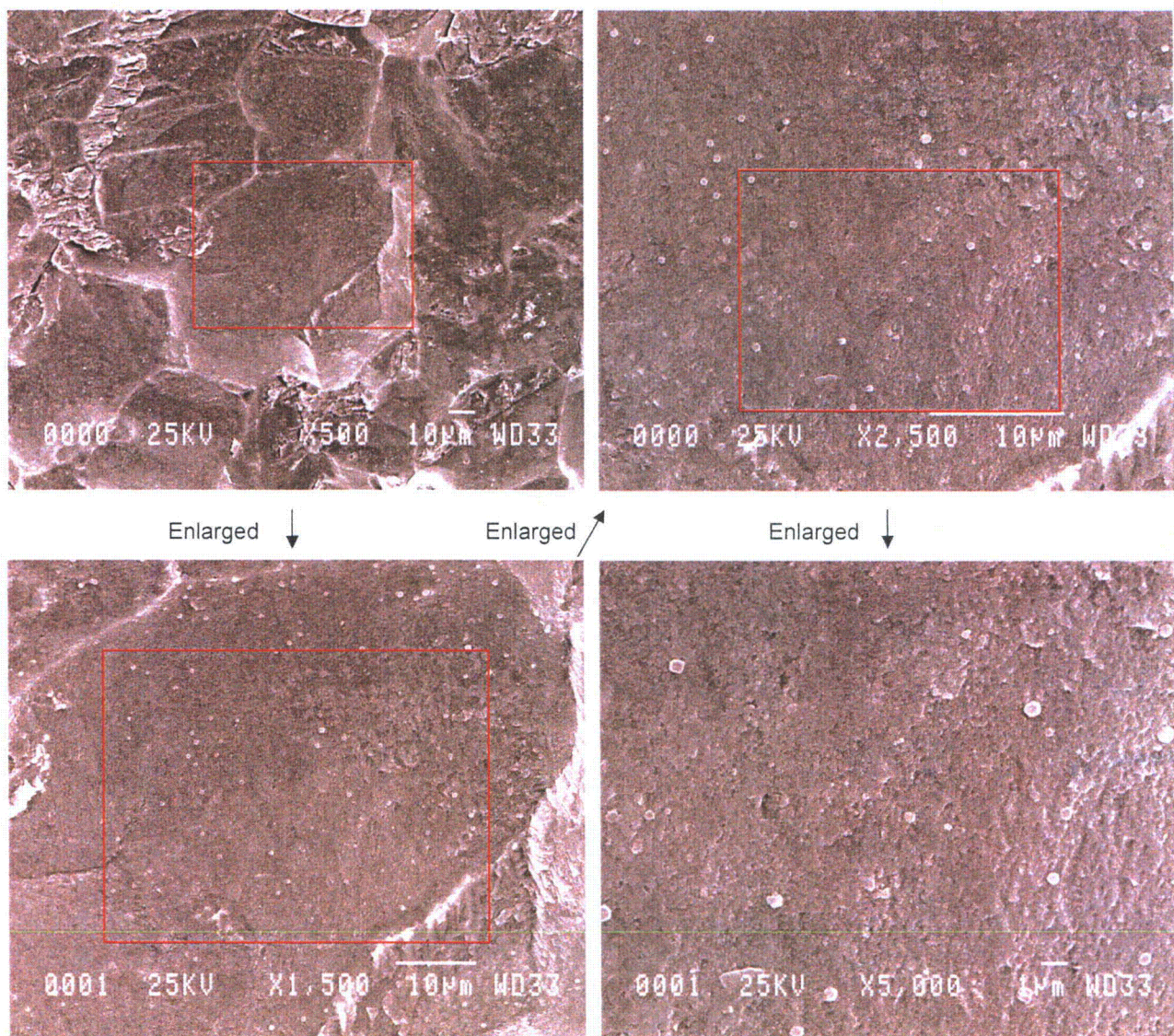
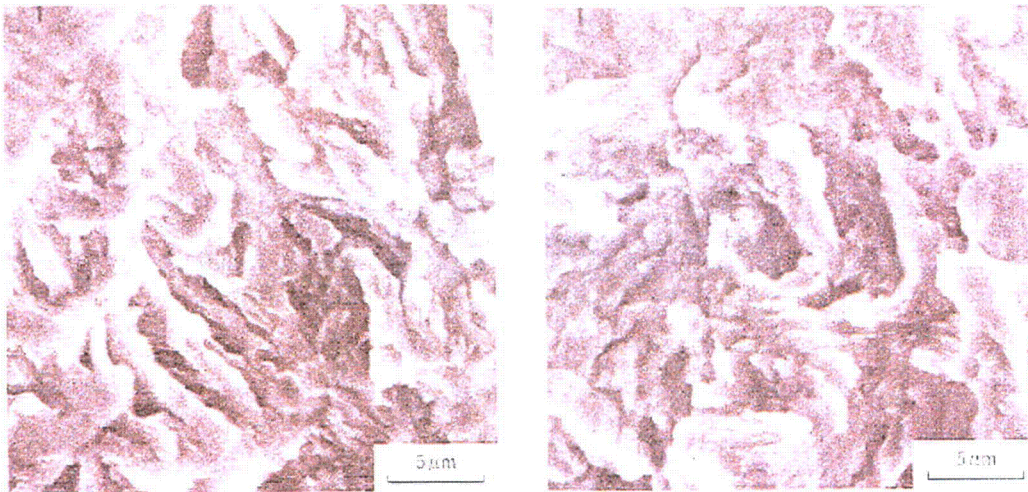
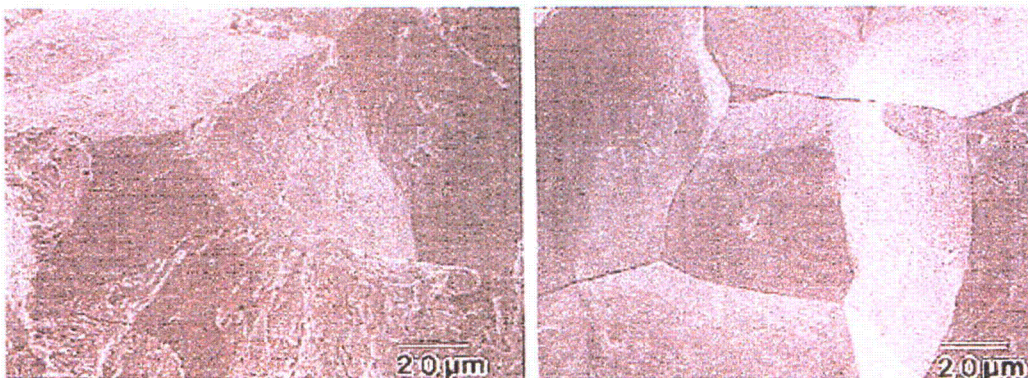


Figure S.2(4) SEM pictures of the fracture surface
(Sample C, TP C-1, location A)



(a) Fracture surface of hydrogen-induced cracking in 1%Cr-0.5%Mo steel

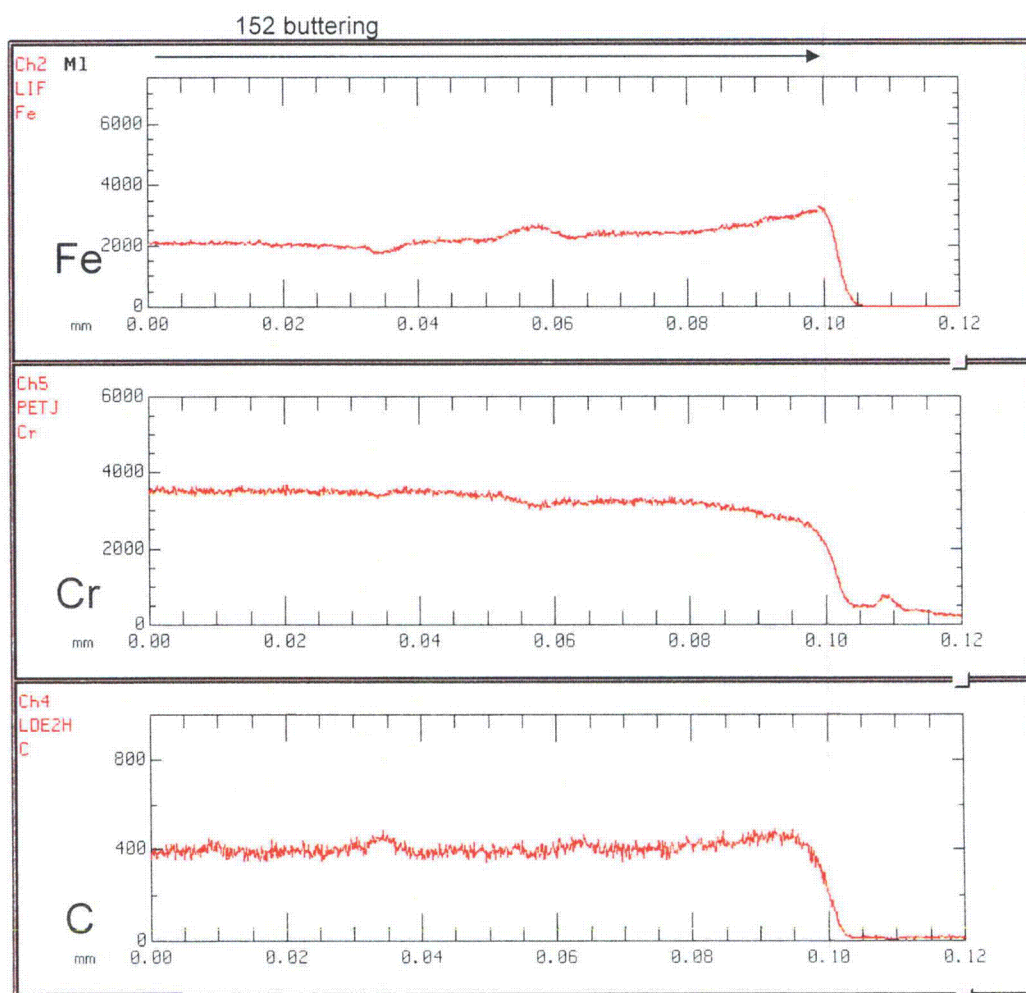


(b) Fracture surface of hydrogen-induced cracking in 2%Cr-4%Mo steel

Figure S.2(5) SEM pictures of the fracture surface of hydrogen-induced cracking for reference
("Fractography" edited by The Society of Materials Science Japan, (2000), p.129-130.)

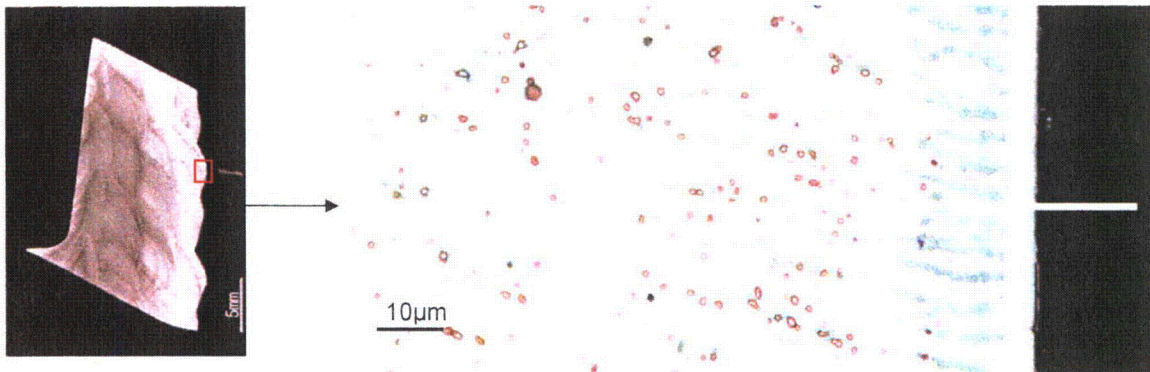


Location of the EPMA observation

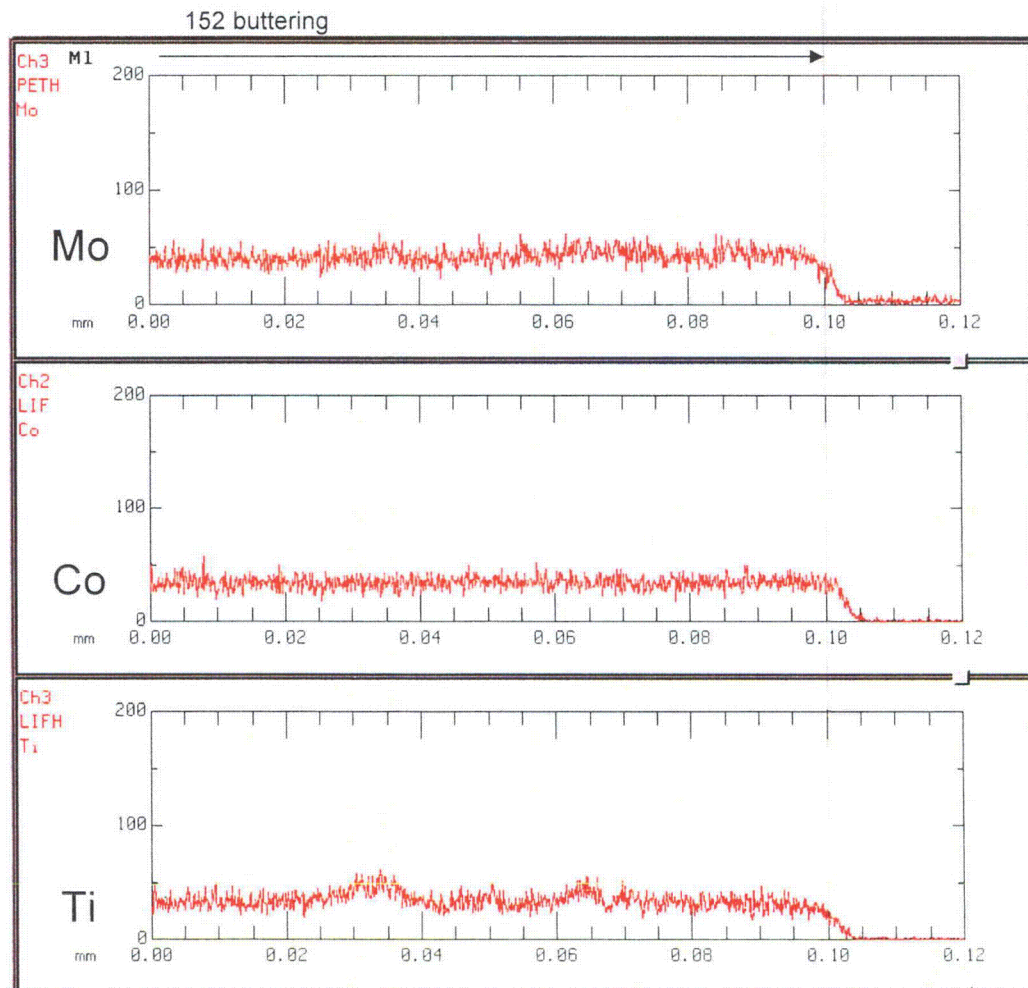


*Resin was removed from the specimen after polishing for the analysis

Figure S.3(1) EPMA line analysis across fusion boundary (sample B, 152 buttering side)

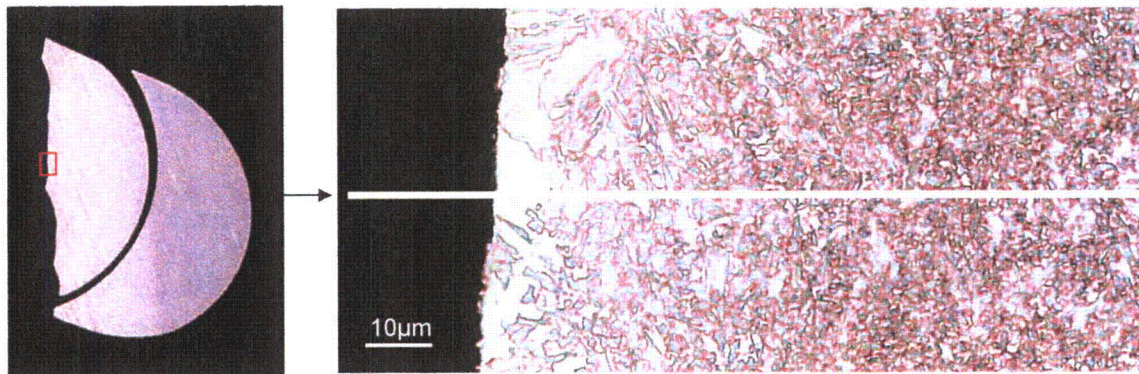


Location of the EPMA observation

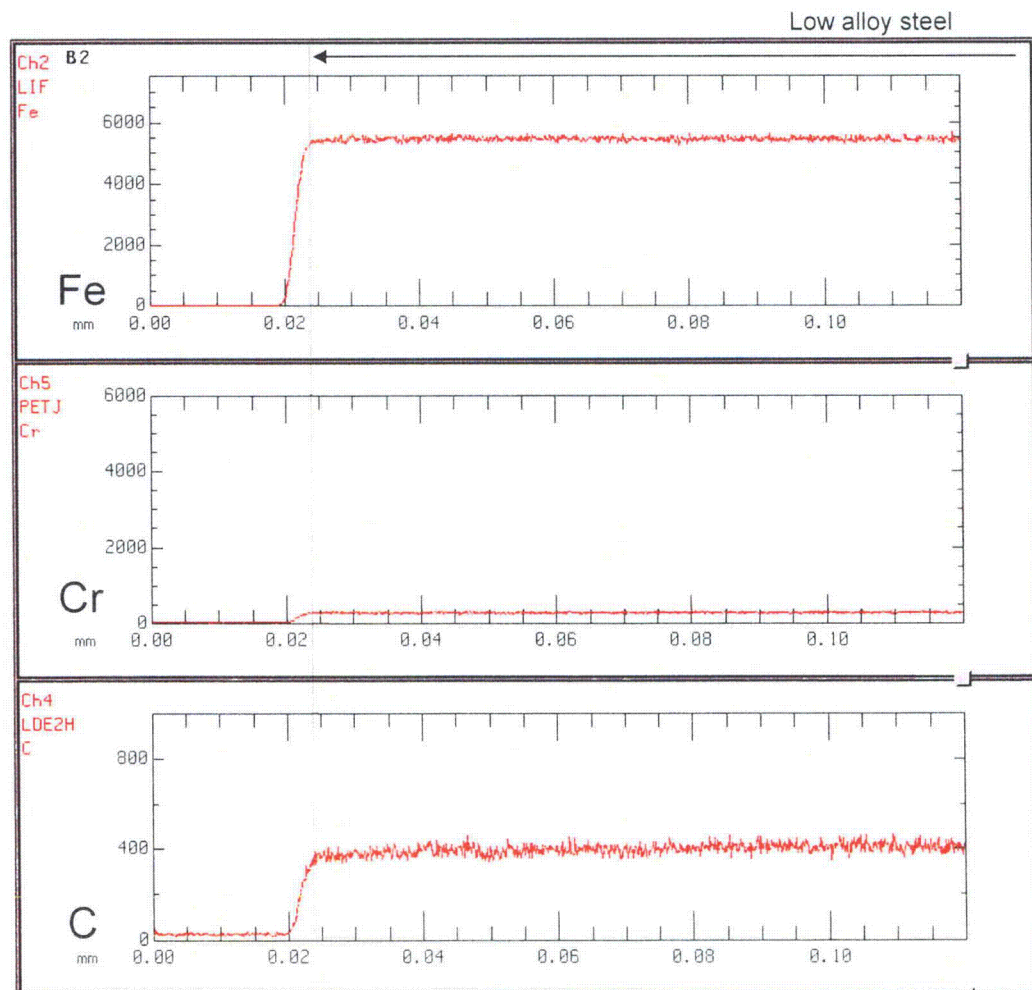


*Resin was removed from the specimen after polishing for the analysis

Figure S.3(2) EPMA line analysis across fusion boundary (sample B, 152 buttering side)

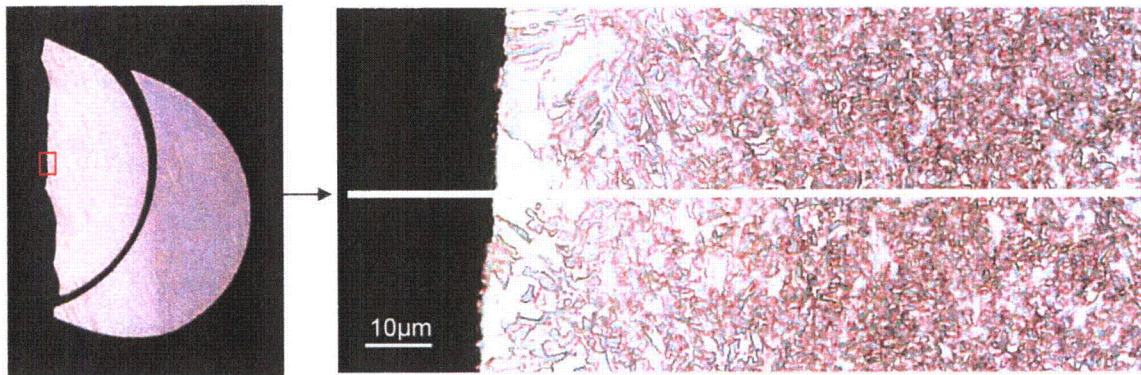


Location of the EPMA observation

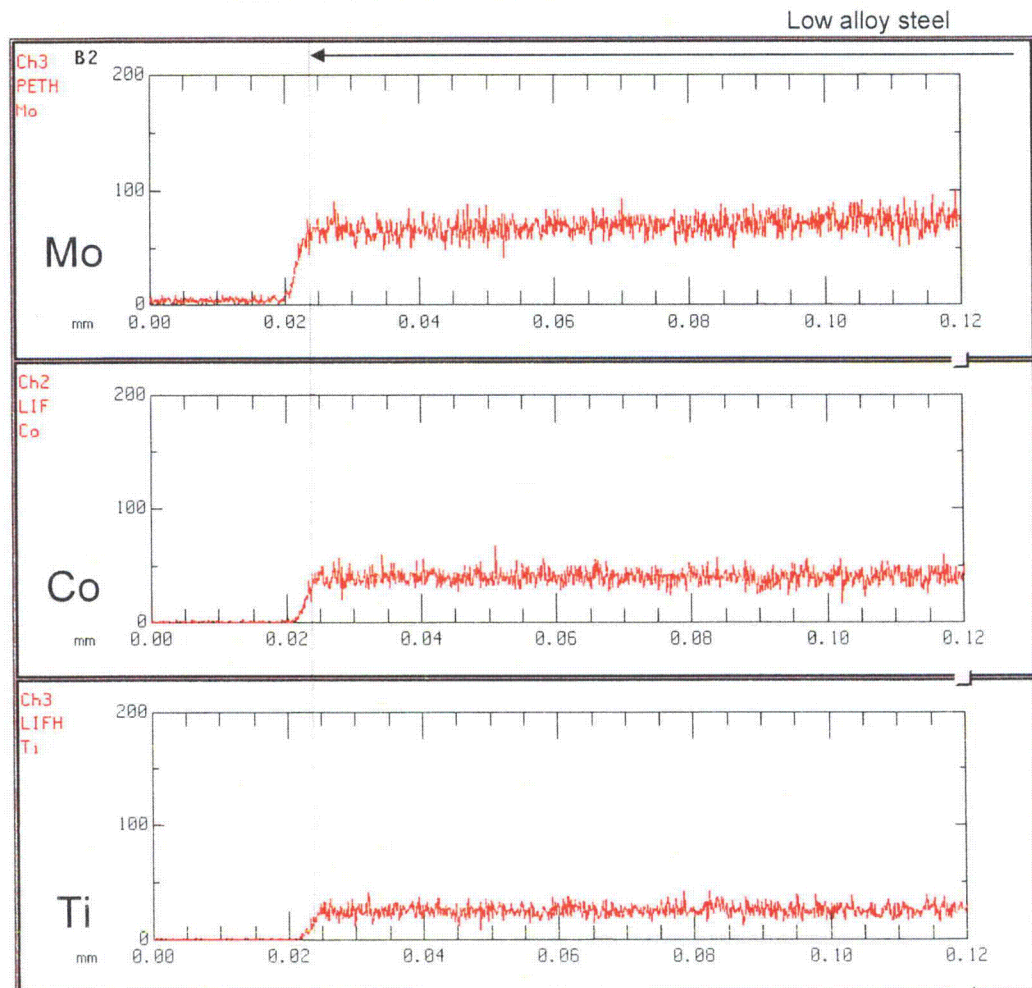


*Resin was removed from the specimen after polishing for the analysis

Figure S.3(3) EPMA line analysis across fusion boundary (sample B, Low alloy steel side)

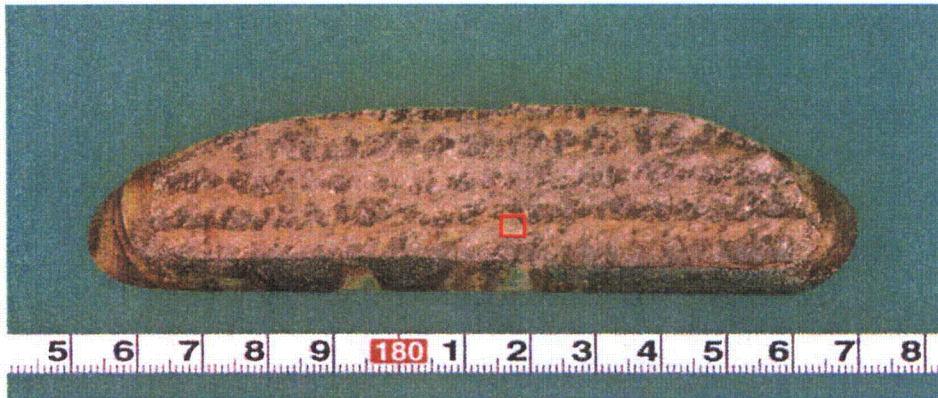


Location of the EPMA observation



*Resin was removed from the specimen after polishing for the analysis

Figure S.3(4) EPMA line analysis across fusion boundary (sample B, Low alloy steel side)



Location of the Composition mapping

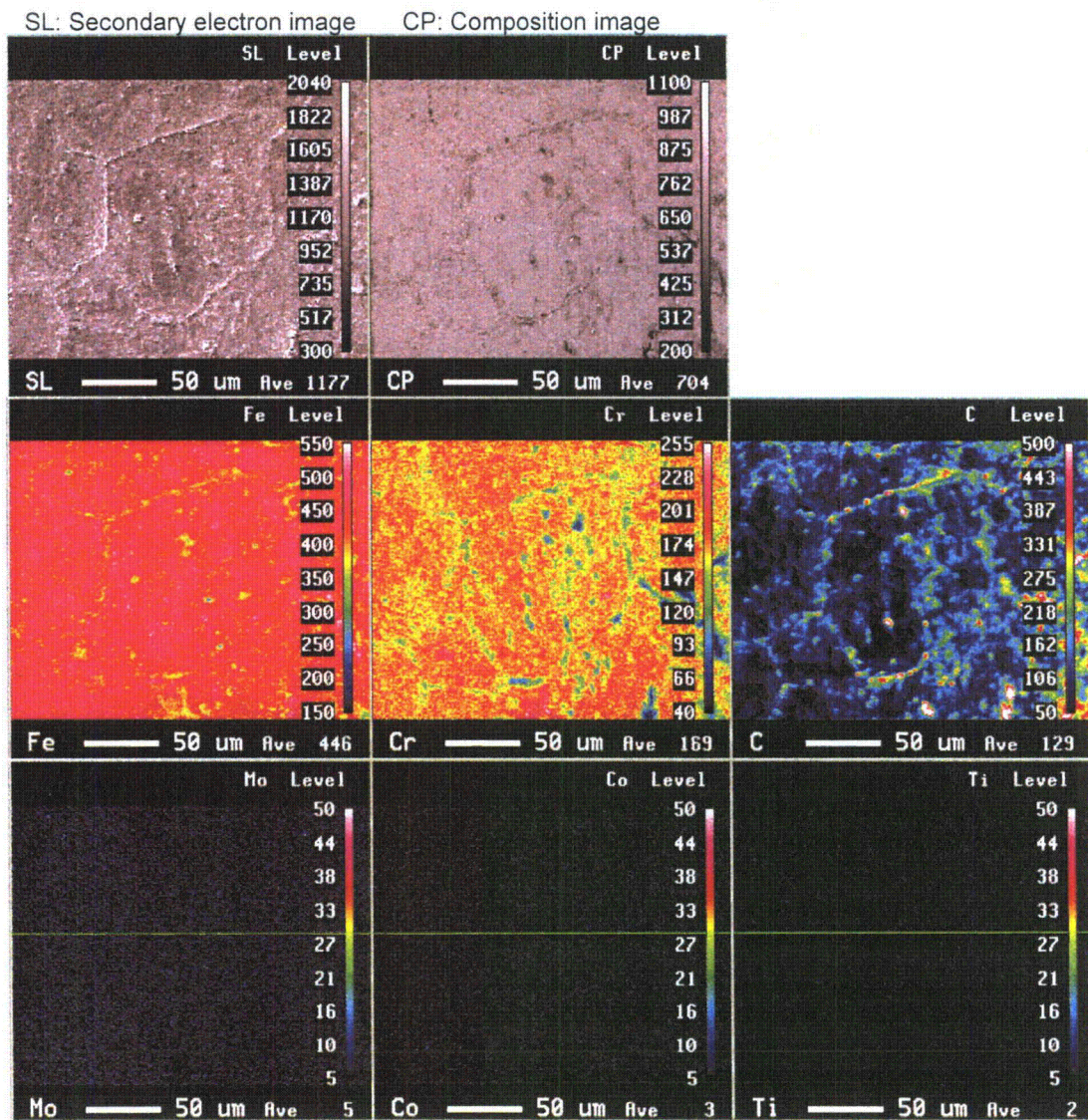
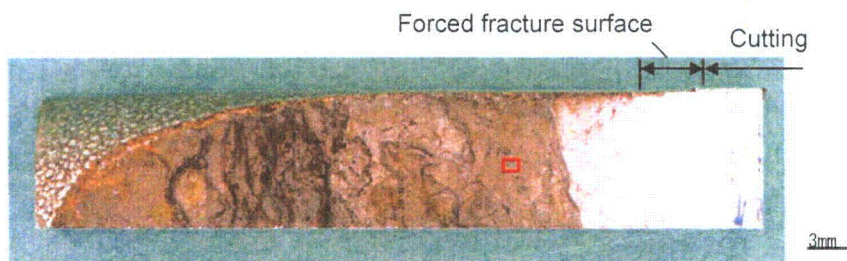


Figure S.4(1) Compositional mapping by EPMA on the fracture surface

(Sample B, 152 buttering side)

MITSUBISHI HEAVY INDUSTRIES, LTD.



Location of the Composition mapping

SL: Secondary electron image CP: Composition image

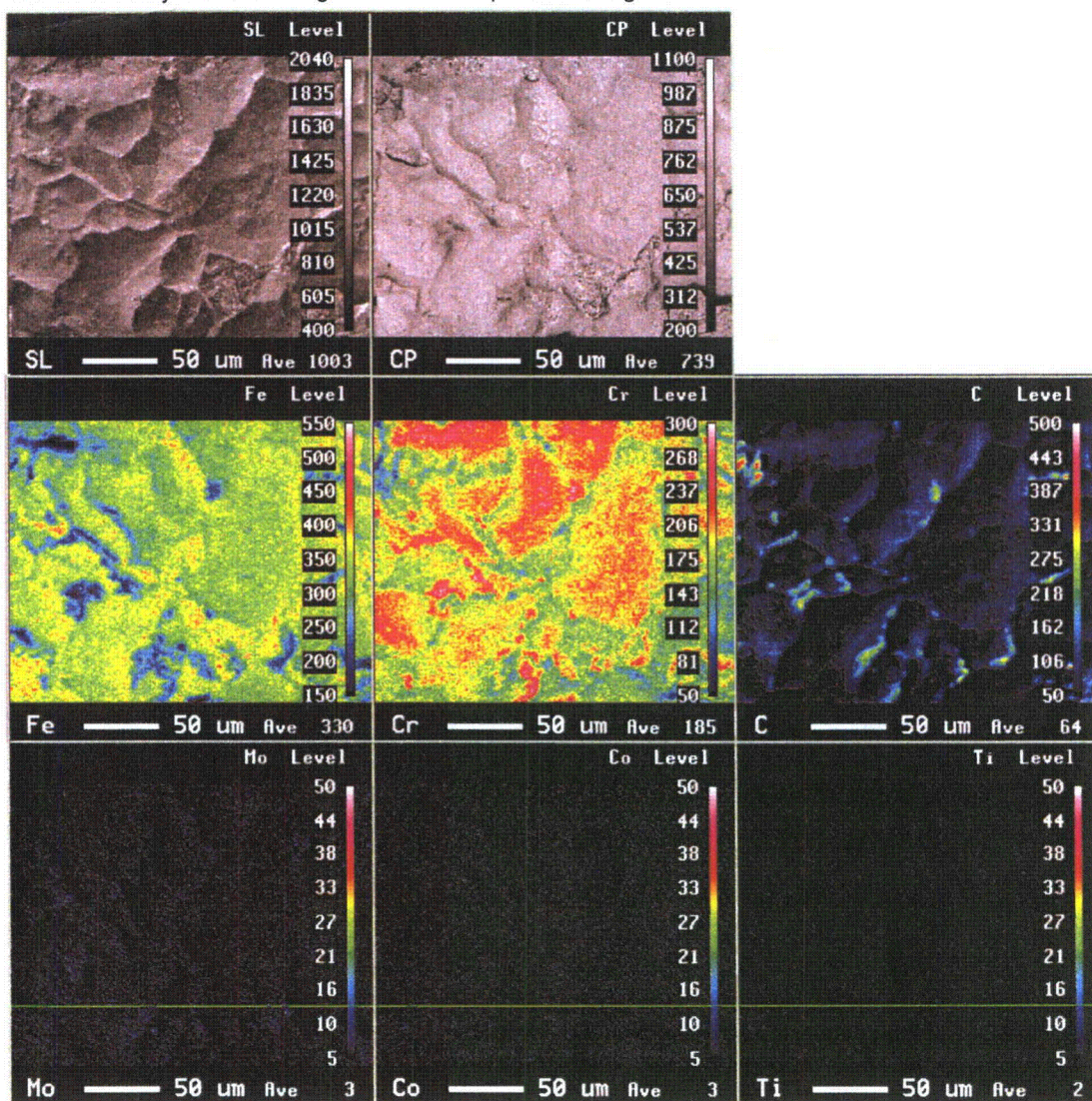


Figure S.4(2) Compositional mapping by EPMA on the fracture surface
(Sample C, TP C-1, stainless steel clad side)